SEED PRIMING WITH GREEN SYNTHESIZED NANOPARTICLES IMPROVE GERMINATION, GROWTH, AND YIELD WHILE MAINTAINING QUALITY OF ONION AND WATERMELON

A Dissertation

by

PRATIBHA ACHARYA

Submitted to the Office of Graduate and Professional Studies of
Texas A&M University
in partial fulfillment of the requirements for the degree of

DOCTOR OF PHILOSOPHY

Chair of Committee,	Bhimanagouda S. Patil
Committee Members,	Guddadarangavvanahally K. Jayaprakasha
	Kevin M. Crosby
	John L. Jifon
	Joseph M. Awika
	Subas Malla
Head of Department,	Daniel Lineberger

December 2020

Major Subject: Horticulture

ABSTRACT

Seed priming is a promising approach to improve germination, emergence, and seedling growth by altering pre-germination metabolism and enhancing seedling vigor. Recently, nanopriming gained importance in seed improvement as a result of the small size and unique physicochemical characteristics of nanomaterials. The primary objective of the current research was to characterize the effects of various nanopriming treatments on seed germination, growth, yield and nutritional quality of onion and watermelon.

First, second and third studies focused on green nanomaterial effects on aged onion seeds. Silver nanoparticles (AgNPs) and gold nanoparticles (AuNPs) were synthesized using onion extracts. Similarly, food processing industry byproducts namely, citrus seed and curcumin-removed turmeric oleoresin were used to prepare nanoemulsions for seed treatments. Multiple greenhouse and field studies demonstrated enhanced seed germination, emergence, growth, and yield compared with unprimed and hydroprimed seeds. One-dimensional 1H nuclear magnetic resonance and liquid chromatography coupled with mass spectrometry-based metabolomics revealed the enhancement of germination stimulators, such as γ-aminobutyric acid and zeatin, using nanopriming treatments in onion seeds. Influence of nanoparticles, locations, and the size of the bulbs in the flavonoid and amino acids content was demonstrated in onion.

In fourth, fifth and sixth studies, seeds of two watermelon varieties namely: Riverside (diploid) and Maxima (triploid) treated with two nanomaterials (AgNPs and turmeric nanoemulsion) together with untreated seeds were studied in five locations over two seasons. Higher yield upto 31.6% and 35.6% compared to control were observed in AgNP- treated Riverside and Maxima watermelons, respectively. Physico-chemical properties and

phytochemical profiles were assessed after harvested and stored at 23°C for 0, 10, and 20 d. Levels of health promoting compounds such as carotenoids, L-citrulline and total ascorbic acid were maintained and/or enhanced in watermelons after 10 d of storage compared to untreated fruits at harvest. AgNPs and TNE as the nanopriming treatment in watermelon seeds had no significant differences in the level of phytochemical composition as compared to the unprimed. Total 87 volatile compounds were identified and quantified from the watermelon of two varieties Riverside and Maxima harvested from five different locations. Overall the results demonstrated that nanopriming is an eco-friendly and sustainable technology that can enhance seed germination, growth, and yield of onion and watermelon while maintaining nutritional quality.

DEDICATION

This dissertation is dedicated to my parents, Lekhnath Acharya and Manju Acharya for all their unconditional love and sacrifices. To my father in law Dr. Bishnu Bilas Adhikari and my mother in law Bimala Adhikari who always supported, encouraged, and motivated me. To my loving husband Anil Adhikari for all the encouragement and constant support throughout the highs and lows of this PhD journey, and finally to my daughter Arya Adhikari.

ACKNOWLEDGEMENTS

I would like to express my sincere gratitude to my advisor Dr. Bhimu Patil for providing me the opportunity to pursue graduate studies in his program and for his guidance and encouragement during my PhD. Without his assistance and motivation, it would not be possible for me to have achieved my PhD goals. I am deeply indebted to my committee members, Dr. Jay, Dr. Crosby, Dr. Jifon, and Dr. Awika, for their immense support throughout the course of this research. I extend my sincerest gratitude to Dr. Subas Malla for willing to serve as an alternate committee member during my dissertation. I am also very thankful to Dr. Jashbir Singh for his supervision and help in conducting my research.

Thanks also go to my labmates and colleagues: Rita, Karen, Siddhu, Priyanka, Noorani, Jose, Marisa, Maricella, Jisun, Jason, Diwas, Kishan, Drishti, Varsha, Sarah, Dr. Wilmer and Dr. Tushar and the department faculty and staff for making my time at Texas A&M University a great experience.

Finally, my deepest gratitude to my parents and parents in law for their unconditional love, encouragement and to my husband Anil Adhikari for his patience and love.

CONTRIBUTORS AND FUNDING SOURCES

Contributors

This work was supervised by a dissertation committee consisting of Dr. Bhimanagouda S. Patil [Chair], and Dr. G.K. Jayaprakasha of the Vegetable and Fruit Improvement Center, Department of Horticultural Sciences. My committee members; Dr. Kevin M. Crosby, Dr. John L. Jifon of the Department of Horticultural Sciences and Dr. Joseph M. Awika of the Department of Food Science at Texas A&M University witnessed my results during the committee meetings.

Nanoparticle characterization using X-ray diffraction was conducted using the technical support of Dr. Nattamai Bhuvanesh and internalization study using transmission electron microscopy was performed in the support of Dr. Stanislav Vitha. Similarly, neutron activation analysis was conducted by Dr. Bryan Tomlin, Center for Chemical Characterization, Texas A&M University.

All other work conducted for the dissertation was completed by the student independently under the supervision of the chair of the committee.

Funding Sources

This study was supported by the Texas Department of Agriculture under Grant Number SC-1607-013. This work was also partially supported by the United States Department of Agriculture-NIFA- SCRI-2017-51181-26834 through the National Center of Excellence for Melon at the Vegetable and Fruit Improvement Center of Texas A&M University.
Its contents are solely the responsibility of the authors and do not necessarily represent the official views of the funding agencies.

TABLE OF CONTENTS

Page

LIST OF FIGURES

Page

LIST OF TABLES

Page

1. INTRODUCTION

Nanotechnology is a multidisciplinary field that involves the synthesis, design, fabrication, manipulation and functionalization of the particles at the nanoscale. Nanotechnology encompasses knowledge from different fields of study and applied in myriad areas, such as agriculture, engineering, cosmetics, environmental health, health care, food, biomedical sciences, space industries, mechanics, energy science, optics, chemical industries, electronics, drug-gene delivery, photoelectrochemical applications.[1-2] As a reduction in their sizes and high surface to volume ratio, NPs exhibits unique and significantly distinct properties with respect to the corresponding bulk materials.[2-3] Most commonly used method for the preparation of stable, colloidal, and well-dispersed NPs is chemical reduction in the presence of reducing agents and stabilizers.[2] These reducing agents and stabilizers used for commercial synthesis of NPs are highly reactive and toxic chemical compounds and may pose a risk to the environment and humans.[4] Moreover, they are expensive for large-scale applications. An alternative to the use of toxic chemicals for the synthesis of NPs is the use of plant-based phytochemicals, also known as green synthesis methods because of the environmentally benign process. Use of plants extracts are cost-effective, eco-friendly, sustainable, and bio-renewable platforms, for the production of new, greener, and safer nanoparticles (NPs).

Green nanotechnological approach is a rapidly expanding in sustainable agriculture that promises to revolutionize food production to meet the rising global demand. Global population is sky rocketing and expected to be around 10 billion by 2050. To fulfill the needs of 10 billion people, the world needs to produce 50% more food by 2050.[5-6] With the escalating population, demand for high agricultural produce with higher nutrition composition also increases.

Nanotechnology has emerged as one of the most promising solutions to overcome the shortcomings of traditional agricultural practices which have restricted the utilization of available farmlands to full its potential. In agriculture, nanotechnology promises to improve crop productivity and quality at every stage like seed storage, priming, germination, fertigation, post-harvest storage.

An important target point for NP application in enhancing crop performance is the seed and germination stages. Seed germination and seedling emergence are critical factors that determine crop success and ultimately yields.[7] For rapid and uniform seed germination and seedling emergence, priming is a commonly used method that enables the seed to imbibe water to proceed to the first stage of germination.[8] Nanopriming, in which a NP suspension or emulsion is used as a priming medium, is a newly introduced, innovative method for improving seed germination and growth. NPs offer advantages over conventional priming methods as they have high surface to volume ratio, small sizes, and increased reactivity which enable NPs to penetrate the pores of seeds, spread inside, and activate phytohormones that stimulate growth. Nanopriming is very effective in the aged seeds and those which are difficult to germinate. Aged onion seeds and triploid watermelon seeds are characterized as showing poor germination and slow post-germination growth. So, they were selected as the model crop for the study.

Nanotechnology has been actively pursued in recent years in agriculture but the long-term evaluation of their impacts on crop growth, yield and quality is rather limited. Consequently, it is imperative to conduct the comprehensive study during all steps of the crop cycle, from sowing to harvesting stage in order to fill a major gap between existing laboratory research and the field applications. It is also critical to understand the internalization of NPs in plant tissues and their impact in the food chain by assessing the health promoting compounds.

Herein, an approach for utilization of plant extract and agro industrial byproducts has been developed to obtain environmentally benign nanomaterials and applied as nanopriming agent in onion and watermelon seeds. These treated seeds were examined for germination, emergence, growth, yield and the nutritional composition of the final produce of onion and watermelon.

1.1. Objectives

1) To determine the effect of green synthesized NPs in the seedling growth, yield, and quality of onion (*Allium cepa* L.)
2) To evaluate the growth promoting metabolites in nano treated onion seedlings using ^{1}H nuclear magnetic resonance and liquid chromatography coupled with mass spectrometry.
3) To assess the influence of NP treatments, growing locations and bulb size on flavonoids and amino acids content of onion.
4) To investigate the effect of NP mediated seed priming method on the germination, growth, yield, and quality of watermelons.
5) To determine the effect of nanoparticle treatments, storage period, and the growing environments on the nutritional composition of watermelons.
6) To assess the influence of post-harvest storage and growing environments on volatile compounds of triploid and diploid watermelons.

2. GREEN-SYNTHESIZED NANOPARTICLES ENHANCED SEEDLING GROWTH, YIELD, AND QUALITY OF ONION (*Allium cepa* L.)*

2.1. Introduction

Nanotechnology has the potential of revolutionizing the food and agricultural industries by enhancing crop productivity and quality.[9] Nanoparticles (NPs) can boost plant metabolism,[10] can enter into plant root and leaf cells, and can carry chemicals into these cells.Galbraith [11] NPs cause many physiological and metabolic changes in plants, depending on the chemical composition, surface area, size, reactivity, and dose of NPs used.[12]

One target point for NP use in enhancing crop performance is the seed germination and seedling growth. Seed germination and seedling emergence are critical factors that determine crop success and ultimately yields.[7] For rapid seed germination and uniform seedling emergence, seed priming is a commonly used method to imbibe water leading to the first stage of germination.[8] In nanopriming, NP suspension or emulsions were used as a priming media, for improving seed germination and growth. Nanoparticles penetrate the pores of seeds, spread inside, and activate phytohormones that stimulate growth.[12-13] Due to their small sizes, high surface area to volume ratio, and increased reactivity, NPs offer advantages over conventional priming methods.

The commonly used method for the synthesis of NPs is chemical reduction. Certain reducing agents, such as hydrazine hydrate and sodium borohydride used for the commercial synthesis of NPs are highly reactive toxic chemicals and pose risk to the environment and humans.[14-16] An alternative plant-based phytochemical was used as reducing agents for the green synthesis because of the environmentally benign process. Green synthesis of NPs is economical, biocompatible, and a promising approach compared with the NPs synthesized using toxic chemicals.[15] In order to prepare environmentally benign NPs, we used onion extract as a reducing agent for the preparation of silver NPs (AgNPs) and gold NPs (AuNPs). In the present study, we have used agro-food industrial byproducts for the green synthesis of NPs.

Turmeric is an important spice crop of the Zingiberaceae family and curcumin is the primary active compound. Curcumin is commercially produced using oleoresin of turmeric and the mother liquor (approximately 70–80% of the starting oleoresin) that remains after isolation of curcumin has no commercial value.[17] Therefore, this byproduct can be used for the formulation of turmeric oil nanoemulsion (TNE). Similarly, citrus peel and seeds are major byproducts from the citrus processing industry and these can be used in the formulation of citrus nanoemulsions (CNE). The waste from the citrus industry (peels, seeds, and pulp) represents about 50% of the raw materials.[18] These agro-food industrial byproducts can be potentially turned into value added nanobiomaterials to improve the agriculture production.

We hypothesized that the phytochemicals (phenolics, terpenoids, proteins, amino acids, polysaccharides, and flavonoids) present in plant extracts and agro-industrial byproducts could be effectively utilized as reducing agents for the synthesis of NPs. To the best of our knowledge, there are no reports on the use of TNE, CNE, AgNPs and AuNPs to enhance onion seed germination and productivity by maintaining the quality. A limited number of studies have

evaluated the effect of nanoparticles in plant from the seed germination stage to the final nutritional quality of the produce.[19-20] Therefore, we have investigated these treatments along with control treatments to determine their positive effects on growth, yield, and quality of onion for the first time.

2.2. Materials and methods

2.2.1. Materials

All solvents and chemicals used in this study were of analytical grade. Silver nitrate ($AgNO_3$), sodium tetracloroaurate ($NaAuCl_4$), and the surfactants polysorbate (Tween 20) and sorbitan monolaurate (Span 20) required for preparing silver and gold NPs and nanoemulsions, respectively, were procured from Sigma-Aldrich (Sigma-Aldrich, St. Louis, MO, USA). The curcumin-removed turmeric oleoresin (CRTO) was obtained from Sami Labs Limited, (Bangalore, India). Citrus fruits (*Citrus aurantium* L.) were received from the Texas A&M University Kingsville Citrus Center Orchard, Weslaco, TX. Nanopure water (NANOpure, Barnstead, Dubuque, IA, USA) and seeds extracted from these citrus fruits were used for the entire study.

For onions, seeds of variety Legend, which was developed at the Vegetable and Fruit Improvement Center at Texas A&M University were used in the experiment. 'Legend' is a variety bred from the 1015Y Texas Super-sweet onion, specifically for higher content of health-promoting compounds. To observe the effect of the nanoparticles on onion seed germination, naturally aged onion seeds were used, which were kept in cold storage for 10 years. These seeds were selected for their poor germination and slow post-germination growth.

2.2.2. Formulation of turmeric oil and citrus seed oil nanoemulsions

Nanoemulsions is a mixture of immiscible liquids in which one of the liquids is dispersed in the form of nano-scale droplets (20–300 nm).[21] Nanoemulsions are produced by high- or low-energy methods. As compared to high-energy approaches, there are some advantages using low-energy approaches such as effectiveness at producing smaller droplets, lower energy costs, and ease of implementation.[22] Owing to these advantages, in the current study, formation of nanoemulsion was carried out using a low energy method based on spontaneous emulsification as previously described, with some minor modifications.[22] In brief, in this spontaneous emulsification method, 2 mL oil (citrus or turmeric oil) and a lipophilic surfactant (25 mL) were mixed together and the mixture was poured into 75 mL of aqueous phase with overnight continuous stirring using magnetic stirrer at ambient temperature. The lipophilic phase was prepared by adding 250 mg of Span 20 in 25 mL of nanopure water followed by two hours of stirring on a magnetic stirrer. Similarly, the aqueous phase was prepared by adding 450 mg of Tween 20 in 75 mL of nanopure water with continuous stirring by a magnetic stirrer for two hours.

2.2.3. Green synthesis of silver and gold nanoparticles

Chopped onion bulbs (50 g) were boiled with 100 mL of nanopure water for 10 min, then filtered through Whatman filter paper 1 followed by a Chromafil A-45/25, 45 µm syringe filter (Macherey-Nagel Inc., Bethlehem, PA, USA) to obtain particle-free reducing agent. Silver nanoparticles (AgNPs) were prepared by treating 1 mL of freshly prepared onion extract in 10 mL of 0.01 M silver nitrate ($AgNO_3$) at 80 °C with continuous stirring using a magnetic stirrer to obtain dark reddish-brown color, indicating the formation of AgNPs. Gold nanoparticles (AuNPs) were also prepared by using onion extracts. During the synthesis of AuNPs, 1 mL of

onion juice was added to 19 mL of 0.001 M sodium tetrachloroaurate dihydrate ($NaAuCl_4$) at 90 °C with continuous stirring. Change of the yellowish color to a purple-red color indicates the conversion of gold to AuNPs.[23]

2.2.4. Characterization of nanoemulsions and nanoparticles

Mean particle size (PS), zeta potential (ZP), and polydispersity index (PDI) of the synthesized nanomaterials were measured using a dynamic light scattering technique through photon correlation spectroscopy (Malvern Zetasizer Nano-ZS model, Malvern, UK).[24] Samples were diluted 30-fold (by volume) using nanopure water to avoid multiple scattering effects. An average of three measurements per sample was analyzed and each measurement was an average of 13 runs. Data were reported as hydrodynamic diameter and considered as a mean particle size. Optical absorption measurements of prepared silver and gold NPs were carried out by ultraviolet-visible spectroscopy (UV-2900 Hitachi spectrophotometer) by diluting two-fold with nanopure water.

Similarly, the morphology of the NPs was captured through transmission electron microscopy (TEM) at 100 kV. The samples were deposited on a copper grid followed by drying for TEM. In order to fully understand and confirm the crystal structure and crystalline size of the NPs, X-ray diffraction (XRD) technique was used. The powder form of AgNPs and AuNPs were subjected to X-ray diffraction analysis (D8 Powder Eco) at 40 kV and 25 mA with Cu Kα radiation. The scan 2θ range was 10–80°.

2.2.5. Identification of phytochemicals coated in nanoparticles

The synthesized AgNPs and AuNPs (15 ml each) were centrifuged, decanted and rinsed with 10 ml of nanopure water. The rinsed nanopellet was mixed with 200µL of methanol. Samples were vortexed for 1 min and analyzed by 1290 Agilent rapid resolution LC system

(Agilent, Santa Clara, CA) to detect the phytochemicals involved as reducing agents in silver and gold NP synthesis. The separation was conducted on a Zorbax C18 column (1.8 µm, 50 × 2.1 mm) (Agilent, Santa Clara, USA) at 30 °C with a flow rate of 0.2 mL/min and 3 µL sample injection volume. Separation of the compound was achieved using a binary mobile phase consisting of (a) 0.1% formic acid in water and (b) methanol. A gradient program of 0% b (0–4 min), 80% b (4–12 min), and 100% b (12–17 min) and again 0% b (17-20 min) was used. Mass spectral analyses were carried out using the quadrupole time-of-flight mass spectrometry (ESI-Q-TOF-MS) (Bruker Daltonics, Billerica, MA, USA) equipped with an electrospray ionization source in positive ion mode according to the published paper.[25]

2.2.6. Seed priming treatments

Seed priming treatments included control, hydro priming, priming with turmeric oil nanoemulsion (TNE), citrus nanoemulsion (CNE), silver nanoparticles (AgNPs), and gold nanoparticles (AuNPs). TNE and CNE were diluted with nanopure water in a ratio (1:3). AgNPs and AuNPs were used at 31.3 ppm and 5.4 ppm, respectively. The concentration of gold and silver element in the priming solution was obtained from instrumental neutron activation analysis (INAA). The unprimed dried seeds and hydroprimed seeds were used as controls. Seeds were immersed in priming media for 12 h at ambient temperature, and the proportion of seed weight to priming solution was 1:5 g/mL.[8]

2.2.7. Assays for peroxidase activity

The peroxidase (POD) activity after the treatment of onion seeds was determined by the method of Jiang et. al.[26] with slight modifications. Approximately 200 mg of seed was weighed and ground to a fine powder in liquid nitrogen, homogenized in 1.8 ml of 50 mM potassium phosphate buffer (pH 7.0) and then centrifuged at 10,000 g for 10 min. POD activity was

determined in the Synergy™ HT Multi-Mode Microplate Reader (BioTek, Instruments, Winooski, VT) at 465 nm by using a 96-well flat bottom plate. The reaction mixture contained 125 µL potassium phosphate buffer (50 mM, pH 7.0), 25 µL 16 mM H_2O_2, 25 µL of 64 mM guaiacol, and 25 µL of enzyme extract. The amount of enzyme that cause an increase of 0.001 absorbance value per minute was defined as one unit of POD activity.

2.2.8. Quantification of internalized nanomaterials in onion seeds

2.2.8.1. Nanoemulsions

The nanoemulsion-treated seeds were washed with water three times to remove the adhering emulsion, then the seeds were crushed using a pestle and mortar. First, a known amount (100 mg) of TNE-treated sample was extracted twice with 0.6 mL hexane. Then the pooled extract was filtered and used for GC-MS analysis. The GC-MS analysis was carried out using a GC-MS (Thermo Fisher Scientific, Inc., San Jose, CA, USA) with a Dual-Stage Quadrupole (DSQ II) mass spectrometer equipped with an electron ionization (EI) source. A polar phase column Rtx-Wax (30 m X 0.25 mm i.d. 0.25 um film thickness; Restek Corporation, Bellefonte, PA, USA) was used for quantitation. Helium gas was used as a carrier gas with a flow rate of 1 mL/min. The initial oven temperature was maintained at 50 °C, then increased to 230 °C at a rate of 10 °C/min, then held for 5 min, with a total run time of 23 min. A sample volume of 2 µL was injected into the GC injector at 225 °C. Electron impact (EI) data from m/z 40 to 400 were acquired at a scanning speed of 16.67 scans/sec. The temperature of mass transfer line and ion source were maintained at 280 °C and 285 °C, respectively. Xcalibur software (v. 2.0.7., Thermo-Fisher Scientific, San Jose, CA, USA) was used to record and process the data.

For the citrus seed oil nanoemulsion, fatty acids were characterized by GC-MS after derivatizing to volatile methyl esters. The crushed seed material (100 mg) was extracted with

hexane as mentioned above and used for methylation with trimethylchlorosilane (Sigma, St. Louis, MO, USA). Fatty acid methyl esters (FAMEs) were produced by esterification of fatty acids in the presence of 100 μL trimethylchlorosilane in 1 mL methanol at 70 °C for 15 min. GC-MS was used to identify and quantify the volatiles and fatty acids present in the CNE. The GC-MS method for identifying FAMEs in CNE-treated seed consisted of an initial oven temperature of 80 °C, then the temperature was increased to 150 °C at a rate of 10 °C/min, held for 2 min and finally increased to 220 °C at a rate of 5 °C/min and again held for 2 min, with a total run time of 25 min. The rest of the mass spec conditions were the same as above. For both treatments, equivalent amounts of hydroprimed seeds were extracted and used as controls.

2.2.8.2. AgNPs and AuNPs in onion seeds

Mass fractions of Au and Ag were quantified by instrumental neutron activation analysis (INAA).[27] INAA measures the chemical elements in material and it involves converting a small number of atoms in a sample into radioactive atoms. In order to quantify the elements present in the onion seeds, three sets of treated samples were irradiated for 14 h. Following a 6-d decay interval, gamma-ray spectra were acquired for 0.5 h each using an HPGe detector. These spectra were used to quantify Au using the 411 keV gamma-ray peak from radioisotope ^{198}Au ($t_{1/2}$ = 2.6935 d). The second set of gamma-ray spectra were acquired for 1 h each following an 11-d decay interval. These spectra were used to quantify Ag using the mean values of three gamma-ray peaks (658 keV, 885 keV, and 1384 keV) from the radioisotope ^{110m}Ag ($t_{1/2}$ = 249.76 d). The NAA software package from Canberra Industries was used for the data reduction.

2.2.9. Observation of seed ultrastructure

Randomly selected AgNP and AuNP primed seeds were dissected, pre-fixed using Trump's fixative, and washed with Trump's buffer, then post-fixed with 1% osmium tetroxide.

After dehydration through a series of acetone concentrations, the specimens were infiltrated with Spurr's resin and polymerized for 24 h at 65 °C. Leica Ultracut UCT ultra-microtome was used to made ultrathin seed sections. TEM images were obtained using a JEOL 1200Ex transmission electron microscope (JEOL, Tokyo, Japan) at an accelerating voltage of 100 kV.

2.2.10. Influence of nanoemulsions and nanoparticles on onion seed emergence

The study was conducted in the greenhouse of the VFIC, Department of Horticultural Science, Texas A&M University in 2015–16 and 2016–17. To assess the effects of nanopriming on seed emergence (appearance of the cotyledon from the soil surface), treated and untreated onion seeds were sown in a greenhouse. The greenhouse experiment was laid out in a completely randomized design with four replications and six treatments including control, hydropriming, TNE priming, CNE priming, priming in AgNPs and AuNPs. The unprimed dried seeds and hydroprimed seeds were used as a control. Each replication included 200 seeds from each of the treatments. Observations of the total emerged onion seed were taken on the 6^{th} and 21^{st} days after sowing (DAS), respectively. Emergence percentage (EP) was calculated using the published equation.[28]

2.2.11. Effect of nanoparticles on onion production

In the first season (2015–16), 45-day-old onion seedlings were transplanted in the field of the Horticultural farm at Texas A&M University, College Station (30°36'N, 96°18'W). The experiment was performed in a randomized complete block design with three replications. Forty plants were transplanted per plot. The required soil moisture level was maintained by drip and manual irrigation in the field. Weeding and fertilization were conducted according to the needs of the crop. In the first year, plant height and leaf number were recorded for onions grown at College Station. To validate the effect of treatment, a multi-location field trial was conducted in

second year at three different production regions of Texas (Eastern, Central, and Lower Rio Grande Valley), i.e. College Station, Uvalde (29°12'N, 99°47'W), and Weslaco (26°15'N, 97°98'W). The second-year project was conducted during the fall season of 2016–17 and growth parameters such as plant height, leaf surface area, number of leaves, leaf diameter and neck diameter were observed in all three locations (Weslaco, Uvalde, and College Station). Length and leaf diameter are the good predictors of onion's leaf area.[29-30] Therefore, leaf surface area was measured in a non-destructive way calculating the cone surface area using longest leaf length and leaf diameter. Onion yield was calculated after the final harvest.

2.2.12. Influence of nanoparticles on quality parameters

2.2.12.1. Chlorophyll analysis

Chlorophyll *a* (Chl *a*) and chlorophyll *b* (Chl *b*) were determined according to a published method[31] with slight modifications. Onion leaves from all the treatments were collected from three locations at 75 days after transplanting (DAT). Onion leaf samples (5 g) were extracted with 10 mL of acetone in dark conditions. Extracted samples were vortexed for 1 min and sonicated for 30 min. Samples were centrifuged for 15 min at 4480 g and filtered. The residue was re-extracted twice with 5 mL and 3 mL of acetone. Both extracts were combined and used for the HPLC analysis according to our published method mentioned above.

2.2.12.2. Color measurement

A chroma meter was used for measurement of surface color and surface darkness/lightness and color intensity. Data output is in the form of L*, a*, and b* values. L* corresponds to levels of darkness/lightness between black and white. The a* value signifies the balance between red and green. Similarly, the b* values signifies the balance between yellow and blue.

2.2.12.3. Measurement of pungency, soluble solids, and sugars

After harvesting, onions were categorized into colossal (≥100 mm diameter), large (75–100 mm), medium (50–75 mm) and small (≤50 mm) size in the second year. Due to the production of fewer colossal onions, bulbs were categorized into large (>75 mm), medium (50–75 mm) and small (<50 mm) in the first year. The neck, basal plate, and skin of the different sized onion bulbs were removed. Pyruvic acid content in the onion juice was determined by an automated dinitrophenyl hydrazine method previously developed by our group.[32-34] Hand refractometer was used for the measurement of soluble solids content (SSC) in the juice and expressed as Brix. Sugar was measured by the method used in our earlier report.[35] The HPLC system with a autosampler, binary pump, refractive index detector (Perkin Elmer LC 200 Series, Norwalk, Conn., USA), and Rezex RNM-carbohydrate Na+ (8%), (300×7.8 mm) column was used for the quantitation of the sugar. A 20 μL injection volume was used and the column temperature was maintained at 90 °C. Nanopure water was used as a mobile phase with a flow rate of 0.5 mL/min. Standard curves of glucose, fructose, and sucrose were used to calculate the sugar concentration. Different size grade of onions from each treatment were analyzed separately.

2.2.13. Statistical analysis

Field experiments for all locations were planted as randomized complete block designs with three replications. Greenhouse experiments and all the lab experiments were carried out in a completely randomized design. Analysis of variance (ANOVA) of field data was carried out, using JMP pro 14 software. Excel software was used to prepare graphs and mean comparison was done by Student's *t*-test at 5% probability. The multivariate analysis was performed by using MetaboAnalyst 3.0 (http://www.metaboanalyst.ca/).

2.3. Results and discussions

2.3.1. Formulation and characterization of the nanoemulsions

The prepared nanoemulsions were optically opaque, homogeneous, and physically stable to gravitational separation. Dynamic light scattering was used to calculate the particle size (PS), polydispersity index (PDI), and zeta potential (ZP) for the characterization of nanoemulsions. The mean particle sizes recorded for TNE and CNE were 141.3 ± 1.69 nm and 139.8 ± 0.79 nm, respectively (Figure A1A–A1B). The PDI was 0.2 for both nanoemulsions. TNE and CNE had ZP values of -1.19 ± 0.05 mV and -1.74 ± 0.11 mV, respectively. The mobility and the uptake of NPs are affected with their coagulation or flocculation in the process of application.[36-37] The ZP provides information on the stability of the nanoparticle dispersion that can be used to predict the stability of the nanoparticulate dispersion.[23] The nanomaterials with low zeta potentials tend to coagulate or flocculate. Therefore, in our study, we used freshly prepared nanoemulsions for the seed treatment.

2.3.2. Green synthesis and characterization of the AgNPs and AuNPs

Reduction of metal ions to metal NPs can be visualized by color change. A reddish dark brown color was observed when Ag^{+} ions were reduced to AgNPs after addition of onion extract, indicating the reduction of Ag^{+} to Ag^{o}. Similarly, when onion extract was added to the gold salt solution, the reaction mixture color gradually changed from yellow to purple-red, indicating the formation of AuNPs.[38] The color change confirmed that the phytochemicals present in onion extract reduced the metal ions into metal NPs.

2.3.3. Characterization of nanoparticles

2.3.3.1. Dynamic light scattering

Dynamic light scattering was used to observe the size distribution of AgNPs and AuNPs coated with phytochemicals.[39] Onion phytochemicals (reducing agents) coated on AgNPs and AuNPs causes substantial change in the hydrodynamic radii of NPs. The PS values of AgNPs and AuNPs were 116.2 ± 2.40 nm and 93.68 ± 2.06 nm, respectively (Figure A1C–A1D), suggesting that onion phytochemicals (flavonoids, sugars) are capped on AgNPs and AuNPs. Similarly, droplet stability is significantly affected by the interfacial surface tensions present on emulsion droplets. In our study, PDI for AgNPs and AuNPs were observed to be 0.1. A negative ZP, -2.20 ± 0.29 mV and -8.51 ± 1.26 mV was recorded for AgNPs and AuNPs, respectively indicating less tendency for the particles to aggregate as compared to the nanoemulsions. The negative ZP value shown by biosynthesized AgNPs and AuNPs could be due to the bio-organic components present in the plant extract.

2.3.3.2. UV-Vis spectroscopy

In the UV-Vis spectrum (Figure A1E), a single broad resonance peak was observed between 410–450 nm, which confirmed the synthesis of AgNPs,[40] and a surface plasmon resonance (SPR) peak (Figure A1F) located between 500–580 nm confirmed the synthesis of AuNPs.[41]

2.3.3.3. TEM analysis

TEM provides information about the morphology, size, and dispersion of the nanoparticles. A TEM image (Figure 1A) of the AgNP sample showed that NPs exhibit typical spherical and ellipsoidal morphologies. The size range of AgNPs was 19–37 nm. Similar morphology and size were obtained in the AgNPs prepared using makrut lime (*Citrus hystrix*)

leaf extract.[42] Similarly, TEM results of AuNPs (Figure 1B) showed that nanoparticles are polydisperse with anisotropic morphology. TEM provides sizes of the metallic-gold cores.[23] Synthesized AuNPs are mostly spherical or near spherical. Some anisotropic larger particles with triangular shapes were also observed with the size range of 30–113 nm. The obtained AuNPs were highly dispersed and non-aggregated. Similar TEM images were acquired with AuNPs synthesized using cocoa extract[38] and the rhizome extract of galanga (*Alpinia galanga* L.).[43]

2.3.3.4. XRD analysis

Powder XRD was performed to understand the crystal structure of AgNPs and AuNPs. The AgNPs showed Bragg Reflection peaks at 38.2°, 44.4°, 64.7° and 77.5° in the 2θ range between 10° and 80°, which were assigned to (111), (200), (220), and (311) crystallographic planes of cubic silver.[44] The synthesized AgNPs are pure crystalline silver which was confirmed by the lack of additional diffraction peaks.[43] The peak corresponding to (111) plane is the predominant orientation as it is more intense than the other planes (Figure 1C). The average nanocrystallite size of AgNPs was calculated by Debye-Scherrer's equation[45] and was found to be 86.1 nm.

The crystalline nature of synthesized AuNPs was also confirmed by powder XRD (Figure 1D). The XRD image displays four prominent diffraction peaks at 2θ value of 38.1°, 44.3°, 64.5°, and 77.5° assigned to (111), (200), (220), and (311) Miller indices, respectively, which are characteristic of the face-centered cubic crystalline structure of metallic gold (JCPDS No. 040784).[45] Along with the gold phase, NaCl and KCl phase were also obtained. The NaCl and KCl phase resulted from the combination of sodium and potassium present in the onion extract, with the chloride ion provided by the gold salt. The presence of minerals (Na and K) in onion

extract were confirmed by inductive coupled plasma-atomic emission spectroscopy (ICP-AES). Similar NaCl phase was obtained in preparing the AuNPs using different forms of albumins.[46] The average crystallite size of synthesized AuNPs estimated by Debye-Scherrer formula was found to be 68.9 nm. The crystal structure is an important property in nanoparticles research, which can influence the behavior of the nanomaterials. The peak corresponding to (111) plane is more intense than the other planes, suggesting that (111) is the predominant orientation. Larger particles will have narrower and intense peaks. The NPs with lower size was always observed to have higher toxicity to the plant compared to larger NPs.[47] Therefore, the intense crystallographic plane indicated the higher crystallite size of nanoparticles resulting enhanced growth and yield of onion seeds.

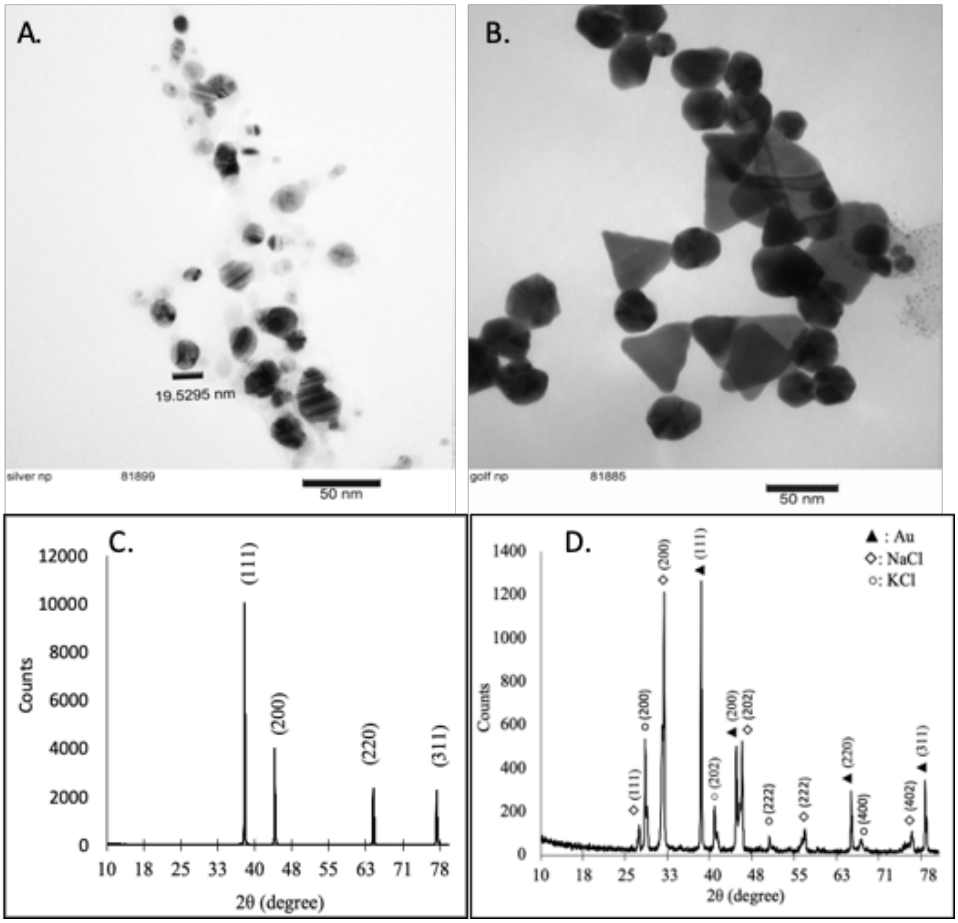

Figure 1 TEM images of (A) silver nanoparticles and (B) gold nanoparticles, X-ray diffraction pattern of (C) silver and (D) gold nanoparticles synthesized using onion extract.

2.3.4. Plausible mechanism of AgNPs and AuNPs formation using onion extract

The high-resolution mass spectrometry was used to identify the phytochemicals found in onion extract coated onto AgNPs and AuNPs. Figure 2 presents the results of 11 phytochemicals separated from onion extract, and from AgNPs and AuNPs. The mass tandem and +bbCID spectra of all the compounds are presented in Figure A2. Onion extract contains three major quercetin derivatives (quercetin 4'-glucoside, quercetin 7,4'-diglucoside, and quercetin 3,7,4'-triglucoside), two isorhamnetin glucosides (isorhamnetin 4'-glucoside and isorhamnetin 3,4'-diglucoside), free

proteinogenic amino acids (phenylalanine, tryptophan), γ-glutamyl peptides (γ-Glu-Leu, γ-Glu-Phe), and *S*-substituted cysteine derivatives (γ-Glu-Cys(2-CP)-Glyc; γ-Glu-Cys(Prop-1-enyl). Interestingly, all identified phytochemicals from onion extract were also found in AgNPs but only phenylalanine and γ-glutamyl derivatives were observed in the AuNPs.

These observations confirm that the synthesized NP were coated with onion phytochemicals. The absence of quercetin glucosides on AuNPs could be due to the formation of oxidation products during the reaction. Indeed, certain oxidative products were reported for the reaction of quercetin with $[AuCl_4]^-$.[48] Previous studies suggested that various functional groups like hydroxyl and carbonyl groups are present in flavonoids, which could play a dual role in reducing and capping metallic NPs.[49] It is possible that flavonoids reduce Au^{3+} ions into Au^0 NPs and prevent agglomeration to stabilize NPs in aqueous medium. Moreover, onions are rich in sugars which can have a significant role in metal nanoparticle synthesis.[50] Our mass spectrometry analysis showed various phytochemicals found in onion extract coated onto AgNPs and AuNPs surface. Phytochemicals like proteins, amino acids, phenolics, terpenoids, polysaccharides, and flavonoids could be responsible for the reduction of Ag^+ and Au^{3+} ions into AgNPs and AuNPs, respectively.

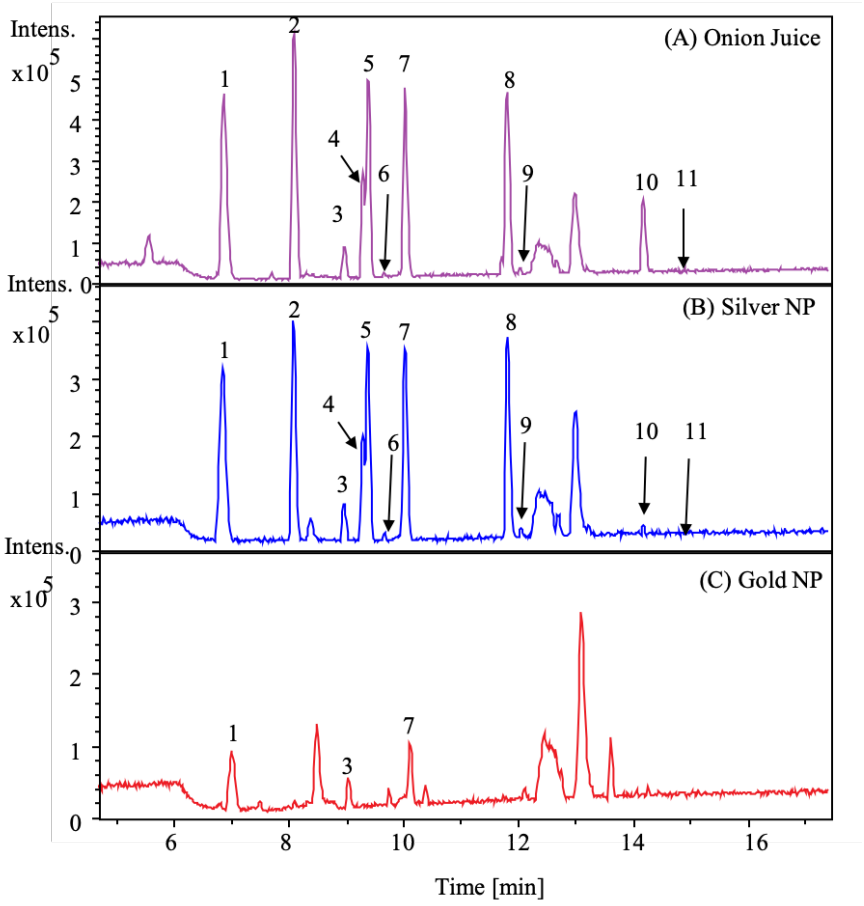

Figure 2 UPLC chromatograms of onion extract (A), silver (B) and gold NPs (C). Chromatograms were obtained from HR-ESI-QTOFMS analysis in positive ionization mode. Phytochemicals were identified by mass spectra as Peak- 1: phenylalanine; 2: γ-Glu-Cys(2-CP)-Glyc; 3: γ-Glu-Leu; 4: tryptophan; 5: γ-Glu-Cys(Prop-1-enyl); 6: quercetin 3,7,4′-triglucoside; 7: γ-Glu-Phe; 8: quercetin 7,4′-diglucoside; 9: isorhamnetin 3,4′-diglucoside; 10, quercetin 4-glucoside and 11: isorhamnetin 4′-glucoside. The presence of above peaks in NPs indicates that, nanoparticles were coated with certain phytochemicals present in the onion extract.

2.3.5. Internalization studies

2.3.5.1. Nanoemulsions

Internalization of the volatiles and fatty acids present in the TNE- and CNE-treated seeds, were determined by GC-MS and results are summarized in Table 1. Ar-turmerone is the major

compound present in the TNE and was used as a marker to understand TNE internalization into the onion seeds. The results showed that 418.49 ± 15.22 μg/g of the ar-turmerone was found in seeds treated with TNE, which was 7.61% of the ar-turmerone present in the TNE.

When seeds were treated with CNE, fatty acid methyl esters (palmitic, oleic, stearic, and linoleic acids methyl esters) were identified after methylation and were quantified based on the area of certified fatty acid methyl esters. Palmitic, oleic, stearic and linoleic acids were found in control (unprimed) onion seeds and were also reported in the literature.[51] Therefore, quantification of the fatty acids in the control seeds was done, and the control seeds had less fatty acids than the treated seeds, indicating that the fatty acids in the priming solution were internalized in the treated seeds. Our results demonstrated that 5.20% of linoleic acid, 4.61% of oleic acid, 2.25% of stearic acid, and 1.48% of palmitic acid in the CNE are internalized in the CNE-treated onion seeds.

2.3.5.2. Ag and Au nanoparticles

Internalization of silver (Ag) and gold (Au) NPs after AgNP and AuNP treatments, were determined by INAA and the results are summarized in Table 1. The concentration of Ag and Au was found to be 46.57 μg/g and 1.31 μg/g, respectively in AgNP- and AuNP-treated onion seeds. Moreover, these elements were present at trace or below the detection limit (40 ng/g for Ag and 0.4 ng/g for Au) levels in the unprimed and hydroprimed onion seeds. The concentration of Ag in the AgNP priming solution was 31.3 μg/ml and Au in the AuNP priming solution was 5.4 μg/ml. After 12 h of priming, the percentage of Ag and Au absorbed by the onion seeds was 29.75% and 4.86%, respectively. This result supported that Ag^{+} and Au^{3+} ions released from AgNPs and AuNPs penetrate the outer seed coat into seed tissues.

Table 1 Internalization of compounds in nanoparticle-treated onion seeds

Nanopriming solution	Compounds quantified	Compound internalized in seed (µg/g FW)	Compound internalized (%) in seed after nanopriming
TNE	Ar-Turmerone	418.49 ± 15.22	7.61
CNE	Palmitic acid Methyl ester	20047.50 ± 4072.52	1.48
	Stearic acid Methyl ester	8108.06 ± 2106.83	2.25
	Oleic acid Methyl ester	63579.86 ± 9587.56	4.61
	Linoleic acid Methyl ester	96707.87 ± 10749.75	5.20
AgNPs	Ag	46.56 ± 4.88	29.75
AuNPs	Au	1.31 ± 0.02	4.86

Values (µg/g FW) represent mean ± standard error of the mean (n = 3).
GC-MS was used to identify and quantify the major compound present in nanoemulsion-treated onion seeds. Silver and gold concentrations quantified by instrumental neutron activation analysis (INAA) after treating onion seeds with NPs.

These findings were also confirmed by TEM images of onion seeds (Figure 3) that showed AgNPs and AuNPs inside the embryo in the treated seeds. No particles were observed in the control unprimed onion seeds. Another study showed that AgNPs accumulated in maize (*Zea mays*) seeds after AgNP priming. [43] Transport of NPs into plant cells is influenced by characteristics of the NP, and the physiology of different plant species.[52] Since NP-treated seeds germinated and grew very well as compared to unprimed and hydroprimed seeds, AuNPs and AgNPs that accumulated in the seeds might have improved the imbibition process or activated certain metabolic events that enhanced seed germination.

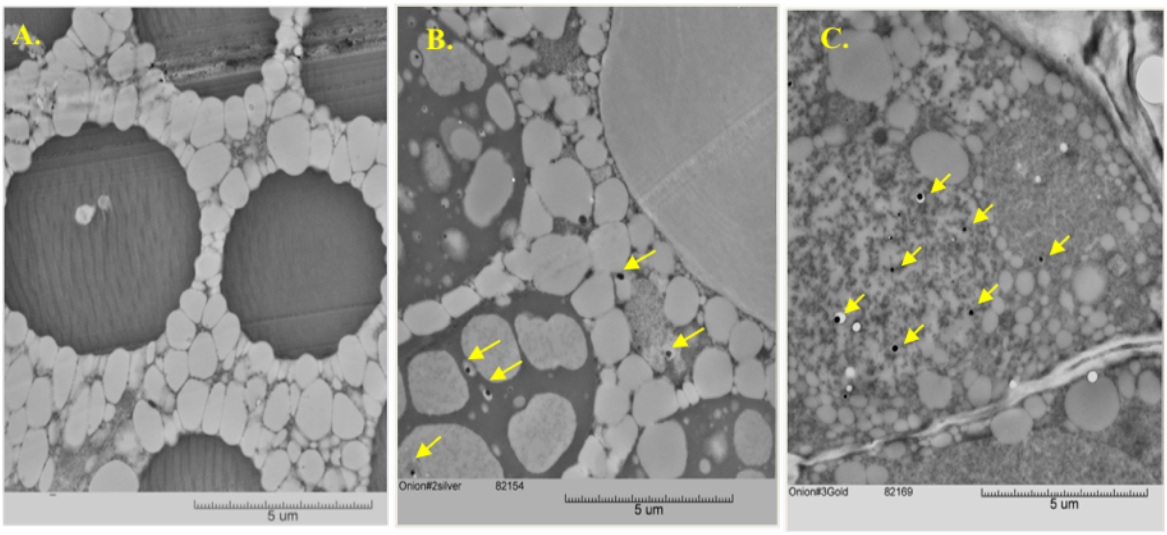

Figure 3 TEM images shows (A) unprimed, (B) AgNP-primed and (C) AuNP-primed onion seeds. Arrows indicate the AgNPs (B) and AuNPs (C) in onion seeds after 12 h of nanopriming.

2.3.6. Influence of green nanopriming on the emergence of onion seedlings

All NPs used in this study had a beneficial effect on seed emergence when evaluated at 6 and 21 DAS. The emergence percentage (Figure 4) was significantly higher in treated seeds as compared with unprimed and hydroprimed seeds in both years and on both observation dates ($p \leq 0.05$). At 6 DAS, the percent emergence was lowest in unprimed (T1) seeds in 2015–16 (38.55%) and 2016–17 (36.25%) followed by hydropriming (T2), although there was no significant difference between the two control treatments (Figure 4A). The same trend was observed at 21 DAS (Figure 4B). The seeds treated with AuNPs (T6) showed significantly earlier emergence ($p \leq 0.05$), in comparison to other treatments at 6 and 21 DAS in 2015–16. In 2016–17, all the treatments had significantly higher emergence percentage compared to the unprimed (T1) at 6 and 21 DAS, but there were no significant differences among the other

treatments. A combined analysis of both year data revealed significant differences in mean emergence percentage between the unprimed and NP treatments.

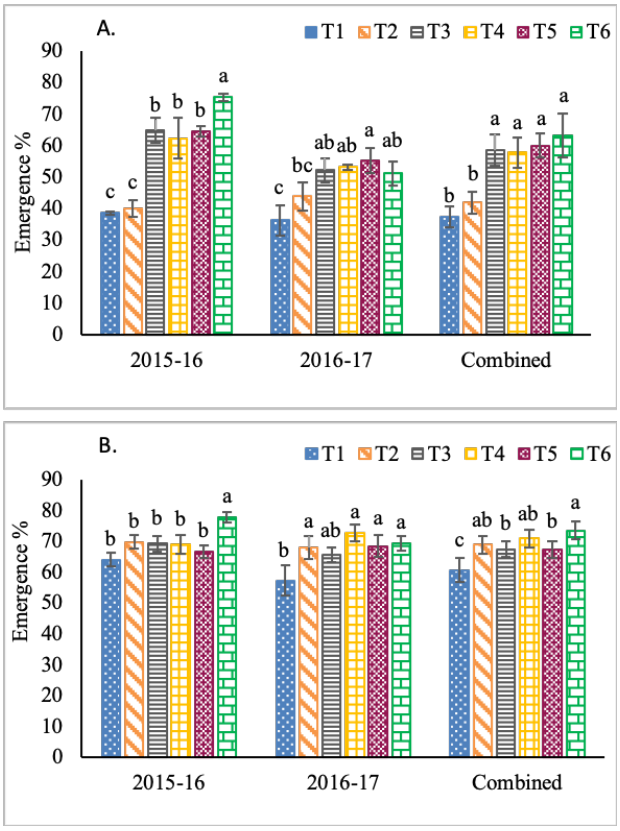

Figure 4 Effect of nanopriming on emergence percentage of onion at (A) 6 days after sowing (DAS) and (B) 21 DAS. T1: unprimed, T2: hydroprimed, T3: turmeric nanoemulsion, T4: citrus nanoemulsion, T5: silver nanoparticle, and T6: gold nanoparticle. Same letters above a bar indicate there was no significant difference at ($p \leq 0.05$) in between the treatments.

These results indicate that priming with NPs has a statistically significant effect on seedling emergence in onion seeds, as the best results in this study were obtained with AuNPs in repeated experiments. The beneficial effects of AuNPs on seed germination have been reported

in previous studies in maize,[43] *Gloriosa superba*,[53] and rice (*Oryza sativa* L.)[42] In onions, priming with polyethylene glycol has been reported to decrease the time for onion seedling emergence[54]. However, to the best of our knowledge, this is the first study to demonstrate the benefits of AuNPs on onion seed priming.

The onion seeds used in this study were 10 years old and characterized as showing poor germination and slow post-germination growth. In general, onion seeds have poor shelf life and tends to lose viability quickly under sub-tropical conditions. Some of the detrimental effects of aging are related with damages occurring at the membrane, nucleic acid, and protein levels.[55] Low enzyme activity, declines in the antioxidant potential of the cell, and retardation of biochemical and physiological reactions causes poor germination in aged vegetable seeds.[56] Slow seed germination can expose seedlings to adverse environmental conditions resulting in poor seedling vigor and ultimately economic losses for the growers. Seed priming can be utilized to reduce economic losses due to poor seedling emergence.

Nanopriming modulated antioxidant enzyme activity in seeds. Significantly higher activity of peroxidase (POD) was observed in the nanoprimed seeds as compared to the dry and hydroprimed seeds (Figure A3). There were no significant differences in between the NPs-treated seeds. POD is a primary antioxidant enzyme that catalyzes the conversion of H_2O_2 to H_2O.[26] Interestingly, the increase in POD activity coincides with the rapid seed germination which suggested that there is connection between the seed germination and POD activity.[42] Priming improves water uptake in seed since primed seeds exhibited faster imbibition and causes production of reactive oxygen species (ROS) in oxidative window range to stimulate germination and seedling growth.[43, 57] ROS react with plant polyphenols causing loosening of cell wall, which is vital for cell growth.[58] Thus seed priming with NPs at optimized concentrations might mediate

production of ROS, In this study also, onion seedlings (Figure 5A–5B) demonstrated a beneficial growth effect of all the NP treatments as compared to control treatments (unprimed and hydroprimed).

In a previous seed priming study using AgNPs in rice, the authors hypothesized that NPs penetrate the seed coat by creating new pores and up-regulate aquaporin genes; this facilitates water and H_2O_2 diffusion into cells, resulting in higher seedling emergence.[42] Similarly, the authors observed increased α amylase activity in AgNP-treated rice seedlings; this activity enhanced the starch metabolism required for seedling growth.[42] We believe that priming onion seeds with nanoemulsions and metal NPs might result in a similar phenomenon, resulting in higher onion seed germination compared to unprimed in the present study.

Significant enhancement of soybean growth was recorded in plants treated with thymol nanoemulsion[59] as a result of the antibacterial properties of thymol. In our study, ar-turmerone is the major compound found in the byproduct from curcumin manufacture and this compound has been found to have antibacterial[17] and antifungal properties.[60] Nanoscale ar-turmerone could be a potential plant growth-promoting agent, causing higher seed germination compared to the controls.

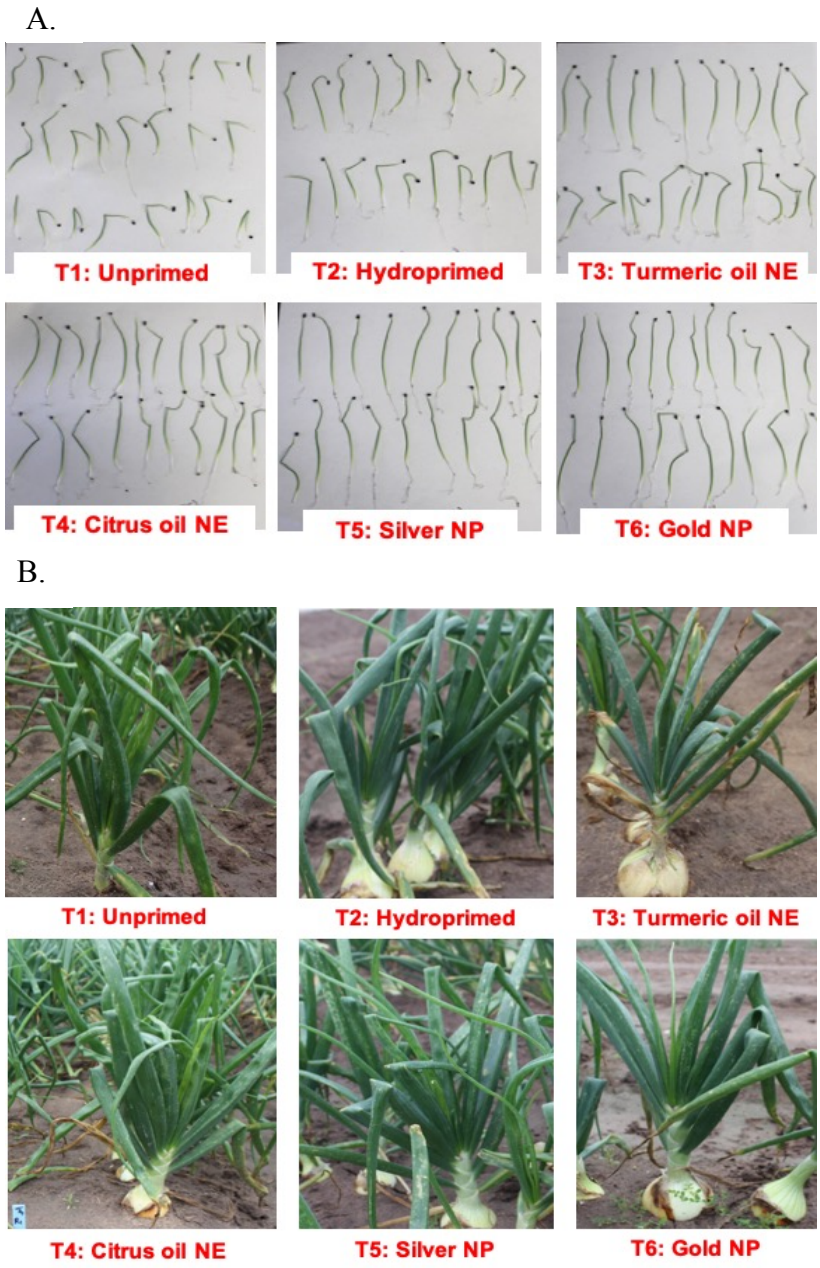

Figure 5 Onion plants at (A) 10 days after sowing in the greenhouse study and (B) 100 days after transplanting in the field study.

In our study, the citrus nanoemulsion was prepared with a very low dose of citrus seed oil. Lipids when exogenously applied, cause changes in ROS levels in plants. Lipid treatment

can be beneficial to the plant, stimulating the release of optimum amounts of ROS and resulting in improved germination and development. Several studies have reported the beneficial effects of exogenous lipid application in seed germination.[61-62] For example, the germination percentage of fatty acid-treated alder tree seed (*Alnus glutinosa*) at 35 °C and cotton seed (*Gossypium hirsutum* Pima S-5) at 14 °C were significantly higher than control.[61-62] A low concentration of the saturated fatty acid myristic acid improved germination rate and increased seedling growth in *Brassica napus*.[63] At higher concentrations of fatty acids, the ROS level was significantly higher leading to oxidative stress and therefore causing a decrease in germination percentage. The higher germination percentages compared to the control observed for the nanoemulsion-treated seeds in our study might be due to the release of ROS at optimum levels.

2.3.7. Green nanopriming enhanced onion growth and yield

Growth parameters are a measure of the overall health of plants. To understand the effect of green nanopriming on physiology and growth, we measured traits such as plant height and number of leaves in plants grown at College Station in 2015–16 (Figure A4). Additionally, leaf length, leaf diameter, leaf surface area, and neck diameter were measured at 75 DAT (Figure A5) and 100 DAT (Figure A6) in onions grown at Weslaco, Uvalde and College Station in 2016–17 and the results are summarized in Table 2. The measurements taken at 75 DAT are representative of early physiological growth (pre-bulb growth stage) whereas those taken at 100 DAT are representative of the bulb initiation stage. All the statistical analysis and treatment mean comparisons were done at 5% probability.

Table 2 Summary of growth parameters for different treatments that were significantly different from controls

Growth parameters	2015–16		2016–17					
	College Station		Weslaco		Uvalde		College Station	
	75 DAT	100 DAT	75 DAT	100 DAT	75 DAT	100 DAT	75 DAT	100 DAT
Plant height	T5, T6	T5	T4, T6	NS	T6	T6	NS	NS
Number of leaves	T5, T6	T6	T3, T4, T6	T3, T4, T6	T6	T4, T5, T6	NS	NS
Leaf length			T4, T6	NS	T6	T6	NS	NS
Leaf diameter			T6	T3, T4, T6	T6	T4, T5, T6	T6	NS
Neck diameter			T3, T4, T6	T6	T6	T4, T6	T6	NS
Leaf surface area			T4, T6	T3, T4, T6	T6	T6	T6	NS

T1: unprimed, T2: hydroprimed, T3: turmeric nanoemulsion, T4: citrus nanoemulsion, T5: silver nanoparticle, T6: gold nanoparticle. Controls are (T1) unprimed and (T2) hydroprimed. First year, only plant height and number of leaves were recorded. NS: Not significant; DAT: Days after transplanting.

We observed a beneficial effect of all the NP treatments as compared to control treatments (unprimed and hydroprimed) across locations and at both observation dates. During the first year, AgNPs (T5) and AuNPs (T6) had significantly increased plant height and numbers of leaves compared to plants from unprimed and hydroprimed seeds at 75 DAT in College Station. At 75 DAT, in the second year, only AuNPs (T6) had significantly enhanced effects compared to control treatment groups in Uvalde and College Station whereas in Weslaco, priming with TNE (T3) and CNE (T4) also appear to have beneficial effects on some growth parameters. At 75 DAT, AuNPs

(T6) had a significant effect on almost all the growth parameters recorded across all locations and years.

The effect of NP treatment on growth parameters was not significantly different from control at College Station (2016–17) at 100 DAT whereas significant differences were observed between the treatments in Uvalde (2016–17), Weslaco (2016–17), and College Station (2015–16). At 100 DAT, the effect of AuNPs (T6) was significantly stronger than that of the other treatments in almost all cases. We observed that onions grown at Weslaco had enhanced growth performance followed by Uvalde and College Station. This differential effect on growth parameters among the three locations could be due to environmental factors such as weather conditions, soil type (Table A1 and A2), water availability, etc. However, in all the three research locations, among NP/nanoemulsion treatments, when onion seeds were soaked in AuNPs, stronger positive effects were observed on onion growth parameters.

Similarly, significantly higher yield was observed in AuNP treated onion in Weslaco (86,946 lb/acre) and Uvalde (116,259 lb/acre) as compared to the control which was 56,639 lb/acre in Weslaco and 101,602 lb/acre in Uvalde (Figure 6). The effect of treatment on the yield of onion bulbs was not significant ($p \leq 0.05$) in College Station, 2015–16. Due to severe weather conditions (Table A1) survival rate was very poor, and onions could not be harvested from all the blocks in College Station during 2016–17. Among the three locations, we observed higher onion bulb yield in Uvalde followed by Weslaco and College Station (Figure 6). In a combined analysis of both years, the yield of AuNP-treated onions was higher by 14.1% and 23.9% compared to the hydroprimed and unprimed onions, respectively.

Our results with AuNPs in onion are consistent with previous work. [53, 64-65] For example, AuNPs improved the germination index, number of leaves, node elongation, and seed yield in the

medicinal plant *Gloriosa superba*.[53] Earlier, Kumar *et al.*[64] reported that AuNPs enhanced water uptake capacity of seeds resulting higher seed germination, vegetative growth, and seed yield in *Arabidopsis thaliana.* These researchers also highlighted the improved free radical scavenging potential, due to increased enzyme activity in AuNP-treated plants. Similarly, various growth and yield related parameters were positively affected by AuNP treatment in *Brassica juncea*.[65] In AuNP-treated seedlings, decreased levels of microRNAs (miR 398, miR408, miR164, miR167) and enhanced levels of miR169 were reported; these altered microRNAs are correlated with the improved germination, growth and yield.[64] Thus, AuNP priming could be a broadly useful alternative method for promoting plant growth and yield.

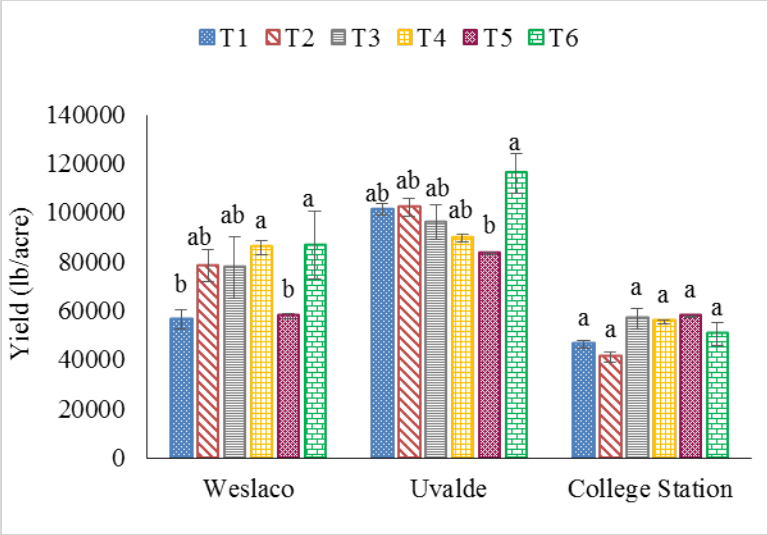

Figure 6 Effect of nanopriming on yield of onion bulbs grown in Weslaco (2016–17), Uvalde (2016–17) and College Station (2015–16). Due to bad weather conditions, no yield data could be measured from the fields in College Station (2016–17). Weather data are given in Table A1. T1: unprimed, T2: hydroprimed, T3: turmeric nanoemulsion, T4: citrus nanoemulsion, T5: silver nanoparticle, and T6: gold nanoparticle. Mean comparison is in between the treatments for each location. Same letters above a bar indicate there was no significant difference ($p \leq 0.05$).

2.3.8. Positive impact of green nanopriming on physiology and quality of onions

2.3.8.1. Chlorophyll level

Studies on the interactions between chlorophyll and NPs are critical for understanding the photo-physical behavior of plants exposed to NPs.[66] Chl *a* and Chl *b* were significantly higher in the CNE-, AgNP- and AuNP-treated plants compared to the unprimed and the hydroprimed treated onion plants grown at College Station, 2015–16 (Figure 7). The Chl *a* and Chl *b* contents of onion leaves grown at all three locations (Weslaco, Uvalde and College Station) during 2016–17 are summarized in Figure 8A and 8B, respectively. Chl *a* was higher in AuNP-treated samples in Weslaco and Uvalde (2016–17). However, Chl *b* was higher in CNE-treated samples, but was not significantly different from AuNP-treated samples. All the primed onions gave higher Chl *a* and *b* in College Station samples (2016–17) compared to unprimed. Previous studies have reported positive effects of metal NPs on the photosynthetic system.[67] It has been reported that AuNP treatment induces higher chlorophyll contents in *Brassica juncea*[65] and wheat[68] leading to an increase in the total photosynthate produced. Increased absorbance and fluorescence quenching were found at increased AuNP concentrations.[66] Metal NPs can increase the efficiency of chemical energy production and the improvement mechanisms may act as an artificial light-harvesting system.[67]

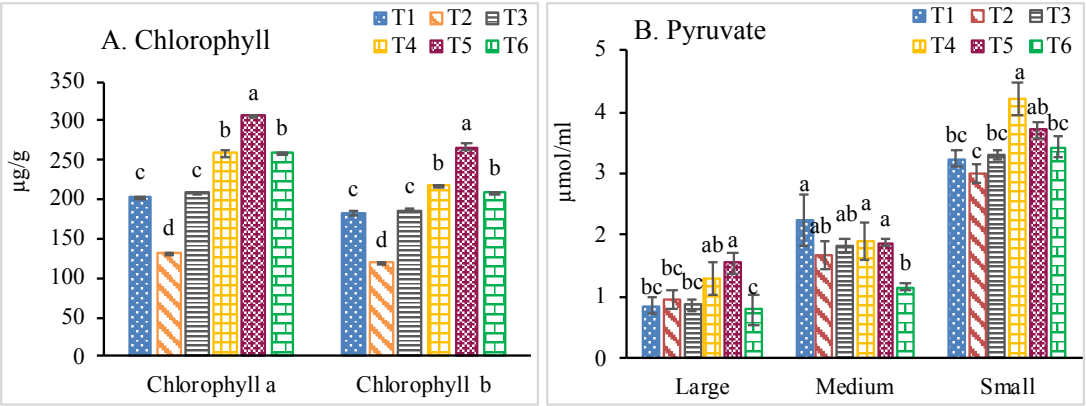

Figure 7 Effect of nanopriming on (A) Chlorophyll and (B) Pyruvate level of large (>100 mm), medium (50 to 75 mm) and small (<50 mm) size onions grown at College Station, 2015–16. T1: unprimed, T2: hydroprimed, T3: turmeric nanoemulsion, T4: citrus nanoemulsion, T5: silver nanoparticle, and T6: gold nanoparticle. Same letters above a bar indicate there was no significant difference ($p \leq 0.05$).

2.3.8.2. Pungency of onions

The irritating lachrymatory factor propanthial S-oxide released by onions when chopped is due to the presence of alliinase, 1-propenyl L-cysteine sulphoxide (PRENCSO), and lachrymatory factor synthase.[69-70] The commonly accepted method to measure the pungency level is by quantifying the pyruvic acid content of the onion.[34] According to the National Onion Association, the most common sizes sold in the U.S. retail shops are medium sized, 2 to 3.75 inches in diameter. A separate analysis of the pyruvate level of different sized onions was conducted for all three locations in 2016–17 (Weslaco, Uvalde and College Station) and one location in 2015–16 (College Station). Consumer preferred onions with low pungent sensation, which positively correlated to lower pyruvate concentrations. Data from College Station (2015–16) showed lower pyruvate levels in large and medium sized onions treated with AuNPs as compared to the unprimed (Figure 7).

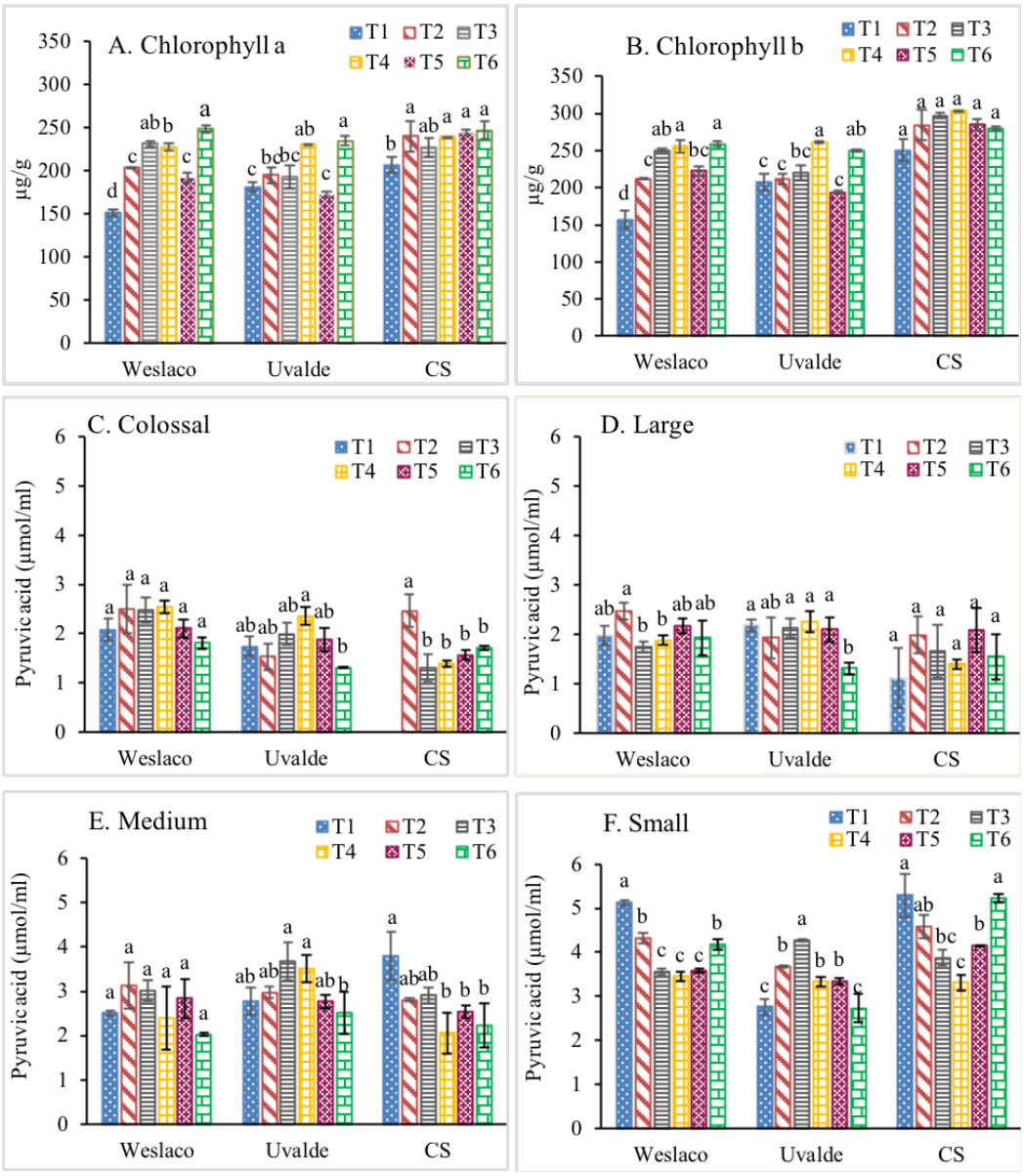

Figure 8 Effect of nanopriming on (A) chlorophyll a, (B) chlorophyll b, and (C) pyruvate level of colossal (>100 mm), (D) large (75 to 100 mm), (E) medium (50 to 75 mm) and (F) small (<50 mm) size onions grown at Weslaco, Uvalde, and College Station (2016–17). T1: unprimed, T2: hydroprimed, T3: turmeric nanoemulsion, T4: citrus nanoemulsion, T5: silver nanoparticle, and T6: gold nanoparticle. Mean comparison is in between the treatments for each location. Same letters above a bar indicate there was no significant difference ($p \leq 0.05$).

In the second year (2016–17), the pungency level was relatively lower in AuNP-treated onion plants grown in Uvalde for colossal, large, and medium sized bulbs compared to the control (Figure 8C, 8D, and 8E). However, no significant difference in the pyruvate level was observed in between AuNP-treated and unprimed onions of colossal, large and medium size grown in Weslaco. All primed small sized onions grown at Weslaco had significantly less pyruvate compared to the control (Figure 8F). No colossal sized onions were harvested in College Station and compared to hydroprimed all the treated onions had significantly lower pyruvate levels. The CNE-, AgNP-, and AuNP-treated medium size onions grown at College Station had significantly lower pyruvate levels. The pungency of the different size onions in all treatments ranged between 0.8 and 5.29 μmol/mL, which is similar to reported values.[35, 70]

In both years and all the locations, AuNP-treated medium sized onions were found to be relatively less pungent compared to the unprimed onions. AuNPs might alter the level of PRENCSO, allinase, or lachrymatory factor synthase resulting in the change in pungency level. Partial least squares discriminant analysis (PLS-DA) was conducted for pyruvate levels in different sized onions from all three locations including six treatments. The first principle component (PC1) explained 75.4% of the variance and the second components (PC2) explained 10.8% of the variance (Figure 9A). In all treatments and locations, pungency levels declined as bulb size increased. A reduced pungency levels in larger bulbs might be caused by the dilution effect. Similar results have been obtained in the previous studies.[70]

2.3.8.3. Sugar content

The overall onion flavor is determined by the ratio of sugar to pungency.[71] PLS-DA was also conducted for sugar content in onion. Data from all three locations, six treatments, and four size categories were used as observation and the sucrose, glucose, and fructose content of onions

were used as variables. PC1 explained 82.2% of the variance and PC2 explained the remaining 17.4% of the variance (Figure 9B). PC1 appeared to be providing the linear contrast between sucrose, and glucose and fructose combined while PC2 offered no clear contrast between observations. A scatterplot of PC1 and PC2 was plotted, and the data points were color coded according to location. Three distinct clusters of observations are visible in the scatter plot, which indicates that location-specific differences exist in sugar content of onions in this experiment. However, no trend was found in sugar content as influenced by the nanopriming treatments and the bulb size. Similarly, no linear relationships between the total sugar contents and pungency level were observed. Previous studies have also reported insignificant correlations between pyruvic acid concentration and sugar level in onions.[35]

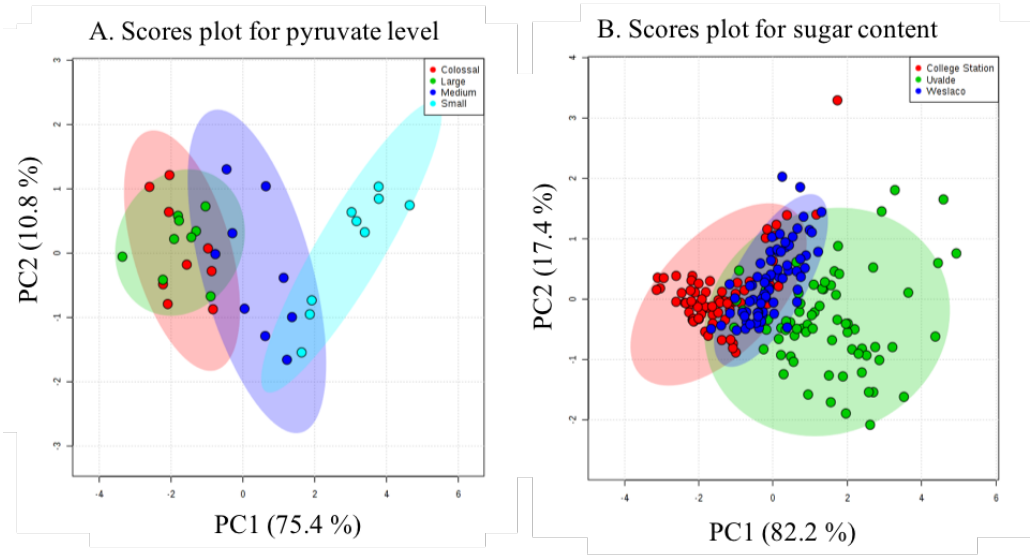

Figure 9 Partial least squares discriminant analysis (PLS-DA) scores plot for (A) pyruvate level of colossal (>100 mm), large (75 to 100 mm), medium (50 to 75 mm) and small (<50 mm) sized onions (B) sugar content of onions grown at three different locations of Texas (Weslaco, Uvalde and College Station) in 2016–17.

2.4. Conclusions

In the present study, environmentally friendly synthesized NPs used were prepared from plant extracts and characterized. Based on TEM and INAA results, it was confirmed that AgNPs and AuNPs can internalize into the seed and improve water uptake resulting better germination and growth. All the nanopriming treatments exhibited positive effects compared to the unprimed onion seeds. Among all the treatments, applying AuNPs as priming agent at low concentrations (5.4 ppm) resulted in enhancement of germination, plant height, leaf length, leaf diameter, neck diameter, and leaf surface area at both early and later plant development stages without toxicity symptoms. The average yield of AuNP-treated onions from all the locations was increased by 23.9% compared to unprimed onions. Increased chlorophyll content in the leaves and reduced pungency level in the bulbs were evident in the AuNP treatment compared to the unprimed and hydroprimed. Although AgNPs gave good results in seed germination, that treatment was not equivalent to AuNPs for growth, yield, and quality of onion. Moreover, AuNPs worked at low concentrations and did not need to be applied to the soil; preventing the large dispersal of NPs into the ecosystem. Results of our studies presented a new green method for the production and use of nanoparticles paving the way for excellent opportunities for their application in onion production. Therefore, green nanopriming could be further used as an emerging technique for sustainable agriculture.

3. ^{1}H NUCLEAR MAGNETIC RESONANCE AND LIQUID CHROMATOGRAPHY COUPLED WITH MASS SPECTROMETRY-BASED METABOLOMICS REVEAL ENHANCEMENT OF GROWTH-PROMOTING METABOLITES IN ONION SEEDLINGS TREATED WITH GREEN-SYNTHESIZED NANOMATERIALS*

3.1. Introduction

Seed germination is a key stage in the plant's life cycle and rapid, synchronous germination followed by establishment of vigorous seedlings, is crucially important for agriculture.[72] Germination begins with the absorption of water by the dry seed, followed by embryo expansion, and ends with the radicle breaking through the seed coat.[73] This process is characterized by a transition from a quiescent to a metabolically active state and involves catabolic and anabolic processes.[74] The next step, seedling establishment, involves mobilization of reserves accumulated during seed development and activation of metabolic and developmental processes during the seed-to-seedling transition.[72]

Seed dormancy and germination are regulated by several plant hormones[75] and growth regulators.[76] Gibberellins (GA) breaks dormancy, promotes germination, and stimulates stem elongation and leaf expansion.[77] GAs promote germination by negatively regulating abscisic acid (ABA) levels.[78] ABA is a universal sesquiterpenoid plant hormone and an essential repressor of seed germination.[78-79] Indole 3-acetic acid (IAA) is the most common auxin in plants, that regulates plant growth and development, and also functions in stress resistance.[77] Jasmonic acid

---

(JA), its precursor *cis*(+)-12-oxophytodienoic acid (OPDA), and associated metabolites, including methyl jasmonate (MeJA) and jasmonic acid isoleucine (JA-Ile) are all involved in mediating the response to biotic as well as abiotic stimuli.[80]

Responses to hormonal signals in the endosperm and embryo influence the rate of seed germination.[73] Moreover, plant hormones interact and hence the production of each might depend on the production of the others.[73] In addition, the endogenous concentrations of a hormone are controlled by the balance between biosynthesis and deactivation and regulate plant physiological responses.[72] Therefore, profiling of all hormones and their metabolites is imperative to understand the regulatory networks of hormone metabolism.[75] Since the physiological actions of a hormone depend on its endogenous concentrations, it is critical to determine the precise level of endogenous hormones.[75] Among the various technologies used for primary plant metabolite profiling, ^{1}H nuclear magnetic resonance (NMR) and liquid chromatography coupled with mass spectrometry (LC-MS) proved to be robust methodologies.[81]

In recent years, nanotechnology has the potential to play an important role in enhancement of seed germination and seedling establishment.[82-84] Nanoparticles (NPs) have been highly studied due to their extremely small size and large surface area to volume ratio, which contribute to their unique physical and chemical properties compared to bulk materials of an identical chemical composition.[2, 85-86] Different studies demonstrated the internalization of NPs into seeds, and activation of phytohormones that stimulate seed germination and growth.[83, 87] However, most growers and commercial industries are reluctant to use the nanotechnology in agriculture owing to the use of toxic chemical reducing agents and cost for escalating the production of nanomaterials.[88] This demands the application of green synthesized nanomaterials using plant extracts which are environmentally benign and economically viable for mass

production. Similarly, plant physiology affects the interaction with nanoparticles, so results observed in a crop are not necessarily valid for another one which makes imperative to conduct studies in different crop species.

In this present study, plant-based phytochemicals were used for the synthesis of NPs, which are sustainable alternative to chemical synthesis methods as they are of low cost, fast, efficient, and generally lead to the formation of crystalline NPs.[89] In the present study, onion water extract was used as reducing agent for the preparation of silver and gold NPs. Furthermore, agro-industrial byproducts were also used for the synthesis of turmeric nanoemulsion (TNE) and citrus oil nanoemulsion (CNE) using a low-energy method.[83] The rising market for curcumin generates byproducts with no commercial value, as approximately 40% of the oil remains in the mother liquor after isolation of curcumin from oleoresin; we used this curcumin-depleted turmeric oleoresin for formulation of TNE.[17, 90-91] Similarly, citrus seeds and peels are byproducts from the citrus processing industry and we used these in the formulation of CNE.[92-93] About 19% of total citrus fruits in the world and 48% of the total United States citrus production are used in the processed fruit market.[94] The waste from this industry, such as peels, seeds, and pulp, represents about 50% of the raw processed fruit[78] and generates 11,769,450 tons of byproduct in the world and 1,880,000 tons in the USA. The phytochemicals present in these agro-industrial byproducts were used for the formation of nanomaterials, which were applied as priming agents to enhance onion seed germination.

We recently demonstrated that nanopriming at relatively low doses can penetrate onion seed coats, stimulate germination, and enhance growth, yield, and quality of onion.[83] Increasing use of nanomaterials in agriculture makes it imperative to understand their effects on plant physiology. However, the data about potential phytotoxicity, metabolite profiles, and

physiological effects of nanomaterials on seed germination remain limited. Metabolomics can be used to better understand the effects of nanomaterials. We hypothesized that the enhancement of seed germination and seedling growth are associated with signature metabolite profiles. Distinct and time-dependent changes in plant hormone levels are to be expected and hormonal profiling will provide a comprehensive picture of these changes. The present study investigated the effect of seed priming with different nanomaterials on seedling growth and hormonal profiles of onion. Our results highlight the dynamics of metabolism across developmental stages during the seed-to-seedling transition in onions. To our knowledge, this is the first study that examines the effect of green-synthesized nanomaterials on endogenous hormones of onion seeds and seedlings.

3.2. Materials and methods

3.2.1. Chemicals and Materials

All solvents and chemicals used in this study were of analytical grade. Standards for phytohormones (IAA, ABA, ZA, GA, JA, and JA-Ile), and γ-aminobutyric acid (GABA) were procured from Sigma-Aldrich Chemical Co (St. Louis, MO, USA). OPDA was purchased from Cayman Chemical (Ann Arbor, MI, USA). Two cultivars of onion seeds, Legend and the pink root-resistant cultivar 50147 were obtained from Prof. Kevin Crosby at Texas A&M University. In order to see the effect of the NPs on onion seed germination and hormonal changes, naturally aged onion seeds were used, which were kept in cold storage for 10 years. These seeds were selected for their poor germination and slow post-germination growth.

3.2.2. Green synthesis of nanomaterials and their characterization

In the present study, all the nanomaterials used were synthesized and characterized adapting a protocol we developed in our laboratory.[82-83] Briefly, silver nanoparticles (AgNPs) and gold nanoparticles (AuNPs) were synthesized using a green process involving the use of

onion extracts as reducing agents. Chopped onion bulb (50 g) was boiled with 100 mL of nanopure water for 10 min, then passed through Whatman filter paper grade 1. AgNPs were prepared by treating 1 mL of freshly prepared onion water extract in 10 mL of 0.01 M silver nitrate ($AgNO_3$) at 80 °C with continuous stirring using a magnetic stirrer to obtain dark reddish-brown color. Similarly, during the synthesis of AuNPs, 1 mL of onion extract was added to 19 mL of 0.001 M sodium tetrachloroaurate dihydrate ($NaAuCl_4$) at 90 °C with continuous stirring to obtain a purple-red color. Further, NPs were characterized by UV-Vis spectrophotometry, dynamic light scattering, transmission electron microscopy (TEM), X-ray diffraction (XRD), and LC-MS. [82-83]

Additionally, two nanoemulsions were prepared from turmeric and citrus byproducts using a low-energy method based on spontaneous emulsification. The prepared nanoemulsions were characterized by using dynamic light scattering technique, according to our published protocol.[24, 82, 95-96] In this spontaneous emulsification method, 2 mL oil (citrus or turmeric oil) and a 1% lipophilic surfactant (25 mL) were mixed together and the mixture was poured into 75 mL of aqueous phase (0.5%) with overnight continuous stirring at ambient temperature. The lipophilic phase was prepared by adding 125 mg of Span 20 in 25 mL of nanopure water followed by 2h of stirring on a magnetic stirrer. Similarly, the aqueous phase was prepared by adding 450 mg of Tween 20 in 75 mL of nanopure water with continuous stirring by a magnetic stirrer for 2h.

3.2.3. Pre-sowing seed treatments

Seed priming treatments, the concentrations of priming solutions, and the priming duration were similar to the conditions in our published protocol.[83] Briefly, priming treatments included water (hydropriming), TNE, CNE, and priming with suspensions of AgNPs and AuNPs.

TNE and CNE were diluted with nanopure water in a ratio (1:3) and used as a priming solution. Similarly, AgNPs and AuNPs were used at 31.3 ppm and 5.4 ppm, respectively. The concentrations of gold and silver element in the priming solution were obtained from instrumental neutron activation analysis (INAA). The unprimed dried seeds and hydroprimed seeds were used as controls. Seeds were immersed in priming media for 12 h at a room temperature at a ratio of 1 g of seed per 5 mL of medium. Seeds were dried at ambient temperature after rinsing a couple of times with nanopure water.

3.2.4. Incubator study for seed samples to measure plant hormones

The incubator study was conducted in darkness at 25 °C using Legend and 50147 onion seeds with six treatments: unprimed seeds, hydroprimed seeds, and seeds primed with TNE, CNE, AgNPs, and AuNPs. Seeds of uniform size were placed in 100 x 15 mm petri dishes with 100 seeds per dish and each test was replicated three times. Initially, 10 mL distilled water was added to each petri dish to moisten the sterile germination paper. Two mL of distilled water was added on alternate days to all petri dishes to prevent drying. Radicle emergence to 2 mm or more was scored as germination and was recorded at 24 h intervals for 3 days. Every 24 h, seed samples were collected for plant hormone measurements.

3.2.5. Seedling development in the greenhouse for emergence and metabolites study

Emergence tests were conducted using two cultivars of onion seeds (Legend and 50147). For emergence tests, seeds with different treatments were sown in the greenhouse. Seeds of each treatment were individually sown in 200-cell plastic trays with three replications containing a professional growing mix (Sun Gro Horticulture Inc, Agawam, MA, USA) composed of fine sphagnum peat moss, vermiculite, dolomitic limestone, and wetting agent. A seed was considered emerged when the cotyledons rose completely above the medium. Trays were thoroughly

moistened and moisture levels were maintained throughout the experiment. Onion seedlings were harvested on a weekly basis for 3 weeks (7, 14 and 21 days after sowing). The harvested seedlings were immediately stored at −80 °C until extraction for plant hormone and metabolite measurements.

3.2.6. Sample preparation for ^{1}H nuclear magnetic resonance (NMR spectra)

To evaluate the physiological responses in nanomaterial-treated onion seedlings, a ^{1}H NMR-based metabolomics platform was used. In the ^{1}H NMR spectrum, the chemical shifts and coupling constants give valuable information about the quantitative relationship between intramolecular and inter-molecular resonances. ^{1}H NMR can analyze any class of compound. ^{1}H NMR is the easiest in terms of sample preparation and can simultaneously detect a certain primary metabolites needed for seed germination.[97] The onion seedling samples were collected at 1, 2, and 3 weeks after sowing of treated and untreated seeds. The seedlings were immediately crushed using liquid nitrogen, ground, and lyophilized (Labconco Freeze Drying System, KS, USA). Dried seedling tissue (50 mg) was extracted with 2 mL of 0.75% (w/w) 3-(trimethylsilyl) propionic-*2,2,3,3-d*$_4$ acid, sodium salt (293040-25G) (TSP) (Sigma-Aldrich Chemical Co, St. Louis, MO, USA). The mixture was vortexed for 1 min, sonicated for 1 h, and centrifuged (Eppendorf 5417C, Eppendorf, Hamburg, Germany) at 10,000 rpm for 10 min. Finally, 550 µL of supernatant was used for NMR.

3.2.7. NMR analysis

1D ^{1}H NMR spectra were obtained on an ECS-400 spectrometer (JEOL-USA, Peabody, MA, USA) composed of fully digitized circuitry including RF generator, NMR lock, and digital matrix shim, equipped with a z-field gradient unit, operating at 400 MHz. 1D ^{1}H NMR spectra were acquired using a single pulse sequence with a 5 mm multinuclear inverse probe head

connected to NM-ASC24 auto-sample changer. 1D ^{1}H NMR spectra were acquired using a single pulse sequence without water suppression using the following conditions: acquisition point 131,072, total transients 128, relaxation delay 16 s, number of scans 32, and instrument calculated receiver gain automatically. Free induction decays were processed with line broadening of 0.2 Hz prior to Fourier transformation. Acquisition and processing of spectra were made with the Delta software version 4.3.6 (Windows NT). The spectrometer was locked on D_2O and all spectra were acquired at 25 °C. The ^{1}H NMR spectra were recorded with the standard pulse sequence for presaturation of the water signal at δ4.86 ppm, and the spectral width of δ10 ppm. The spectra were recorded with relaxation delays of 2, 4, 8, 12, and 16 s.

3.2.8. Data processing

^{1}H NMR spectra was analyzed using MNOVA (Version 14, Mestrelab Research, CA, USA). The chemical shift region of significance between 0.5 and 12.0 ppm was divided into small bins of equal width (0.04 ppm bin size). The region from 4.6 to 4.7 ppm was excluded to eliminate the signal from D_2O. Multivariate analysis of the binned NMR data was conducted with MetaboAnalyst 3.0 (http://www.metaboanalyst.ca/MetaboAnalyst/).

3.2.9. Untargeted LC-MS metabolomics study

In the present study, the targeted metabolites are hydrophilic in nature, and thus, LC-MS is an ideal platform for their analysis. Therefore, in our study, LCMS-based metabolomics was selected to detect the induced alteration in nanomaterial-treated onion seedlings. Extraction of freeze-dried samples (1-, 2-, and 3-week-old onion seedlings) were performed in accordance with our previously described procedures[13] with minor modifications. Briefly, 1.5 mL of methanol was added to 50 mg freeze-dried seedling samples, vortexed for 30 s and sonicated (Cole-Parmer Ultrasonic 8893, Vernon Hills, IL, USA) for 2 h at 4 °C, centrifuged at 13,000 rpm

for 10 min (Eppendorf 5417C, Eppendorf, Hamburg, Germany). The supernatant was collected, and a second extraction was performed with 0.5 mL of methanol. Both extracts were pooled and stored at -80 °C until further use. One µL of the pooled sample was injected into UPLC/ESI-HR-QTOFMS. The column conditions, gradient program, flow rate, and operating parameters of the mass spectrometer were in accordance with our published protocol.[13] Briefly, separation was achieved on a reversed-phase Eclipse Plus C18 RRHD column (1.8 µm, 50 × 2.1 mm). Binary mobile phase, 0.1% aqueous formic acid (A) and 0.1% formic acid in acetonitrile (B) was used with the gradient program: 0−2 min, 0% B; 2−15 min, 0−80% B; 15−18 min, 80−100% B; 18−20 min, 100−0% B. The flow rate was 0.3 mL min^{-1}, and the column temperature was set at 70 °C. Mass spectra were acquired in positive ionization mode using electrospray ionization (ESI) on a maXis Impact mass spectrometer (Bruker Daltonics, Billerica, MA, USA). Raw data were processed using Data Analysis 4.3 software (Bruker Daltonics) to get molecular features. The multivariate analysis was performed for all processed data using MetaboAnalyst 3.0.

3.2.10. Analysis of hormones by LC-MS

Seed samples from 0, 24, 48, and 72 h after seed treatments were collected and ground in liquid nitrogen with a mortar and pestle, then lyophilized (Labconco Freeze Drying System, KS, USA) to get freeze-dried powder. For each sample, 100 mg of dried tissue was weighed in 2.0 mL microcentrifuge tubes, and 300 µL of isopropanol: water: glacial acetic acid (79:20:1, v/v) was added. Samples were vortexed for 30 s, sonicated for 1 h at 4 °C, and centrifuged (13,000 rpm) for 10 min. After separation of supernatant, the residue was reextracted with 100 µL of isopropanol: water: glacial acetic acid (79:20:1, v/v).

Similarly, greenhouse seedling samples from the 1st, 2nd and 3rd week after sowing were harvested for analysis of hormones and ground in liquid nitrogen. Seedling samples (500 mg

each) were extracted with 300 µL of isopropanol: water: glacial acetic acid (79:20:1, v/v). The supernatant was collected, and second extraction was performed with 150 µL of isopropanol: water: glacial acetic acid (79:20:1, v/v).

Final pooled extracted samples were used for UPLC/ESI-HR-QTOFMS quantitative analysis of plant hormones. The column conditions, gradient program, flow rate and the operating parameters of the mass spectrometer were in accordance with the published protocol.[13, 98-99] In brief, the separation of plant hormones was achieved on the Eclipse Plus C18 RRHD (1.8 µm, 50 × 2.1 mm) column with flow rate of 0.15 mL min^{-1}. The gradient mobile phases used were (A) 0.1% aqueous formic acid and (B) 0.1% formic acid in acetonitrile. The following gradient system was applied for the elution compounds as follows, 0 min, 0% B; 11 min, 80% B; 15 min, 100% B; 16 min 0% B.

3.2.11. Statistical analysis

Results were expressed as a mean ± standard error (SE) with three replications. Analysis of variance (ANOVA) was carried out using JMP pro 14 software. Microsoft Excel was used for data visualization and mean comparison was done by using Student's *t*-test. The normality of data was verified by evaluating the scatter plot of residuals given by JMP pro 14 software. The residuals were normally distributed for all ANOVA test. The effects of nano-treatment were considered statistically significant when $p \leq 0.05$. The multivariate analysis was performed by using MetaboAnalyst 3.0 (http://www.metaboanalyst.ca/).

3.3. Results and discussion

3.3.1. Synthesis and Characterization of Nanomaterials

The synthesis and characterization of TNE, CNE, AgNPs, and AuNPs were previously published.[83] Dynamic light scattering technique was used to calculate the particle size (PS) for the characterization of nanoemulsions. The mean particle sizes recorded for TNE and CNE were 141.3 ± 1.69 and 139.8 ± 0.79 nm, respectively. Nanoparticles were characterized by UV-Vis spectrophotometry, dynamic light scattering technique, TEM, XRD, and LC-MS. In the UV−vis spectrum, a single broad resonance peak was observed between 410 and 450 nm, which confirms the synthesis of AgNPs, and a peak located between 500 and 580 nm indicates the presence of AuNPs. TEM image of the synthesized nanoparticles showed the size range of 19−37 nm for the AgNPs and 30−113 nm for the AuNPs. The crystalline nature of the synthesized AgNPs and AgNPs were confirmed by the XRD. Similarly, LC-MS results verify that the synthesized NPs were coated with onion phytochemicals.

3.3.2. Effect of Priming with Green Nanomaterials on Seed Germination and Seedling Emergence

The effects of seed priming with various nanopriming agents on the germination of onion cultivars Legend and 50147 are shown in Figure 10a and 10b. AgNP and AuNP treatments had the highest germination percentages for Legend and 50147 onion cultivars, respectively. In both cultivars, unprimed seeds had the lowest germination percentage. Upon sowing, primed seeds rapidly absorb water and revive the seed metabolism than non-primed seeds resulting increased germination rate, uniformity of emergence, and resistance of seedlings against unfavorable environmental conditions.[79] Several studies have demonstrated the positive influence of different nanoparticles on seed germination. In onion seeds, previous studies have reported the beneficial

effects of low concentrations of nano-size titanium dioxide,[100-101] zinc-supported multiwalled carbon nanocomposite,[102] and zinc oxide nanoparticles.[103] Application of carbon nanotubes[12] and nanosilicon dioxide[104] significantly enhanced the germination of tomato (*Solanum lycopersicum* L.) seeds compared to control. The beneficial effects of gold nanoparticles on seed germination have been previously reported in maize (*Zea mays* L.),[43] *Gloriosa superba* L.,[53] and rice (*Oryza sativa* L.).[42] Similarly, enhanced germination was observed using AgNPs in rice[42] and *Boswellia ovalifoliolata* N.P.Balakr. & A.N.Henry.[105] These results suggest that plant physiology affects the interaction with nanoparticles, resulting in different effects of nanoparticles in the different crops.

Figure 10c and 10d show the emergence percentage in the greenhouse study of Legend and 50147 cultivars. The hydropriming and NP priming treatments had higher seedling emergence compared to the unprimed control. The seedling emergence trend was similar in both onion cultivars. Significantly higher seed emergence was observed at 6 and 21 days after sowing in the nanoprimed onion seeds as compared to the unprimed and hydroprimed seeds in our published manuscript.[83] Several other studies have demonstrated the positive effects of different types of NPs as seed-priming agents to enhance emergence of barley (*Hordeum vulgare* L.), soybean (*Glycine max* L.), corn,[106] spinach (*Spinacia oleracea* L.),[107] rice[42] and watermelon (*Citrullus lanatus* (Thunb.) Matsum. & Nakai.).[82]

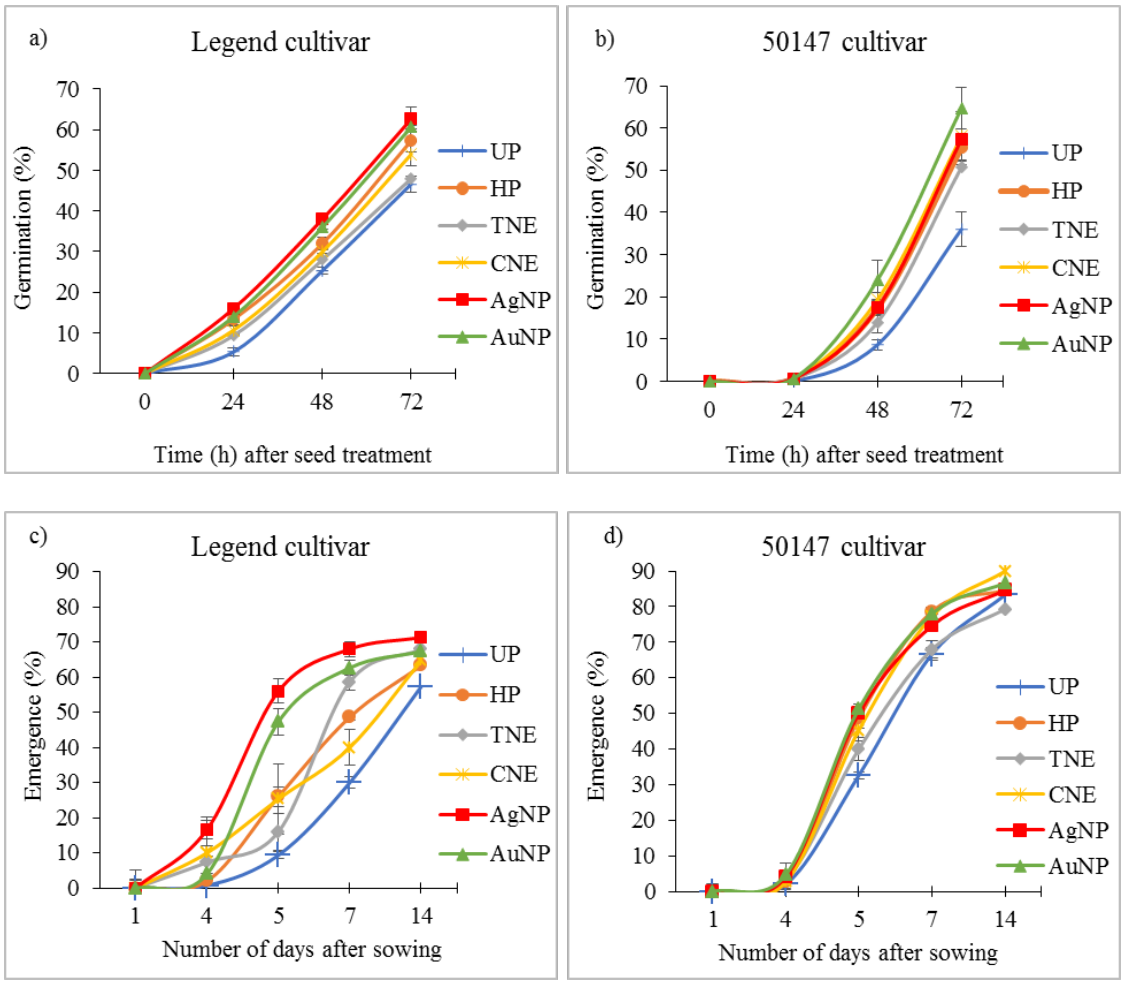

Figure 10 Effect of nanopriming on germination percentage of (a) Legend and (b) 50147 onion cultivars and emergence percentage of (c) Legend and (d) 50147 onion cultivars. Values are expressed as means ± SE of three replicates. UP: unprimed, HP: hydroprimed, TNE: turmeric nanoemulsion, CNE: citrus nanoemulsion, AgNP: silver NPs, and AuNP: gold NPs.

In this study, nanopriming treatments showed a beneficial effect on onion seed germination (Figure 11a) and seedling emergence (Figure 11b). We have studied the internalization of these nanomaterials into onion seeds using TEM, INAA and GC-MS.[83] The internalized nanomaterials might facilitate water uptake in seeds and cause production of reactive oxygen species in a beneficial range, resulting higher seed germination and seedling growth[42-43]

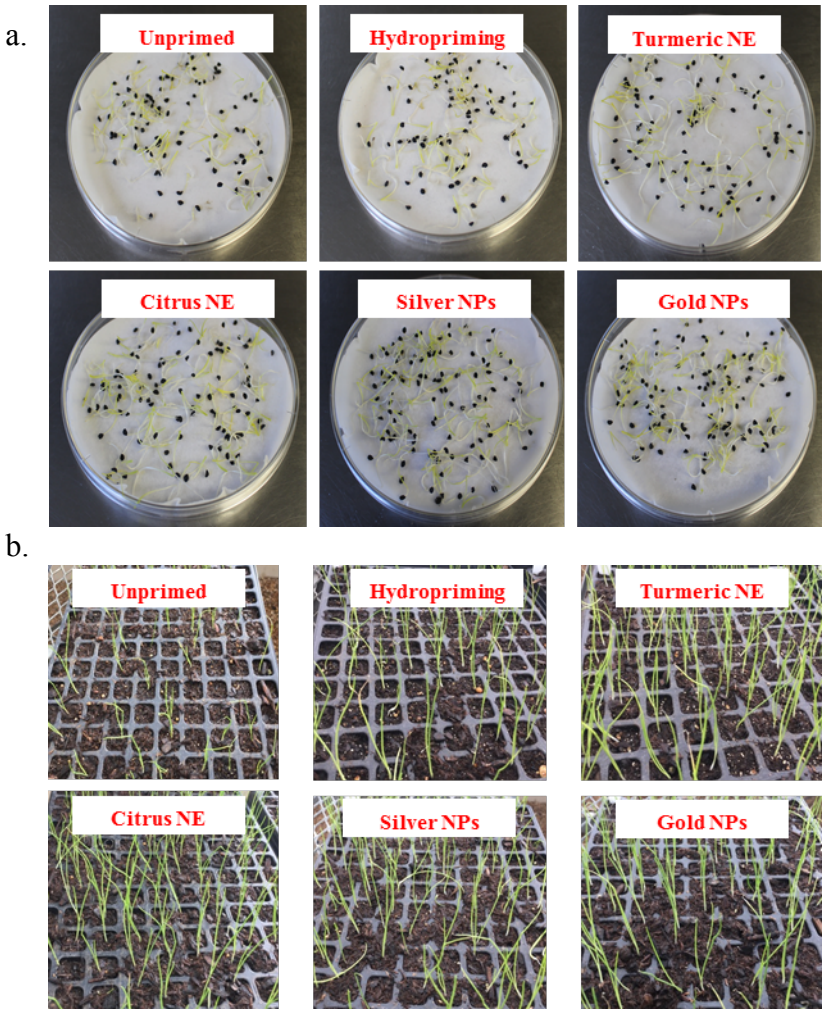

Figure 11 Influence of different nanopriming treatments on (a) onion seed germination in incubator studies and (b) seedling growth in greenhouse studies.

3.3.3. Effect of Nano treatments on Overall Metabolic Profiles of Onion Seedlings using ^{1}H NMR Data

To visualize general trends, grouping, and the differences between control and nano-treated plants in the ^{1}H NMR data, we conducted Partial Least Squares Discriminant Analysis (PLS-DA), which is a supervised clustering method, to maximize the separation between groups. PLS-DA of the metabolomics data from 1-, 2- and 3-week-old onion seedling samples produced

principal components (PCs). Together, PC1 and PC2 explained 93.9%, 48.4%, and 99.2% of the total variance for 1-, 2-, and 3-week-old onion seedlings, respectively (Figure 12). The score plots from PC1 and PC2 clearly separated the control and nano-treated plants, reflecting differences in metabolic profiles at all stages of seedlings. However, no difference was found between nano-treatments in 1-week and 3-week-old seedlings. Together, these data show that nano-treatments changed the pattern of metabolites in onion seedlings.

Identification of metabolites present in our samples were identified using ^{1}H NMR. Primary metabolites including sugar (glucose), seven amino acids (methionine, L-isoleucine, valine, threonine, L-citrulline, arginine, and tyrosine) and three organic acids (acetate, butyrate, and citrate) were identified in the ^{1}H NMR published spectra[108-109] by authentic known standards. Metabolites altered within the same treatment at different developing stage of onion seedlings were shown in Figure B1-B6. Figure B1 shows the identified metabolites from unprimed onion extract. Irrespective of the nano-treatments, all the metabolites were enhanced significantly in the later stage of seedling growth as compared to first and second weeks. Increased sugar signals in the third week were most likely due to increased photosynthate availability due to higher leaf biomass. Similarly, Figure B7, B8 and B9 depicts the overlay of ^{1}H NMR spectra of 1-,2-, and 3-week-old onion seedlings for all the treatments, respectively.

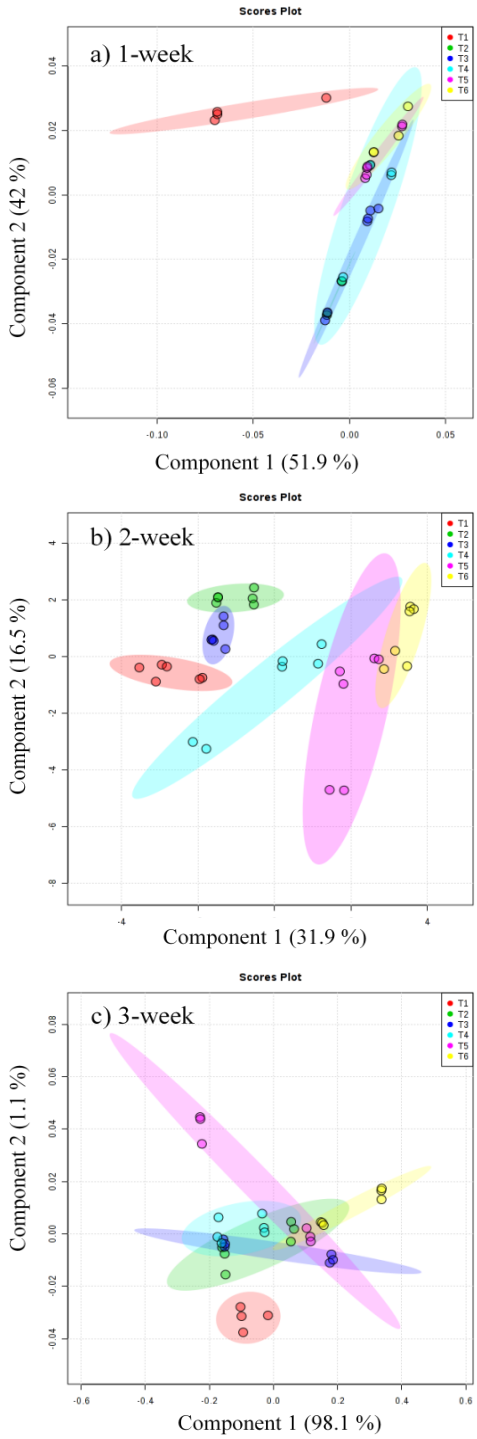

Figure 12 Partial least-squares discriminant analysis (PLS-DA) score plots of overall metabolic profile in the 1H NMR data of (a) 1-week (b) 2-week and (c) 3-week-old seedlings. T1: unprimed, T2: hydroprimed, T3: turmeric nanoemulsion, T4: citrus nanoemulsion, T5: silver nanoparticles, and T6: gold nanoparticles.

3.3.4. Global Metabolic Response to NP Priming in Onion Seedlings in the LC-MS data

LC-MS was used to identify and quantify metabolites in onion seedlings. PLS-DA was performed to visualize the influence of priming on the global metabolic response of 1-, 2-, and 3-week-old onion seedlings. The PLS-DA score plots of unprimed, hydro-primed, and nano-primed onion seedling samples are presented in Figure 13a, 13b, and 13c. NP priming treatments formed separate clusters from hydro-primed and unprimed groups in all the score plots, indicating that NP priming influences the metabolome of onion seedlings.

Furthermore, the variable importance on projection (VIP) score plots were obtained from the PLS-DA models. The compounds responsible for clustering in six different treatments were identified based on their VIP scores (Figure 13d, 13e, and 13f). Seed germination inhibitors like JA, OPDA, daminozide, mepiquat chloride, MeJA, ABA, gallic acid, and coumaric acid were high in unprimed (T1) and hydroprimed (T2) seedlings during the 1^{st} and 2^{nd} weeks after sowing. Similarly, germination stimulators like GABA, GA, kinetin, and spermidine were low in the unprimed and hydroprimed as compared to the NP-treated onion seedlings. These changes in the germination stimulators and the inhibitors during the initial growth stages might regulate seed germination and explain the enhanced seed emergence in the NP-treated onion seeds.

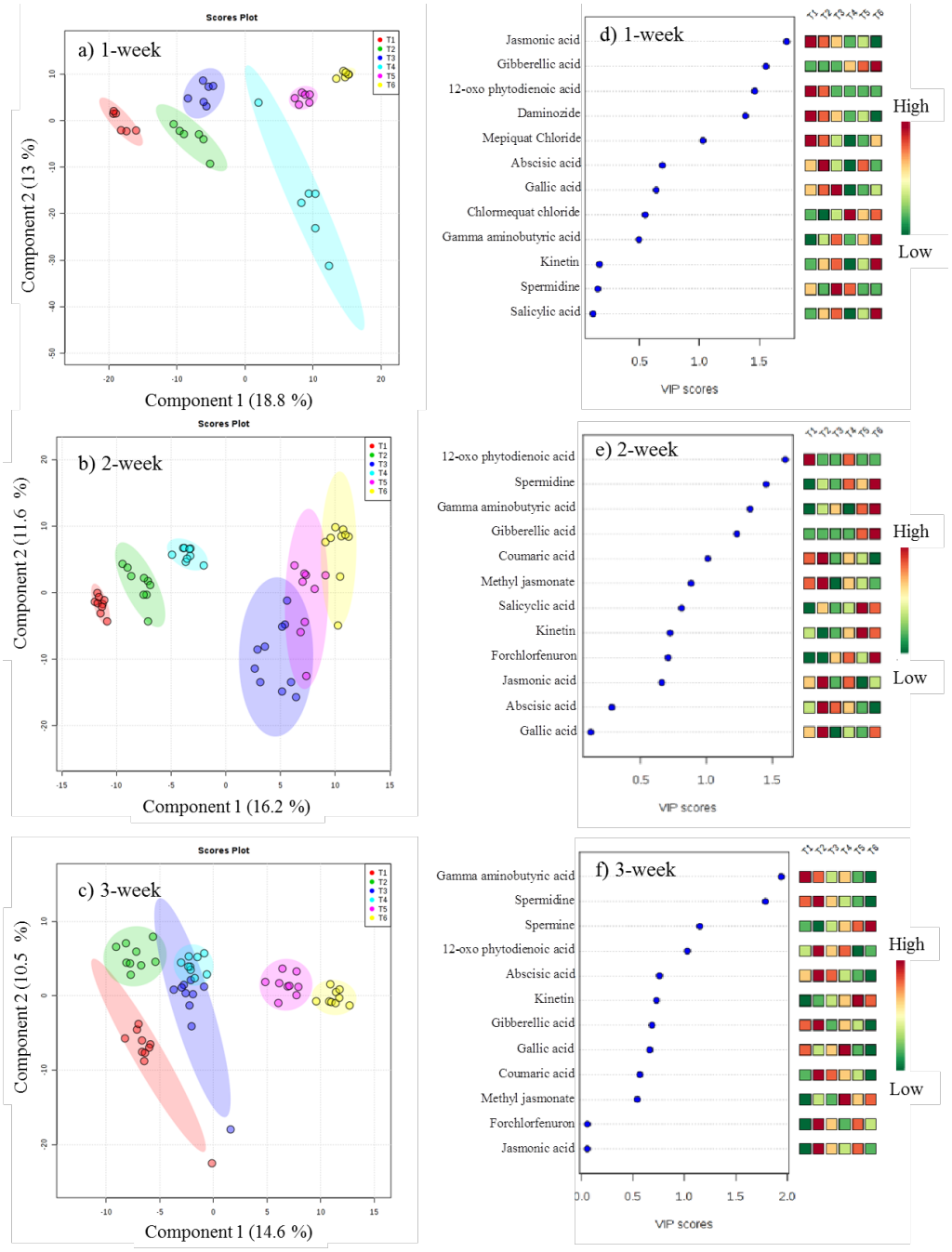

Figure 13 Partial least-squares discriminant analysis (PLS-DA) score plots of overall metabolic profile in the LC-MS data of (a) 1-week (b) 2-week and (c) 3-week-old onion seedlings. The discriminating metabolite features based on variable importance on projection (VIP) scores from PLS-DA of (d) 1-week (e) 2-week and (f) 3-week-old onion seedlings of different priming treatments compared to unprimed and hydroprimed controls. T1: unprimed, T2: hydroprimed, T3: turmeric nanoemulsion, T4: citrus nanoemulsion, T5: silver nanoparticles, and T6: gold nanoparticles.

3.3.5. Seed Priming Treatment-Specific Modulation of Plant Hormones up to 72 h Treatment in Incubator

UPLC/ESI-HR-QTOFMS was used for separation, identification and measurement of plant hormones (Figure 14).

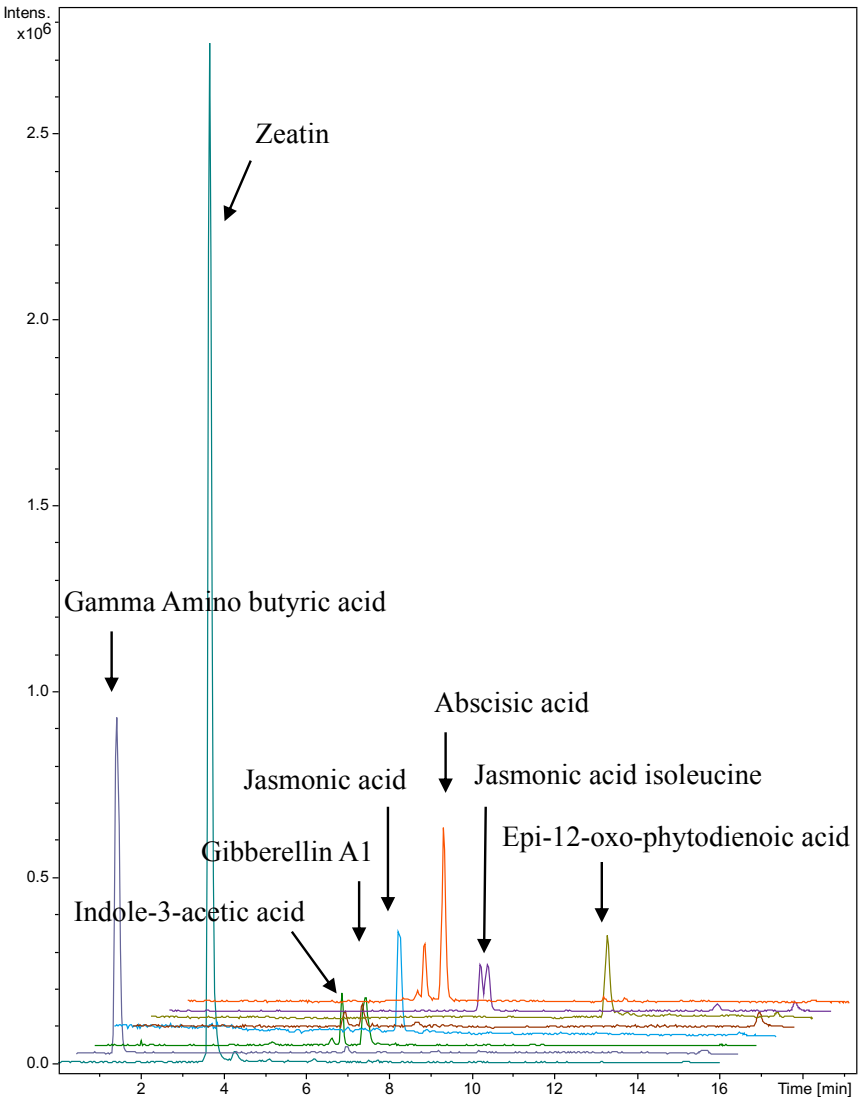

Figure 14 UHPLC/HR-QTOFMS separation and identification of plant hormones

The mass tandem and + bbCID mass spectra of the tested plant hormones are presented in Figure 15. Plant hormones were identified based on the UV, MS, and +bbCID mass spectra, and the published literature.[13] We quantified zeatin (ZA), GABA, and IAA levels in the onion seeds at 0, 24, 48, and 72 h after nanopriming treatments. For the first time, we found that priming treatments with nanomaterials selectively modulated ZA and GABA levels in onion seed germination as compared to the unprimed and hydroprimed controls (Figure 16a, 16b, 16c, and 16d). Conversely, no significant changes were observed in the levels of IAA in the onion seedlings after priming treatments during 0 and 24 h of seed priming (Figure 16e). In later stage at 48 and 72 h, a significantly enhanced IAA level was observed in the nanoprimed Legend cultivar as compared to the unprimed control but not in 50147 cultivar (Figure 16f). Auxin by itself is not necessary for seed germination.[110] However it is important in post-emergence growth of young seedlings.

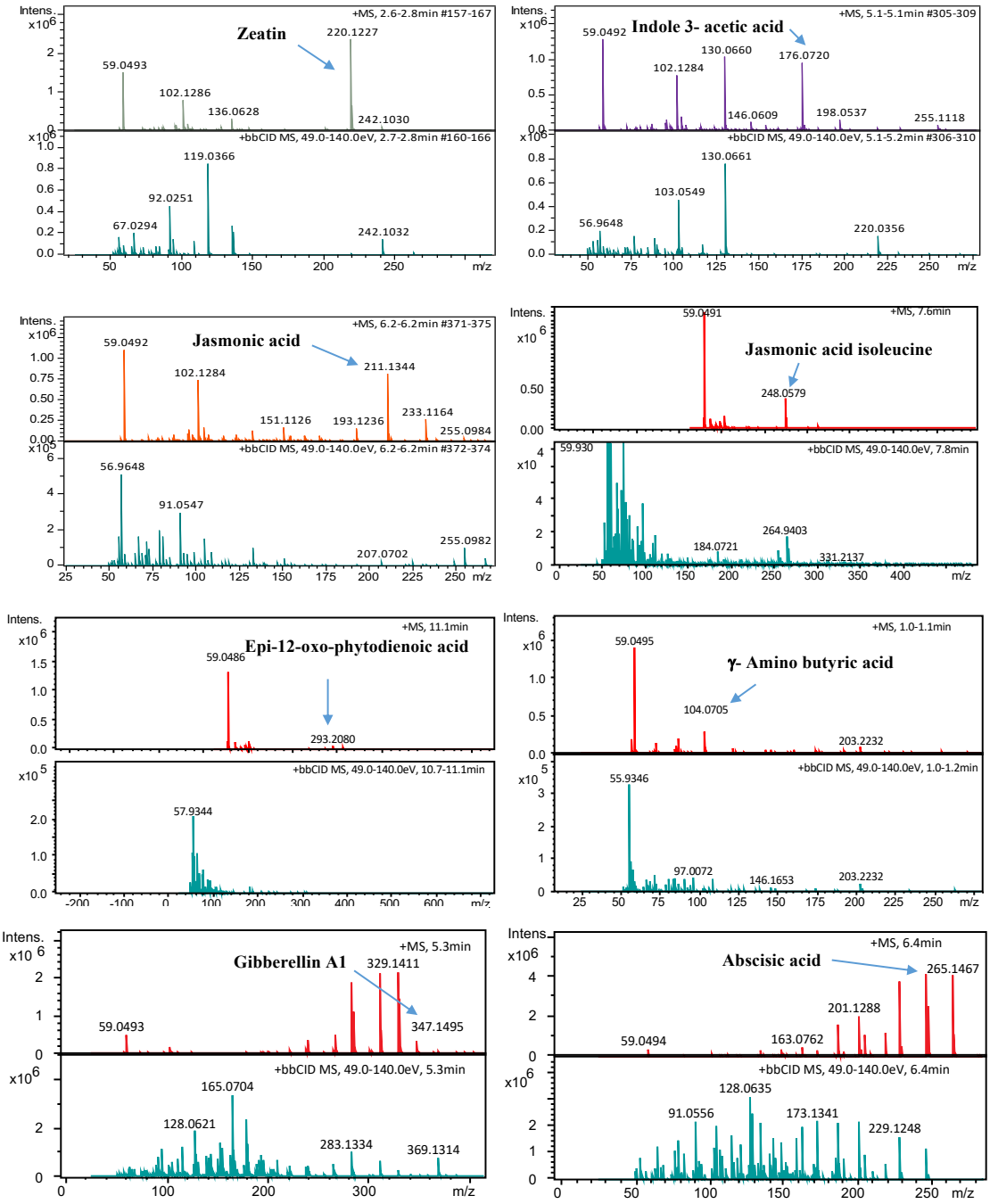

Figure 15 Tandem mass spectra of certain plant hormones present in onion seedlings in positive ionization mode.

Cytokinins enhance seed germination and act in all stages of germination.[110] They regulate the utilization of storage proteins during seed germination. Their effects on seed germination also contribute to the alleviation of stresses such as salinity, drought, heavy metals, and oxidative stress.[110] Cytokinins function in controlling seed size, which controls growth of the embryo, endosperm, and seed coat and might affect seed germination.[111] The level of endogenous cytokinin is generally low in dry seeds and then increases during seed germination.[112] In our study, the ZA level was significantly lower in the unprimed seed compared to the nanoprimed seeds of both onion cultivars, which might promote seed germination and plant growth.

Amino acids can provide an alternative substrate for energy production in germinating seeds.[113] GABA is a well-known non-protein amino acid and the content of GABA in brown rice,[74, 114] barley[6] and Arabidopsis[72] increases during seed germination. In addition, germinating seeds had enhanced activity and transcript levels of glutamate decarboxylase, the first enzyme of the GABA shunt.[115] Moreover, GABA contributes to TCA cycle respiration in imbibed seeds and plays an important role in balancing carbon and nitrogen metabolism and in storage reserve accumulation.[116] The GABA pool can play a significant role in imbibed seeds when energy and oxygen levels are low and storage reserves are not yet readily available.[113, 115] Significantly higher level of GABA were observed at 0, 24, 48, and 72 h of treatment in NP-treated seeds as compared to unprimed seeds. Higher accumulation of GABA in the nanoprimed seeds of both onion cultivars might contribute to the higher seedling emergence rate as compared to the control seeds.

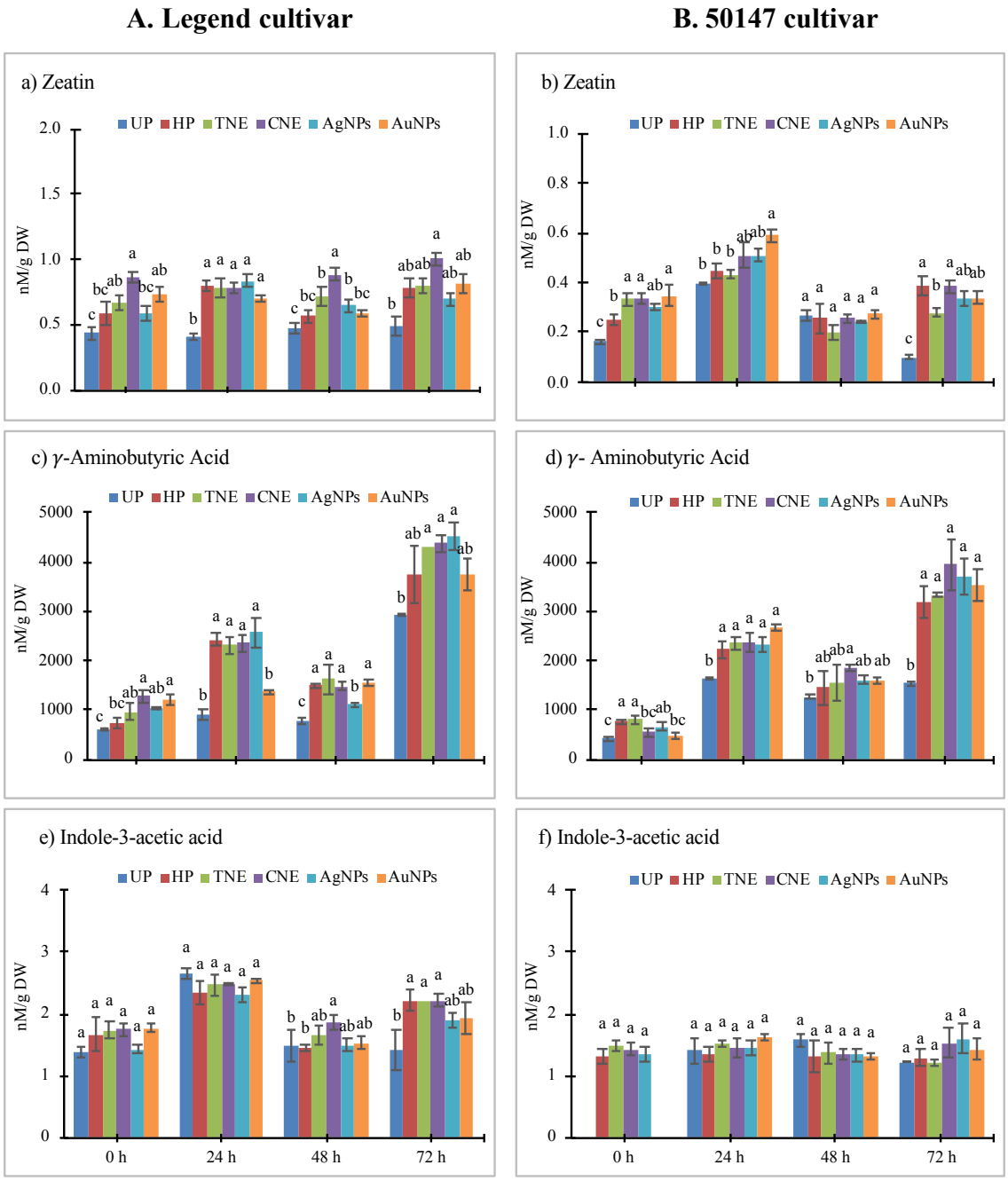

Figure 16 Zeatin (ZA), γ-aminobutyric acid (GABA) and Indole-3-acetic acid (IAA) in incubator study at 0, 24, 48, and 72 h of priming (a) Legend and (b) 50147 onion seed cultivars with different nano-priming treatments compared to replicates. Values are expressed as means ± standard error of three replicates. Different letters in the row indicate significant differences according to Student's *t*-test ($p \leq 0.05$). UP: unprimed, HP: hydroprimed, TNE: turmeric nanoemulsion, CNE: citrus nanoemulsion, AgNPs: silver nanoparticles, and AuNPs: gold nanoparticles.

Along with these germination stimulators, nanopriming treatments significantly affected germination inhibitors in onion seeds. ABA inhibits seed germination, delaying radicle protrusion and endosperm weakening, as well as enhancing expression of specific transcription factors.[117] In our study, the level of ABA was higher in the unprimed Legend seeds compared to nanoprimed seeds at 0 and 24 h of treatment (Figure 17a). The enhanced ABA level in the untreated seed might have adverse effects in the germination and growth of the unprimed seeds.

Jasmonic acid (JA), its precursor OPDA, and associated metabolites, including JA-Ile (collectively referred to as jasmonates), are all involved in mediating stress responses[80] and promoting seed dormancy. OPDA acts with ABA in repressing Arabidopsis seed germination.[118-119] OPDA also acts through the dormancy-promoting factor MOTHER-OF-FT-AND-TFL1 (MFT), the ABA-sensing protein ABA-INSENSITIVE5 (ABI5), and the gibberellin-sensing protein RGL2 (Ral Guanine Nucleotide Dissociation Stimulator Like 2).[120] ABA, ABI5, RGL2, and MFT are key components of the OPDA pathway that represses seed germination. Significantly higher levels of OPDA, JA, and JA-Ile were observed in the unprimed Legend seeds as compared to the nano-primed seeds at 72 h (Figure 17a). Considering this, lowering of OPDA, JA and JA-Ile accumulation with nanopriming could be an effective strategy to break dormancy, improve seed germination, and enhance seedling growth. However, the effect was not observed within 72 h of the treatment in the 50147 cultivar (Figure 17b). The distinct phytohormone contents in the two cultivars might be due to their different genetic makeup, seed morphology or just by random chance. The Legend cultivar was developed at the Vegetable and Fruit Improvement Center, TAMU, and was bred from 1015 Y Texas Super Sweet Onion for higher content of health-promoting compounds, and 50147 was bred for pink root resistance.

a) Legend cultivar

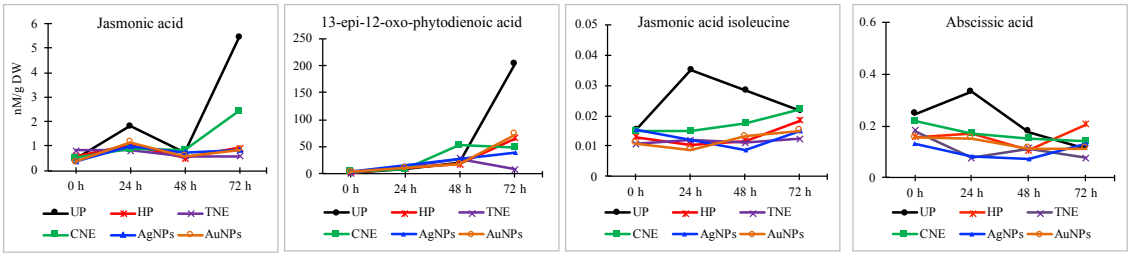

b) 50147 cultivar

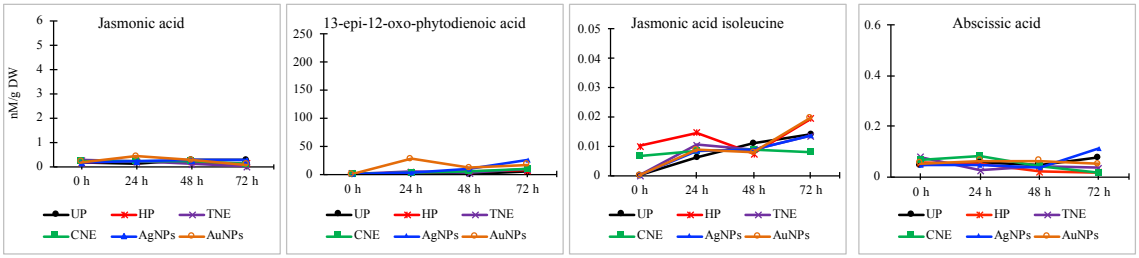

Figure 17 Jasmonic acid (JA), 12-oxo phytodienoic acid (OPDA), jasmonic acid isoleucine (JA-Ile), and abscisic acid (ABA) in incubator study at 0, 24, 48, and 72 h of priming (a) Legend and (b) 50147 onion seed cultivars with different nano-priming treatments compared to unprimed and hydroprimed treatment. UP: unprimed, HP: hydroprimed, TNE: turmeric nanoemulsion, CNE: citrus nanoemulsion, AgNPs: silver nanoparticles, and AuNPs: gold nanoparticles.

3.3.6. Plant Hormone Levels after NP Priming in Greenhouse-Grown Onion Seedlings

The levels of plant hormones in onion seedlings were measured in three consecutive weeks after NP priming to understand how the plant carries the effect of seed priming through development, based on metabolic signatures. Figure 18 and 19 show the hormone levels in the Legend and 50147 cultivars, respectively. Interestingly, NP priming enhanced the levels of ZA in 50147 cultivar only in the 1st week (Figure 19a). However, the level of ZA in the 3rd week of the treatment was significantly higher in the unprimed onion seeds and hydroprimed seeds of 50147 and Legend cultivars, respectively, compared with the other treatments (Figure 19a and 18a). This suggests that the seed germination enhancers accumulated in the later stages of germination in unprimed and hydroprimed seeds as compared to the nanoprimed seeds.

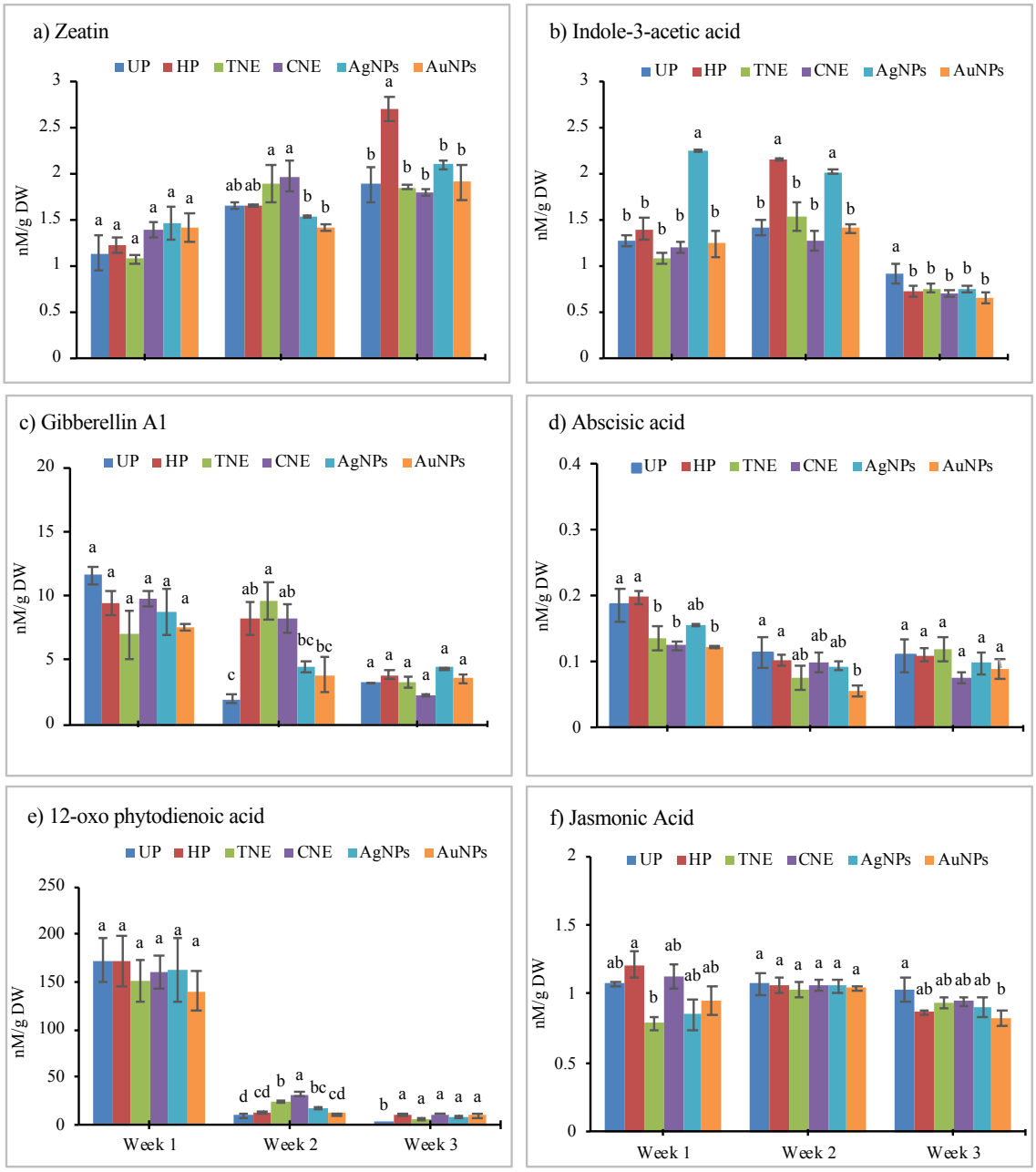

Figure 18 Levels of plant growth hormones in greenhouse study of 1-, 2-, and 3-week-old onion seedlings of Legend cultivar with different nano-priming treatments compared to unprimed and hydroprimed treatments. Values are expressed as means ± standard error of three replicates. Different letters in the row indicate significant differences according to Student's *t*-test ($p \leq 0.05$). UP: unprimed, HP: hydroprimed, TNE: turmeric nanoemulsion, CNE: citrus nanoemulsion, AgNPs: silver nanoparticles, and AuNPs: gold nanoparticles.

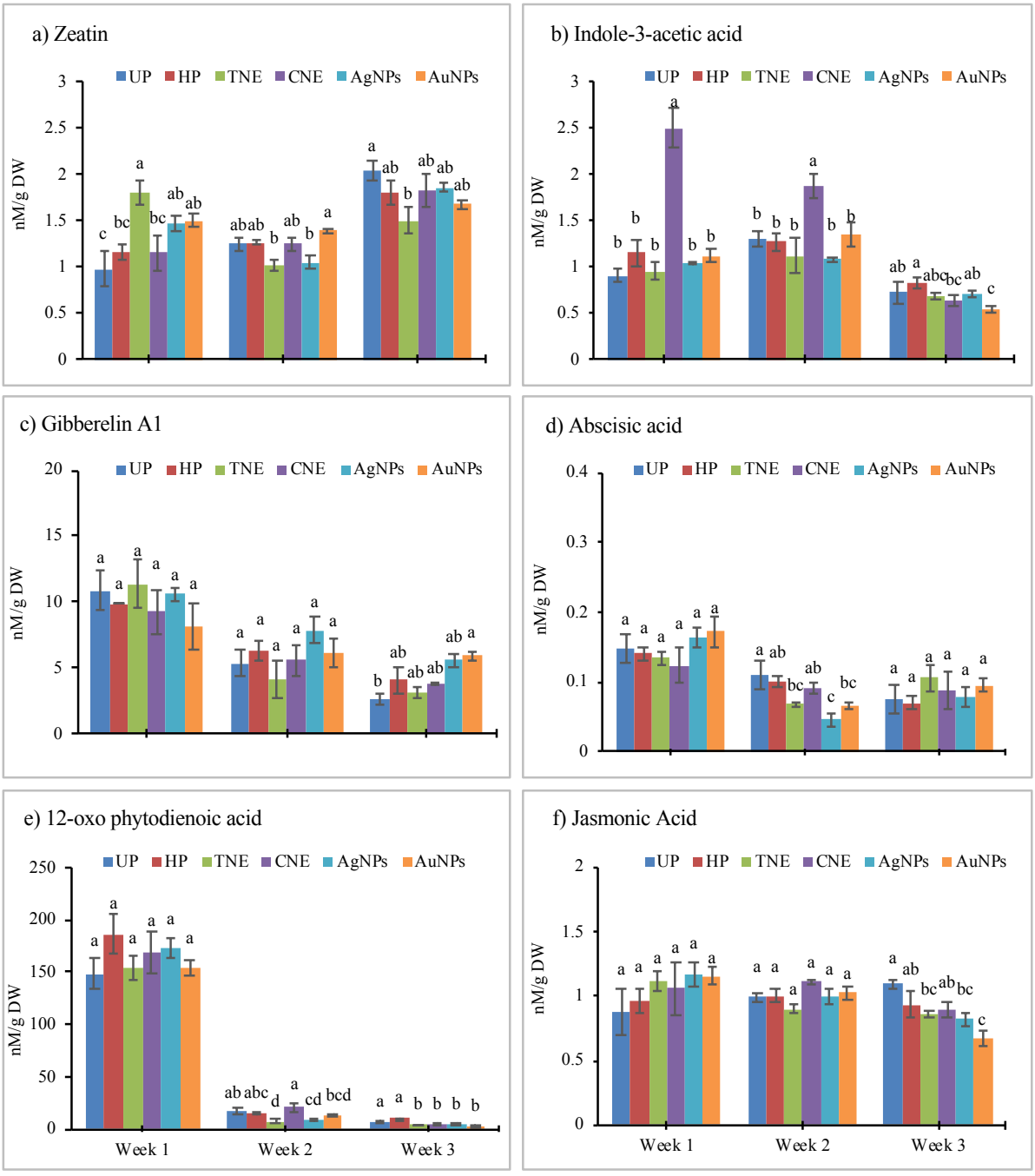

Figure 19 Levels of plant growth hormones in greenhouse study of 1-, 2-, and 3-week-old onion seedlings of 50147 cultivar with different nano-priming treatments compared to unprimed and hydroprimed treatments. Values are expressed as means ± standard error of three replicates. Different letters in the row indicate significant differences according to Student's *t*-test ($p \leq 0.05$). UP: unprimed, HP: hydroprimed, TNE: turmeric nanoemulsion, CNE: citrus nanoemulsion, AgNPs: silver nanoparticles, and AuNPs: gold nanoparticles.

Interestingly, NP priming had no significant impact on the levels of GA compared to unprimed and hydroprimed seedlings of both cultivars. GA stimulates seed germination by inducing hydrolytic enzymes that weaken the seed coat, mobilizing seed nutrient storage compounds, and stimulating embryo expansion.[121] However, the balance of endogenous ABA and GA levels plays an important role in controlling seed germination.[122] This suggests that although the level of GA was not significantly different between the treatments, the ratio of GA and ABA might play a crucial role in enhancing seed emergence in the NP-treated seeds.

A significant increase in IAA levels was observed in the AgNP and CNE priming treatments during the 1st week of treatment in Legend and 50147 cultivars, respectively. Hydroprimed and unprimed Legend seeds had significantly higher levels of IAA during the second and third weeks of priming, respectively. This shows that IAA accumulated in the later stages of germination in unprimed and hydroprimed seeds as compared to the nanoprimed seeds. Figure 18d–18f and 19d–19f show the post-emergence changes in the endogenous ABA, OPDA, and JA in the Legend and 50147 onion seedlings. In the first week of treatment, there were no significant differences in levels of the three hormones in treated and untreated onion seedlings. Although the level of ABA was statistically equivalent in the Legend onions, the trend reflects the earlier findings that unprimed seeds had higher levels compared to the treated seedlings. In the second and third weeks, ABA accumulation was higher in the unprimed onion seeds as compared to the treated seedlings. A significant drop in OPDA was observed in 2- and 3-week-old onion seedlings as compared to the 1st week. Our results indicate that maintaining the interplay of seed germination enhancers and inhibitors is critical to get a suitable combination of enhanced seed germination, strong plant growth, and robust defense responses.

3.4. Conclusions

Herein, we demonstrated that nanomaterials prepared using agro-industrial byproducts effectively enhanced onion seed germination. Given the low dosage of nanoparticles used in this work, the material cost for commercial application of AgNPs and AuNPs is about $3-5/acre and $8-13/acre, respectively, making this a cost-efficient seed treatment method. Seed priming with these green synthesized nanomaterials was nontoxic, similar to unprimed and hydroprimed seeds.[83] This study demonstrate that the seed priming treatments significantly inhibited plant hormones and growth regulators like abscisic acid and *cis*(+)-12-oxo-phytodienoic acid (OPDA). Similarly, enhanced germination stimulators like γ-aminobutyric acid (GABA) and zeatin (ZA) were observed in the treated onion seeds and seedlings. These nanomaterials can be applied sustainably to induce seed germination stimulators and repress inhibitors during the early stages of seedling development in onion. However, further studies are needed to observe the effect of nanopriming in the plant metabolites during the later phase of plant growth and development in onions.

4. MULTIVARIATE APPROACH REVEALS THE INFLUENCE OF NANOPARTICLE TREATMENTS, GROWING LOCATIONS AND SIZE OF ONION BULBS ON FLAVONOIDS AND AMINO ACIDS

4.1. Introduction

Sufficient food production with suitable quality for the growing world population has made it necessary to revise common crop production systems. Nanotechnology is an innovative method that has potential to revolutionize the advancement in agriculture in terms of nanoagriculture.[123] This technology can resolve the traditional agricultural problems through designing, engineering and fabricating materials at the nano-scale that has novel physical, chemical and biological properties compared to its bulk product. However, the applications of nanotechnology in agriculture are still underdeveloped and there are still debates and controversy on environmental concerns of the nano particles (NPs)-based agricultural products. Several studies demonstrated the positive impact of nanoparticles in the growth and yield of plants[124-125] but very few studies have been conducted through the entire life cycle of a plant. The knowledge regarding the impact of nanoparticles on nutritional quality of produce remains largely unknown. This study reports the interaction of green synthesized nanoparticles with onion cultivar grown at three different locations of Texas.

Onion represent one of the most important vegetable crops and is cultivated under different climatic conditions nearly worldwide. With a production of about 97 million tonnes of bulbs from 5.2 million ha, onion is the second most produced vegetable after tomato world- wide in the year 2017. In terms of production, the United States rank 3rd (after China and India) with production of 3.1 million tons of onions from 53,650 ha.[126] It is grown nearly worldwide from

tropical to cool temperate climates and used as food and spice in diets of almost all cultural areas. Onion is a plant with a long history of traditional medicinal uses. Onion extracts and the isolated bioactive compounds from onion has wide range of biological effects including antioxidant, antidiabetic, antiproliferative, anti-obesity, antimicrobial and anti-inflammatory effects on human health.[127]

Flavonoid is an important group of phytochemical presents in onion that possess a distinct flavor and aroma and are proved to have beneficial effects to human health. The epidemiological studies associate their possible role in preventing cardiovascular diseases, cancer and other age related diseases.[128-129] This health-promoting activity seems to be related to the antioxidant (free-radical scavenging) activity of flavonoids.[129-130] Quercetin is the major flavonoid present in the onion that chelates certain transition metals, acts as a potent electron donor, and scavenges free radicals which inhibits lipid oxidation in vitro.[131] Quercetin is nonpolar and is therefore found as glycosides in plants. Quercetin derivative viz; diglucoside and monoglucoside comprised upto 93% of total flavonol content.[132] The flavonoid content in onion is strongly influenced by several factors such as variations in variety, color,[133] growth stage, soil type, location,[134] cultivation practices, field curing,[135] scales,[136] light,[137] storage,[136] and processing.[138-139] Compared to red and white onions, yellow onions contain a high level of quercetin.[133]

Along with flavonoids, onions are rich in amino acid content as well. Beyond protein formation, free amino acids are an important nitrogen reservoir, which additionally contributes to the nutritional value of the *Allium* species. Amino acids play significant roles in plant growth by producing metabolic energy, providing resistance to stress and controlling cellular pH.[140] They are also involved in various physiological functions like glucose homeostasis, gastrointestinal

health, cell signaling, satiety and development of flavor.[141] Another role of free amino acids is their participation in the Maillard reaction during industrial processing.[142] Free amino acid content are strongly influenced by different cultivars,[141] ploidy level,[143] stage of development at harvest and the long term storage.[142] As per our knowledge, no reports are available on influence of nano treatments and size of the bulb on amino acid content in onion.

Recently, more interest has been focused on the sweet and less pungent onion cultivars because of their appealing sweetness and lower pungency. Therefore, in the present study, the sweet yellow onion variety Legend was used. We investigated the influence of nanoparticles, location and the size of the bulbs in the flavonoid content of Legend variety. Our previous study has demonstrated the significant effect of nanopriming in the seed germination, growth, and yield of onion.[83] However, there are no reports on the seed priming using turmeric oil and citrus oil nanoemulsions, or silver and gold NPs in the flavonoid content of onions. Similarly, the effect of location and bulb size in the flavonoid content of Legend cultivar is not reported. For the first time, a comprehensive metabolite profiling approach targeting all relevant compounds in onion was applied to examine the impact of nano-treatments and growing environment on the metabolite composition of onion bulbs.

4.2. Materials and methods

4.2.1. Chemicals and seed materials

All solvents and chemicals used in this study were of analytical grade. Methanol, acetonitrile, phosphoric acid, quercetin-3-*O*-glucoside and amino acid standards were obtained from Sigma-Aldrich (St Louis, MO, USA). Silver nitrate ($AgNO_3$), sodium tetracloroaurate ($NaAuCl_4$), and the surfactants polysorbate (Tween 20) and sorbitan monolaurate (Span 20) required for preparing silver and gold NPs and nanoemulsions, respectively, were procured from

Sigma-Aldrich (Sigma-Aldrich, St. Louis, MO, USA). The curcumin-removed turmeric oleoresin (CRTO) was obtained from Sami Labs Limited, (Bangalore, India). Citrus fruits (*Citrus aurantium* L.) were received from the Texas A&M University Kingsville Citrus Center Orchard, Weslaco, TX. Nanopure water (NANOpure, Barnstead, Dubuque, IA, USA) and seeds extracted from these citrus fruits were used for the entire study. For onions, seeds of variety Legend, which was developed at the Vegetable and Fruit Improvement Center (VIFC) at Texas A&M University were used in the experiment.

4.2.2. Seed treatment and the field study

Seed priming treatments included control, hydro priming, priming with turmeric oil nanoemulsion (TNE), citrus nanoemulsion (CNE), silver nanoparticles (AgNPs), and gold nanoparticles (AuNPs). The description of formulation of nanoemulsions and nanoparticles and their characterization has been reported in previous studies.[83] Briefly, low energy method based on spontaneous emulsification method was used where 2 mL oil (citrus or turmeric oil) and a lipophilic surfactant (25 mL) were mixed together and the mixture was poured into 75 mL of aqueous phase with overnight continuous stirring using a magnetic stirrer at ambient temperature. The lipophilic phase was prepared by adding 125 mg of Span 20 in 25 mL of nanopure water and aqueous phase was prepared by adding 450 mg of Tween 20 in 75 mL of nanopore water with continuous stirring by a magnetic stirrer for two hours. Similarly, onion juice was used as a reducing and stabilizing agent to prepare AgNPs and AuNPs. Seeds were immersed in priming media for 12 h at room temperature and then dried after rinsing with water. Multi-location field trial was conducted in three different production regions of Texas (Eastern, Central, and Lower Rio Grande Valley), i.e. College Station (30°36’N, 96°18’W), Uvalde

(29°12'N, 99°47'W), and Weslaco (26°15'N, 97°98'W). The detail description of the field study has been reported in the previous study.[83]

4.2.3. Sample preparation for flavonoid extraction

After harvesting, onions were categorized into colossal (≥100 mm diameter), large (75–100 mm), medium (50–75 mm) and small (≤50 mm) size. The neck, basal plate, and skin of the different sized onion bulbs were removed and blended for 2 minutes. Blended samples (10 g) were extracted with 15 mL of methanol by vortexing for 1 min, homogenization for 3 min, sonication for 1 h and centrifugation (Beckman Model TJ-6) at 4480 × *g* for 15 min. The residue was re-extracted with 10 mL and 5 mL of methanol. All three extracts were pooled and filtered through Whatman #1 filter paper. Onion homogenates [6 treatments × 4 bulb sizes × 3 locations × 3 agronomic replicates = 216 samples] were extracted and subjected to HPLC analysis.

4.2.4. LC/ESI-HR-QTOF-MS for global metabolic response and identification of flavonoids

The methanol extracts were analyzed for flavonoid identification using an Agilent 1290 liquid chromatography (Santa Clara, CA, USA) equipped with a diode array detector and coupled to a maXis Impact high-resolution mass spectrometer (LC/ESI-HR-QTOF-MS) (Bruker Daltonics, Billerica, MA, USA). Chromatographic separation was carried out on a Zorbax Eclipse Plus C_{18} column (1.8 µm, 50 × 2.1 mm) (Agilent, Santa Clara, USA) at 30 °C with a flow rate of 0.2 mL/min. The mobile phase was composed of (A) 0.1% formic acid in water and (B) 0.1% formic acid in acetonitrile. The solvent gradient was 0% B (4 min), 0–80% B (8 min), 80–100% B (5 min), and 3 min isocratic at 100% A.

Mass spectral analyses were performed in positive ionization mode according to our previous methodology.[25] The capillary voltage was set at 3500 V and nebulizer gas pressure was

3.2 bar. The transfer time of the source was 80 µs and prepulse storage time was 80 µs. Nitrogen was used as a nebulizer and drying gas. The drying gas flow rate and temperature was kept at 8.0 L/min and 250 °C, respectively. MS/MS fragmentation pattern was obtained in multiple reaction monitoring (MRM) mode by different collision energies of 5, 10, 15, 20, 40, and 70 eV to obtain mass data for the intact precursor ion at low energy and their product ions at series of higher collision energy. The ion energy in quadrupole was kept at − 5.0 eV with 5.00 m/z isolation mass width and a set collision cell RF 500 Vpp was used. Full scan MS and bbCID data acquisition was performed at m/z 50–2000. The mass spectrometer calibration was performed by nine sodium formate clusters using high-precision calibration (HPC) mode. The calibration solution was injected at the end of each run using a Cole Palmer syringe pump (Vernon Hills, Illinois, USA) directly coupled to the interface, equipped with a Hamilton syringe (Reno, Nevada, USA). The accurate mass data for the precursor ions were processed using the Data Analysis 4.3 software Determination of molecular formula was carried out by mass accuracy, isotopic patterns, adduct and fragment information using SmartFormula. Same samples were analyzed for comprehensive metabolites profiling of onion bulbs.

4.2.5. Quantification of onion flavonoids by HPLC

Flavonoid analysis was performed in a 1525 HPLC system (Waters, Milford, MA) equipped with a 2996 photodiode array detector and a 717plus autosampler using a previously published method with slight modifications.[144] Chromatographic separation was performed on a X bridge C_{18} column (4.6 mm × 150 mm, 3.55 µm). A gradient mobile phase consisted of (A) 0.03 M phosphoric acid in water and (B) water/acetonitrile (1:1, v/v) at a flow rate of 0.5 mL/ min. The solvent gradient was 2 min isocratic at 10% B, 10–70% B (13 min), 70–10% B (1 min) and 4 min isocratic at 10% B. The column was equilibrated 2 min before the next injection. A 20

µL sample was injected and the chromatograms were monitored at 280 nm. Empower-2 software was employed for processing the data.

4.2.6. Derivatization of free amino acids and bioamines

Methanolic extracts were used for the quantification of amino acids for which the extracts were derivatized using dansyl chloride reagent in the presence of sodium borate buffer (pH 9.4). For derivatization, 350 µL of methanol extract was mixed with 125µL dansyl chloride, 300µL buffer and 50µL of diamino heptane (internal standard) in a centrifuge tube. The tubes were placed in water bath shaker maintained at 60°C for 30 min. To stop further derivatization and stabilize the sample mixture, 60µL of 2N acetic acid was added to sample and allowed to cool down to room temperature. The tubes were centrifuged, and the samples were transferred to vials for HPLC analysis.

4.2.7. HPLC-FLD for quantitation of amino acids

Amino acids were separated based on previously used method[145] and modified to suit onion samples. Analysis was carried out on Perkin Elmer Series 200 HPLC system consisted with binary pump, autosampler (Shelton, Connecticut, USA), a Gastorr TG-14 inline HPLC mobile phase degasser (FLOM USA, San Diego, CA, USA) and an Eppendorf TC-50 controller with CH-30 column heater (Eppendorf, Westbury, NY, USA). Detection of amino acids was achieved by using 1260 Infinity fluorescence detector controlled by Instant Pilot model G4208A (Agilent Technologies, Santa Clara, CA, USA). The system was supported by an interface (PE Nelson 900) and a Link box (PE Nelson 600). For the separation, Zorbax Eclipse XDB-C8 (4.6 x 150 mm, 5µm) was used with guard cartridge. The mobile phase consisted of formic acid 1% as solvent A and a combination of formic acid 1%, triethylamine 1% dissolved in 4L water as solvent B. Isocratic method with 36-min run time was used to separate amino acids with flow

rate 0.6 mL/min and sample injection volume was 10µL. The gradient method included 85% A to15% B (8 min), 80% A and 20% B (12min) , 55% A and 45% B (4 min), 50% A to 50% B (5min), 0%A to 100% B (7min) and 85% A to 15% B (4min). The excitation and emission of the fluorescence detector were set at 340 nm and 455 nm respectively for monitoring the derivatized amino acids. Perkin Elmer TotalChrom version 6.3.2. software was used to process the data.

4.2.8. Statistical analysis

The two-way analysis-of-variance (ANOVA) with size of onion bulbs and the seed treatment, and their interaction was performed using JMP pro 14 software. Excel software was used to prepare graphs and mean comparison was done by Student's *t*-test at 5% probability. Results of flavonoids and amino acids were subjected to multivariate statistical analysis using MetaboAnalyst 4.0 (http://www.metaboanalyst.ca/). Results are presented as mean ± standard error of mean.

4.3. Result and discussion

4.3.1. Global Metabolic Response to NPs Priming in onion flavonoid

To gain a fundamental insight into the structure of the generated data set, a supervised multivariate method, partial least squares-discriminant analysis (PLS-DA) was performed. An untargeted UPLC/ESI-HR-QTOFMS metabolomics approach was used to understand the effect of different size and nanopriming treatments on global metabolic responses of onion. The PLS- DA score plots of unprimed (T1), hydroprimed (T2), TNE (T3), CNE (T4), AgNPs (T5), and AuNPs (T6) treated onion bulb extracts from three different locations, Weslaco, Uvalde and College Station are presented in Figure 20.

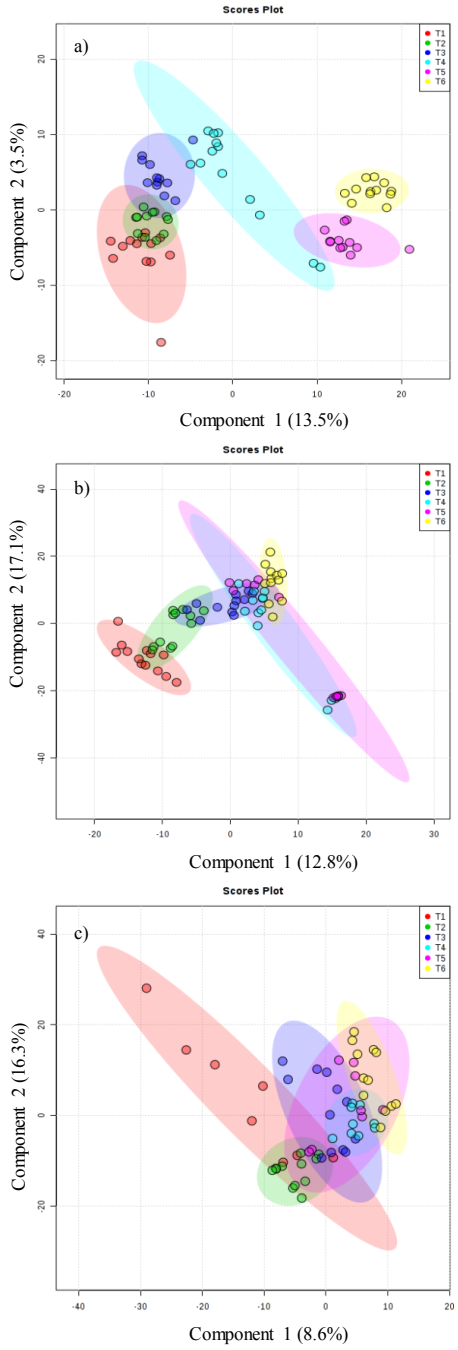

Figure 20 Partial least squares discriminant analysis (PLS-DA) score plots of global metabolic responses of onion juice to different NPs priming treatments compared to unprimed control onions harvested from a) Weslaco b) Uvalde, and c) College Station. Ellipses represent 95% confidence intervals. T1: Unprimed, T2: Hydroprimed, T3: Turmeric nanoemulsion, T4: Citrus nanoemulsion, T5: Silver nanoparticles, and T6: Gold nanoparticles.

In Weslaco harvested onion, the first principle component (PC1) explained 13.5% of the variance and the second principle component (PC2) explained 3.5% of the variance. Similarly, in Uvalde and College Station, PC1 explained 12.8% and 8.6%, respectively, while PC2 explained 8.6% and 16.3% respectively. Nanopriming had separate clusters from hydroprimed and unprimed groups in score plots, which indicate that NP priming influences the metabolome of onion bulbs (Figure 20). However, there was no clear separation of clusters in between the nanopriming treatments.

In addition, distinct clusters for each size category of onion extract further revealed that metabolic alterations in the onion in response to nanopriming was size dependent (Figure 21). In Weslaco, Uvalde, and College Station harvested onion, PC1 explained 5.5%, 10.4% and 20.6% of variance, respectively. Similarly, PC2 explained 5.6%, 5% and 3.2% of variance in Weslaco, Uvalde, and College Station onion samples, respectively. In all treatments and locations, metabolome declined as bulb size increased. A reduced metabolite in larger bulbs might be caused by the dilution effect.

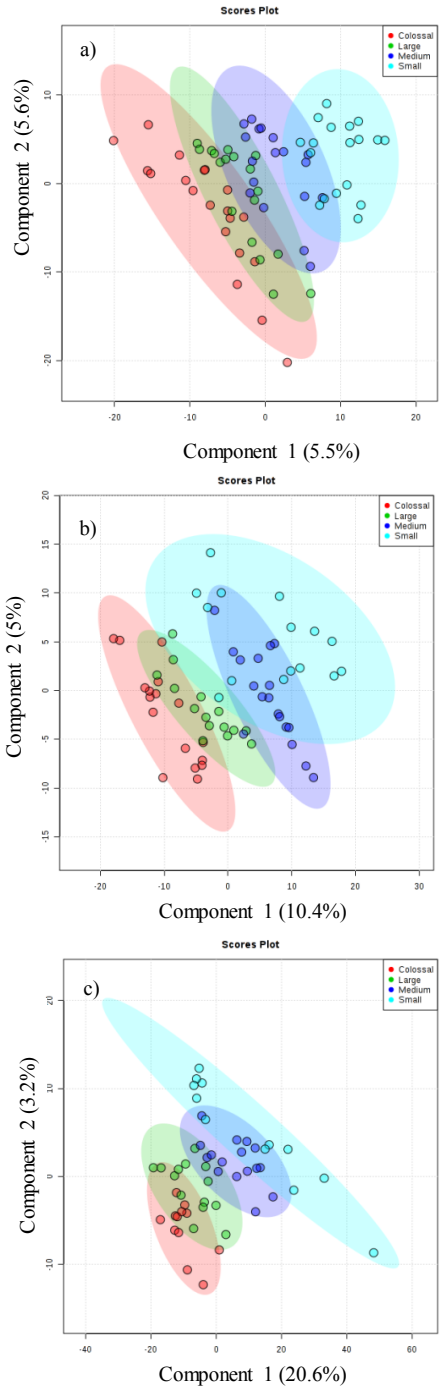

Figure 21 Partial least squares discriminant analysis (PLS-DA) score plots of global metabolic responses of onion juice to different bulb size i.e. jumbo (>100 mm), large (75−100 mm), medium (50−75 mm), and small (<50 mm) sized onions harvested from a) Weslaco b) Uvalde, and c) College Station. Ellipses represent 95% confidence intervals.

4.3.2. Metabolic profiling of onion using LC-HR-ESI-QTOF-MS

In the present study, 8 flavonoids were identified using LC-HR-ESI-QTOF-MS in positive ionization mode (Figure 22). The tandem mass spectra, +bbCID spectra, protonated accurate mass and mass error of identified flavonoids are presented in Figure 23 and Figure C1. A peak eluted at retention time (t_R) 5.7 min exhibits UV spectrum (λ_{max}) at 320 nm which corresponds to characteristic flavonoid moiety. A MS spectrum showed an accurate mass at *m/z* 789.2083$[M+H]^+$ (mass error 0.12 ppm). The precursor ion loss a glucose molecule to give a product ion at *m/z* 465.1028 $[M+H-162-162]^+$. It further loss a one glucose molecule to give a promonent base peak at *m/z* 303.0502 $[M+H-465-162]^+$ $(Y_0)^+$ which corresponded to the aglycone moiety. Thus, based on the UV, MS and +bbCID mass spectra, and published literatures present peak was identified as quercetin 3,7,4′-triglucoside. Similarly, another peak eluted at t_R 6.7 min represents the molecular ion peak at *m/z* 627.1566 $[M+H]^+$ (mass error -1.63 ppm) and product ion at *m/z* 465.1026 $[M-162]^+$ and *m/z* 303.0520 $[M+H-465-162]^+$ $(Y_0)^+$ was identified as quercetin 3, 4′-di-*O*-glucoside. LC-HR-QTOF-MS spectra of the precursor ion (t_R 6.9 min) showed as accurate mass at *m/z* 641.1715 $[M+H]^+$ (mass error -0.42 ppm). The precursor ion losses two molecule of glucose to prominent product ion peak at *m/z* 317.0656 $[M+H-162-162]^+$ which attributed to aglycone isorhamnetin moiety. Thus, the present peak identified as isohamnetin 4′-glucoside. Two peaks eluted at 7.4 and 7.9 min displays a molecular ion at *m/z* 465.1038 $[M+H]^+$ (mass error -2.25 ppm) and at *m/z* 465.1047 $[M+H]^+$ (mass error -4.18 ppm), respectively. Both peaks were identified as derivatives of quercetin glucoside. Both the peaks loss a one molecule of glucose which displayed a prominent product ion at *m/z* 303.0509 $[M+H-162]^+$ and *m/z* 303.0518 $[M+H-162]^+$, respectively. Thus, the present peaks identified as quercetin-3-*O*-glucoside and quercetin-4-*O*-glucoside, respectively. A peak (t_R 8.2

min) was identified as Isohamnetin 4′-glucoside having a precursor ion at *m/z* 479.1200 $[M+H]^+$ (mass error -3.3 ppm) and a product ion at *m/z* 317.0670 $[M+H-162]^+$ $(Y_0)^+$. Similarly, two minor peaks eluted at t_R 9.0 and 9.8 min showed UV-spectra (λ_{max}) at 320 nm. The MS spectra of both peaks displayed a precursor ion at *m/z* 303.0509 $[M+H]^+$ (mass error -3.20 ppm) and 287.0551[M+H]+ (mass error -0.3 ppm), respectively, which corresponds to the presence of aglycone quercetin and kaempferol.

Onion metabolites other than major flavonoids were also identified such as derivative of γ-glutamyl peptides, amino acid and flavonoids glucoside (Table 3 and Figure C2). Amino acid valine, methionine, tryptophan, phenylalanine, leucine and cystine were accumulates in conjugated form as γ-glutamyl peptides. A mass spectrum of γ-Glu-Met, γ-Glu-Val, and γ-Glu-Tyr showed an accurate mass at *m/z* 279.101 $[M+H]^+$ (mass error -12.8 ppm), *m/z* 247.130 $[M+H]^+$ (mass error -4.2 ppm), and *m/z* 311.125 $[M+H]^+$ (mass error -12.8 ppm), respectively.

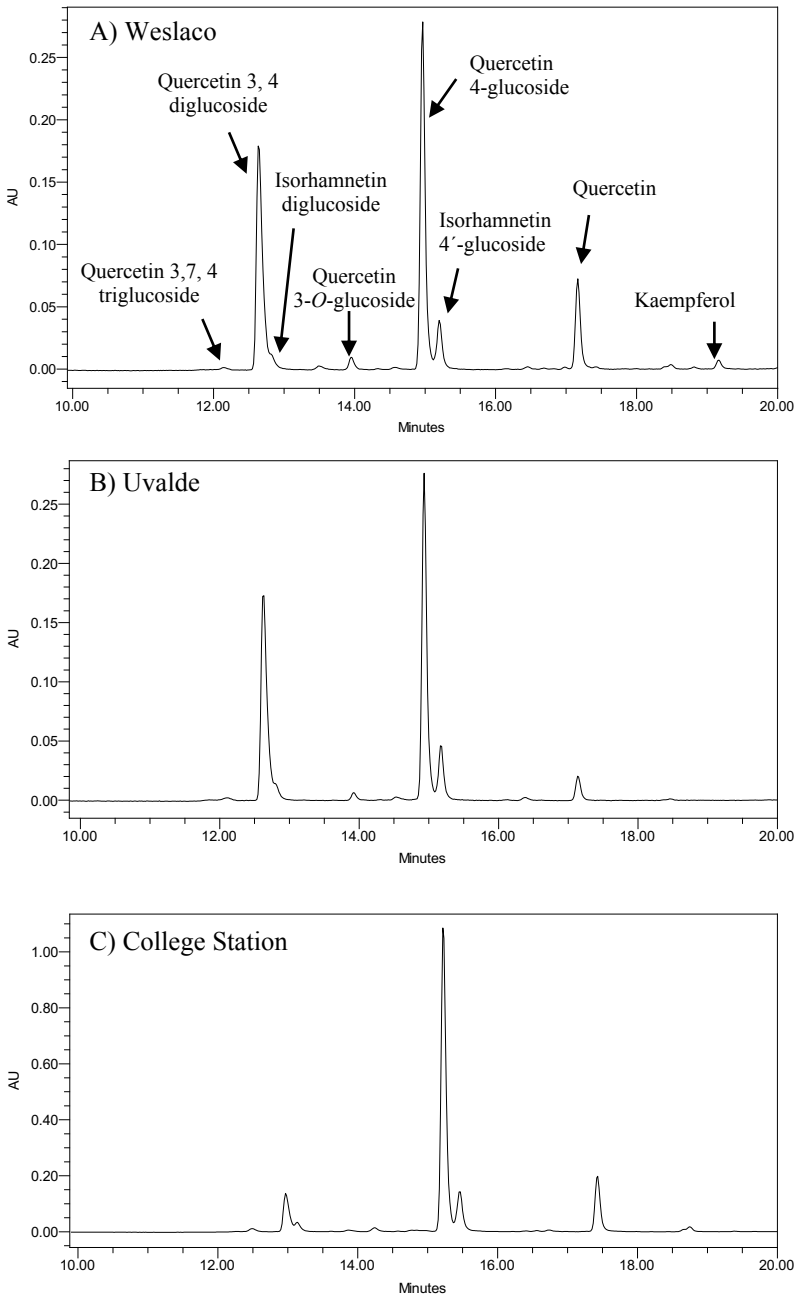

Figure 22 HPLC chromatograms of onion extract harvested from (A) Weslaco, (B) Uvalde, and (C) College Station. The chromatogram indicates that the level of flavonoid content was affected by growing locations.

Table 3 Metabolites identified by UHPLC/HR-ESI-QTOFMS in positive ion mode other than flavonoids.

RT (min)	Identified Compound	Molecular formula	Experimental Mass	Theoretical Mass	Mass error (ppm)
3.2	γ Glu-Met	$C_{10}H_{18}N_2O_5S$	279.105	279.101	-12.830
3.3	γ Glu-Val	$C_{10}H_{18}N_2O_5$	247.130	247.129	-4.257
3.4	Phenylalanine	$C_9H_{11}NO_2$	166.089	166.086	-18.334
4.2	γ Glu-Tyr	$C_{14}H_{18}N_2O_6$	311.125	311.124	-3.976
4.7	Cys (2-CP)-Gly	$C_9H_{16}N_2O_5S$	265.086	265.085	-0.871
4.9	γ Glu-Cys (2-CP)-Gly Hexoside	$C_{20}H_{33}N_3O_{13}S$	556.185	556.181	-7.756
5.1	Tryptophan	$C_{11}H_{12}N_2O_2$	205.099	205.097	-9.001
5.4	γ Glu-leu	$C_{11}H_{20}N_2O_5$	261.148	261.144	-14.559
5.5	γ-Glu-Cys (Prop-1-enyl)	$C_{11}H_{18}N_2O_5S$	291.106	291.101	-16.424
5.7	γ Glu-Cys (Propyl)	$C_{11}H_{20}N_2O_5S$	293.117	293.117	-2.153
5.8	γ Glu-Phe	$C_{14}H_{18}N_2O_5$	295.133	295.129	-13.391
6.2	γ Glu-Trp	$C_{16}H_{19}N_3O_5$	334.141	334.140	-2.553
6.7	γ Glu-Cys (S Prop-1-enyl)-Gly	$C_{13}H_{21}N_3O_6S_2$	380.096	380.094	-2.752
6.9	γ Glu-Cys (S Propyl)-Gly	$C_{13}H_{23}N_3O_6S_2$	382.110	382.110	-0.251
8	Kaempferol -3-O-B-Glc	$C_{21}H_{20}O_{11}$	449.108	449.108	-0.361
8.6	N-(p-Coumaroyl)-tyramine	$C_{17}H_{17}NO_3$	284.128	284.128	1.830

We also identified S-alkylated and S-alkenyl cysteine derivatives, γ Glu-Cys (Propyl) and γ-Glu-Cys(Prop-1-enyl) with a molecular ion peak at *m/z* 293.117 $[M+H]^+$ (mass error -2.1 ppm) and 291.106 $[M+H]^+$ (mass error -16.4 ppm). Cysteine derivative of carboxy propyl (CP) were also observed, Cys (2-CP)-Gly (*m/z* 265.3086 $[M+H]^+$; -0.87 ppm) and γ-Glu-Cys(2-CP)-Gly-hexoside (*m/z* 556.185 $[M+H]^+$; -7.75 ppm). A minor peak eluted at t_R 8 min represents a molecular ion peak at *m/z* 449.1080 $[M+H]^+$ (mass error -0.361 ppm) and product ion at *m/z* 287.0553 $[M-162]^+$ was identified as kaempferol-3-*O*-gluciosde.

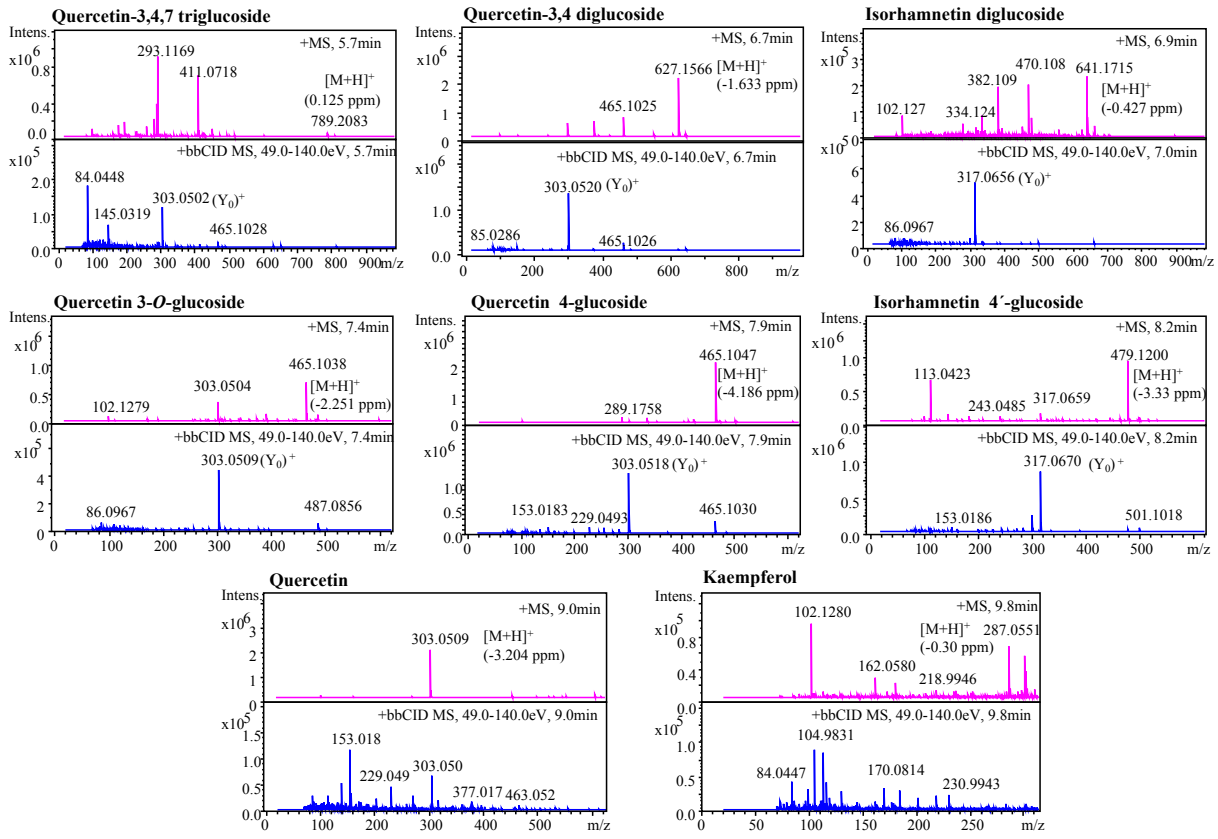

Figure 23 Tandem mass spectra in positive ionization mode. 1: quercetin 3,7,4′-triglucoside; 2: quercetin 3,4-diglucoside; 3: isorhamnetin diglucoside; 4: quercetin 3-O-glucoside; 5: quercetin 7,4′-diglucoside; 6: quercetin 4-glucoside; 7: isorhamnetin 4′-glucoside; 8: quercetin; and 8: Kaempferol.

4.3.3. Influence of bulb size in flavonoid content

The flavonoid composition was determined in the colossal, large, medium and small sized onions of the nano-treated and untreated onions harvested from three different locations. As indicated by the two-way ANOVA (Table 4), the levels of flavonoids were strongly affected by the size of the onion bulbs.

Table 4 Influence of bulb size and nanopriming in the flavonoid content (μg/g) of onion

Factors		Quercetin 3,7,4 triglucoside	Quercetin 3,4 diglucoside	Isorhamnetin diglucoside	Quercetin 3-*O*-glucoside	Quercetin 4-glucoside	Isorhamnetin 4'-glucoside	Quercetin	Kaempferol
Weslaco									
Bulb size (S)	Colossal	0.57c	44.49c	9.76bc	4.32ab	60.89b	9.81b	13.01b	0.52b
	Large	0.92bc	47.75c	9.11c	2.65b	64.04b	11.11b	11.82b	0.94a
	Medium	1.20ab	60.57b	11.19ab	3.52ab	69.92b	15.30a	13.25a	0.90a
	Small	1.50a	89.30a	17.01a	5.61a	100.57a	18.63a	16.88a	0.91a
Treatments (T)	Control	0.73ab	50.08c	7.08c	3.98a	65.15b	14.56a	18.31ab	1.28a
	HP	0.71b	52.68c	11.13b	5.62a	78.97ab	13.76a	21.73a	1.01ab
	TNE	1.15ab	65.61ab	13.20b	4.23a	87.26a	14.53a	14.64bc	0.68bc
	CNE	1.33ab	60.92bc	11.06b	2.81a	74.20ab	12.25a	8.13d	0.29d
	AgNP	1.51a	58.89bc	12.60b	4.79a	70.95ab	11.94a	11.35cd	0.54cd
	AuNP	0.87ab	74.99a	15.54a	2.73a	66.61b	15.26a	8.27d	1.09ab
Interaction	(S x T)	*	**	**	NS	**	**	*	**
Uvalde									
Bulb size (S)	Colossal	0.54b	29.45b	6.08b	2.55a	39.66b	8.50b	8.03b	0.41b
	Large	0.97ab	46.10a	8.82a	2.61a	69.92a	13.98a	10.92a	0.56a
	Medium	1.40a	52.66a	9.17a	4.78a	68.40a	12.31a	9.30ab	0.38b
	Small	0.94ab	48.32a	9.24a	2.74a	65.27a	11.73a	10.28ab	0.44ab
Treatments (T)	Control	0.74ab	51.06ab	9.00ab	2.20b	67.33ab	11.99a	7.11de	0.23c
	HP	0.42b	30.28c	7.12b	1.49b	38.60c	8.34b	5.70e	0.26c
	TNE	0.94ab	40.10bc	7.91ab	2.05b	54.81bc	10.75ab	10.32bc	0.49b
	CNE	1.35a	55.86a	9.63a	8.31a	81.73a	14.31a	12.82ab	0.68a
	AgNP	1.05ab	40.69bc	8.37ab	2.75b	57.32bc	12.23a	13.14a	0.79a
	AuNP	1.28a	46.83ab	7.94ab	2.23b	65.11ab	12.15a	8.70cd	0.22c
Interaction	(S x T)	*	**	**	*	NS	*	NS	NS
College Station									
Bulb size (S)	Colossal	1.79c	19.03bc	5.51b	4.42b	71.46c	11.11c	32.37b	1.29b
	Large	3.20b	16.42c	5.84b	5.32ab	111.09b	15.61b	40.98ab	2.75b
	Medium	6.25a	31.21a	8.47a	7.21a	163.97a	25.66a	49.38a	4.47a
	Small	3.18b	23.82b	7.86a	4.71b	123.04b	17.28b	35.68b	2.12b
Treatments (T)	Control	2.87ab	19.12c	4.55c	4.33a	108.03b	18.11bc	30.09bc	2.63ab
	HP	2.44b	22.03c	8.28b	6.62a	91.58b	13.59c	36.81b	2.83ab
	TNE	4.58a	8.74d	5.22c	4.61a	172.46a	23.01a	61.31a	3.96a
	CNE	3.30ab	9.46d	3.54c	6.78a	106.63b	15.30c	52.86a	2.49ab
	AgNP	4.34ab	33.80b	8.42b	5.47a	123.32b	20.49ab	33.54bc	2.79ab
	AuNP	4.10ab	42.57a	11.50a	4.67a	102.32b	13.99c	23.00c	1.25b
Interaction	(S x T)	**	**	**	**	**	**	**	**

Statistical analysis was performed using two-way ANOVA and means were compared using Student's t-test. Different letters indicate significant differences at *P < 0.05, **P < 0.01. HP: Hydroprimed, TNE: Turmeric nanoemulsion, CNE: Citrus nanoemulsion, AgNP: Silver nanoparticles, AuNP: Gold nanoparticles, and NS: Non-significant.

Small-sized onions had a significantly higher content of all the quantified flavonoids in onions extract harvested from Weslaco. The level of kaempferol, isorhamnetin and quercetin aglycones were not significantly different in between the small and medium sized onions. Besides, kaempferol, all the other quantified flavonoids were significantly lower in colossal sized onions from Uvalde. However, there was no significant differences in between small, medium and large sized onions. Medium sized onions from College Station had the significantly higher flavonoids which was followed by the small, large and colossal onions. In general, onions of small and medium size had higher level of flavonoid content as compared to the large and the colossal onions. These findings show the need for sampling onion bulbs with a typical average size when the intention is to characterize onions as regards to their levels of flavonoids. Our data are in agreement with Vermelha da Po´voa onions where small sized had a higher content of total flavonols than large onion.[146] However, no significant differences in quercetin glucoside content between small, medium and large onions were found in other studies.[134, 147]

4.3.4. Influence of nanopriming and location in the flavonoid content

The two-way ANOVA (Table 4) demonstrated the significant treatment difference in the level of flavonoids in most of the cases in all three locations. However, no treatment effect was demonstrated in the Quercetin 3-*O*-glucoside level of onions harvested from Weslaco and College Station. Similarly, isorhamnetin 4'-glucoside from Weslaco onions was also not affected by the nano-treatments. The ability of crops to synthesize selected secondary metabolites was not systematically affected by the nanopriming treatments across different bulb size and geographical locations. There is limited research regarding the effect of nanoparticles in the flavonoid content. Flavonoid concentration in cerium oxide nanoparticles treated medium amylose rice samples increased by 12.5% relative to the control.[148] These results indicate that

biosynthesized nanomaterials were nonphytotoxic pertaining to the nutritional quality of the onion.

Similarly, the level of different flavonoids was different in the three different studied locations (Table 4). Quercetin 3,4 diglucoside and isorhamnetin diglucoside were higher in the onion harvested from Weslaco. However, remaining quantified flavonoids; Quercetin 3, 7, 4 triglucoside, quercetin 3-*O*-glucoside, quercetin 4-glucoside, isorhamnetin 4'-glucoside, quercetin and kaempferol were found at enhanced level in the samples from College Station as compared to the Weslaco and Uvalde. Our data are in agreement with 'Sweet Vidalia' onions where significant effect of location was observed.[149] Patil et. al.,[134] also observed the location effect in the quercetin concentration of onion. This location effect could be owing to the difference in soil type, light intensity, and weather condition in between the three different locations.

4.3.5. Multivariate analysis of effect of nanopriming treatments on amino acids

The total flavonoid was found higher in Weslaco harvested onion samples as compared to the other two locations, Uvalde and College Station. Therefore, we quantified the amino acids level in Weslaco onion samples and did multivariate analysis to see the overall comprehensive picture. Quantification of each amino acid was carried out using individual reference standard. To visualize general trends, grouping, and the influence of each nano treatments, we conducted Partial Least Squares Discriminant Analysis (PLS-DA), which is a supervised clustering method. The first principle component (PC1) explained 22.6% of the variance, and the second component (PC2) explained 10.5% of the variance (Figure 24). The score plots from PC1 and PC2 clearly separated the control (T1 and T2) and nano-treated plants, reflecting differences in amino acids profiles.

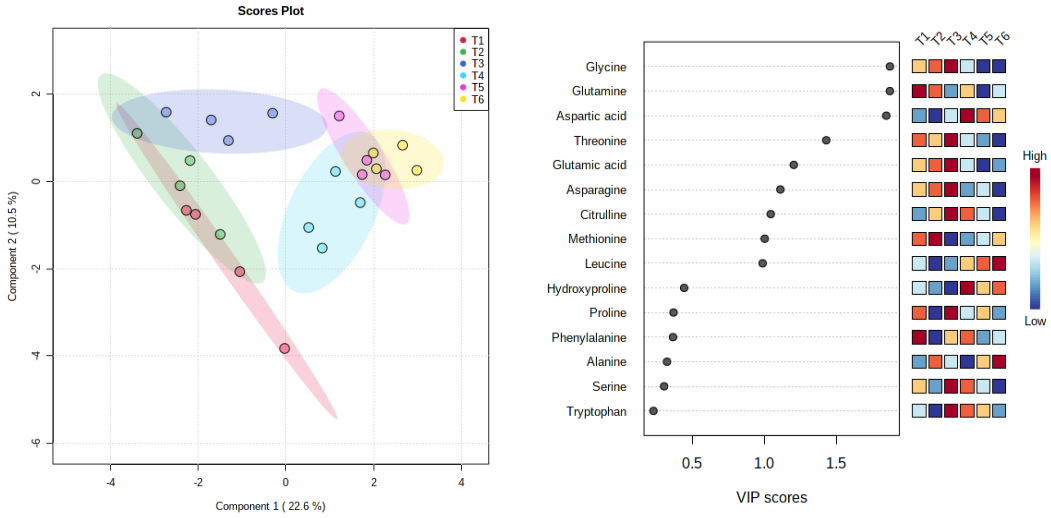

Figure 24 Partial least squares discriminant analysis (PLS-DA) score plots of amino acids present in onions harvested from Weslaco. Ellipses represent 95% confidence intervals. T1: Unprimed, T2: Hydroprimed, T3: Turmeric nanoemulsion, T4: Citrus nanoemulsion, T5: Silver nanoparticles, and T6: Gold nanoparticles.

However, no difference was found between nano-treatments. Together, these data show that nano treatments changed the pattern of amino acids in onion. Furthermore, the variable importance on projection (VIP) score plots were obtained from the PLS-DA models. The compounds responsible for clustering in six different treatments were identified based on their VIP scores exceeding 1.0 The common amino acids with VIP scores > 1.0 were glycine, glutamine, aspartic acid, threonine, glutamic acid, asparagine, citrulline, methionine and leucine. Among them, glycine, glutamine, and aspartic acid were most discriminating metabolite scoring >1.5.

4.3.6. Amino acid composition of onion bulbs

A total of 19 amino acids were found in the studied onion cultivar Legend. Table 5 shows the content of all amino acids (μg/mL) in onions among nano-priming treatments and different bulb sizes. The most abundant amino acids were asparagine, aspartic acid, glutamic acid, glutamine and arginine. There were no significant differences in arginine, serine, valine, phenylalanine and isoleucine among the nano-priming treatments. For the other amino acids, differential effect of treatments was observed. Glutamine was found significantly high in unprimed control treatment. Similarly, aspartic acid, beta alanine, alanine, and leucine were highest in AuNPs treated onion. Total amino acid is higher in all the nano-treated onion samples compared to the unprimed and hydroprimed control treatment. Accumulation of amino acids under stress conditions has been reported in published literature.[140, 150] Stress lead to the protein breakdown, causing the overall increase in free amino acids. Also, increase in the levels of specific amino acids have shown beneficial effect in a stressful environment.[150] Application of nanopriming causes the oxidative stress in the plant which might contribute to the higher amino acids level compared to the control.

Similarly, differential effect of bulb size was observed in the level of amino acids. Arginine, serine, hydroxyproline, threonine, valine, isoleucine and leucine were not significantly different among the different size of onion bulbs. Asparagine, citrulline, glutamic acid, aspartic acid, glycine, proline, and tryptophan were significantly high in the small sized onions as compared to the others. However, level of glutamine, beta alanine, alanine, methionine, phenylalanine was found significantly high in the colossal onions and the level reduces with the size of onions.

Amino acid composition in food is very crucial owing to their role as protein building blocks. Arginine was reported as the most abundant amino acid in different onion cultivars.[142-143] Arginine have an major role as a source of nitrogen, which is an extremely important amino acid during the period of maturation.[143] Glutamic acid and arginine might be responsible for the color of onion seed.[151] Glutamine was found as the most crucial "umami" substrate responsible for specific onion taste.[152] Content of free amino acid are widely influenced by different cultivars,[141] ploidy level,[143] stage of development at harvest and the long term storage of onion.[142] Yellow onion contained the highest amounts of amino acids compared to the red onions and shallots.[109] However, in comparison with white onions, the total amino acids was significantly low in yellow onion cultivars.[141]

4.4. Conclusion

In conclusion, eight flavonoids were quantified in onions using LC-HR-ESI-QTOF-MS in positive ionization mode. Similarly, a total of 19 amino acids were found in the studied onion cultivar among which the most abundant amino acids were asparagine, aspartic acid, glutamic acid, glutamine and arginine. The levels of flavonoids were strongly affected by the location and size of the onion bulbs. In all the locations, relatively small-sized onions had a higher content of all the flavonoids and the trend was similar in total amino acids. Differential effect of treatments was observed in the amino acids content of onion. In addition, multivariate analysis demonstrated the distinct clusters for each size and treatment category of onion extract which further revealed that metabolic alterations in the onion in response to nanopriming was size and treatment dependent. Results indicated that biosynthesized nanomaterials had differential effect on the nutritional quality of onion.

Table 5 Effect of nano-priming treatments and the bulb size in the level of amino acids (μg/mL) present in onions. Statistical analysis was performed using two-way ANOVA and means were compared using Student's t-test. Different letters indicate significant differences at $*p < 0.05$, $**p < 0.01$. HP: Hydroprimed, TNE: Turmeric nanoemulsion, CNE: Citrus nanoemulsion, AgNP: Silver nanoparticles, and AuNP: Gold nanoparticles.

Amino acids	Treatment (T)						Size (S)				Interaction
	T1	**T2**	**T3**	**T4**	**T5**	**T6**	**Colossal**	**Large**	**Medium**	**Small**	**T × S**
Arginine	476.99^{a}	457.48^{a}	482.73^{a}	396.79^{a}	479.02^{a}	509.37^{a}	460.34^{a}	435.43^{a}	494.61^{a}	477.88^{a}	**
Asparagine	1701.52^{a}	1760.20^{a}	1856.67^{a}	1435.67^{b}	1457.44^{b}	1472.53^{b}	1602.02^{ab}	1441.03^{b}	1684.09^{a}	1728.88^{a}	**
Glutamine	734.27^{a}	567.40^{b}	366.15^{cd}	387.06^{cd}	315.89^{d}	430.47^{c}	503.41^{a}	486.52^{a}	461.16^{ab}	416.40^{b}	**
Citrulline	37.94^{c}	51.10^{b}	58.96^{a}	48.36^{b}	36.02^{c}	15.01^{d}	30.63^{d}	35.92^{c}	40.34^{b}	48.04^{a}	**
Serine	58.80^{a}	52.56^{a}	65.02^{a}	59.09^{a}	57.53^{a}	52.23^{a}	53.98^{a}	53.97^{a}	57.94^{a}	64.28^{a}	**
Glutamic acid	1043.98^{c}	1309.30^{b}	1618.57^{a}	746.44^{d}	675.52^{d}	666.35^{d}	849.55^{b}	907.35^{b}	1107.52^{a}	1175.69^{a}	**
Hydroxyproline	481.87^{a}	487.06^{a}	150.01^{b}	520.42^{a}	488.44^{a}	488.94^{a}	428.55^{a}	401.52^{a}	407.29^{a}	407.13^{a}	*
Aspartic acid	1122.16^{d}	723.20^{e}	1840.76^{c}	3081.67^{a}	2477.45^{b}	2524.82^{b}	1882.08^{b}	1847.98^{b}	1871.12^{b}	2245.53^{a}	**
Threonine	70.85^{b}	69.51^{b}	83.24^{a}	57.46^{b}	60.52^{b}	70.37^{ab}	68.61^{a}	63.14^{a}	72.43^{a}	70.45^{a}	**
Glycine	13.47^{b}	17.73^{a}	18.00^{a}	11.83^{b}	5.01^{c}	5.06^{c}	8.18^{b}	11.11^{ab}	9.20^{ab}	12.20^{a}	**
Beta alanine	30.91^{a}	11.90^{c}	19.59^{b}	22.43^{b}	23.71^{b}	32.26^{a}	30.52^{a}	22.53^{b}	17.90^{b}	22.91^{b}	**
Alanine	32.15^{c}	52.23^{ab}	37.71^{bc}	15.15^{d}	41.32^{bc}	55.71^{a}	48.58^{a}	43.30^{ab}	35.21^{bc}	29.09^{c}	**
Proline	72.20^{a}	21.12^{d}	74.53^{a}	57.94^{c}	67.56^{ab}	61.88b^{c}	53.56^{bc}	56.46^{ab}	61.73^{ab}	65.07^{a}	**
Methionine	16.25^{b}	35.70^{a}	13.66^{b}	13.63^{b}	14.59^{b}	15.56^{b}	20.81^{a}	17.32^{ab}	18.50^{b}	16.29^{b}	*
Valine	311.08^{a}	298.96^{a}	298.81^{a}	298.96^{a}	291.89^{a}	318.67^{a}	302.93^{a}	288.27^{a}	310.88^{a}	310.17^{a}	**
Tryptophan	53.04^{b}	48.22^{b}	61.65^{a}	54.23^{ab}	55.79^{ab}	53.91^{ab}	46.40^{c}	53.28^{b}	57.29^{ab}	60.92^{a}	**
Phenylalanine	89.17^{a}	75.19^{a}	82.64^{a}	82.34^{a}	77.04^{a}	83.71^{a}	86.17^{a}	84.74^{a}	84.63^{a}	71.19^{b}	**
Isoleucine	35.47^{a}	30.03^{a}	37.76^{a}	33.66^{a}	34.44^{a}	33.01^{a}	33.90^{a}	31.26^{a}	34.15^{a}	36.93^{a}	*
Leucine	89.9^{ab}	71.05^{c}	83.38^{bc}	93.14^{ab}	90.75^{ab}	101.18^{a}	86.69^{a}	86.58^{a}	88.89^{a}	90.77^{a}	**

5. NANOPARTICLE-MEDIATED SEED PRIMING IMPROVES GERMINATION, GROWTH, YIELD, AND QUALITY OF WATERMELONS (*Citrullus lanatus*) AT MULTI-LOCATIONS IN TEXAS*

5.1. Introduction

Rapid and uniform seed germination is important for adequate crop establishment to ensure economic sustainability and efficient use of production resources in commercial agriculture.[7] This situation is particularly evident in high-value specialty crops such as watermelons where demand and production of seedless (triploid) varieties has become very popular compared to traditional seeded (diploid) varieties.[153] However, seedless (triploid) varieties have several production limitations, including low seed germination rates compared with diploid varieties, and generally lower stand establishment rates as a result of seedling sensitivity to environmental stresses. Seed characteristics partly account for these limitations. Triploid watermelon seeds are smaller in size, which has been associated with a limited amount of reserves to support germination and seedling growth. Significantly smaller lipid bodies and lower starch levels have been reported in triploid compared to the diploid seeds and these observations were correlated with significantly lower average germination rates for triploid seeds.[154,155] Besides size, other seed characteristics such as their thick seed coat, weak embryos, dense endotesta layers, and strong adherence of the seed coat to the cotyledon[156] have also been noted as being significantly different from those of seeded varieties. Triploid seeds also tend to

* Reprinted with permission from Acharya, P., Jayaprakasha, G. K., Crosby, K. M., Jifon, J. L., & Patil, B. S. (2020). "Nanoparticle-mediated seed priming improves germination, growth, yield, and quality of watermelons (*Citrullus lanatus*) at multi-locations in Texas." Scientific reports, 10(1), 1-16. Copyright 2020 Springer Nature.

have an airspace surrounding the embryo, which may contribute to moisture deficit sensitivity.[156] It is possible that these seed characteristics have implications for water imbibition and onset of germination.

Semi-permeable layers in the seed coat of many crop species allow gas exchange and water uptake while restricting solute leakage. Watermelon seed coats have a thick aniline blue-staining layer,[157] which may affect water permeability and consequently, seed germination. Thicker seed coats in triploid watermelon varieties could further lead to oxygen deprivation, resulting in poor germination, inconsistent emergence, and poor stand establishment.[156] To improve seed coat permeability to water and oxygen, treatments such as seed coat removal, scarification, and seed nicking have been investigated with varying degrees of success for enhancing seed germination and seedling vigor. However, seedling vigor of triploid seeds is still lower than that of diploids.[158] Therefore, to improve seed germination and seedling vigor, novel seed priming techniques are needed.

Seed priming prior to sowing is a promising strategy to provide value-added solutions that enhance the yield and quality potential of high-value crops. Priming has been shown to result in higher emergence rates, vigorous seedling growth, and faster stand establishment rates. Priming induces an increase in the activity of enzymes such as amylases, proteases, and lipases that break down macromolecules for growth and development of the embryo. Priming also alleviates stress at the germination stage and ultimately results in higher rates of seedling emergence and successful seedling establishment.[159,28] These biological effects ultimately benefit farmers because they reduce the time, expense of re-seeding, additional irrigation, fertilization, and weed management on weak plants.

More recently, nanotechnology has emerged as an advanced seed priming technology for smart agriculture. Important and unique features of nanoparticles, such as their surface to mass ratio, which is much larger than that of other particles and materials, allows them to efficiently enhance catalysis, as well as to adsorb and deliver substances of interest.[160] Nanoparticles derived from metals or their compounds have been developed and used as carriers for biological systems. Our group has demonstrated significantly improved germination in diploid and triploid watermelon varieties with iron nanoparticle priming compared to the unprimed group.[13] This is probably due to the fact that nano-priming has the added advantage of being able to trigger certain metabolic processes that are normally activated during the early phase of germination. Consequently, nano-priming enhances the rate of emergence and subsequent growth, yield, and quality of the crop.

Synthesis of plant-based nanoparticles is a further refinement of nanotechnology that uses sustainable manufacturing processes to produce safe and innocuous nanoscale biomaterials for agricultural applications. Agro-industrial byproducts from turmeric and onions were used in this study to develop value-added nanomaterials that are environmentally benign and economically viable for large-scale production. Turmeric oil extracted from curcumin-removed turmeric oleoresin was used for the formulation of turmeric oil nanoemulsion (TNE). For preparing silver nanoparticles (AgNPs), onion peel extract was used as a reducing agent. Silver-based 'green' nanoparticles have the added protective advantage because silver has proven anti-bactericidal and anti-fungicidal properties.[161]

Based on the unique physical and chemical properties of nanoparticles and the aforementioned benefits as a delivery mechanism in biological systems, we hypothesized that seed priming with plant-based nanoparticles would improve germination/emergence rates, seedling

vigor, and other growth parameters of triploid watermelons. Accordingly, this study investigated the effects of seed priming with green nanoparticles on various aspects of watermelon production, from seed germination to fruit yield and postharvest nutritional quality. The study also involved multi-location field investigations to assess if the nanoparticle-mediated benefits are region-specific. To the best of the authors' knowledge, this is the first study to report the effects of nanopriming on seed germination, growth, yield, and nutritional qualities of watermelon.

5.2. Materials and Methods

5.2.1. Chemicals and Materials

Silver nitrate ($AgNO_3$) and surfactants polysorbate (Tween 20) and sorbitan monolaurate (Span 20) required for preparing AgNPs and TNE, respectively, were procured from Sigma-Aldrich (Sigma-Aldrich Chemical Co, St. Louis, MO, USA). The curcumin-removed turmeric oleoresin (CRTO) was obtained from Sami Labs Limited (Bangalore, India). Two hybrid varieties of watermelon seeds, Riverside (diploid) and Maxima (triploid) were obtained from Origene America Inc. (Alamo, TX, USA).

5.2.2. Formulation of nanoemulsions using turmeric oil

Turmeric oil nanoemulsion formation was carried out using a low energy method based on a spontaneous emulsification procedure[22] with minor modifications. The lipophilic phase was prepared by adding 250 mg of Span 20 in 25 mL of nanopure water followed by two hours of stirring on a benchtop magnetic stirrer (VWR International, Missouri City, TX, USA) at 1500 rpm. Similarly, the aqueous phase was prepared by adding 450 mg of Tween 20 in 75 mL of nanopure water with agitation by a magnetic stirrer for two hours. In this spontaneous emulsification method, 2 mL turmeric oil and lipophilic surfactant (25 mL) were mixed together and then the mixture was

poured into 75 mL of aqueous phase while continuously stirring the system with the magnetic stirrer at ambient temperature and kept under vigorous stirring overnight to prepare the TNE.

5.2.3. Green synthesis of silver nanoparticles

AgNPs were prepared using onion peel water extract as a reducing agent. Onion peel (25 g) was boiled for 10 min in 200 mL of nanopure water. The extract was filtered through Whatman filter paper grade 1 followed by a cellulose filter for the synthesis of AgNPs. AgNPs were prepared by adding 0.5 mL of freshly prepared onion extract to 10 mL of 0.01 M $AgNO_3$ solution at 80°C with continuous stirring for 5 minutes. A reddish dark brown color was observed after addition of onion peel extract indicating the formation of AgNPs.

5.2.4. Characterization of nanoemulsions and nanoparticles

The prepared nanomaterials were characterized by using a dynamic light scattering (DLS) technique (Malvern Zetasizer Nano-ZS model, Malvern, UK), according to our published protocol[24]. Ultraviolet-visible spectroscopy (UV-2900 Hitachi spectrophotometer) was used for optical absorption measurements of prepared AgNPs.

Similarly, the morphology and size of the AgNPs was captured by transmission electron microscopy (TEM) at 100 kV. X-ray diffraction (XRD) was used to fully understand and confirm the crystal structure and crystalline size of the AgNPs. The powder forms of AgNPs were subjected to X-ray diffraction analysis (D8 Powder Eco) at 40 kV and 25 mA with Cu Kα radiation. The scan 2θ range was 20–80°.

5.2.5. Seed treatments

Two varieties of watermelon seeds, Riverside and Maxima, were primed with TNE and AgNPs in 2017 and 2018. One-part TNE was diluted with ten parts of nanopure water to make the priming solution. A 2.5% suspension of synthesized AgNPs was used, which contains 31.3

ppm of Ag. The concentrations of nanopriming agents were selected based on preliminary experiments. The unprimed seeds were used as control. In third year 2019, along with unprimed seeds, $AgNO_3$ primed (same concentration as AgNPs), and hydroprimed seeds were also added as controls. Seeds were immersed in priming media for 12 h, in the dark, at room temperature, and the proportion of seed weight to priming solution was 1:5 g/mL. Seeds were dried at ambient temperature after rinsing 2–3 times with nanopure water.

5.2.6. Quantification of internalized nanomaterials in watermelon seeds

5.2.6.1. TNE in watermelon seeds

TNE-treated seeds were washed with water repeatedly to remove the adhering emulsion, then the seeds were crushed. A known amount (100 mg) of TNE-treated sample was extracted with 0.6 mL hexane twice and the pooled extract was filtered and used for GC-MS analysis for the identification and quantification of the major volatile compounds. The Thermo Finnegan gas chromatograph (Thermo Fisher Scientific, Inc., San Jose, CA, USA) coupled with an electron ionization (EI) source with a Dual-Stage Quadrupole (DSQ II) mass spectrometer (Thermo Scientific, Austin, TX, USA) was used for volatile analysis. Chromatographic separation was carried out on a polar phase column Rtx-Wax of 30 m × 0.25 mm i.d. 0.25 um film thickness) (Restek Corporation, Bellefonte, PA, USA). Helium was used as a carrier gas with a flow rate of 1 mL/min and sample volume 2 µL was injected into the GC injector at 225°C. The initial oven temperature was maintained at 50°C, then increased to 230°C at a rate of 10°C/min, held for 5 min, with a total run time of 23 min. Electron impact (EI) data from m/z 40 to 400 were acquired at a scanning speed of 16.67 scans/sec. The temperatures of ion source and mass transfer line were maintained at 285°C and 280°C, respectively. The data were processed using Xcalibur software (v. 2.0.7., Thermo-Fisher Scientific, San Jose, CA, USA).

5.2.6.2. AgNPs in watermelon seeds

Mass fractions of Ag were determined by comparative instrumental neutron activation analysis (INAA).[27] In order to identity and quantify Ag in watermelon seed samples, three sets of control and AgNP-treated seeds were irradiated for 14 h using 1-MW TRIGA reactor. Following an 11-d decay interval, gamma-ray spectra were acquired for 1 h each using an HPGe detector. These spectra were used to quantify Ag using the mean values of three gamma-ray peaks (658, 885, and 1384 keV) from the radioisotope ^{110m}Ag ($t_{1/2}$ = 249.76 d). The data reduction was conducted using the NAA software package (OpenVMS alpha processor-based Genie-ESP software) from Canberra Industries (Meriden, CT, USA).

5.2.7. Observation of seed ultrastructure

Randomly selected AgNP-primed seeds were dissected and pre-fixed using Trump's fixative and washed with Trump's buffer. Post-fixation with 1% osmium tetroxide was done. The specimen was infiltrated after dehydration through a series of acetone concentrations, then it was fixed in Spurr resin, and polymerized at 65°C for 24 h. Leica Ultracut UCT ultra-microtome was used to prepare Ultrathin sections. TEM images were obtained using a JEOL 1200Ex (JEOL, Tokyo, Japan) TEM at an accelerating voltage of 100 kV.

5.2.8. Assessment of germination of watermelon seeds

The incubator study was conducted in darkness at 30°C using Riverside (diploid) and Maxima (triploid) seeds with three treatments: control (unprimed seeds), TNE- and AgNP-treated seeds. Uniform size seeds were placed in 100 x 15 mm Petri dishes with 25 seeds per dish and each test was replicated three times. Radicle emergence to 2 mm or more was scored as germination and was recorded at 24 h intervals for ten days. Two mL of distilled water was added in alternate days to all petri dishes to prevent drying. The number of germinated seeds was

counted every day. Final germination percentage (FGP), time to 50% germination (T50), germination rate (GR), and mean germination time (MGT) were considered to study the effect of nanopriming on the germination of watermelon seeds and calculated using the published equation[162]. This experiment was repeated in the second year, 2018. In the third year 2019, the incubator study was conducted with five treatments: unprimed, hydroprimed, TNE-, $AgNO_3$- and AgNP-treated seeds. Based on the International Seed Trade Association (ISTA) guidelines, 400 seeds were tested for each treatment. For each treatment, 16 petri dishes containing 25 seeds in each replicate were tested.

5.2.9. Analysis of sugar by HPLC

Germinated seed samples from each group were collected in 24-h intervals starting from the samples just after priming (i.e., 0 h) to 96 h. Seeds were ground in liquid nitrogen with a mortar and pestle and freeze-dried. Aliquots of 100 mg freeze-dried seed samples were transferred into 1.5 mL centrifuge tubes and 600 μL of nanopure water was added. All samples were vortexed for 30 s, sonicated for 15 minutes, and centrifuged (10,000×g, 10 min). The supernatant was separated, and the residue was reextracted with 400 μL of nanopure water. Both extracts were combined and used for the HPLC analysis according to our published method[108].

5.2.10. Emergence study

A seedling was considered emerged when the cotyledons were completely raised above the media. Emergence tests were conducted using Riverside (diploid) and Maxima (triploid) seeds with a total of three treatments, i.e. control (unprimed seeds), TNE, and AgNPs. For emergence tests, seeds with different treatments were sown at the greenhouse. Twenty seeds of each treatment were individually sown in 200-cell plastic trays containing a commercial growing medium with three replications. Various results have been obtained in previous studies relating

cucurbit seed orientation to emergence.[163] In this experiment, the seeds were oriented with the radicle end up at a 90° angle to reduce the seed coat adhered to cotyledons. Trays were thoroughly moistened and moisture levels were maintained throughout the experiment. Stem length and diameter were recorded at 21 days after sowing and the same seedlings were used as watermelon transplants for the field experiment. The entire emergence experiment in the greenhouse was repeated in the second year, 2018. In third year 2019, emergence study was conducted with total five treatments: unprimed, hydroprimed, TNE-, $AgNO_3$- and AgNP-treated seeds. All the other parameters remained the same.

5.2.11. Measurement of chlorophyll in watermelon seedlings

The interaction between Chl molecules and NPs was investigated in watermelon seedlings at 21 days after sowing (DAS) to understand the potential toxicity of seed priming with the TNE and AgNPs. Leaf samples were ground in liquid nitrogen with mortar and pestle and extracted in dark conditions. One mL of acetone was added to 300 mg of leaf sample. Each sample tube was vortexed (30 s), sonicated (15 min at 4°C), and centrifuged for 10 minutes. After, decanting and filtering the extract, the residue was re-extracted with 0.5 mL of acetone. Both extracts were combined and filtered through 0.45-micron filters then used for the HPLC analysis according to our published method.[99] To understand the potential toxicity of seed priming with AgNPs in comparison with its bulk counterpart $AgNO_3$ at the same concentration, chlorophyll was measured in the leaf tissue of 14-day-old watermelon seedlings collected from the third-year emergence study.

5.2.12. Transplanting watermelon seedlings

Field experiments were conducted to evaluate greenhouse results in field conditions. Growing location and other environmental factors can significantly affect the growth and yield

of watermelon. Watermelons seedlings (5–7 weeks old) were transplanted at four different locations in Texas; Edinburg (26°18′15″N 98°9′50″W), Snook (30°29′25″N 96°28′11″W), Pecos (31°24′56″N 103°30′0″W), and Grapeland (31°29′30″N 95°28′49″W) in the grower's field during the summer season of 2016/17. The four distinct research locations in Texas have unique conditions, which represent different climatic conditions, soil fertility, and soil types. A field trial was conducted with a randomized complete block design with four replications and three treatments, unprimed, TNE, and AgNPs for both varieties (Riverside and Maxima). Field plots were prepared by forming raised beds covered with/without black plastic mulch and drip tape in the bed. A plant-to-plant distance of 3.5 feet was maintained within the row with a planting density of six plants per plot. In the case of triploid (Maxima) plots, two pollen-producing plants (pollinizers) per plot were planted making a 1:3 ratio of diploid and triploid plants. Pollinizers were interplanted in the same row as the triploid variety. The soil was collected from all four locations for routine analysis.

Moreover, to observe the direct seeding effect and to validate the result of the first year, another field trial was conducted in Texas A&M AgriLife Research and Extension Center at Weslaco (26º15'N, 97º98'W) where treated (TNE and AgNPs) and unprimed seeds were directly sown in the field. This project was conducted during the summer season of 2017–18 with a total of six replications and planting density of five plants per plot. In the case of triploid (Maxima) plot, one pollinizer per plot was planted making a 1:4 ratio of diploid and triploid plants in the second year.

5.2.13. Assessment of growth and yield of watermelon plants

Length of the main vine and stem diameter were recorded for 40-day-old vines in all five locations. The length was measured from the base of the plants to the tip of the main vine and the

stem diameter was recorded at the base of the plant. The fields were harvested when more than 90% of the fruits were ripe. Fruit was considered to be ripe by looking for a dried tendril nearest the fruit, a dull sound of the fruit when thumped and a light-colored ground spot, as is normally done for watermelon maturity determination.

In the first year, out of four research locations, fields at Grapeland and Snook were selected for a yield study as shown in the map (Figure D1). Fruit was harvested three times at Grapeland and Snook. In each harvest, the fruit was counted and weighed for each treatment. Total fruit weight for the three harvests combined was calculated. During the second year, owing to the bad weather conditions (heavy storms and rainfall in June that led to flooding in the watermelon field after the first harvest), a single harvest was done in Weslaco. Weather data are given in Figure D2.

5.2.14. Determination of total phenolics and radical scavenging activity

Total phenolics and radical scavenging activity of watermelon fruit harvested from all locations were quantified using our previously published method with slight modifications.[164] Fresh watermelon fruit samples (15 g) were extracted twice with 15 mL methanol and the extracts were pooled. All standards and samples were pipetted in triplicate into 96-well plates. The absorbance was measured using a Synergy HT Multi-Mode Microplate Reader (BioTek, Instruments, Winooski, VT, USA) at 760 nm and 515 nm for total phenolics and DPPH assays, respectively. The total phenolics were expressed as mM Trolox equivalents per gram of fresh weight of samples, and radical-scavenging activity was expressed as mg of ascorbic acid equivalents per gram dry weight.

5.2.15. Mineral content

Nano-treated and untreated watermelon pulp harvested from all the locations in the first year (Snook, Grapeland, Edinburg, and Pecos) and second year (Weslaco) was freeze-dried. Samples from diploid and triploid watermelon cultivars were submitted to the Soil, Water and Forage Testing Laboratory, Texas A&M University, College Station, Texas. The macro-elements nitrogen (N), phosphorus (P), sulphur (S), potassium (K), calcium (Ca), sodium (Na), and magnesium (Mg) were measured along with the microelements iron (Fe), copper (Cu), manganese (Mn), boron (B), and zinc (Zn). Nitrogen content was determined by the high-temperature combustion process. The inductive coupled plasma-atomic emission spectroscopy (ICP-AES) (Spectro Genesis, Deutschland, Germany) was used to estimate the other mineral (P, K, Ca, Mg, Na, S, Fe Cu, Mn, Zn, and B) contents.

5.2.16. Statistical Analysis

One-way analysis of variance (ANOVA) was performed using JMP software (JMP pro 14). Significant differences were tested using a general linear model and means were compared using Student's *t*-test at 5% probability level ($p \leq 0.05$). The results are expressed as means ± standard error of the mean. Microsoft Excel was used for data visualization and graphing.

5.3. Results

5.3.1. Synthesis and characterization of the TNE and AgNPs

Turmeric oil nanoemulsion was prepared using a low-energy method based on a spontaneous emulsification technique. The nanoemulsion was optically opaque, homogeneous, and physically stable. Dynamic light scattering shows the mean particle sizes recorded for TNE

was 171.3 ± 0.52 nm with PDI and ZP values of 0.25 and -1.23 ± 0.16 mV, respectively (Figure. D3A).

In the case of AgNPs, a reddish dark brown color was observed when Ag^{+} ions were reduced to AgNPs after addition of onion peel extract indicating a reduction of Ag^{+} to Ag^{o}. The mean particle sizes recorded for AgNPs was 141.3 ± 0.78 nm with PDI and ZP values of 0.18 ± 0.03 and -1.23 ± 0.16 mV, respectively (Figure D3B). The surface plasmon resonance (SPR) of AgNPs showed a peak centered near 410 nm in UV-vis spectra (Figure D3C), confirming that the phytochemicals present in onion peel extract reduced the silver salt into AgNPs.

Transmission electron microcopy images (Figure 25A and 25B) of AgNP samples showed typical spherical and ellipsoidal morphology with approximate particle diameter of 29 nm. Crystalline nature of synthesized AgNPs was confirmed using X-ray diffraction (XRD). Figure 25C displays four prominent diffraction peaks at 2θ value of 38.19°, 44.38°, 64.49°, and 77.45° indexed as (111), (200), (220), and (311) Miller indices, respectively, which are characteristic of face centered cubic (fcc) crystalline structure of metallic silver (JCPDS file No.04–0783). The average nanocrystalline size of synthesized AgNPs was calculated using Debye-Scherrer's equation and was found to be around 36.5 nm (Table D1).

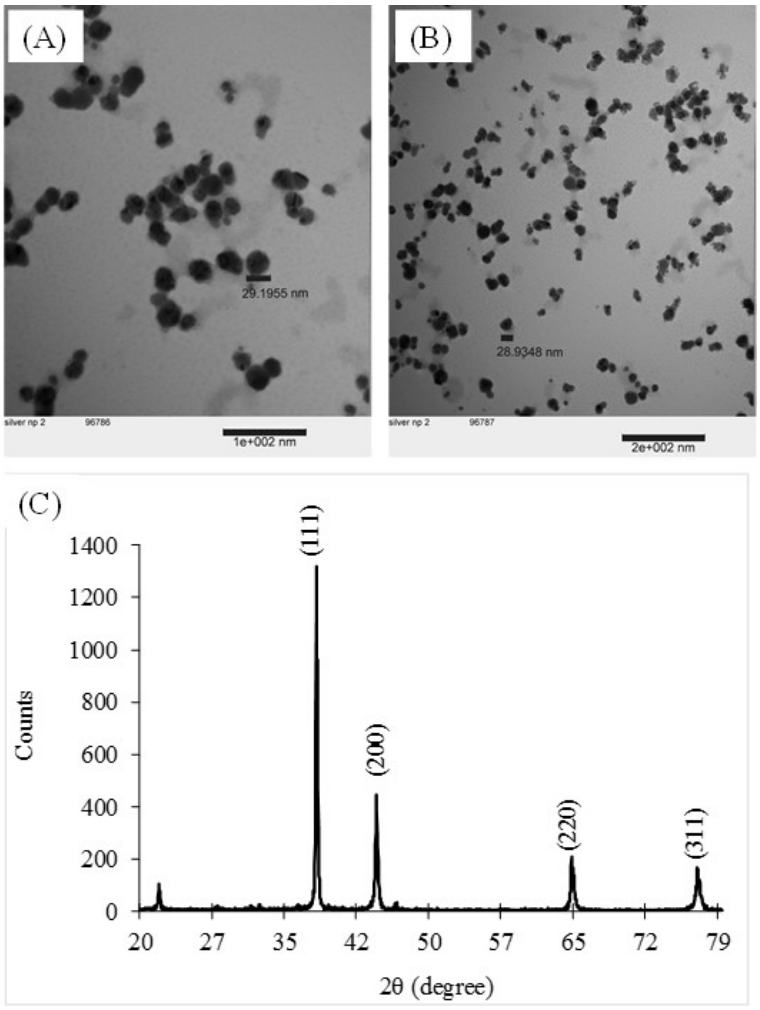

Figure 25 TEM images of silver nanoparticles showing the morphology of synthesized silver nanoparticles at (A) scale bar 100 nm (B) scale bar 200 nm, (C) X-ray diffraction pattern of silver nanoparticles synthesized using onion peel extract.

5.3.2. Enhancement of seed germination, emergence, and seedling growth rate by nanopriming

To examine the effect of nanopriming with AgNPs and TNE, we first assessed seed germination and seedling emergence in 2017 and 2018. The control unprimed treatment required significantly more days for 50% germination of Riverside and Maxima cultivars during the first

and second years, respectively, as compared to AgNP treatment (Table 6). Conversely, seeds of Riverside variety treated with AgNPs had the lowest mean germination times (MGT) and the highest germination rates (GR) compared to the other treatments, showing significant differences in MGT and GR. TNE-treated seeds had significantly higher GR than control, unprimed seeds of Riverside and Maxima cultivars. However, there were no significant differences in the number of days required for 50% seed germination, final germination percentage (FGP), and the final emergence percentage (FEP) when seeds were treated with TNE compared to the unprimed watermelon seeds of both varieties during both planting seasons. No differences were observed in the FGP in both cultivars among the treated and untreated seeds. FEP was significantly higher in the AgNP-treated Maxima seeds. However, no significant difference in FEP was observed for Riverside seeds during both years. The increased FEP suggests that AgNP treatment is more effective at enhancing emergence in triploid cultivars as compared to diploids.

Table 6 Germination and emergence of nanoparticle-treated watermelon seeds in 2017, 2018, and 2019. Data from 2017 and 2018 are presented as mean ± SEM from three replicates containing 25 seeds of each treatment (total 400 seeds, Means denoted by different letters are significantly different at $p \leq 0.05$. Data from 2019 are presented as the mean of 16 replicates containing 25 seeds each ± SEM. Means denoted by the different letters are significantly different at $p \leq 0.05$. UP: Unprimed, HP: Hydroprimed, TNE: Turmeric oil nanoemulsion, AgNO3: Silver nitrate, AgNPs: Silver nanoparticles, FGP: Final germination percentage, MGT: Mean germination time, GR: Germination rate, FEP: Final emergence percentage, DAS: Days after sowing.

Year	Variety	Treatments	Days required for 50% germination	FGP (5 DAS)	MGT (days)	GR (seed/day)	FEP (14 DAS)
2017	Riverside	UP	2.33±0.33^{a}	100±0.00^{a}	2.37±0.09^{a}	0.42±0.02^{c}	96.66±3.36^{a}
		TNE	2.00±0.00^{a}	100±0.00^{a}	1.95±0.08^{b}	0.51±0.02^{b}	93.33±1.68^{a}
		AgNPs	1.66±0.33^{a}	100±0.00^{a}	1.60±0.14^{c}	0.63±0.05^{a}	96.66±3.36^{a}
	Maxima	UP	2.00±0.00^{a}	100±0.00^{a}	2.24±0.07^{a}	0.45±0.01^{c}	70.00±2.91^{ab}
		TNE	2.00±0.00^{a}	100±0.00^{a}	1.76±0.04^{b}	0.57±0.01^{b}	58.30±7.32^{b}
		AgNPs	1.33±0.33^{b}	100±0.00^{a}	1.52±0.08^{c}	0.66±0.03^{a}	80.00±2.91^{a}
2018	Riverside	UP	2.00±0.00^{a}	99±0.67^{a}	2.04±0.01^{a}	0.49±0.00^{c}	98.33±1.67^{a}
		TNE	2.00±0.00^{a}	99±0.67^{a}	1.74±0.03^{b}	0.57±0.01^{b}	98.33±1.67^{a}
		AgNPs	1.00±0.00^{b}	100±0.00^{a}	1.16±0.02^{c}	0.85±0.02^{a}	98.33±1.67^{a}
	Maxima	UP	2.00±0.00^{a}	94±1.71^{a}	2.12±0.02^{a}	0.47±0.00^{c}	58.73±1.67^{a}
		TNE	2.00±0.00^{a}	96±1.79^{a}	1.81±0.03^{b}	0.54±0.01^{b}	72.22±7.22^{ab}
		AgNPs	2.00±0.00^{a}	98±0.89^{a}	1.49±0.05^{c}	0.67±0.02^{a}	85.55±7.22^{a}
2019	Riverside	UP	2.00±0.00^{b}	94±1.36^{b}	2.26±0.04^{a}	0.44±0.01^{d}	90.47±4.76^{a}
		HP	1.93±0.11^{b}	94±0.89^{b}	1.82±0.06^{b}	0.56±0.02^{c}	90.47±4.76^{a}
		TNE	1.18±0.10^{c}	96±1.02^{ab}	1.37±0.06^{c}	0.75±0.03^{b}	95.23±4.76^{a}
		$AgNO_3$	3.00±0.00^{a}	79±1.74^{c}	2.59±0.25^{a}	0.30±0.03^{e}	66.66±4.76^{b}
		AgNPs	1.00±0.00^{c}	98±0.72^{a}	1.17±0.02^{c}	0.86±0.02^{a}	95.23±4.76^{a}
	Maxima	UP	2.00±0.00^{a}	94±1.41^{a}	2.30±0.05^{b}	0.44±0.01^{c}	52.38±4.76^{b}
		HP	1.63±0.13^{b}	95±0.70^{a}	1.82±0.11^{bc}	0.57±0.02^{b}	61.90±4.76^{ab}
		TNE	1.19±0.10^{c}	95±0.40^{a}	1.74±0.13^{bc}	0.65±0.07^{b}	66.66±4.76^{ab}
		$AgNO_3$	–	16±2.55^{b}	3.35±0.59^{a}	0.27±0.04^{d}	0.00±0.00^{c}
		AgNPs	1.00±0.00^{c}	98±0.73^{a}	1.23±0.05^{c}	0.84±0.04^{a}	76.19±4.76^{a}

In third year 2019, the incubator and greenhouse studies were conducted with five treatments: unprimed, hydroprimed, TNE-, $AgNO_3$- and AgNP-treated seeds. The main objective of this experiment was to compare the effect of seed treatment with the same concentration of AgNPs and their bulk counterpart, $AgNO_3$ solution. When the effect of $AgNO_3$ and AgNPs was compared in the repeated germination study, we found that $AgNO_3$ significantly reduced germination in both cultivars (Table 6). In $AgNO_3$-treated watermelon seeds, the FGP was 79% for Riverside and 16% for Maxima, whereas FGP was significantly higher in AgNP-treated seeds (98% for both cultivars).

We also conducted a greenhouse study in the third year to compare the FEP between $AgNO_3$ and AgNP treatments. The FEP was 67% and 95% in Riverside watermelon using $AgNO_3$ and AgNPs, respectively. In Maxima, severe toxicity of $AgNO_3$ was observed, resulting in no emergence. This indicates that the toxicity of bulk metal particles is cultivar and ploidy dependent (Maxima = 3n; Riverside = 2n). Similarly, hydropriming was included as the other control in the third-year incubator and greenhouse study. Although the FGP and FEP were similar in the unprimed and hydroprimed seeds, significantly enhanced growth rate and reduced mean germination time was observed in the hydroprimed seeds as compared to the unprimed control. However, TNE and AgNPs had significantly higher growth rate and reduced mean germination time as compared to the hydroprimed seeds of both cultivars.

5.3.3. Influence of seed germination on primary metabolites

During germination, disaccharides (sucrose) are converted to monosaccharides (glucose and fructose) to fuel development of the germinating seedling (Figure 26).

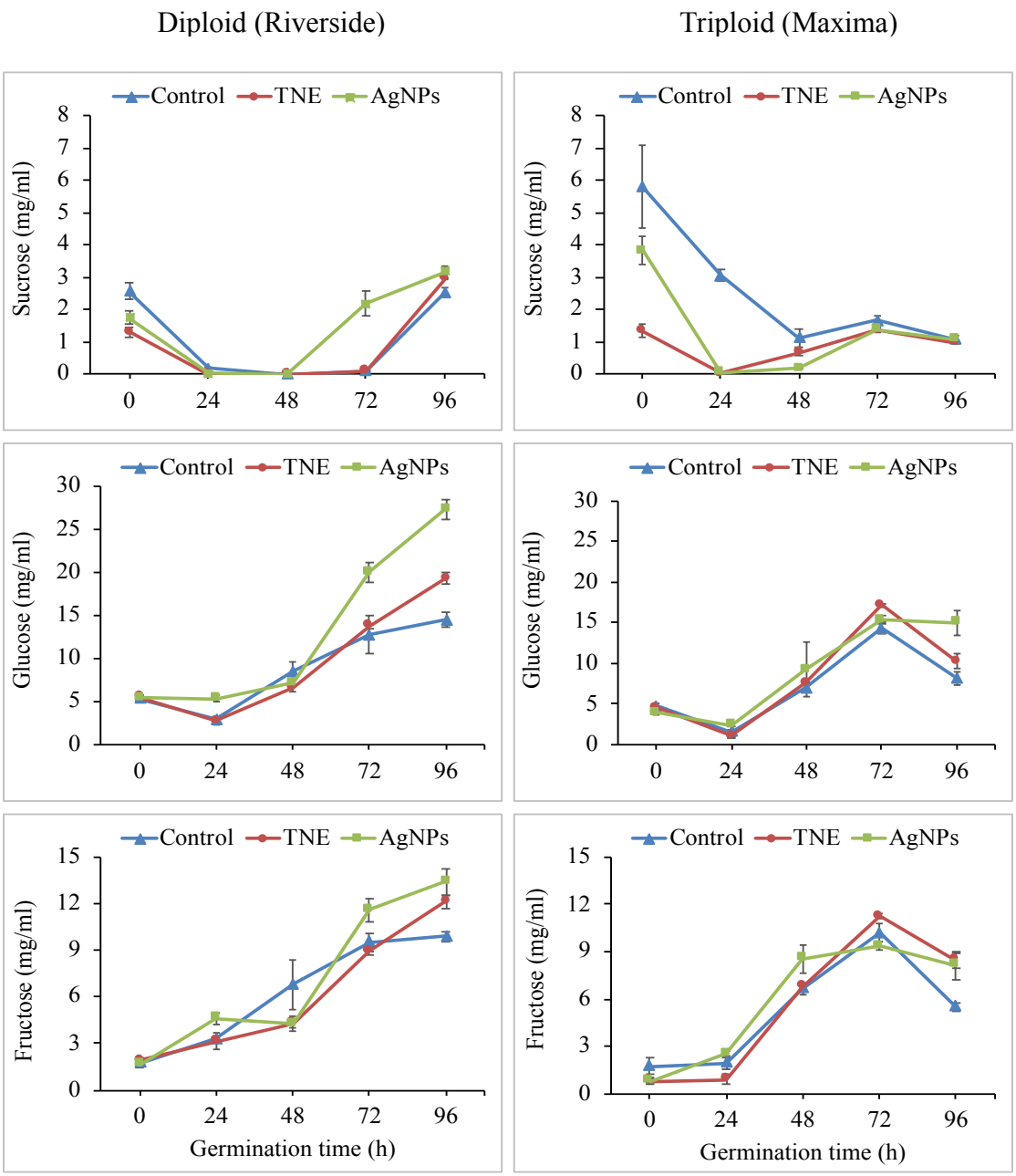

Figure 26 Effect of nanoparticle treatment on diploid (Riverside) and triploid (Maxima) watermelon seeds up to 96 h. Rapid degradation of polysaccharides and disaccharides in nanoparticle-treated samples shown at different time points. Control is unprimed, TNE is turmeric oil nanoemulsion and AgNPs is silver nanoparticles. Values are mean ± SEM (n = 6).

Therefore, we next assessed the effect of nanopriming on this key germination process. An initial reduction in sucrose content of treated and untreated diploid seed was observed at 24 h after priming, suggesting that carbohydrate mobilization and metabolism are highly active in that stage. In the case of triploid seeds, the sucrose level was reduced in nanoprimed seeds at 24 h and in control seeds at 48 h. This shows the influence of nanopriming on seed germination. Glucose and fructose levels peaked at 96 h after priming in the diploid cultivar while in the triploid, glucose and fructose levels declined after 72 h. Interestingly, at 96 h after priming, the glucose and fructose levels were relatively higher in nanomaterial-treated seeds compared to the unprimed control of both varieties.

5.3.4. Effect of nanopriming on photosynthetic pigments

If nanopriming caused toxicity in the developing seedlings, we might see a decrease in photosynthetic pigments; by contrast, if nanopriming improved seedling vigor, we might see an increase in photosynthetic pigments compared with control. Effects of seed priming with TNE and AgNPs on seedling leaf chlorophyll (chl) *a* and *b* contents were assessed at 21 DAS. Seedlings of nano-primed seeds had elevated or similar levels of chl *a* and chl *b* compared to control (Figure 27A and 27B). Nanopriming had a significant influence on chl *a* content of the triploid watermelon seedlings. Although there were no significant differences, both nanotreatments enhanced the chl *a* and chl *b* contents of diploid watermelon seedlings. These results indicate that seed treatment with TNE and AgNPs had no discernable negative effects on watermelon seedling growth.

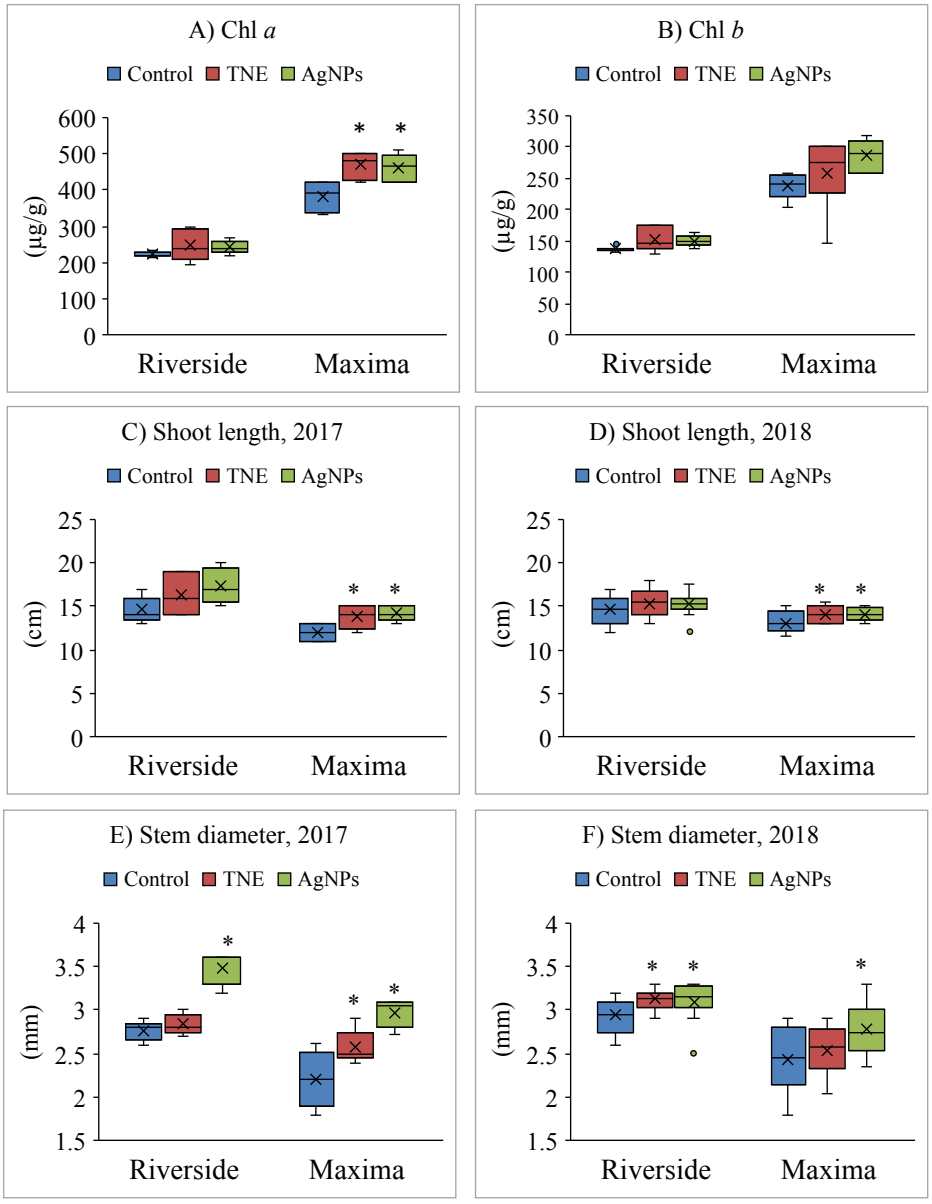

Figure 27 Effect of nanoparticle treatments on chlorophyll content, stem diameter and shoot length in watermelon seedlings at 21 days after transplanting. A) Chlorophyll a (Chl a) and (B) chlorophyll b (Chl b) content in Riverside and Maxima watermelon seedlings at 21 days after sowing (DAS). Boxplots show the shoot length of watermelon grown in (C) first year, 2017 and (D) second year, 2018; stem diameter of watermelon grown in (E) first year, 2017 and (F) second year, 2018. Control is unprimed, TNE is turmeric oil nanoemulsion and AgNPs is silver nanoparticle-treated watermelon seedlings. *denotes statistical differences between treatments at the 5% level according to t test and '×' denotes mean.

5.3.5. Growth of watermelon transplants

To test whether the effects we observed on the seedlings carried over into improved growth later in development, we next examine growth in transplanted plants. To this end, shoot length and stem diameter were recorded at 21 DAS watermelon seeds. Maxima seedlings from both nano-priming treatments had significantly longer shoots compared to the control. Although treated seedlings had longer shoots than the control, there was no significant difference in the Riverside variety. This trend was similar in both planting years (Figure 27C and 27D). AgNP-treated seedlings had significantly larger stem diameters (Figure 27E and 27F) in both Riverside and Maxima cultivars as compared to control during both planting years.

5.3.6. Nanopriming to enhance growth parameters of watermelon vine

To test these effects in field conditions that are relevant to agricultural production, we transplanted watermelon seedlings into growers' fields in four different locations in Texas: Edinburg, Grapeland, Snook, and Pecos (Figure D1). In the field study also, nanoparticle-treated seeds grew very well as compared to the unprimed controls (Figure 28).

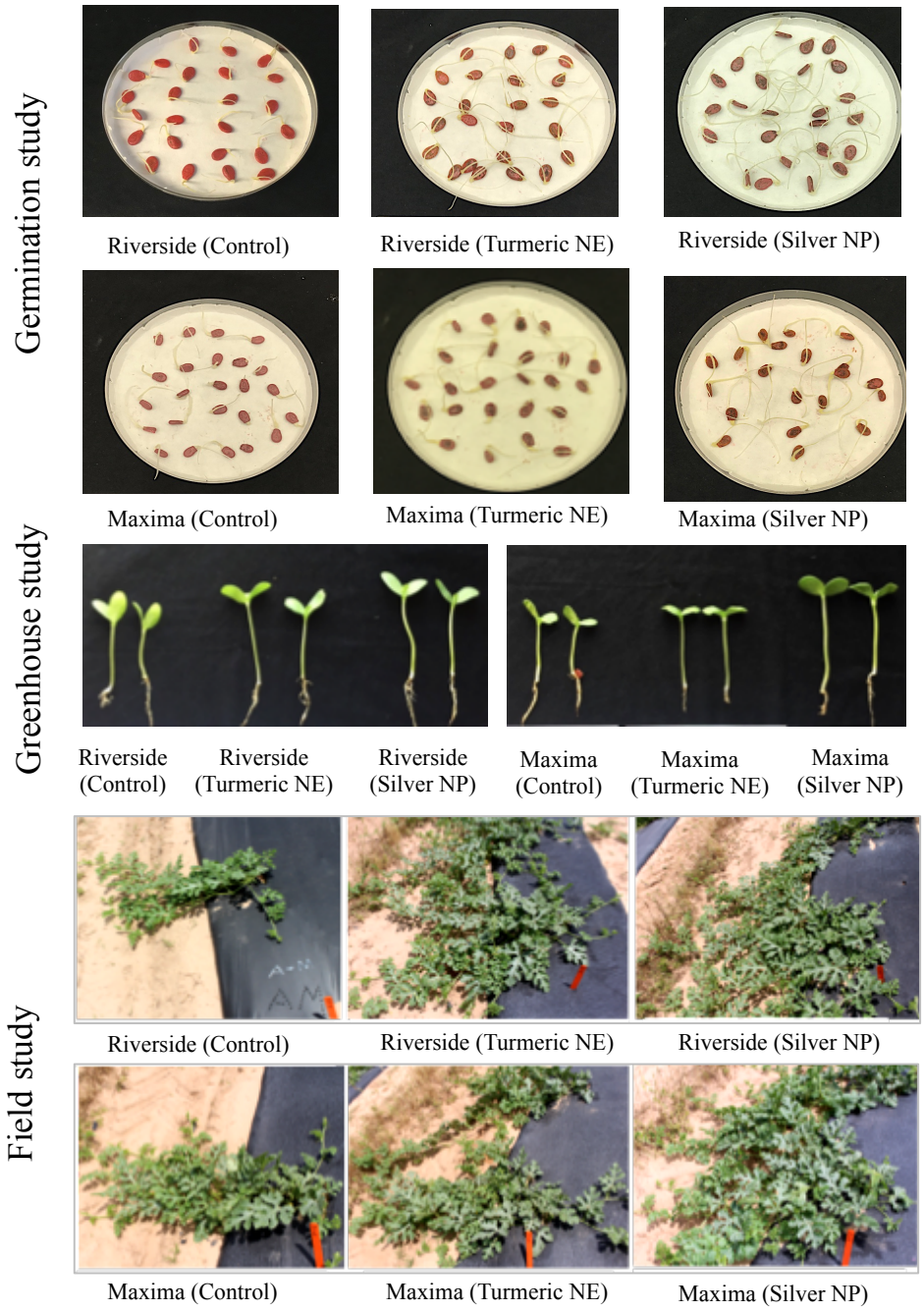

Figure 28 Effect of seed priming with turmeric nanoemulsion and silver nanoparticles on the germination, seedling growth and vine development of diploid (Riverside) and triploid (Maxima) watermelon varieties, compared with unprimed control.

To study the effect of nanopriming on growth, we measured vine length and vine thickness at 40 days after transplanting (DAT) at all the growing locations. The length of the main vine was significantly higher in the AgNP-treated plants as compared to the other treatments in both Maxima and Riverside cultivars grown in Edinburg (Figure 29A and 29B). In Grapeland, Snook, and Pecos, vine length was significantly higher in the AgNP-treated plants as compared to control only in the Maxima cultivar. Effect of the TNE treatment was not significantly different from the control for the vine length of Riverside in all the locations, but TNE treatment enhanced growth of the Maxima cultivar grown in Pecos.

Stem diameter showed a significant difference in Maxima but not in Riverside cultivar grown in Grapeland and Snook (Figure 29C and 29D). AgNP-treated plants had thicker stems as compared to other treatments in the Maxima cultivar. No significant differences were observed in the stem diameter between the treatments in Edinburg. In both cultivars grown at Pecos, stem diameter was significantly higher in NP-treated watermelon plants as compared to the control. During the second year at Weslaco, vine length and thickness were recorded at 40 DAS and AgNP-treated Riverside watermelons had significantly longer vines, but no difference was observed in the Maxima cultivar. Similarly, no significant differences were observed in the stem diameter between the treatments in Weslaco.

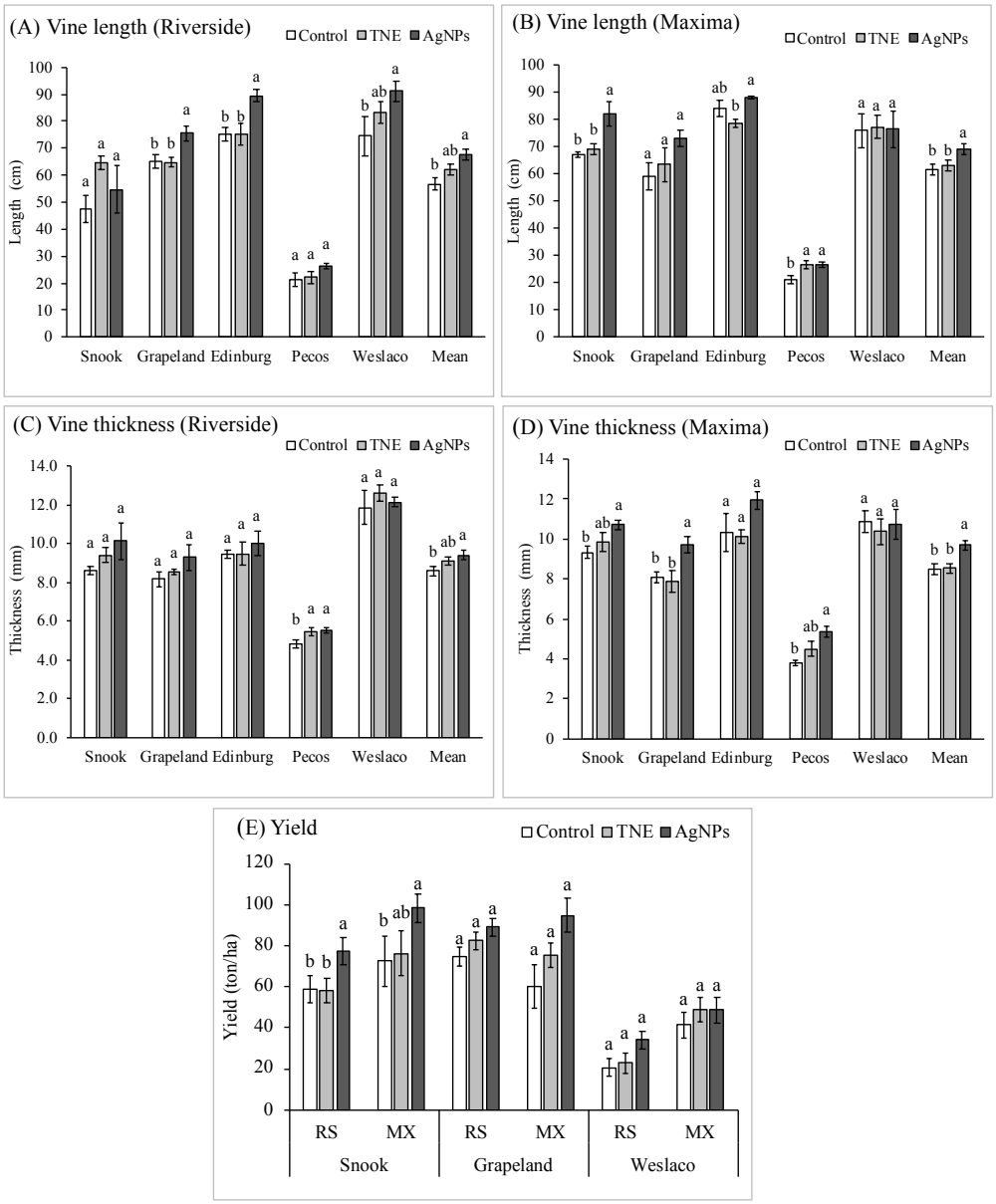

Figure 29 Effects of nanoparticles on the growth parameters at 40-day-old watermelon plants and yield. (A) Vine length (cm) of Riverside, (B) vine length (cm) of Maxima, (C) vine thickness (mm) of Riverside, and (D) vine thickness (mm) of Maxima watermelon plants grown in five locations of Texas (Snook, Grapeland, Edinburg, Pecos, and Weslaco). (E) Effect of nanopriming on yield of watermelon grown in three locations in Texas (Snook, Grapeland and Weslaco). Watermelons were harvested three times during the first year at Snook and Grapeland. Due to bad weather conditions, a single harvesting was done in Weslaco. Control is unprimed, TNE is turmeric oil nanoemulsion and AgNPs is silver nanoparticles treated watermelon. Different letters denote significant difference ($p \leq 0.05$) between treatments. Data represent mean ± SEM.

Watermelons grown at Pecos had poor growth performance at 40 DAT as compared to the other locations. This effect on growth parameters among the five locations (Figure D1) could be due to environmental factors such as weather conditions (Figure D2), soil type (Table D2), and water availability. Pecos has a semiarid to desert climate with hot summers. The low rainfall of this region is reflected in the slow growth of the watermelon vines compared to the other locations.

5.3.7. Effect of nanopriming on watermelon yield

Two nanopriming-based treatments (TNE and AgNPs) were used for this study and compared with the control. Out of four locations, the two fields nearest the university, Grapeland (90 miles) and Snook (14 miles), were selected for yield measurements in the first year. These two locations were selected based on the feasibility of conducting multiple harvests and intensive management. In order to observe the direct seeding effect and to validate the results of the first year, another field trial was conducted in Texas A&M AgriLife Research and Extension Center at Weslaco, which is the best production area for watermelon of the available sites in Texas. In both varieties, AgNP-treated watermelons had a significantly higher yield (tons/ha) than the other two treatments (control and TNE) in Snook (Figure 29E). Higher yield (31.6 %) was observed in AgNP-treated plants compared to control in Riverside watermelons at Snook. Similarly, for Maxima, AgNP treatment increased yield by 35.6% at Snook compared to the control. No significant difference in yield was observed between control and TNE.

In Grapeland and Weslaco, for both varieties, all three treatments showed no statistically significant differences in yield. However, AgNP-treated watermelons had a higher yield as compared to the control in both locations.

5.3.8. Internalization studies

To understand how nanopriming could affect the growth of watermelon plants, we measured the internalization of major active compounds present in TNE by gas chromatography-mass spectrometry (GC-MS; Table D3). Ar-turmerone is the major compound present in the TNE, and it was used as a marker to test internalization into the watermelon seeds. The levels of ar-turmerone internalized in TNE-treated Riverside and Maxima seeds were 2250.18 μg/g and 2422.46 μg/g, respectively.

Internalization of Ag was determined by INAA (Table D3). Ag was detected in the treated seeds of both varieties, while in the unprimed seeds, the Ag level was below the detection limit (detection limit of Ag by INAA is 40 ng/g). The concentration of Ag in the AgNP priming solution was 31.3 μg/mL. After 12 h priming, the concentrations of Ag absorbed by the Riverside and Maxima seeds were 20.86 and 15.63 μg/g fresh weight, respectively. This result suggested that Ag^+ ions released from AgNPs penetrate the seed coat into seed tissues. The findings were further confirmed by TEM images of watermelon seeds (Figure 30) which showed that AgNPs were found inside seed embryos in the treated seeds and no particles were observed in the control, unprimed watermelon seeds.

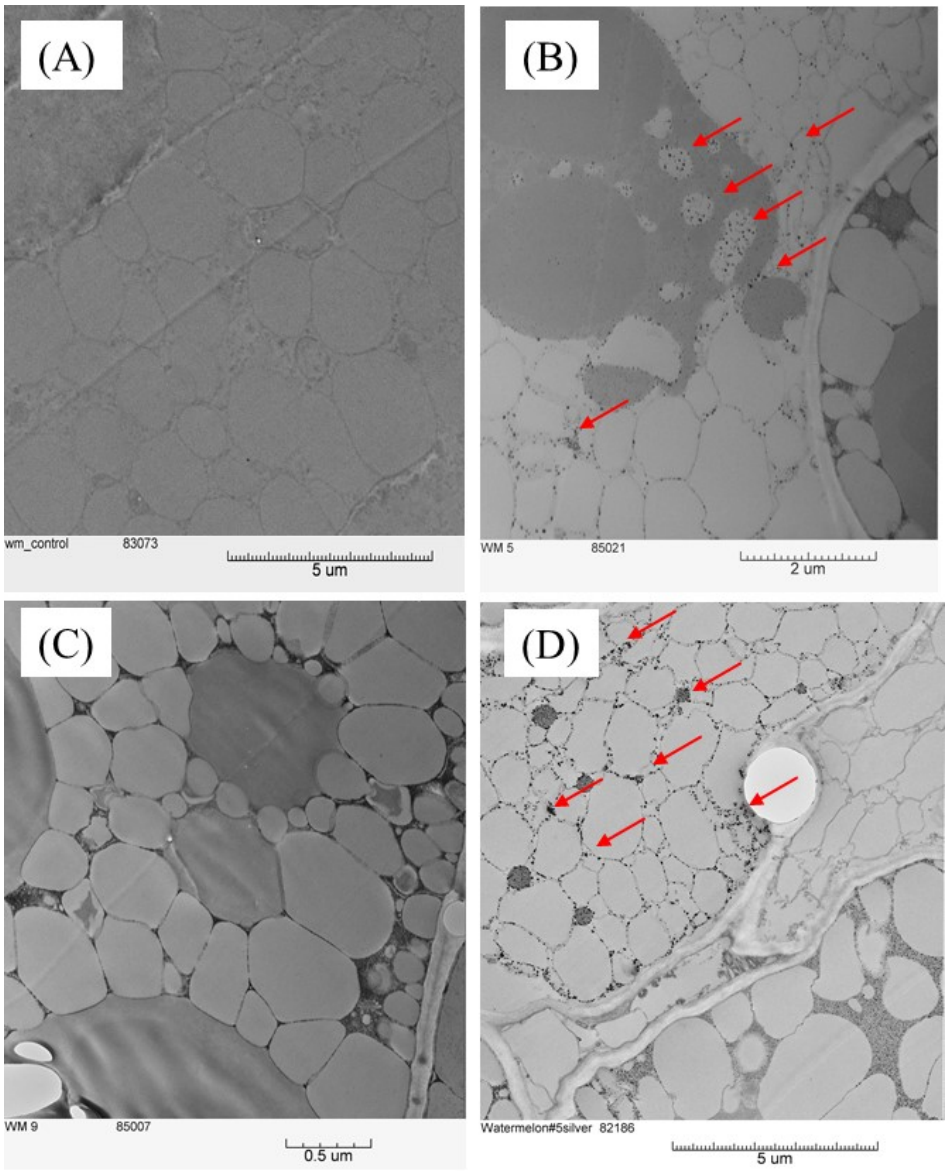

Figure 30 Transmission electron microscopy (TEM) images of internalization of silver nanoparticles in the (A) unprimed triploid (Maxima) seed, (B) AgNP-primed Maxima seed (C) unprimed Riverside seed and (D) AgNP-primed Riverside seed. Arrows indicate regions where AgNPs (dark bead like structures) have accumulated in treated seeds.

5.3.9. Effect of nano-treatments on total phenolics, radical scavenging activity, and elemental composition in watermelon fruit

Phenolic compounds have high antioxidant activities and free radical scavenging capacity, and inhibit the enzymes responsible for reactive oxygen species (ROS) production and reducing highly oxidized ROS. No significant difference ($p \leq 0.05$) was observed in total phenolics content between the treated and the control watermelons (Figure 31A). The radical scavenging activity of all the samples was measured using the 2,2-diphenyl-1-picrylhydrazyl (DPPH) assay. Nano-treatment had no detrimental effect on radical scavenging activity (Figure 31B).

The studied priming treatments had no significant impact on mineral element contents of diploid and triploid watermelon fruit compared with their respective controls (Figure D4). These results indicate that TNE and AgNP treatment did not cause any negative effect on nutritional quality of watermelon fruit.

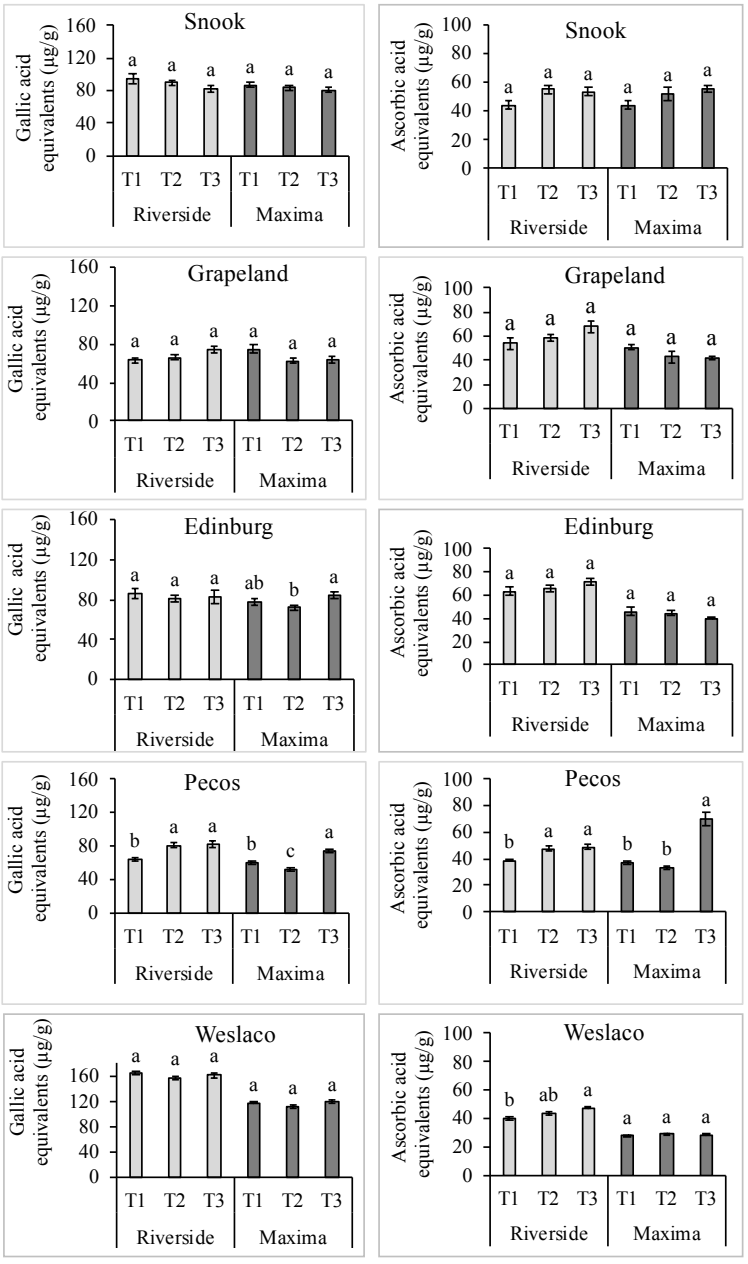

Figure 31 Nanopriming effects on (A) Total Phenolics and (B) Radical scavenging activity of watermelon fruit; Riverside and Maxima by DPPH method. T1: unprimed, T2: turmeric oil nanoemulsion and T3: silver nanoparticles. Data are presented as means ± SEM (n =12). Means denoted by the different letters are significantly different at ($p \leq 0.05$).

5.4. Discussion

5.4.1. Nanopriming stimulated germination of watermelon seeds by modulating primary metabolites

The major form of carbohydrate is soluble sugar and the alteration of soluble sugars in germinating seeds can be a good indicator of seedling emergence and growth. Soluble sugars are mobilized from seeds to various organs in the seedlings during seed germination and early seedling growth.[165] Application of AgNPs enhanced the levels of glucose and fructose at 96 h after priming compared to those in unprimed diploid and triploid seeds (Figure 26). Although sucrose levels decreased during the course of seed germination, the abundance of other carbohydrates (glucose and fructose) increased, which could be due to the conversion of polysaccharides to monosaccharides. This suggests a substantial mobilization from reserves into glycolysis. The data are in agreement with results obtained by gas chromatography analyses of sugars in rice[74] and *Arabidopsis thaliana* seeds.[72] These data corresponded well with the early protrusion of radicles and enhanced growth rate in AgNP-primed seeds compared to other treatments. The germination results agree with previous studies of watermelon, zucchini, and corn crops[166], which showed that, that compared with untreated watermelon, the germination rate was enhanced at all the AgNP concentrations (0.05 to 2.5 mg/mL).[166] Similarly, enhanced germination was observed using AgNPs in rice[8, 42] and *Boswellia ovalifoliolata.*[105]

In the present study, AgNPs and TNE showed great promise for agricultural applications to enhance the germination rate and growth of diploid and triploid watermelon plants as compared to the control unprimed seeds. In TNE, ar-turmerone is the major compound found in the byproduct from curcumin manufacture and this compound has antibacterial[17] and antifungal properties.[60] As a result of the antibacterial properties of thymol, significant enhancement of

soybean seed germination and plant growth was recorded in plants treated with thymol nanoemulsion.[59] Therefore, nanoscale ar-turmerone could be used as an antimicrobial and plant growth-promoting agent, causing higher seed germination compared to the control treatment. Some dose-dependent negative results were reported using chemically synthesized AgNPs in wheat seedlings,[167] which demonstrate the toxicity of the reducing and capping agent. Therefore, green nanoparticles capped with phytochemicals could be benign alternatives for agricultural purposes.

5.4.2. Nanopriming modulated the photosynthetic pigments and growth of transplants

Chlorophyll is positively correlated with photosynthetic rate and the total photosynthate produced.[65] Enhanced chlorophyll content in AgNP-primed seedlings can be attributed to the increase in water and nutrient absorption, leading to better plant growth and physiological development. The increased content of chlorophyll observed in the AgNP-treated seedlings in this study could facilitate the higher accumulation of soluble proteins for plant metabolic activities, which can maintain higher physiological performance. Higher chlorophyll contents could accelerate the rate of photosynthetic CO_2 fixation and subsequently produce more soluble sugars resulting higher biomass of the plants.[65] In treated seedlings of *Brassica juncea*, AgNPs improved the cellular electron exchange efficiency and photosynthetic quantum efficiency, and increase chlorophyll contents, as compared to the control seedlings.[168] The enhanced shoot length and stem diameter of watermelon transplants at 21 DAS could be attributed to the higher rate of photosynthesis in the treated plants. A similar result was obtained in the seedling growth of corn, watermelon, zucchini and pearl millet plants treated with AgNPs.[166,169]

Studies on the interactions between chlorophyll and NPs are imperative for understanding the photophysical behavior of plants exposed to NPs. To understand the potential toxicity of

AgNPs and $AgNO_3$ in seed priming, we measured chlorophyll in the leaf tissue of 14-day-old watermelon seedlings collected from the third-year emergence study. The chlorophyll content significantly decreased in $AgNO_3$-treated seedlings, as compared to AgNPs, when the same concentration was used. AgNP priming had no significant impact on chl *a* and *b* contents when comparing unprimed and hydroprimed seed. Based on these results, we conclude that when used in the same concentrations, $AgNO_3$ bulk treatment is phytotoxic but the synthesized AgNPs are not (Figure D5). In comparative phytotoxicity studies, our group has demonstrated the negative impacts of bulk Fe particles as compared to the Fe nanoparticles on chlorophyll synthesis of watermelon seedlings.[13] Our results are in agreement with similar studies by other groups, which have demonstrated the inhibitory effect of bulk silver particles as compared to silver nanoparticles.[42,170-171] These studies confirmed the phytotoxic effects of silver are not due to nanoparticles but owing to the Ag^+ ions. Indeed, Ag accumulation in seeds primed with AgNPs was lower than those of $AgNO_3$ and this higher Ag accumulation inhibits seed germination and seedling growth in rice,[42] onion,[172] castor,[170] maize,[173] poplar, and Arabidopsis.[174] Differential toxicity of AgNPs and Ag^+ ($AgNO_3$) could be due to the slow surface generation of ROS by AgNPs in contrast to bulk particles.[175]

5.4.3. Nanopriming enhanced growth and yield while maintaining nutritional quality

AgNP-treated watermelon vines had longer and thicker vines as compared to the control and TNE-treated watermelons. Significant differences in yield were also observed in AgNP-treated watermelon of both cultivars at Snook, as well as non-significant increases in Grapeland and Weslaco. The results are in agreement with studies on onion,[83] *Brassica juncea*,[168] common beans, corn[176], safflower cultivars[177], rice[42], and wheat.[178] AgNPs increased plant growth and biochemical attributes of *Brassica juncea*,[168] and seed yield of safflower cultivars.[177] Seed

priming with iron oxide nanoparticles in field crops such as wheat has been shown to be an effective method of increasing yields, and retaining quality, including the nutritive value of grains.[178] In the present study, nanoparticle-treated seeds germinated and grew very well as compared to the unprimed controls (Figure 28). Moreover, AgNPs accumulated in the seeds (Figure 30), which might activate the metabolic events that are vital for the seed germination and seedling growth. The pathway of nanoparticle transport through the xylem and phloem in corn, tomato, and watermelon has been verified previously.[179-181] Internalized nanoparticles are transported through the vascular system of the phloem and could induce gene expression[87] resulting in the enhanced physiological parameters and ultimately productivity.

Along with the growth and the production of the crop, nutritional quality is a major concern. Interestingly, in our study, DPPH and total phenolics in nano-treated and untreated watermelons remained the same, which is in accordance with the literature on cerium oxide-treated medium amylose rice varieties.[148] Similarly, there were no significant differences in the level of macroelements (N, P, S, K, Ca, Na, Mg) and microelements (Fe, Cu, Mn, B, Zn) among the treatments. These findings suggest that the treatment of watermelon seeds with the nanoparticles would be unlikely to induce any negative effects on the nutritional quality of the crop.

5.5. Conclusions

The present study presented a simple, low-cost, and ecofriendly approach to synthesize NPs using agro-industrial byproducts and avoids the use of hazardous and toxic chemicals for direct applications in agriculture. The TNE promoted germination and growth, but AgNPs hold greater promise for agricultural applications. Multiple lab, greenhouse, and field studies suggested that germination and growth parameters of watermelon seeds were enhanced after

treatment with nanoparticles. Therefore, nanopriming could be cost-effective for seed priming and can support sustainable development of agriculture as well as improve the socio-economic status of farmers. Nanoparticle-mediated seed treatments avoid the release of large amounts of nanomaterials into the field, lowering impacts on the environment. Moreover, discarding industrial by-products aggravates disposal problems in the environment; however, these by-products are used in the present study for the synthesis of nanoparticles. To further enhance the effectiveness of the nanomaterial treatments, future efforts should focus on optimization of priming time, the concentration of the priming solution and nanomaterial composition, structure, and activity. Similarly, plant physiology affects the interaction with nanoparticles, so results observed in one crop are not necessarily valid for other crops, which makes it imperative to study different plant species. Therefore, the results of these studies should stimulate investigations to understand nanoparticle–plant surface interactions and the uptake of the green nanoparticles in the plant system.

6. NUTRITIONAL COMPOSITION OF WATERMELONS (*Citrullus lanatus*) AS INFLUENCED BY STORAGE PERIOD AND NANOPARTICLE TREATMENTS

6.1. Introduction

Watermelon (*Citrullus lanatus* (Thumb.) Matsum. & Nakai) is an important vegetable crop with many health benefits. Red-, orange- and yellow-fleshed watermelon cultivars have been developed with varying degrees of sensory and nutritional quality profiles.[182] For instance, red-fleshed watermelon cultivars typically have significantly high amounts of lycopene, a red carotenoid pigment, and a potent antioxidant compound capable of quenching free radicals formed during normal metabolism and may deactivate DNA chain-breaking agents that are associated with various types of cancers.[183-186] Dietary lycopene intake has also been associated with reduced incidence of cardiovascular disease, enhanced skin protection from UV light damage, improved bone mineral density, and improved sperm motility.[187-189]

In addition to lycopene, watermelons are also rich in L-citrulline, a non-protein, non-essential, physiologically-active amino acid which is involved in mammalian metabolic processes. Roles of L-citrulline include aiding in muscle recovery during exercise [190] and blood pressure modulation through vasodilation.[191-192] Watermelon also contain other dietary antioxidants such as polyphenolic compounds, micronutrients, and total ascorbic acid (TAA).

The nutritional composition of fruits and vegetables are influenced by genetics (cultivar), environment (production location) as well as pre-harvest and post-harvest cultural practices.[193-194] During post-harvest storage, many fruits and vegetables still continue normal metabolic processes and react to various biotic and abiotic stresses which affect the secondary metabolism of fresh produce leading to the variation of phytochemical composition.[195] Pre- and post-harvest

manipulations that enhance the shelf-life and/or sensory/nutrition quality of produce can add value and create new opportunities for growers and processors by reaching the health-oriented markets. To achieve this goal, it is important to study the effects of various manipulations such as seed priming and storage duration on health promoting compounds. For watermelons, the usual shelf life after harvest is 14−21 d under 13 °C storage conditions.[196] However, under retail conditions, fruits can remain at near room temperature conditions (23 – 26 °C) for several days. Despite watermelon's non-climacteric nature, significant anabolic processes can continue during postharvest, such as sucrose and lycopene synthesis, as well as catabolic changes in cell wall constitution leading to rheological modification of the pulp.[197] Effects of postharvest storage conditions on nutritional quality have been quantified in watermelon juice and fresh cut but little information is available regarding storage studies in the intact watermelon.[198] In the current study, we assessed the impacts of seed priming and storage duration (10 and 20 d after harvest) on quality and health promoting compounds of intact fresh watermelon fruits.

Seed priming with nanoparticles (NPs) is gaining attention because of the potential for NPs to act as delivery vehicles for key agrochemicals (e.g. pesticides, fertilizers, etc.) and their impacts on yield and quality.[199] Our previous studies demonstrated the beneficial effects of seed nanopriming on seed germination, alteration in growth promoting metabolites, plant growth, and yield in onion[83] and watermelons.[82] There are still many unresolved issues and challenges concerning the biological effects of nanoparticles in the nutritional composition. The application of NPs into the plant system and their possible impact on food safety and quality are a main public concern but limited studies are available to provide strong evidences. Therefore, it is important to elucidate the behavior of NPs in terrestrial ecosystems and their influence in the quality and nutritional composition of fruit. In recent years, silver nano particles have attracted

worldwide attention as it is safe, inexpensive, nontoxic inorganic metal having several beneficiary effects on plant health.[200] Therefore, in this study, the effect of silver nanoparticles on the health promoting compounds and the quality of watermelons were compared with the turmeric oil nanoemulsion and control unprimed samples. For this study, two red-fleshed watermelon varieties namely: Riverside (diploid) and Maxima (triploid) were primed with nanomaterials and grown at multiple locations in Texas over two growing seasons.

The present study was designed to investigate the impacts of treatments with silver nanoparticles (AgNPs), turmeric oil nanoemulsion (TNE) and postharvest storage on fruit quality and phytochemical compound profiles. of diploid and triploid watermelons. To the best of the authors' knowledge, this study represents the first examination of the effect of storage and nanoparticles treatments on the nutritional quality of intact watermelon fruit.

6.2. Materials and methods

6.2.1. Materials

All solvents and chemicals used for these procedures were of analytical grade. Methanol, acetone, acetonitrile, chloroform, tert-butyl methyl ether, hydrochloric acid, meta phosphoric acid, L-ascorbic acid, L-citrulline, and β-carotene were obtained from Sigma-Aldrich (St Louis, MO, USA). Lycopene was purchased from Cayman Chemical Company (Ann Arbor, MI, USA). Tris (2-carboxylethyl) phosphine hydrochloride (TCEP) was purchased from Alfa Aesar (Ward Hill, MA, USA). Nanopure water was used from Barnstead/Thermolyne (Dubuque, IA, USA) for sample preparation and high-pressure liquid chromatography (HPLC) analysis.

6.2.2. Fruit production and sampling procedures

Seeds of two watermelon cultivars: Riverside (a diploid; Origene Seeds Ltd., Alamo, TX., USA) and Maxima (a triploid; Origene Seeds Ltd., Alamo, TX., USA) were treated with

AgNPs and TNE as previously described.[82] Treated seeds, together with untreated controls, were then grown at four different locations in Texas in 2017; Edinburg (26° 18′ N 98° 9′ W), Snook (30° 29′ N, 96° 28′ W), Pecos (31° 24′ N, 103° 30′ W) and Grapeland (31° 29′ N, 95° 28′ W) following commercial watermelon production practices. The same experimental set up was also repeated in 2018 at the Texas A&M AgriLife Research and Extension Center, Weslaco (26° 15' N, 97° 98' W). At the end of the growing season, mature fruits were harvested, labeled and transported to Vegetable and Fruit Improvement Center (VFIC), College station, Texas within two days of harvest. Fruits were immediately rinsed with cold tap water, blotted with tissue paper and stored at room temperature (23 °C) to simulate grocery store retail conditions. Fruits were stored in perforated cardboard boxes (0.56 x 0.57 x 0.56 m) for 30 d. Triplicate samples of stored fruit from each treatment were retrieved at 0, 10 and 20 d for processing and analysis. After 30 d storage, fruits started decaying and were discarded (Figure 32). A total of 270 fruits (5 locations, 2 cultivars, 3 treatments, 3 storage period, 3 samples) were sampled, processed and analyzed. From each fruit sample, 3 subsamples were collected for phytochemical analysis, resulting in a total of 810 samples analyzed.

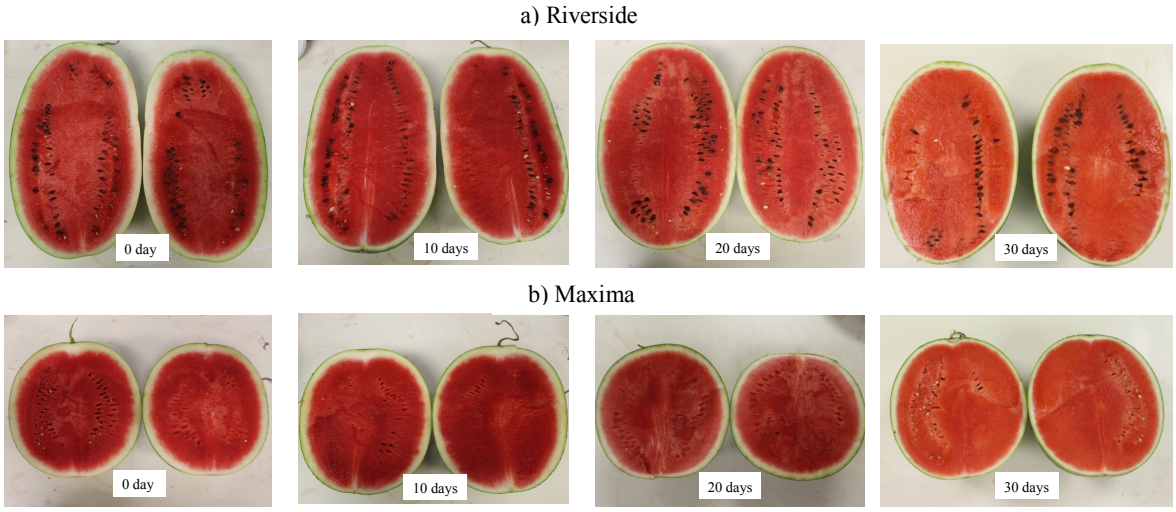

Figure 32 Watermelons during processing at 0 d, 10 d, 20 d and 30 d storage period at room temperature. Samples were taken from the center heart portion for all the phytochemical analysis.

6.2.3. Physico-chemical characteristics

Whole fruits were weighed and then cut at the equatorial region. Exocarp (rind) thickness was measured using a pair of calipers. Fruit mesocarp (flesh) color characteristics were recorded using a Tristimulus reflectance colorimeter (model: CR-400 Chroma Meter; Konica Minolta Sensing Americas, Inc., Ramsey, NJ, USA). Following color measurements, mesocarp samples were collected for juice and subsequent phytochemical analyses. Juice extracted from fruit mesocarp samples was assessed for soluble solid content (SSC) using a hand-held temperature-compensated refractometer (American Optical Corp., South Bridge, MA, USA). Juice pH of the same filtered sample was determined using a pH meter (Orion Star A211, Thermo Fisher Scientific, Waltham, MA, USA).

6.2.4. Extraction and quantitation of carotenoid analysis

Carotenoids in fruit mesocarp samples (5 g) were extracted as per our previous protocol with slight modification.[31] Extraction was accomplished with 10 mL of chloroform and acetone (3:7) under darkness to minimize carotenoid degradation. Samples were homogenized for 1 min, sonicated for 30 min and then centrifuged at 4480 × *g* for 15 min. Upper layer was decanted and lower layer containing carotenoids fraction was transferred to another vial. Same extraction procedure was repeated with 5 mL solvent to ensure the maximum recovery of carotenoids. The two fractions were combined, filtered through a 0.45 µm polytetrafluoroethylene (PTFE) filter and transferred to amber vials for HPLC analysis. HPLC analyses was carried out using a Waters 1525 HPLC system (Milford, MA, USA) equipped with a Waters 2996 photodiode array (PDA) detector and Waters 717 Plus autosampler. The mobile phase comprised of an isocratic mixture of *tert*-butyl methyl ether: methanol, 70:30 (v/v) at a flow rate of 0.5 mL/min for 12 minutes. Samples in the autosampler were maintained at 4 °C throughout the analysis. Carotenoid separation was carried out on a YMC C_{30}, 3-µm column (150 mm × 4.6 mm i.d.) with a guard cartridge (Phenomenex, Torrance, CA, USA). Samples (10 µL) were injected into the HPLC system and chromatograms were monitored at 470 nm. Calibration curves were prepared by injecting six serial dilutions of *β*-carotene and lycopene reference compounds ranging from 0.3 to 0.007 µg/10 µL injection volume and carotenoid levels were expressed as mg/kg.

6.2.5. Total ascorbic acid analysis

Sample preparation and analysis of total ascorbic acid (TAA) was done as per the previously reported protocol.[201] Samples were analyzed after reduction of dehydroascorbic acid by tris(2-carboxyethyl) phosphine hydrochloride (TCEP). Fruit mesocarp samples (4 g) were homogenized in 2 mL of 3 % metaphosphoric acid for 1 min, then sonicated for 30 min in ice-

cold water, vortexed for 1 min and centrifuged (Beckman Model TJ-6, Ramsey, MN, USA) at 4480 × *g* for 15 min. A 300 µL aliquot of the filtered sample was mixed with 300 µL of 5 mM TCEP and incubated for 1 hour at room temperature to reduce sample dehydroascorbic acid to ascorbic acid and the resulting solution was analyzed for TAA using an Agilent HPLC 1200 Series (Foster City, CA, USA) equipped with a diode array detector coupled with a quaternary pump system (P4000) and an autosampler (AS3000). Analysis of TAA was achieved by an isocratic method on a Gemini C_{18} column (4.6 mm × 250 mm, 3 µm) (Phenomenex, Torrance, CA, USA) with 0.03 mol L^{-1} phosphoric acid as mobile phase at a flow rate of 400 µL min^{-1} and 10 µL injection volume. The TAA peak was detected at 254 nm and data were analyzed using Chromquest 4.0 software. TAA levels were monitored and quantified using regression equations and dilution factors obtained from prior calibrations and the final TAA levels were expressed as g per kg of sample.

6.2.6. *L*-Citrulline analysis

For L-Citrulline analysis, samples were first lyophilized (Labconco Freeze Drying System, Kansas, USA) and the freeze-dried powdered samples (0.2 - 0.3 g) were weighed in 15 mL tubes. The samples were extracted with 7 mL water and 0.5 mL of 1 N HCl, by mixing and sonication (Cole-Parmer, IL, USA) for 30 min. The extract was centrifuged and filtered through Whatman No. 1 filter paper and injected to HPLC system according to previously reported methods.[202] The Waters 1525 HPLC system (Milford, MA, USA) was equipped with a Waters 2996 PDA detector and Waters 717 Plus autosampler connected with XBridge C_{18}, 3.5-µm column (150 mm × 4.6 mm i.d.) with a guard cartridge (Phenomenex, Torrance, CA) was used for quantification. HPLC separation was carried out at a flow rate of 0.4 mL/min using a mobile phase of (A) 0.03 mol L^{-1} phosphoric acid, (B) acetonitrile. Absorbance was monitored at

243 nm with a total run time of 14 min and 10 µL injection volume. The L-citrulline concentration was calculated on the basis of linear calibration functions and with regard to dilution factors. The L-citrulline content was expressed as g per kg of freeze-dried watermelon sample.

6.2.7. Statistical analysis

The experiments were set up in a completely randomized design with three replications for all the analysis. Statistical analysis was performed on all raw data using two-way analysis of variance (ANOVA) with JMP Pro 14.0.1 software. A general linear model was used to test significant differences, and means were compared using Student's t-test. Correlations were calculated using Pearson's correlation coefficient (R). The results were expressed as means ± standard error of mean.

6.3. Results

6.3.1. Physico-chemical characteristics

Some of the inherent varietal differences in fruit physico-chemical characteristics such as average fruit mass and shape were conserved and also reflected in responses to seed treatments and storage effects (Table 7; Figure 32). Location effects on fruit physico-chemical characteristics were also weak; hence data were pooled across locations for analysis. Seed priming with TNE or AgNPs was associated with a slight increase in fruit mass. However, this effect was significant only in the diploid variety (Riverside). For both varieties, fruit exocarp (rind) thickness near the peduncle end was significantly greater (12.7 – 15.1 mm) than at the stylar end (4.3 – 8.2 mm). While fruit mesocarp pH did not differ significantly between the two varieties, SSC was generally higher in Maxima compared to Riverside. Seed nanopriming with TNE or AgNPs resulted in heavier fruits and larger fruit diameter for Riverside but not Maxima

(Table 7). Nanopriming also resulted in a significant decrease in fruit mesocarp juice pH and a significant increase juice SSC for Riverside but not Maxima. Seed nanopriming had no effect on exocarp thickness.

Table 7 Combined analysis of physico-chemical characteristics of watermelon fruit, Maxima and Riverside with three treatments harvested from five different locations and stored for 0, 10, and 20 days. Statistical analysis was performed using two-way analysis of variance (ANOVA) and means were compared using Student's t-test. Within a group, means with different letters indicate significant differences at the $P < 0.05$. TNE: Turmeric nanoemulsion, AgNPs: Silver nanoparticles, RT: Rind thickness, NS: Non-significant.

Factors	Treatments	Weight (kg)	Diameter (cm)	Length (cm)	RT at stylar end (mm)	RT at peduncle end (mm)	pH	SSC (%)
Riverside								
Storage (S)	0	9.84a	28.15a	29.74a	6.84a	15.15a	5.66a	9.84a
	10	9.41ab	27.53a	29.26a	5.14b	13.13b	5.70a	9.87a
	20	8.79b	26.36b	29.57a	4.37c	12.78b	5.53b	9.31b
Treatments (T)	Control	8.25b	26.12b	28.69b	5.72a	13.59a	5.56b	9.36b
	TNE	9.63a	28.06a	29.60ab	5.49a	14.06a	5.66a	9.84a
	AgNPs	10.17a	27.86a	30.28a	5.13a	13.40a	5.68a	9.82a
Interaction	(S x T)	NS	NS	NS	NS	NS	NS	NS
Maxima								
Storage (S)	0	8.99a	25.28a	25.52ab	8.28a	15.07a	5.60b	10.17ab
	10	8.80a	24.86ab	26.18a	5.12b	13.87b	5.77a	10.33a
	20	8.17b	24.51b	24.97b	5.06b	12.92b	5.75a	9.98b
Treatments (T)	Control	8.46a	24.86a	25.35a	6.45a	14.04a	5.74a	10.15a
	TNE	8.65a	24.72a	25.55a	6.01a	13.91a	5.70a	10.06a
	AgNPs	8.85a	25.06a	25.77a	6.00a	13.91a	5.71a	10.26a
Interaction	(S x T)	NS	NS	NS	NS	NS	NS	NS

There was a gradual decline in mean fruit fresh mass between 0 and 20 d in storage (Table 7). This fruit weight loss was greater (-11%) in Riverside compared to Maxima (-9%). Average fruit diameter and exocarp thickness also declined slightly for both varieties between 0 and 20 in storage. Mean fruit mesocarp juice pH showed a declining trend with storage time for Riverside but the reverse trend for Maxima. For both varieties, average mesocarp juice SCC initially increased between 0 and 10 d in storage but then decreased thereafter at 20 d in storage.

6.3.2. Changes in carotenoid content

β-carotene, trans-lycopene, and cis isomers (13 cis-lycopene and 5 cis-lycopene) were quantified in this study at 0, 10, and 20 d after harvesting (Figure E1). After 10 d in storage, higher trans-lycopene contents were observed in Riverside fruits from all locations compared to freshly harvested fruits and Maxima fruits (Table 8). However, after 20 d in storage, fruits of both varieties exhibited lower lycopene levels compared to fresh fruits and fruits after 10 d in storage. This trend was similar in cis isomers, 13 cis-lycopene and 5 cis-lycopene (Table 8). Treatment effects on the levels of trans- and cis-lycopenes were weak. Mesocarp β-carotene levels were very low (0.29 to 8.93 mg kg^{-1}) compared to lycopene levels. In combined analysis, β-carotene contents were significantly higher at 20 d in storage compared to freshly harvested fruits of both varieties. Nanopriming had no effects on fruit β-carotene levels compared to the control unprimed watermelons.

Table 8 Carotenoids level (mg kg^{-1}) of watermelon fruit, Riverside and Maxima. Statistical analysis was performed using two-way ANOVA and means were compared using Student's t-test. Different letters indicate significant differences at *P < 0.05, **P < 0.01. TNE: Turmeric nanoemulsion, AgNPs: Silver nanoparticles, lyc: lycopene, car: carotene, NS: Non-significant.

			Riverside				Maxima			
Location	**Factors**		**trans- lyc**	**13 cis lyc**	**5 cis lyc**	**β-car**	**trans-lyc**	**13 cis lyc**	**5 cis lyc**	**β-car**
Edinburg	Storage (S)	0	55.99c	3.55c	5.74c	2.59b	57.97c	4.67b	9.68b	0.90b
		10	123.54a	14.61a	18.95a	5.67a	108.77a	8.45a	14.93a	3.51a
		20	91.11b	6.69b	8.34b	4.76a	77.37b	6.96ab	9.39b	4.18a
	Treatments (T)	Control	90.00a	9.68a	12.36a	4.10a	81.30a	7.43a	11.96a	2.30a
		TNE	90.38a	8.76ab	11.54a	4.06a	76.47a	7.01a	11.47a	3.38a
		AgNPs	90.26a	6.41b	9.12b	4.85a	86.34a	5.65a	10.60a	2.90a
	Interaction	(S x T)	NS	**	**	NS	**	NS	NS	*
Pecos	Storage (S)	0	95.83a	5.04b	14.41a	1.11c	118.67a	6.71b	17.23a	1.34b
		10	104.10a	9.13a	9.13b	1.80b	124.21a	8.76a	8.76b	2.12a
		20	84.63b	3.53c	3.53c	3.27a	94.26b	5.27c	5.27c	2.22a
	Treatments (T)	Control	81.56c	6.20a	7.40a	1.64b	111.01a	6.81a	10.16a	1.76a
		TNE	107.43a	5.95a	9.73a	2.31a	116.41a	7.14a	10.9a	1.80a
		AgNPs	95.46b	5.55a	9.93a	2.23a	109.72a	6.79a	10.19a	2.13a
	Interaction	(S x T)	NS	**	NS	NS	NS	**	**	NS
Grapeland	Storage (S)	0	107.45b	5.27a	7.88b	4.36b	86.43b	4.43a	8.71a	5.21c
		10	122.34a	4.78a	10.11a	5.97a	99.98a	5.25a	9.41a	6.91b
		20	100.02b	4.35a	6.59c	6.85a	73.19c	4.69a	9.42a	8.93a
	Treatments (T)	Control	111.82a	4.77ab	8.09a	5.09b	85.63a	5.18a	9.71a	7.43a
		TNE	104.88a	4.30b	7.79a	5.06b	89.39a	4.15a	9.15a	5.98b
		AgNPs	113.09a	5.33a	8.71a	7.03a	84.58a	5.04a	8.68a	7.64a
	Interaction	(S x T)	NS	*	NS	NS	NS	*	NS	NS
Snook	Storage (S)	0	66.90b	2.63b	8.83b	0.29b	62.63b	2.90b	6.82b	0.69b
		10	84.05a	4.75a	13.74a	1.77a	81.15a	6.78a	16.99a	1.71a
		20	59.48b	5.12a	9.48b	1.72a	56.83b	2.43b	7.31b	0.93b
	Treatments (T)	Control	61.30b	4.18a	10.53a	0.9b	70.66a	4.12a	10.69a	1.14a
		TNE	70.89ab	3.90a	10.76a	0.94b	63.12a	4.09a	10.31a	1.36a
		AgNPs	78.25a	4.42a	10.76a	1.94a	66.83a	3.90a	10.13a	0.83a
	Interaction	(S x T)	NS	*	NS	**	NS	*	NS	NS
Weslaco	Storage (S)	0	67.22b	1.06c	3.13b	0.60b	104.32b	2.03a	6.20a	1.38c
		10	77.65a	1.33b	4.24a	1.16a	119.09a	1.78ab	5.08b	2.25a
		20	50.52c	1.61a	1.41c	0.65b	53.81c	1.50b	2.53c	1.71b
	Treatments (T)	Control	56.66c	1.16c	2.58b	0.76a	87.96a	1.41c	4.32a	1.36b
		TNE	64.01b	1.34b	3.07a	0.75a	94.07a	1.76b	4.76a	1.65b
		AgNPs	74.73a	1.49a	3.13a	0.90a	95.19a	2.15a	4.72a	2.33a
	Interaction	(S x T)	**	**	NS	**	NS	**	**	NS
Combined locations	Storage (S)	0	81.95b	3.49b	8.34b	2.10b	90.20b	4.07b	9.73b	1.83b
		10	102.13a	6.94a	12.44a	2.79ab	106.39a	6.20a	12.71a	3.12a
		20	75.75b	4.25b	5.86c	3.29a	73.16c	4.17b	6.78c	3.60a
	Treatments (T)	Control	80.53a	5.15a	8.34a	2.49a	89.09a	4.98a	9.78a	2.68a
		TNE	88.44a	4.83a	9.28a	2.54a	89.99a	4.81a	10.03a	2.77a
		AgNPs	90.85a	4.71a	9.03a	3.15a	90.67a	4.65a	9.42a	3.10a
	Interaction	(S x T)	NS	NS	NS	NS	NS	NS	NS	NS

6.3.3. Colorimeter values and their correlation with carotenoids

There was a strong location effect on fruit mesocarp color characteristics especially hue values (Table E1). Fruits grown in southernmost location (Weslaco) were significantly redder than those from the other locations as indicated by the lower hue angles (24 – 27 for Weslaco compare to 43 – 50 for other locations). Mesocarp color saturation was also much greater (C* values 48 - 50) for fruits from Weslaco, compared to other locations (C* values 24 – 31). Significant correlation among carotenoids and mesocarp color characteristics were observed (Figure 33).

	l	*a*	*b*	*c*	*h*	*β carotene*	*trans-lycopene*	*13 cis lycopene*	*5 cis lycopene*
l	1.0								
a	-0.5	1.0							
b	-0.2	0.7	1.0						
c	-0.5	1.0	0.8	1.0					
h	0.5	-0.1	0.6	0.0	1.0				
β carotene	-0.6	0.4	0.7	0.5	0.3	1.0			
trans-lycopene	-0.1	0.7	0.2	0.6	-0.4	-0.2	1.0		
13 cis lycopene	-0.2	0.9	0.7	0.9	0.0	0.3	0.8	1.0	
5 cis lycopene	0.0	0.7	0.1	0.6	-0.4	-0.2	1.0	0.8	1.0

Scale: 1, 0.6, 0.3, 0, -0.3, -0.6, -1

Figure 33 Correlation Coefficients among carotenoids and the colorimeter values measured of fruit from watermelon cultivars (Riverside and Maxima) of three treatments (control, turmeric nanoemulsion and silver nanoparticles priming) harvested from five different locations; Edinburg, Pecos, Grapeland and Snook (2017) and Weslaco (2018) at 0 d, 10 d and 20 d of storage.

Fruit β-carotene contents were positively correlated with the color saturation variable b*. For fruits from all locations, there was a gradual fading in mesocarp color (lower L* values) after storage of both varieties resulting negative correlation among the carotenoids and the L* values. The mesocarp color saturation parameters (C* and a*) were positively related with levels of trans- and cis-lycopenes. The result of correlation coefficient was further supported by Table E1 which shows relatively higher a* values during storage, specifically during 10 d after harvesting as compared to the fresh watermelons in most of the locations. Similar higher values of lycopenes were recorded in 10 d stored watermelons (Table 8).

6.3.4. *L*-Citrulline level

L-Citrulline is a non-essential amino acid, a precursor of arginine involved in the nitric oxide cycle and related biological functions, as well as a radical-scavenging phyto-protectant against oxidative stress. In contrast to the carotenoids, L-citrulline was found to be significantly reduced in 10 d after harvesting watermelons as compared to the fresh one during combined analysis of Riverside fruits. Although, the trend is similar in the Maxima watermelons, there was not significantly difference in the level of L-citrulline content during 10 d after harvesting compared to the fresh watermelons. For both varieties, L-citrulline level was significantly reduced in samples from 20 d after harvesting as compared to the fresh (Table 9). The combined analysis showed that the lack of significant differences in the level of L-citrulline in between the nanoparticle treated and untreated watermelons of both cultivars.

Table 9 L-Citrulline (g kg^{-1}) and total ascorbic acid (g kg^{-1}) of watermelon fruit, Riverside and Maxima. L-Citrulline results are expressed in dry weight base. Statistical analysis was performed using two-way ANOVA and means were compared using Student's t-test. Different letters indicate significant differences at *P < 0.05, **P < 0.01. TNE: Turmeric nanoemulsion, AgNPs: Silver nanoparticles, NS: Non-significant.

Location	Factors		Riverside		Maxima	
			L-Citrulline	Total Ascorbic Acid	L-Citrulline	Total Ascorbic Acid
Edinburg	Storage (S)	0	7.35a	73.12a	10.37a	37.65b
		10	3.41b	37.42b	7.97b	45.41a
		20	3.83b	26.57c	5.03c	14.44c
	Treatments (T)	Control	5.52a	41.32b	5.83b	32.49a
		TNE	3.61b	52.84a	8.36a	30.05a
		AgNPs	5.46a	42.97b	9.18a	34.96a
	Interaction	(S x T)	**	**	**	NS
Pecos	Storage (S)	0	11.77a	49.98b	16.17a	43.58b
		10	10.77a	68.06a	14.24b	75.23a
		20	11.75a	22.35c	12.75c	18.83c
	Treatments (T)	Control	10.78b	46.65a	15.13a	39.76b
		TNE	10.99b	44.29a	14.76a	48.90a
		AgNPs	12.52a	49.45a	13.27b	48.97a
	Interaction	(S x T)	NS	**	NS	*
Grapeland	Storage (S)	0	10.21a	75.11a	10.65a	87.72a
		10	9.89a	67.46a	12.60a	55.07b
		20	9.80a	34.78b	11.35a	49.21c
	Treatments (T)	Control	9.03b	45.95c	12.44a	67.04a
		TNE	9.98ab	61.41b	10.69a	60.60a
		AgNPs	10.89a	69.98a	11.48a	64.37a
	Interaction	(S x T)	NS	**	NS	**
Snook	Storage (S)	0	9.08a	76.61b	9.64a	106.09a
		10	9.18a	86.33a	7.90b	55.22b
		20	8.54a	5.47c	5.89c	21.85c
	Treatments (T)	Control	8.56a	54.37a	7.29b	64.86a
		TNE	8.91a	54.85a	7.92ab	62.08ab
		AgNPs	9.31a	59.18a	8.22a	56.21b
	Interaction	(S x T)	NS	**	*	NS
Weslaco	Storage (S)	0	11.58a	23.02a	11.67a	20.96b
		10	10.01b	6.04b	11.13a	35.12a
		20	10.87ab	7.06b	11.40a	14.00c
	Treatments (T)	Control	10.16a	11.48b	10.98a	24.84a
		TNE	11.20a	10.92b	11.30a	22.13a
		AgNPs	11.09a	13.72a	11.92a	23.10a
	Interaction	(S x T)	NS	**	**	*
Combined locations	Storage (S)	0	10.40a	57.52a	11.82a	62.43a
		10	8.89b	54.28a	10.68ab	53.33a
		20	8.60b	19.09b	9.27b	23.80b
	Treatments (T)	Control	8.77a	40.54a	10.58a	46.68a
		TNE	9.10a	43.18a	10.57a	46.16a
		AgNPs	10.02a	47.17a	10.63a	46.72a
	Interaction	(S x T)	NS	NS	NS	NS

6.3.5. Total ascorbic acid

Differential effect of storage and nanoparticle treatment was observed in the level of TAA in different locations and varieties. On average from all the locations and varieties, TAA was maintained in both watermelon varieties at 10 d after harvesting as compared to the fresh watermelons (Table 9). However, TAA was found to be significantly reduced in 20 d after harvesting compared to the fresh and the 10 d storage samples. Similarly, combined data showed no significant differences in the TAA level in between the nano treated and untreated watermelons of both varieties.

6.4. Discussion

6.4.1. Influence of storage in watermelon quality

6.4.1.1. Physico-chemical characteristics

In watermelons, thinning of the rind, increased pH and SSC, and increased flesh redness are indicators of ripeness, whereas a slight loss of SSC and a shift in color from red to red orange are indicators of over ripeness. In our study, slight reduction of the SSC was recorded in the watermelons stored for 20 d after harvesting. Lower SSC (%) was also observed in Black diamond, Summer Flavor 800, and Sugar Shack watermelons stored at 21 °C for 14 d[198] relative to fresh watermelons.

Result indicated significant gradual thinning of rind at both peduncle and stylar end of watermelons stored for 10 and 20 d after harvesting of both varieties, compared to the fresh fruit. A similar loss of rind thickness was reported for Black diamond, Summer Flavor 800, and Sugar Shack watermelons stored at 21 °C for 14 d[198] relative to fresh watermelons. Thinning of the rind was also reported for Charleston Gray and Congo melons stored at 20 °C for 7-10 d.[203]

During the first and second week of storage at 25 °C, rind thickness declined by 8.9 % (1.1 mm) and 17.7 % (2.0 mm), respectively in grafted watermelon cultivars.[204] Despite watermelon's non-climacteric nature, fruits might have undergone various biotic and abiotic stresses and continue their metabolic activities leading to the variation in the physico-chemical properties.

6.4.1.2. Changes in lycopene content

Several factors have been shown to affect the lycopene content of watermelon. Lycopene content varies widely in watermelon germplasm, ranging from 36 to 120 mg kg^{-1} of fresh weight [205]. Environmental conditions during production, such as light intensity, temperature, and irrigation, can alter lycopene content by 10−20 %.[206] It has been suggested that the carotenoids producing enzymes pathways are sensitive to temperature.[207] Despite its non-climacteric nature, lycopene accumulated in the watermelon and consequent color development may evolve during postharvest storage.[197] Redder watermelons were found when stored at ambient temperatures (22−33 °C) for 7−10 d[208] which explained the increased lycopene level in our study at 10 d storage samples. Significant enhancement of fruit lycopene content and further pulp color development was found to be more pronounced in both grafted and non-grafted watermelon fruits at 10 d storage compared to the fresh one.[197] Besides watermelon, room temperature stored tomatoes also showed significant increase in lycopene content during 7 d storage.[209] The first step in the biosynthesis of carotenoids is the condensation of two molecules of geranyl-geranyl diphosphate (GGPP), to form phytoene.[210] An increased pool of GGPP, or the increased activity of enzymes phytoene synthase and phytoene desaturase may have been present in watermelon held at 21 °C, for conversion to lycopene.[198] Employing similar HPLC method parameters, we monitored phytofluene level at 350 nm in randomly selected few watermelon samples.

Results demonstrated the reduced level of phytofluene at 10 d of storage as compared to the fresh watermelons (Figure E2 and E3). This phytofluene might have converted to the trans-lycopene resulting enhanced level of trans lycopene at 10 d as compared to the fresh watermelons.

Again, reduced lycopene was recorded at 20 d as compared to the 10 d of storage in watermelons. The principal cause of lycopene degradation is autooxidation of lycopene which is irreversible and will lead to formation of acetone, methylheptenone, laevulinic aldehyde, and probably glycoxal, which causes typical faded, discolored products having off flavors.[211] The autooxidation of lycopene might have caused the significant reduction at 20 d storage as compared to samples at 10 d of storage.

6.4.1.3. β-carotene level

Result demonstrated significantly higher *β*-carotene content at 20 d after harvesting compared to the fresh watermelons in both varieties during combined analysis. Similar increment of *β*-carotene contents was recorded in the watermelon fruit stored at 21 °C for 14 d indicating enhancement of carotenoid pathway enzymes.[198] Also, in grapefruit, the *β*-carotene levels was found to be gradually increased up to 35 d of storage at room temperature.[164]

Our results indicated that the carotenoid synthesis in watermelons continues to function long after harvest, and the system is enhanced by storage at 23 °C which is in agreement with the previous result.[198] It has been reported that *β*-carotene amount depends on the presence of lycopene, since it is synthesized from lycopene by the enzyme lycopene -*β*- cyclase.[212] Our data on carotenoid composition are consistent with these findings. *β*-carotene content was comparatively low in fresh fruit, then both lycopene and *β*-carotene increased from fresh to 10 d storage stage. Again, the lycopene decrease from 10 to 20 d storage could be due to the onset of

its catabolism, which provoked the significant increase in β-carotene concentration in watermelons at 20 d of harvest.

6.4.1.4. Colorimeter values and their correlation with carotenoids

Chroma measures color saturation or intensity, while a* measures the degree of red (+a*) or green (−a*) color. The a* (redness) and chroma values were highest in watermelons during storage, specifically during 10 d after harvesting as compared to the fresh watermelons. (Table E1). Similar increased in the a and chroma parameter was observed in the mini watermelons with the increase in the ripening stage[212] and in grafted and non-grafted watermelons held at 25 °C for 10 d.[197] In the present study, β-carotene contents of watermelons fruits from the two cultivars were positively correlated with the color variables b*, and chroma (c) values (Figure 33). In our experiment, a* was better correlated than other colorimeter values to the lycopene content of watermelons which is in agreement with the earlier literature on watermelons.[198, 213] The increase in lycopene most likely contributed to the increased in a* values in watermelon. Watermelons from all location were less dark (lower L* values) after storage of both varieties resulting negative correlation among the carotenoids and the L* values. The hue angle measured by tristimulus colorimeters is frequently used to discriminate among subtle visual color differences. A hue angle of 26.7 ° is considered a pure red color, while a hue angle of 28–30° is a reddish-yellow color and 22–24 ° a garnet-red/purplish-red color. In our study the hue angle of the red watermelon cultivars varied from about 24.46 to 31.31° (Table E1). The highest hue angle was recorded in watermelons after 20 d after harvesting i.e. 31.31°, indicating a more reddish-yellow color.[208] A visible orange color in the watermelons were observed when stored at ambient temperatures (22−33 °C) for more than 10 d.[208] Lycopene content and hue were also poorly

correlated in commercial red fleshed watermelons[213] and tomatoes[214] as compared to the a* or chroma values. The correlation coefficient demonstrated the lack of positive correlation between the hue and carotenoids which is in agreement with earlier result.[198] This result concluded that chroma, a function of a* and b* values, was found to be much better indicator of lycopene content than hue in this study.

6.4.1.5. L-Citrulline level and total ascorbic acid

In this study, L-citrulline level ranges from 3.41 to 16.17 (g kg^{-1}) and results were measured in dry weight basis which is in accordance with the earlier research.[202, 215] Significant storage effect was recorded in the grafted watermelons where L-citrulline content was found to be declined during storage at 25 °C at 10 d after harvesting.[197] Degradation of L-citrulline to ammonia and carbon dioxide during storage[146] might cause the reduced level at 10 and 20 d of storage as compared to the fresh watermelons in our study.

The combined analysis demonstrated that the TAA level was maintained in watermelon of both varieties at 10 d after harvesting as compared to the fresh watermelons. Similar result was obtained in the intact watermelons stored for 9 d where vitamin C content was maintained as fresh watermelons.[216] At 20 d of storage at room temperature, our study demonstrated the significant loss of TAA. Previous studies have directly correlated degradation of vitamin C due to storage temperature and storage period.[217-218] Ascorbate oxidase has been proposed to be the major enzyme responsible for enzymatic degradation of ascorbic acid. Ascorbic acid first oxidizes reversibly to dehydroascorbic acid in the presence of ascorbate oxidase, which undergo further oxidation followed by hydrolytic steps or direct hydrolysis irreversibly to 2,3-diketogulonic acid.[219] Thereafter, the 2,3-DKGA degrades to form threonic and oxalic acids and

these irreversible degraded products has no vitamin C activity.[220] This explains the reduction of TAA in the 20 d after harvesting watermelons fruits.

6.4.2. Nanoparticle treatments in nutritional composition of watermelons

Results indicated no significant treatment effect in the weight, length, diameter, rind thickness, pH and the SSC level of the Maxima fruit. However, when combined across locations for the Riverside fruits, both nano treatments had significantly enhanced physico-chemical parameters compared to the unprimed watermelons. This observed distinct differences in the diploid and triploid varieties may be due to their different genetic makeup and seed morphology. Similarly, in both cultivars, content of TAA, β-carotene, L-citrulline, trans and cis lycopene level were not significantly different in between the control and the nanopriming treatments during combined analysis.

From our previous study, a positive impact of nanoparticles on seed germination, growth and yield has been observed.[82] Despite the growing research and publications on the interaction of nanoparticles with plants, knowledge of the implications of NPs in the nutritional value of food crops is still limited. Therefore, assessment of health promoting compounds in nanoparticle treated watermelon could lay foundation for NPs potential impact in the nutritional quality of the final produce. From this study, the lack of treatment differences and enhanced positive impacts were observed in the AgNPs treated crops. AgNPs and TNE did not show any negative impact on the phytochemical content of both watermelon cultivars. Taken together, these results indicate that biosynthesized nanomaterials were nonphytotoxic regarding the nutritional quality of the watermelon.

6.5. Conclusion

A storage study was done in the intact watermelons stored at 10 and 20 d after harvesting and were compared with the fresh watermelons. Physico-chemical characteristics such as weight, length, diameter, and SSC (%) and the nutritional composition were maintained in the watermelons stored for 10 d at 23 °C. Lycopene and its isomers level were significantly high at 10 d of storage compared to the fresh watermelons. However, in both varieties, physico-chemical characteristics and phytochemical composition was found to be significantly reduced in 20 d storage samples. It is possible that watermelons continue their metabolic activities after harvest and might have undergone various biotic and abiotic stresses.

Along with the storage study, the effect of AgNPs on phytonutrients and quality of watermelons were compared with the TNE and the control unprimed samples. AgNPs and TNE as the nanopriming treatment in watermelon seeds had no significant differences in the level of phytochemical composition as compared to the unprimed. These observations demonstrate the differential impacts that preharvest cultural management factors (including cultivar selection, growth location and seed treatment) can have on the nutritional quality of foods. Our results also elucidate that plant mediated nanoparticles have future application in the production of watermelon without deteriorating the nutritional quality.

7. POST-HARVEST STORAGE AND GROWING ENVIRONMENTS ALTER THE VOLATILE COMPOUND PROFILES OF TRIPLOID AND DIPLOID WATERMELONS

7.1. Introduction

Watermelon (*Citrullus lanatus*) is a warm-season crop cultivated throughout the world and is in high demand due to it's refreshing taste, attractive color, good flavor and potential health benefits.[221] Important health-promoting phytochemicals present in watermelon include lycopene, β-carotene, flavonoids, phenolic compounds, L-citrulline, and vitamins.[222] Watermelon is a heat-sensitive fruit and environmental factors greatly affect its quality and flavor factors.[223] For example, different growing environments with different weather conditions affect the total volatile content, which affects fruit aroma.

Fruits and vegetables remain physiologically active after harvest and their metabolic processes continue during postharvest handling and storage. During this process, abiotic stresses can accelerated metabolic responses, degradation of substrates and changes in bioactive compounds in fruits and vegetables.[224] Postharvest storage of produce can lead to loss of reserves that provide energy to maintain the nutritional and qualitative aspects, which can lead to changes in phytonutrients and volatile composition.[224-225]

Volatile compounds play a key role in watermelon quality as they contribute to the aroma profile. The typical aroma of each fruit results from a combination of several volatile substances, such as esters, alcohols, acids, aldehydes, ketones, acetals, hydrocarbons, ethers and heterocyclic compounds that result from different biochemical pathways for aroma production.[226-228] Most volatiles are formed after fruit cutting followed by the introduction of oxygen and the release of enzymes.[229] Aroma formation in fresh-cut watermelon is a dynamic enzymatic process; therefore

the aroma is not long lasting and constantly changing.[230] The abundance of volatile compounds in fruit is influenced by many factors including cultivar, agronomic practices, types of treatment used, ripeness, growing environment, and postharvest handling.[231] Therefore, it is important to investigate the qualitative and quantitative pattern of volatile compounds that occur due to different growing location, cultivars and storage period.

Although there have been several previous studies have examined fruits that are closely related to watermelon, such as cantaloupe and honeydew melons, there have been a limited number of reports concerning volatile flavor compounds of watermelon. Previously reported storage studies on watermelon volatiles have mostly focused on juice and cut slices. To the best of our knowledge, there is little information available concerning the aroma profiles of watermelons that were stored as whole, uncut fruit. To address this, here we studied the volatile profiles of Riverside and Maxima cultivars as influenced by the growing environment and storage.

7.2. Materials and methods

7.2.1. Chemicals

n-Alkanes (C_6–C_{24}) used for the Kovat index (KI) calculation were obtained from Sigma-Aldrich (Saint Louis, MO, USA). Ethanol served as the solvent for dissolving reference standards, perillyl alcohol (internal standard) and SPME fibers were purchased from Sigma-Aldrich.

7.2.2. Fruit samples

Watermelons were grown in five different locations in Texas: Edinburg (26°18′N 98°9′W), Snook (30°29′N,96°28′W), Pecos (31°24′N, 103°30′W), and Grapeland (31°29′N, 95°28′W) in the local growers' fields during the summer season of 2017 and Texas A&M Agrilife Research and Extension Center at Weslaco (26°15′N, 97°′W) during the summer season of 2018. Watermelons

of two cultivars, Riverside (diploid) and Maxima (triploid) were collected, cleaned with damp paper towels and stored in heavy duty cardboard boxes (22 x 22.5 x 22 in) at room temperature (23°C) for 20 d to simulate retail store conditions. Three watermelons of each cultivar from each location were analyzed at 0, 10, and 20 d of storage. Three samples were taken from each watermelon for volatile analysis.

7.2.3. Sample extraction

For extraction of fruit volatiles, samples were taken from the center heart portion of the flesh of each watermelon. Approximately 3 g of blended watermelon pulp was put in 20-mL sample vials and 10 µL internal standard perillyl alcohol (250 ppm) was added into the vials. Vials were immediately frozen and kept at -20°C until analysis. Flavor and off-flavor aromas have been assessed in watermelon samples by solid-phase microextraction (SPME). SPME was chosen because it is rapid, less laborious, relatively inexpensive, and does not require solvents, purge and trap, preconcentration, or vigorous extraction and heating (which may alter endogenous compounds), and the absorptive nature of the fibers permits assays at nondestructive temperatures.

7.2.4. HS-SPME-GC-MS analysis of volatile aroma compounds

Volatile compounds were identified using a Thermo Finnigan GC–MS (Thermo Fisher Scientific, Inc., San Jose, CA, USA) equipped with an electron ionization source with a Dual-Stage Quadrupole (DSQ II) mass spectrometer (Thermo Scientific, Austin, TX, USA). The GCMS sequence was set up and the method started with the vials being placed into a thermostatic stirrer for 30 min maintained at 60°C. The headspace volatile sampling was carried out by 50/30 µm divinylbenzene/carboxen/polydimethylsiloxane (DVB/CAR/PDMS) SPME fiber. Separation was achieved with a Zebron ZB-Wax column (20 m x 0.25 mm ID with 0.25 µm film thickness). Helium was used as the carrier gas at a constant flow rate of 1 mL/min in

splitless mode. The initial oven temperature was maintained at 50°C for 1 min, then increased to 170°C at a rate of 6°C/min. Finally, it was ramped up to 225°C at a rate of 25°C/min and held for 1 min with a total run time of 24 min. The injector, ion source and mass transfer line temperature were maintained at 225°C, 285°C and 280°C respectively. The ionization voltage was 70 eV, the mass range was 45–450 amu and the scan rate was 11.7 scans per second.

7.2.5. Identification and quantification of watermelon volatile compounds

Identification of volatile compounds was achieved by comparison of their mass spectra from the National Institute of Standards and Technology (NIST MS search 2.0) and Kovats indices (KI) against those in the literature. The KI values were calculated by the retention time of *n*-alkane standards (C_6–C_{24}) analyzed under the same chromatographic conditions as those of the samples. The data were processed using Xcalibur software (v. 2.0.7., Thermo-Fisher Scientific, San Jose, CA, USA). The regression equation of perillyl alcohol was used to calculate the concentration of volatile compounds and results were expressed as µg/kg of sample equivalence to perillyl alcohol.

7.2.6. Statistical analysis

Results of GC-MS data were subjected to multivariate statistical analysis. Multivariate analysis was performed by exporting GC–MS data in Excel format to online software, MetaboAnalyst 4.0 (http://www.metaboanalyst.ca/). Partial least square discriminant analysis (PLS-DA) were performed to evaluate metabolite patterns among different varieties, storage period and locations. All results were expressed as means ± standard error (SE).

7.3. Results and discussions

7.3.1. Volatile composition in Riverside and Maxima watermelon cultivars

Volatile compounds responsible for the characteristic flavor and aroma of fruits are produced via metabolic pathways and depend on many factors including species, variety and

treatment.[232] In this study, the volatile compositions of Riverside and Maxima grown in five different environments in Texas (Snook, Pecos, Grapeland, Edinburg and Weslaco) were compared across three different storage period (0 d, 10 d and 20 d) for each cultivar (Figure 34).

Our SPME GC-MS analysis identified a wide range of volatile compounds were identified in the watermelon fruits using SPME GC-MS. The 87 identified and quantified volatiles compounds, together with their retention times are listed in Table 10. The quantified volatiles were grouped into seven classes: alcohols, aldehydes, ketones, furan, hydrocarbons, acids and ester compounds. The most represented compounds were C6 and C9 aldehydes and alcohols. Among the aldehydes, (Z)-6-nonenal, (E)-2-nonenal, (E,Z)-2,6-nonadienal and nonanal were prevalent (Table F1-F5). For the fresh watermelon samples, the Riverside cultivar had the highest amount of (Z)-6-nonenal (3129.3 μg/kg) in fruit from Snook and nonanal (2836.43 μg/kg) in fruit from Edinburg. (E,Z)-2,6-nonadienal (1452.22 μg/kg) and (E)-2-nonenal (3030.85 μg/kg) were recorded highest in Maxima fruit from Pecos. Among the alcohols, fresh samples of Maxima harvested from Snook at 0 d had the largest amounts of (Z)-3-nonen-1-ol (5473.49 μg/kg), (Z,Z)-3,6-nonadien-1-ol (3881.69 μg/kg), (E)-6-nonen-1-ol (803.13 μg/kg) and 1-nonanol (1604.81 μg/kg) as compared with the other cultivar and other locations (Table F1).

Table 10 Identification information of the volatile compounds recovered in Riverside and Maxima watermelon via SPME GC-MS. Identification of volatile compounds was achieved by comparison of their mass spectra and Kovats indices (KI). RT: Retention time, MW: Molecular weight

S.N	RT	Compounds	MW	Measured KI	Lit KI	R match	Library
1	2.30	Ethanol	46.07	1068	900	954	wileyregistry8e
2	3.64	Hexanal	100.16	1127	1078	897	wileyregistry8e
3	5.04	D-limonene	136.23	1189	1180	914	wileyregistry8e
4	5.48	β-limonene	136.23	1208	1183	842	wileyregistry8e
5	5.50	Pyridine	79.10	1209	1185	842	wileyregistry8e
6	5.71	2-Pentylfuran	138.21	1218	1239	951	wileyregistry8e
7	5.80	(E)-2-Hexenal	98.14	1222	1248	896	replib
8	6.54	Cyclodecane	140.27	1255	1271	789	wileyregistry8e
9	6.58	Acetoin	88.11	1256	1272	870	wileyregistry8e
10	6.80	trans-2-(2-Pentenyl)furan	136.19	1266	1282	749	mainlib
11	6.99	Octanal	128.21	1274	1291	779	wileyregistry8e
12	7.57	6-Methyl-5-hepten-2-one	126.10	1300	1323	987	wileyregistry8e
13	7.84	(E)-2-Heptenal	112.17	1312	1334	866	replib
14	8.53	1 Hexanol	102.17	1342	1359	881	wileyregistry8e
15	8.60	Nonanal	142.23	1345	1370	981	wileyregistry8e
16	9.07	Perilline	150.22	1366	1431	877	wileyregistry8e
17	9.58	Acetic acid	60.05	1389	1452	862	wileyregistry8e
18	9.79	1-Octen-3-ol	128.21	1398	1456	949	wileyregistry8e
19	9.85	(E)-2-Octenal	126.19	1400	1457	723	replib
20	10.00	(E)-4-Nonenal	140.22	1408	1458	848	wileyregistry8e
21	10.26	(Z)-6-Nonenal	140.22	1420	1459	829	wileyregistry8e
22	10.42	(E)-6-Nonenal	140.22	1428	1469	948	mainlib
23	10.70	6-Methyl-5-hepten-2-ol	128.00	1442	1473	867	mainlib
24	10.76	(Z)-2-Nonenal	140.00	1444	1528	898	wileyregistry8e
25	11.03	Benzaldehyde	106.00	1457	1534	900	wileyregistry8e
26	11.20	Methyl nonanoate	172.00	1466	1536	911	wileyregistry8e
27	11.23	Decanal	156.00	1467	1538	876	wileyregistry8e
28	11.35	(E)-2-Nonenal	140.22	1473	1543	898	replib
29	11.90	Pinocarvone	150.00	1500	1553	833	wileyregistry8e
30	11.92	1-Octanol	130.14	1500	1565	921	wileyregistry8e
31	12.33	(E,Z)-2,6-Nonadienal	138.10	1520	1573	979	wileyregistry8e
32	12.33	Ethyl-3-nonenoate	184.00	1520	NA	712	wileyregistry8e
33	12.34	6-Methyl-3,5-heptadien-2-one	124.00	1521	1582	814	wileyregistry8e
34	12.72	(Z)-3-Nonenyl acetate	184.00	1539	1590	789	wileyregistry8e
35	12.89	β-cyclocitral	152.00	1547	1598	724	wileyregistry8e
36	12.98	(Z)-5-Octen-1-ol	128.12	1552	1608	805	ni
37	13.34	(E)-2-Decenal	154.25	1569	1630	793	wileyregistry8e
38	13.35	cis-Pinocarveol	152.23	1570	1653	833	wileyregistry8e
39	13.48	Methyl 6-nonynoate	262.27	1576	NA	769	wileyregistry8e
40	13.77	4,5-Difluoroctane	150.00	1590	NA	987	wileyregistry8e
41	13.88	1-Nonanol	144.00	1595	1666	957	wileyregistry8e
42	14.10	(Z)-Citral	152.12	1609	1678	955	wileyregistry8e
43	14.32	(Z)-3-Nonen-1-ol	142.14	1625	1682	894	mainlib
44	14.44	(E,E)-2,4-Nonadienal	138.00	1634	1686	777	wileyregistry8e
45	14.68	(Z)-6-Nonen-1-ol	142.00	1652	1696	909	wileyregistry8e
46	14.83	(E)-2-Nonen-1-ol	142.23	1663	1713	894	wileyregistry8e
47	14.92	(E)-6-Nonen-1-ol	142.00	1669	1714	951	wileyregistry8e
48	15.03	(E)-Citral	152.00	1677	1733	954	wileyregistry8e
49	15.52	(Z,Z)-3,6-Nonadien-1-ol	140.22	1730	1762	881	mainlib
50	15.82	(E,Z)-2,6-Nonadien-1-ol	140.22	1736	1766	911	replib
51	15.85	L-Perrillaldehyde	150.00	1738	1768	880	replib
52	15.91	Methoxy-phenyl-oxime	179.22	1742	1773	853	mainlib
53	16.35	(E,E)-2,4-Decadienal	152.23	1775	1795	886	wileyregistry8e
54	16.36	(E)-Geraniol	154.00	1776	1802	723	wileyregistry8e
55	16.74	cis-Geranylacetone	194.31	1803	1813	886	ni
56	16.95	Myrtenol	152.00	1817	1813	785	wileyregistry8e
57	17.07	α-Ionone	192.29	1824	1818	879	wileyregistry8e
58	17.20	trans-Geranylacetone	194.00	1833	1820	987	wileyregistry8e
59	17.59	Benzyl alcohol	108.00	1858	1822	901	wileyregistry8e
60	17.76	Isolimonene	136.23	1869	NA	768	mainlib
61	17.84	Hexanoic acid	116.00	1874	1826	961	replib

Table 10 continued

S.N	RT	Compounds	MW	Measured KI	Lit KI	R match	Library
62	18.18	Benzene ethanol	122.00	1896	1912	928	wileyregistry8e
63	18.30	Tetradecanal	212.37	1903	1924	789	wileyregistry8e
64	18.54	β-Ionone	192.00	1919	1955	897	wileyregistry8e
65	18.66	cis-Jasmone	164.24	1926	1960	776	wileyregistry8e
66	18.77	Benzothiazole	135.18	1933	1962	934	wileyregistry8e
67	18.97	6,10 Dimethyl-5,9 undecadien-2-ol	196.00	1946	1968	798	wileyregistry8e
68	19.43	β-Ionone-5,6-epoxide	208.00	1976	1995	899	mainlib
69	19.89	2 Hexenoic acid	114.00	2007	2002	850	wileyregistry8e
70	19.97	γ-Nonalactone	156.00	2013	2028	913	wileyregistry8e
71	20.07	Pentadecanal	226.00	2021	2042	765	wileyregistry8e
72	20.74	5 Pentyl-2(5H)-furanone	154.00	2077	2052	960	wileyregistry8e
73	21.23	Cuminol	150.00	2117	2068	855	wileyregistry8e
74	21.35	Octanoic acid	144.00	2127	2072	950	replib
75	21.59	(E,E)-Pseudoionone	192.00	2147	2073	869	mainlib
76	21.98	Nonanoic acid	158.00	2179	2144	957	wileyregistry8e
77	22.35	Methyl hexadecanoate	256.00	2210	2170	935	replib
78	22.62	Ethyl pentadecanoate	270.45	2232	2179	875	wileyregistry8e
79	22.63	Ethyl hexadecanoate	284.00	2233	2202	863	replib
80	22.71	3-Nonenoic acid	156.00	2240	NA	897	wileyregistry8e
81	23.18	Dihydroactinidiolide	180.24	2279	2337	840	wileyregistry8e
82	23.35	Farnesyl acetone	262.00	2293	2382	795	replib
83	23.80	Methyl 9-octadecenoate	296.48	2330	2400	770	ni
85	24.00	2 Decenoic acid	170.00	2346	2428	830	wileyregistry8e
86	24.03	Methyl octadecanoate	298.00	2349	2445	846	ni
84	24.14	Ethyl 9-octadecenoate	310.00	2358	2476	789	ni
87	24.19	Methyl octadecadienoate	310.00	2362	2488	796	ni

Although C6 and C9 compounds in fruits are often considered oxidation products, they are characteristic of the volatile fraction of fruits belonging to the Cucurbitaceae family. Watermelon aroma results from a combination of aldehydes and alcohols, which dominate qualitatively and quantitatively, with other compounds such as ketones and furans.[233] Key aroma characters determined by alcohols include fresh melon [(Z)-3-nonen-1-ol], pumpkin-cucumber [(Z,Z)-3,6-nonadien-1-ol], flower-green (hexanol), herbaceous (1-nonanol) and pumpkin-like, green melon [(Z)-6-nonen-1-ol].[234-235] Similarly, aldehydes determine the other key aroma characteristics of watermelon such as fat-cucumber-melon [(E)-2-nonenal], green (hexanal), cucumber-green [(E,Z)-2,6-nonadienal], melon-orange peel (nonanal), honeydew melon-fruity [(Z)-6-nonenal], earthy [(E)-6-nonenal] and flower aroma elicited by ketone 6-methyl-5-hepten-2-one.[234] The C9 double unsaturated alcohol (Z,Z)-3,6-nonadienol has been reported to be an

important aroma compound and is described as having a watermelon, fruity, fresh, cucumber aroma.[228]

Among 14 identified ketones, 6-methyl-5-hepten-2-one, trans-geranylacetone, β-ionone, (E,E)-pseudoionone, and farnesyl acetone were the most abundant. 6-Methyl-5-hepten-2-one, geranylacetone and β-ionone have been reported to be important contributors to the unique flavor of watermelon.[236] *β*-Ionone and dihydroactinidiolide were formed from peroxidase-mediated catabolism of *β*-carotene.[237] Other volatiles such as 6-methyl-5-hepten-2-one, (E,E)-pseudoionone, geranyl acetone, and farnesyl acetone are derived from breakdown of lycopene and other noncyclic tetraterpenoids.[229, 238] We expected to detect these compounds due to the high concentration of lycopene found in the red-fleshed watermelon analyzed in the study.

In this study, important hydrocarbons were also detected in the watermelon samples. However, these hydrocarbons were location specific. D-limonene, β-limonene, cyclodecane and pyridine were identified in Weslaco samples while isolimonene was only observed in Grapeland samples. Perilline and 4,5 difluoroctane were identified in most of the locations. Limonene was detected for the first time in watermelon with different flesh colors by Liu et. al. (2012).[239] In addition, fatty acid ester compounds like methyl nonanoate, ethyl 3-nonenoate, (Z)-3-nonenyl acetate, methyl 6-nonynoate, ethyl pentadecanoate, ethyl and methyl hexadecanoate, methyl- and ethyl 9-octadecanoate, methyl octadecanoate and methyl octadecadienoate were found. Among these, ethyl hexadecanoate and methyl and ethyl 9-hexadecanoate were abundant. No acetate or non-acetate esters were found in this study.

7.3.2. Effects of cultivar and location on total volatile contents

For the freshly harvested samples (0 d of storage), the triploid seedless cultivar Maxima had much higher total volatile contents than diploid seeded Riverside cultivar. The genotypic

variation in carotenoid composition results in differences in the terpenoid volatile profile and the fruit taste because important aroma volatiles are derived from the degradation of carotenoid pigments.[238-240] Lycopene is the major carotenoid present in watermelon and its content varies widely in watermelon germplasm, ranging from 36–120 μg/g FW of fresh weight.[205] In another study, lycopene content was 60–66 μg/g FW for triploids and 45–80 μg/g FW for diploid fruits.[206] Similarly, a higher total volatile content was recorded in the triploid cultivar (Maxima) as compared to the diploid (Riverside) cultivar which could be directly related to the carotenoid content.

Along with cultivars, we observed an effect of location on the volatile contents of watermelon. The total volatile content in Maxima was higher in fruit grown in Snook and Grapeland as compared to the other three locations. A similar trend was observed in the Riverside cultivar. For both cultivars, fruit from Weslaco and Edinburg had lower total volatile content. Among all the locations, Snook-Grapeland and Weslaco-Edinburg share geographical proximity. Therefore, variation in total volatile content could be due to the environmental conditions such as temperature, rainfall, and humidity. Geographical and weather differences among the growing locations were discussed in our earlier published paper.[82] Similar strong genotype and environmental effects on volatile compounds were observed in melon[241] and other berries like blueberry,[242] strawberry[243] and blackcurrant.[244] The carotenoids-producing enzymes pathways are sensitive to temperature of growing environment.[207] For example, lycopene production in watermelon fruit was inhibited above 37 °C.[245] Effect of location in the carotenoid content and the direct role of these carotenoid pigments in the volatile content might result in variation among locations.

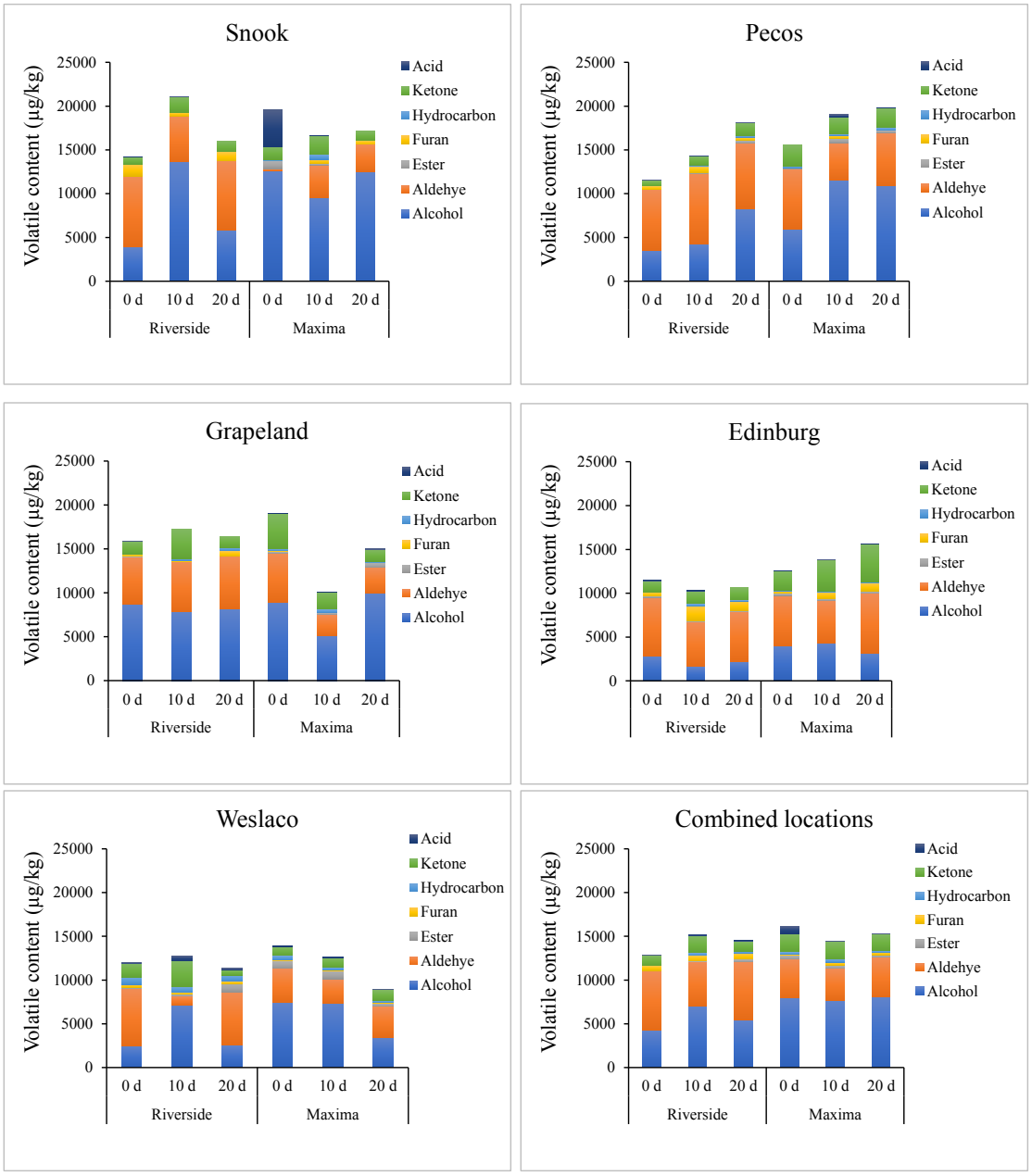

Figure 34 Volatile content of 'Riverside' and 'Maxima' watermelon grown at five different locations of Texas and analyzed at different storage period.

7.3.3. Relative contents of all classes of volatiles

The relative content of each class of volatile compounds present in Riverside (Figure 35) and Maxima (Figure 36) were calculated for all the locations. The average data from all locations demonstrated a higher relative content (%) of alcohols at 10 d (Figure 35 and 36). However, the average relative content of aldehydes was low at 10 d of storage (33.8%) compared with the fresh (51.43%) and 20 d (46.35%) samples in Riverside. A similar trend was observed in Maxima. In most of the locations, C9 aldehydes like nonanal and (Z)-6-nonenal were present in lower levels at 10 d compared with 0 d. By contrast, alcohols like (E)-6-nonenol, (Z,Z)-3,6-nonadien-1-ol, and (E,Z)-2,6-nonadien-1-ol were present at higher levels at 10 d compared with 0 d (Table F1-F5).

Analysis of the relative contents of these volatiles may reveal metabolic relationships among compounds and identify key compounds responsible for appealing and off-putting aromas. For example, in pasteurized watermelon juice, the aldehyde content decreased significantly in 14 d storage at 4°C, but the alcohol, acid, and ester content of the juice increased.[246] We observed that the relative content of aldehyde at 10-d storage period was very low in Riverside cultivar grown at Weslaco as compared to the other storage period and locations (Figure 35). Interestingly, for the same storage period at Weslaco, the relative content of total acid at 10-d storage period was very high. Similarly, in case of Maxima, relative content of aldehyde at fresh 0 d samples of Snook were very low while, the acid content for the same sample was high compared to others. This showed the negative correlation of acid and aldehyde content in watermelons among locations.

In another storage study of cut watermelon, no significant difference was found for (Z)-3-nonen-1-ol during storage while the percentages of (E,Z)-2,6-nonadienal, (Z,Z)-3,6-nonadienol,

(Z)-6-nonen-1-ol, and (E)-2-nonenal differed significantly.[228] Irrespective of treatments, a significant increase in (Z)-6-nonen-1-ol was observed during storage of cut watermelon slices up to 12 d.[247] According to the authors, the increase in (Z)-6-nonen-1-ol during storage of fresh-cut slices may be particularly important as it might contribute to the pumpkin-like off-odors and squash-like off-flavors often attributed to overripe whole watermelon during storage. In agreement with previous studies, we measured a higher total alcohol content and lower aldehyde content at 10 d storage (Figure 35 and Figure 36). However, at 20 d storage, total alcohol content was reduced and aldehyde was enhanced in both cultivars. Most of the earlier studies were conducted in fresh cut watermelon or in watermelon juices. None of the studies reported the volatile profile in watermelon stored as intact, uncut fruit for 20 d.

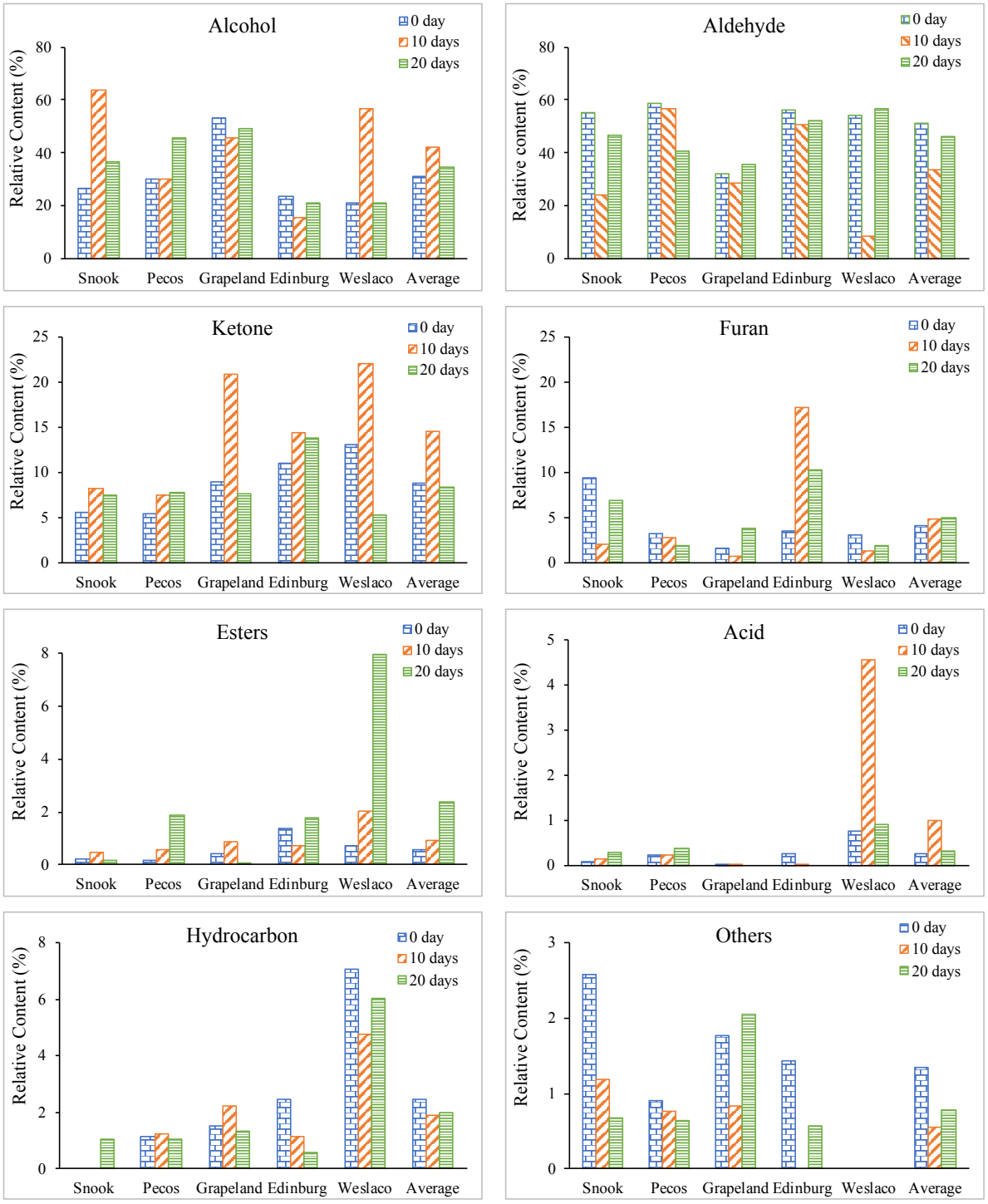

Figure 35 Relative contents (%) of all class of volatiles at 0,10 and 20 days of storage period from Riverside cultivars grown at five different locations.

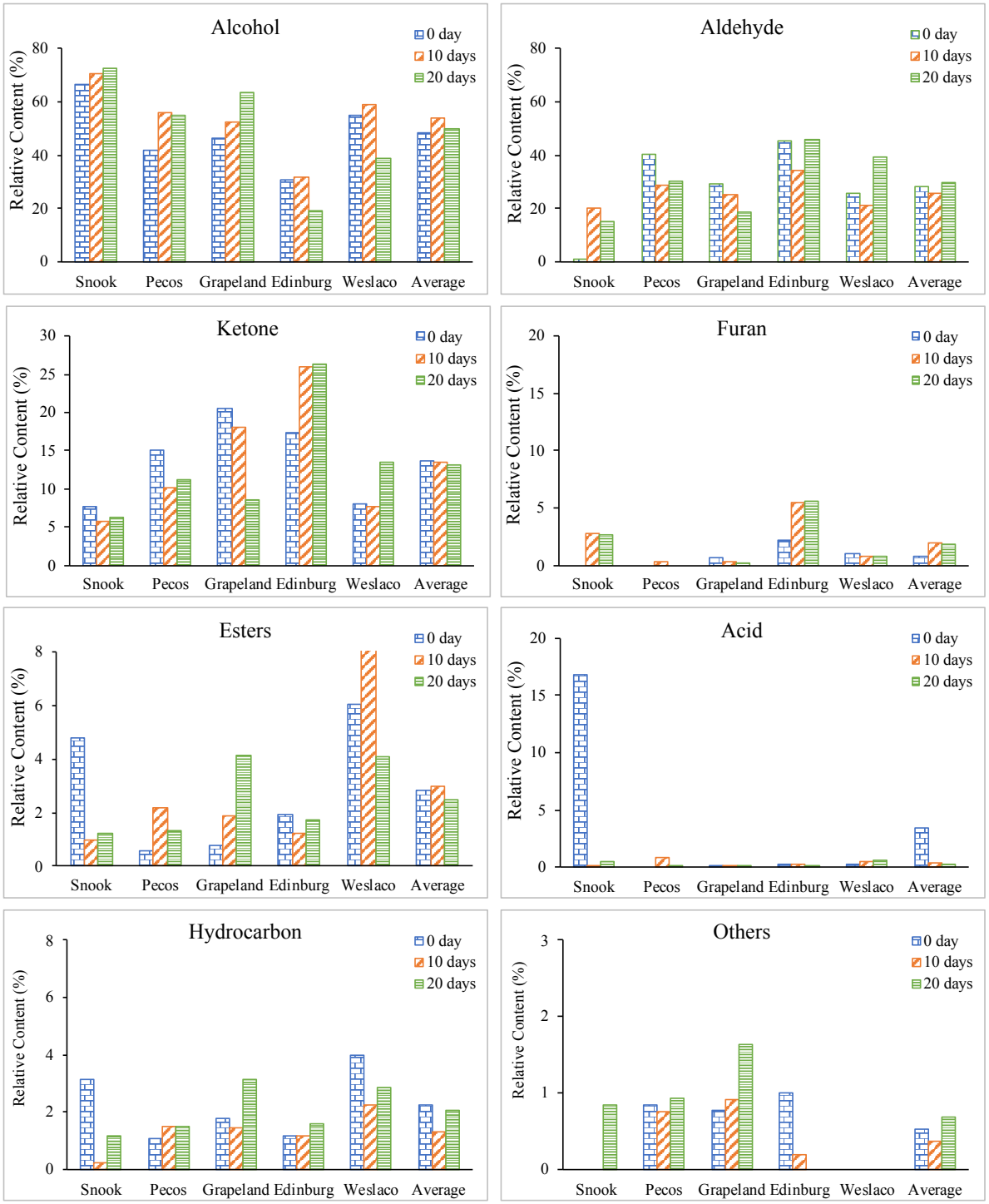

Figure 36 Relative contents (%) of all class of volatiles at 0,10 and 20 days of storage period from Maxima cultivars grown at five different locations.

7.3.4. Multivariate analysis of volatiles

To visualize the general trends, grouping, and the differences between cultivars, locations and storage period, we conducted partial least squares discriminant analysis (PLS-DA), which is a supervised clustering method to maximize the separation between groups. Data from all five locations, two cultivars, and three storage periods were used as observations and the different volatile contents of watermelon were used as variables. PLS-DA of the volatile data of watermelon samples produced principal components (PC). Together, PC1 and PC2 explained 20.7, 13, and 22.6% of the total variance for cultivar, storage period, and location effect, respectively (Figure 37). The score plots from PC1 and PC2 clearly separated the Maxima and Riverside cultivars, reflecting differences in volatile profiles of diploid and triploid watermelons (Figure 37a). Consistent with this separation, Beaulieu et. al (2006)[248] reported the different volatile profiles of seedless cultivars as compared to their seeded counterparts. Similarly, a distinct separation of volatiles was observed for 0 and 20 d storage. PC1 separated volatiles at 0 and 20 d storage while PC2 separated observations at 10 vs. 0 and 20 d. The score plots from PC1 and PC2 separated the Edinburg, Snook, Grapeland, and Weslaco locations, reflecting an effect of location on watermelon volatiles. Together, these data demonstrate that cultivar, location, and storage period produce specific changes in the volatile profiles of watermelon.

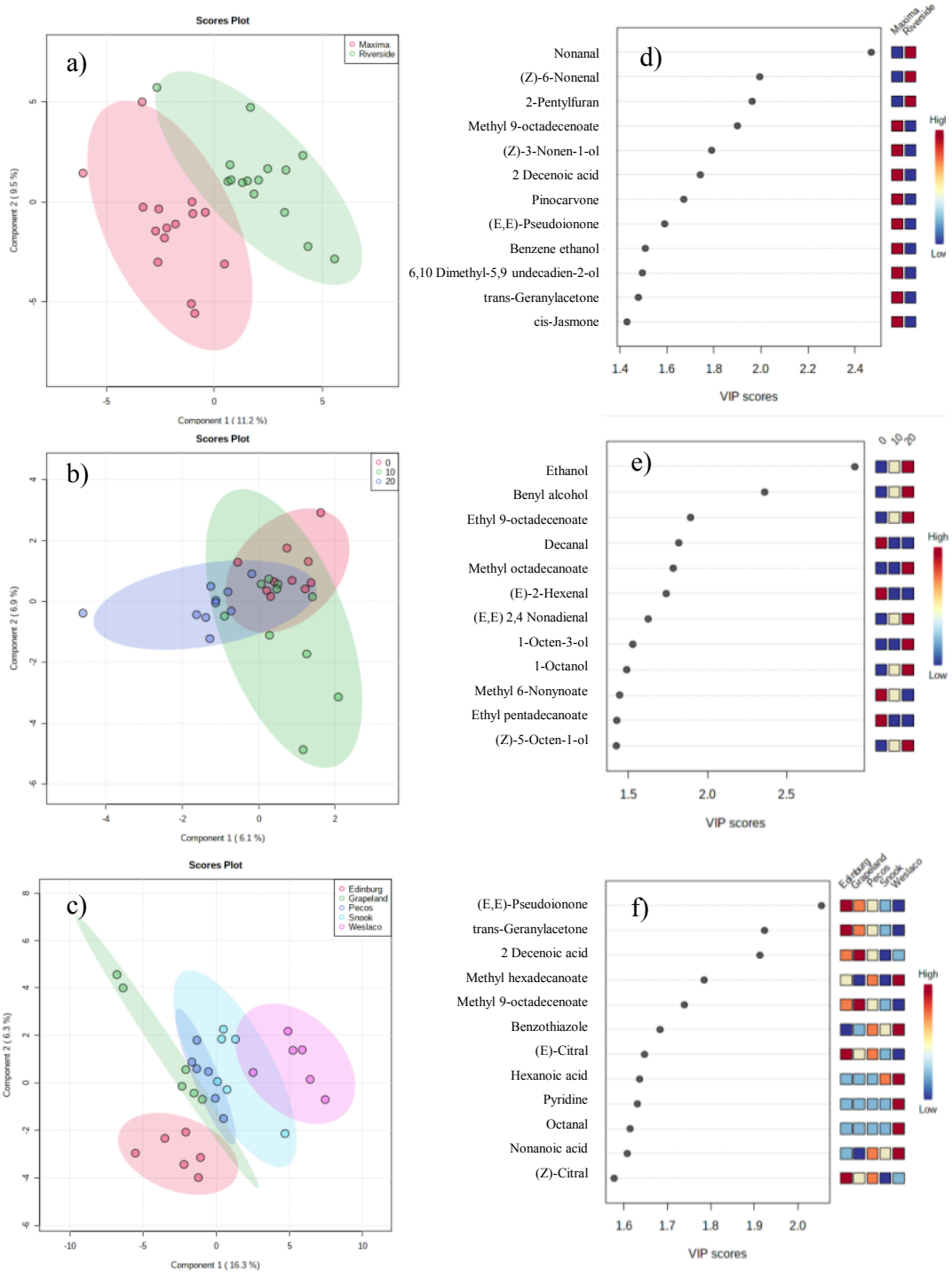

Figure 37 Partial least squares discriminant analysis (PLS-DA) scores plot corresponding to a model aimed at the discrimination between a) cultivars b) storage periods and c) locations. The colored-ellipses denote 95% confidence intervals. Variable importance on projection (VIP) scores from the PLS-DA model indicating the most discriminating volatile metabolites between d) cultivars e) storage periods and f) locations.

Furthermore, the variable importance in projection (VIP) score plots were obtained from the PLS-DA models. The major compounds responsible for clustering in two different cultivars are nonanal, (Z)-6-nonenal, 2-pentylfuran, methyl 9-octadecenoate, (Z)-3-nonen-1-ol, and 2 decenoic acid, and most of the compounds were high in Maxima compared with Riverside. Similarly, alcohols [ethanol, benzyl alcohol, 1-octanol, 1-octen-3-ol], aldehydes [decanal, (E)-2-hexenal], and esters [ethyl 9-octadecenoate, methyl octadecenoate] are responsible for the distinct clusters among the storage periods studied. VIP score plots showed the enhanced level of these alcohols and esters at 20 d and of aldehydes at 0 d of storage. The major compounds responsible for clustering in the five different locations are (E,E)-pseudoionone, trans-geranylacetone, and 2 decenoic acid. These compounds were high in Snook and Weslaco samples and low in Edinburg and Grapeland.

7.4. Conclusions

The SPME system was found to be a reliable and convenient sampling technology for rapid qualitative and quantitative analysis of volatiles from watermelon. Using SPME and GC-MS, we identified and quantified 87 volatile compounds from the two varieties of watermelon harvested from five different locations and stored for up to 20 d. The identified volatiles include alcohols, aldehydes, ketones, furans, ester, hydrocarbons, and acid groups. Irrespective of the location, cultivar, and storage period, the most prevalent class of compounds were alcohols and aldehydes, followed by ketones. The average relative content of alcohol was high at 10 d of storage compared to the fresh watermelon samples while aldehyde content was low at 10 d in both cultivars. The total volatile content of the fresh samples was higher in the triploid cultivar Maxima as compared to the diploid Riverside and both cultivars showed location-specific volatile profiles. Multivariate

analysis demonstrated the distinct separation of volatiles for two different cultivars, three different storage periods, and five growing locations. Taken together, our results elucidated the different effects that preharvest factors (cultivar selection, growing location) and postharvest factors have on the volatile components of intact watermelon.

8. CONCLUSIONS

The present study presented a low-cost, and ecofriendly approach to synthesize NPs using agro-industrial byproducts and avoids the use of hazardous and toxic chemicals for direct applications in agriculture. Herein, we compared nanomaterial treatments with control untreated onion plants from sowing to maturity and also the changes in nutritional quality of onion bulbs. There were a total of six treatments: unprimed, hydroprimed, TNE, CNE, AgNPs and AuNPs. All the nanopriming treatments exhibited positive effects compared to the unprimed onion seeds. Among all the nanopriming treatments, applying AuNPs as priming agent at low concentrations (5.4 ppm) resulted in enhancement of germination, plant height, leaf length, leaf diameter, neck diameter, and leaf surface area at both early and later plant development stages. The average yield of AuNP-treated onions from all the locations was increased by 23.9% compared to unprimed onions. Based on TEM and INAA results, AgNPs and AuNPs were internalized into the seed and those might have helped to improve water uptake, resulting in better germination and growth. Increased chlorophyll content in the leaves and reduced pungency level in the bulbs were evident in the AuNP treatment compared to the unprimed and hydroprimed cases. The other study on the metabolites profile of onion seeds demonstrates that the seed priming treatments significantly inhibited plant hormones and growth regulators, such as abscisic acid and OPDA. Similarly, enhanced germination stimulators, such as GABA and ZA, were observed in the treated onion seeds and seedlings. These nanomaterials can be applied sustainably to induce seed germination stimulators and repress inhibitors during the early stages of seedling development in onion. Nutritional composition of the treated and untreated onions from different locations were also analyzed. The levels of flavonoids were strongly affected by the location and

size of the onion bulbs. In all the locations, relatively small-sized onions had a higher content of all the flavonoids and the trend was similar in total amino acids also. In addition, multivariate analysis results distinct clusters for each size and treatment category of onion extract which further revealed that metabolic alterations in the onion in response to nanopriming was bulb size and nano-treatment dependent. Taken together, results indicate that biosynthesized nanomaterials had differential effect on the nutritional quality of onion.

Similarly, in watermelon study, AgNPs and TNE were applied as nanopriming agents and tested in five different growing environments. The TNE promoted germination and growth, but AgNPs hold greater promise for watermelon production. Multiple lab, greenhouse, and field studies suggested that germination and growth parameters of watermelon seeds were enhanced after treatment with nanoparticles. A yield increase upto 32% and 36% compared to control was observed in AgNPs treated diploid and triploid watermelons, respectively. Total phenolics content, radical scavenging activities, and macro and micro nutrients level in the watermelon fruit were maintained in nanotreatments. A storage study was done in the intact watermelons stored at 10 and 20 d after harvesting and were compared with the fresh watermelons. Physico-chemical characteristics such as weight, length, diameter, and SSC (%) and the nutritional composition were maintained in the watermelons stored for 10 d at 23 °C. Lycopene and its isomers level were significantly high at 10 d of storage compared to the fresh watermelons. However, in both varieties, physico-chemical characteristics and phytochemical composition was found to be significantly reduced in 20 d storage samples.

Along with the storage study, the effect of AgNPs on phytonutrients and quality of watermelons were compared with the TNE and the control unprimed samples. AgNPs and TNE as the nanopriming treatment in watermelon seeds had no significant differences in the level of

phytochemical composition as compared to the unprimed. In the other study, the influence of post-harvest storage and growing environments on volatile compounds of triploid and diploid watermelons were studied. A total of 87 volatile compounds were identified and quantified from the watermelon of two varieties Riverside and Maxima harvested from five different locations by SPME-GCMS. Identified volatiles include alcohols, aldehydes, ketones, furans, ester, hydrocarbon and acid. Harvested watermelons were stored for 20 days to evaluate the storage effect and samples were analyzed at 0-, 10- and 20- days of storage period. Irrespective of locations, cultivars and the storage period, the most prevalent class of compounds were alcohol and aldehyde followed by ketone group. Average relative content of alcohol was high at 10 d of storage period compared to the fresh watermelon samples while aldehyde content was reduced at 10 days in both cultivars. For the fresh samples, total volatile content was higher in triploid cultivar Maxima as compared to the diploid Riverside and location specific volatile content was observed in both cultivars. Taken together, our results elucidated the differential impacts that preharvest cultural management factors (including cultivar selection, growing location) and postharvest storage factor can have on the volatile component of intact watermelon.

This nanopriming techniques avoid the incorporation of NPs in the soil; this prevents the dispersal of large amounts of NPs into the ecosystem lowering the human impacts on the environment. Application of these synthesized nanoparticles as priming agent will boost ongoing efforts for sustainable development of nanomaterials by minimizing the contamination in food chains. The findings reflect the situation in real field condition by repeatedly growing in the multilocation field, which is quite relevant for commercial watermelon production. Given the low dosage of NPs used in this work, the material cost for commercial application of AgNPs and AuNPs is about $3−5/acre and $8−13/acre, respectively, making this a cost-efficient seed

treatment method. Our results also elucidate that plant mediated nanoparticles have future application in the production of onion and watermelon without deteriorating the nutritional quality. To further enhance the effectiveness of the nanomaterial treatments, future efforts should be focused on optimization of priming time, priming solution concentration and nanomaterial composition, structure, size, and activity. Similarly, plant physiology affects the interaction with nanoparticles, so results observed in one crop are not necessarily valid for other crops, which makes it imperative to study different plant species. Therefore, the results of these studies should stimulate investigations to understand nanoparticle plant surface interactions and the uptake of the green nanoparticles in the plant system.

REFERENCES

1. Parida, U. K.; Das, S.; Jena, P. K.; Rout, N.; Bindhani, B. K., Plant mediated green synthesis of metallic nanoparticles: Challenges and opportunities. In Fabrication and self-assembly of nanobiomaterials, Elsevier: 2016; pp 149-177.

2. Mohammadinejad, R.; Karimi, S.; Iravani, S.; Varma, R. S., Plant-derived nanostructures: types and applications. Green Chemistry 2016, 18 (1), 20-52.

3. Ma, X.; Geiser-Lee, J.; Deng, Y.; Kolmakov, A., Interactions between engineered nanoparticles (ENPs) and plants: phytotoxicity, uptake and accumulation. Science of the total environment 2010, 408 (16), 3053-3061.

4. Alam, M. N.; Roy, N.; Mandal, D.; Begum, N. A., Green chemistry for nanochemistry: exploring medicinal plants for the biogenic synthesis of metal NPs with fine-tuned properties. Rsc Advances 2013, 3 (30), 11935-11956.

5. Searchinger, T.; Waite, R.; Hanson, C.; Ranganathan, J.; Dumas, P.; Matthews, E.; Klirs, C., Creating a sustainable food future: A menu of solutions to feed nearly 10 billion people by 2050. Final report. WRI: 2019.

6. Pastor, A.; Palazzo, A.; Havlik, P.; Biemans, H.; Wada, Y.; Obersteiner, M.; Kabat, P.; Ludwig, F., The global nexus of food–trade–water sustaining environmental flows by 2050. Nature Sustainability 2019, 2 (6), 499-507.

7. Chen, K.; Arora, R., Priming memory invokes seed stress-tolerance. Environ. Exp. Bot. 2013, 94, 33-45.

8. Basra, S.; Farooq, M.; Wahid, A.; Khan, M. B., Rice seed invigoration by hormonal and vitamin priming. Seed Sci. Technol. 2006, 34 (3), 753-758.

9. Servin, A. D.; White, J. C., Nanotechnology in agriculture: next steps for understanding engineered nanoparticle exposure and risk. NanoImpact 2016, 1, 9-12.

10. Giraldo, J. P.; Landry, M. P.; Faltermeier, S. M.; McNicholas, T. P.; Iverson, N. M.; Boghossian, A. A.; Reuel, N. F.; Hilmer, A. J.; Sen, F.; Brew, J. A., Plant nanobionics approach to augment photosynthesis and biochemical sensing. Nat. Mater. 2014, 13 (4), 400-408.

11. Galbraith, D. W., Nanobiotechnology: silica breaks through in plants. Nat. Nanotechnol. 2007, 2 (5), 272-273.

12. Khodakovskaya, M.; Dervishi, E.; Mahmood, M.; Xu, Y.; Li, Z.; Watanabe, F.; Biris, A. S., Carbon nanotubes are able to penetrate plant seed coat and dramatically affect seed germination and plant growth. ACS Nano 2009, 3 (10), 3221-3227.

13. Kasote, D. M.; Lee, J.; Jayaprakasha, G. K.; Patil, B. S., Seed Priming with Iron Oxide Nanoparticles Modulate Antioxidant Potential and Defense Linked Hormones in Watermelon Seedlings. ACS Sustainable Chem. Eng. 2019.

14. Geraldes, A. N.; da Silva, A. A.; Leal, J.; Estrada-Villegas, G. M.; Lincopan, N.; Katti, K. V.; Lug; atildeo, A. B., Green nanotechnology from plant extracts: synthesis and characterization of gold nanoparticles. Adv. Nanopart. 2016, 5 (03), 176.

15. Sharma, D.; Sabela, M. I.; Kanchi, S.; Bisetty, K.; Skelton, A. A.; Honarparvar, B., Green synthesis, characterization and electrochemical sensing of silymarin by ZnO nanoparticles: experimental and DFT studies. J. Electroanal. Chem. 2018, 808, 160-172.

16. Pu, F.; Huang, Y.; Yang, Z.; Qiu, H.; Ren, J., Nucleotide-based assemblies for green synthesis of silver nanoparticles with controlled localized surface plasmon resonances and their applications. ACS Appl. Mater. Interfaces 2018, 10 (12), 9929-9937.

17. Negi, P.; Jayaprakasha, G.; Jagan Mohan Rao, L.; Sakariah, K., Antibacterial activity of turmeric oil: a byproduct from curcumin manufacture. J. Sci. Food Agric. 1999, 47 (10), 4297-4300.

18. Choi, I. S.; Lee, Y. G.; Khanal, S. K.; Park, B. J.; Bae, H.-J., A low-energy, cost-effective approach to fruit and citrus peel waste processing for bioethanol production. Appl. Energy 2015, 140, 65-74.

19. Zhao, L.; Peralta-Videa, J. R.; Rico, C. M.; Hernandez-Viezcas, J. A.; Sun, Y.; Niu, G.; Servin, A.; Nunez, J. E.; Duarte-Gardea, M.; Gardea-Torresdey, J. L., CeO2 and ZnO nanoparticles change the nutritional qualities of cucumber (Cucumis sativus). J. Agric. Food Chem. 2014, 62 (13), 2752-2759.

20. Rawat, S.; Pullagurala, V. L.; Hernandez-Molina, M.; Sun, Y.; Niu, G.; Hernandez-Viezcas, J. A.; Peralta-Videa, J. R.; Gardea-Torresdey, J. L., Impacts of copper oxide nanoparticles on bell pepper (Capsicum annum L.) plants: a full life cycle study. Environ. Sci.: Nano 2018, 5 (1), 83-95.

21. Anton, N.; Vandamme, T. F., The universality of low-energy nano-emulsification. Int. J. Pharm. 2009, 377 (1-2), 142-147.

22. Chang, Y.; McClements, D. J., Optimization of orange oil nanoemulsion formation by isothermal low-energy methods: influence of the oil phase, surfactant, and temperature. J. Agric. Food Chem. 2014, 62 (10), 2306-2312.

23. Nune, S. K.; Chanda, N.; Shukla, R.; Katti, K.; Kulkarni, R. R.; Thilakavathy, S.; Mekapothula, S.; Kannan, R.; Katti, K. V., Green nanotechnology from tea: phytochemicals in tea as building blocks for production of biocompatible gold nanoparticles. J. Mater. Chem. 2009, 19 (19), 2912-2920.

24. Shanmugam, H.; Acharya, P.; Jayaprakasha, G. K.; Patil, B. S., Nanoformulation and characterization of nomilin with different poly (lactic-co-glycolic acid) resomers and surfactants for the enhanced inhibition of α-amylase and angiotensin-converting-enzyme. J. Funct. Foods 2017, 37, 564-573.

25. Singh, J.; Jayaprakasha, G.; Patil, B. S., An optimized solvent extraction and rapid identification of unidentified flavonoid glucuronide derivatives from spinach by UHPLC-HR-QTOF-MS. Talanta 2018.

26. Jiang, H. S.; Qiu, X. N.; Li, G. B.; Li, W.; Yin, L. Y., Silver nanoparticles induced accumulation of reactive oxygen species and alteration of antioxidant systems in the aquatic plant Spirodela polyrhiza. Environ. Toxicol. Chem. 2014, 33 (6), 1398-1405.

27. Greenberg, R. R.; Bode, P.; Fernandes, E. A. D. N., Neutron activation analysis: a primary method of measurement. Spectrochim. Acta, Part B 2011, 66 (3-4), 193-241.

28. Ashraf, M.; Foolad, M., Pre-sowing seed treatment—A shotgun approach to improve germination, plant growth, and crop yield under saline and non-saline conditions. Adv. Agron. 2005, 88, 223-271.

29. Córcoles, J.; Domínguez, A.; Moreno, M.; Ortega, J.; de Juan, J., A non-destructive method for estimating onion leaf area. Ir. J. Agric. Food Res. 2015, 54 (1), 17-30.

30. Gamiely, S.; Randle, W.; Mills, H.; Smittle, D., A rapid and nondestructive method for estimating leaf area of onions. HortScience 1991, 26 (2), 206.

31. Barkat, N.; Singh, J.; Jayaprakasha, G. K.; Patil, B. S., Effect of harvest time on the levels of phytochemicals, free radical-scavenging activity, α-amylase inhibition and bile acid-binding capacity of spinach (Spinacia oleracea). J. Sci. Food Agric. 2018, 98, 3468–3477.

32. Yoo, K. S.; Lee, E. J.; Patil, B. S., Improved Consistency in DNPH-Mediated Pyruvic Acid Analysis of Onion Juice by Modifying the Sample Processing Order. J. Food Sci. 2011, 76 (1).

33. Yoo, K. S.; Pike, L. M., Development of an automated system for pyruvic acid analysis in onion breeding. Sci. Hortic. 1999, 82 (3-4), 193-201.

34. Metrani, R.; Jayaprakasha, G. K.; Patil, B. S., Optimized method for the quantification of pyruvic acid in onions by microplate reader and confirmation by high resolution mass spectra. Food Chem. 2018, 242 (Supplement C), 451-458.

35. Lee, E. J.; Yoo, K. S.; Jifon, J.; Patil, B. S., Characterization of shortday onion cultivars of 3 pungency levels with flavor precursor, free amino acid, sulfur, and sugar contents. J. Food Sci. 2009, 74 (6).

36. Chen, H., Metal based nanoparticles in agricultural system: behavior, transport, and interaction with plants. Chem. Speciation Bioavailability 2018, 30 (1), 123-134.

37. Vogel, R.; Pal, A. K.; Jambhrunkar, S.; Patel, P.; Thakur, S. S.; Reátegui, E.; Parekh, H. S.; Saá, P.; Stassinopoulos, A.; Broom, M. F., High-resolution single particle zeta potential characterisation of biological nanoparticles using tunable resistive pulse sensing. Sci. Rep. 2017, 7 (1), 17479.

38. Fazal, S.; Jayasree, A.; Sasidharan, S.; Koyakutty, M.; Nair, S. V.; Menon, D., Green synthesis of anisotropic gold nanoparticles for photothermal therapy of cancer. ACS Appl. Mater. Interfaces 2014, 6 (11), 8080-8089.

39. Li, C.; Zhou, L.; Yang, H.; Lv, R.; Tian, P.; Li, X.; Zhang, Y.; Chen, Z.; Lin, F., Self-assembled exopolysaccharide nanoparticles for bioremediation and green synthesis of noble metal nanoparticles. ACS Appl. Mater. Interfaces 2017, 9 (27), 22808-22818.

40. Jyoti, K.; Baunthiyal, M.; Singh, A., Characterization of silver nanoparticles synthesized using Urtica dioica Linn. leaves and their synergistic effects with antibiotics. J. Radiat. Res. Appl. Sci. 2016, 9 (3), 217-227.

41. Santhoshkumar, J.; Rajeshkumar, S.; Kumar, S. V., Phyto-assisted synthesis, characterization and applications of gold nanoparticles–A review. Biochem. Biophys. Rep. 2017, 11, 46-57.

42. Mahakham, W.; Sarmah, A. K.; Maensiri, S.; Theerakulpisut, P., Nanopriming technology for enhancing germination and starch metabolism of aged rice seeds using phytosynthesized silver nanoparticles. Sci. Rep. 2017, 7 (1), 1-21.

43. Mahakham, W.; Theerakulpisut, P.; Maensiri, S.; Phumying, S.; Sarmah, A. K., Environmentally benign synthesis of phytochemicals-capped gold nanoparticles as nanopriming agent for promoting maize seed germination. Sci. Total Environ. 2016, 573, 1089-1102.

44. Li, S.; Wang, Q.; Bu, Y., A Green and General Strategy to Synthesize Hollow CdS/Ag Nanocomposites for Superior SERS Performance. CrystEngComm 2019.

45. Aromal, S. A.; Philip, D., Benincasa hispida seed mediated green synthesis of gold nanoparticles and its optical nonlinearity. Phys. E 2012, 44 (7-8), 1329-1334.

46. Miranda, É. G.; Tofanello, A.; Brito, A. M.; Lopes, D. M.; Albuquerque, L. J.; de Castro, C. E.; Costa, F. N.; Giacomelli, F. C.; Ferreira, F. F.; Araújo-Chaves, J. C., Effects of gold salt speciation and structure of human and bovine serum albumins on the synthesis and stability of gold nanostructures. Front. Chem. 2016, 4, 13.

47. Rastogi, A.; Zivcak, M.; Sytar, O.; Kalaji, H. M.; He, X.; Mbarki, S.; Brestic, M., Impact of metal and metal oxide nanoparticles on plant: a critical review. Front. Chem. 2017, 5, 78.

48. Shestakov, A.; Golovanova, S.; Lariontseva, N.; Sadkov, A.; Martynenko, V.; Levchenko, L., Deep oxidation of rutin and quercetin during their reaction with HAuCl4 in aqueous solutions. Russ. Chem. Bull. 2015, 64 (10), 2477-2485.

49. Raghunandan, D.; Bedre, M. D.; Basavaraja, S.; Sawle, B.; Manjunath, S.; Venkataraman, A., Rapid biosynthesis of irregular shaped gold nanoparticles from macerated aqueous extracellular dried clove buds (Syzygium aromaticum) solution. Colloids Surf., B 2010, 79 (1), 235-240.

50. Panigrahi, S.; Kundu, S.; Ghosh, S.; Nath, S.; Pal, T., General method of synthesis for metal nanoparticles. J. Nanopart. Res. 2004, 6 (4), 411-414.

51. Golubkina, N.; Nadezhkin, S.; Agafonov, A.; Kosheleva, O.; Molchanova, A.; Russo, G.; Cuciniello, A.; Caruso, G., Seed oil content, fatty acids composition and antioxidant properties as affected by genotype in Allium cepa L. and perennial onion species. Adv. Hortic. Sci. 2015, 29 (4), 199-206.

52. Judy, J. D.; Unrine, J. M.; Rao, W.; Wirick, S.; Bertsch, P. M., Bioavailability of gold nanomaterials to plants: importance of particle size and surface coating. Environ. Sci. Technol. 2012, 46 (15), 8467-8474.

53. Gopinath, K.; Gowri, S.; Karthika, V.; Arumugam, A., Green synthesis of gold nanoparticles from fruit extract of Terminalia arjuna, for the enhanced seed germination activity of Gloriosa superba. J. Nanostruct. Chem. 2014, 4 (3), 115.

54. Brocklehurst, P.; Dearman, J., Interactions between seed priming treatments and nine seed lots of carrot, celery and onion. I. Laboratory germination. Ann. Appl. Biol. 1983, 102 (3), 577-584.

55. Rao, R.; Singh, P.; Rai, M., Storability of onion seeds and effects of packaging and storage conditions on viability and vigour. Sci. Hortic. 2006, 110 (1), 1-6.

56. Liu, G.; Porterfield, D. M.; Li, Y.; Klassen, W., Increased oxygen bioavailability improved vigor and germination of aged vegetable seeds. HortScience 2012, 47 (12), 1714-1721.

57. Wojtyla, Ł.; Lechowska, K.; Kubala, S.; Garnczarska, M., Molecular processes induced in primed seeds—increasing the potential to stabilize crop yields under drought conditions. J. Plant Physiol. 2016, 203, 116-126.

58. Tenhaken, R., Cell wall remodeling under abiotic stress. Front. Plant Sci. 2015, 5, 771.

59. Kumari, S.; Kumaraswamy, R.; Choudhary, R. C.; Sharma, S.; Pal, A.; Raliya, R.; Biswas, P.; Saharan, V., Thymol nanoemulsion exhibits potential antibacterial activity against bacterial pustule disease and growth promotory effect on soybean. Sci. Rep. 2018, 8:6650.

60. Jayaprakasha, G. K.; Negi, P. S.; Anandharamakrishnan, C.; Sakariah, K. K., Chemical composition of turmeric oil-A byproduct from turmeric oleoresin industry and its inhibitory activity against different fungi. Z. Naturforsch., C, J. Biosci. 2001, 56 (1-2), 40-44.

61. Bartkowski, E. J.; Katterman, F. R.; Buxton, D. R., Influence of exogenous fatty acids on cottonseed germination. Physiol. Plant. 1978, 44 (3), 153-156.

62. Wanner, H.; Stocker, H., Different effects of long chain fatty acids on seed germination. Biochem. Physiol. Pflanz. 1977, 171 (5), 391-399.

63. Addinall, R. Effects of exogenous myristic acid on growth and germination of Brassica napus L. under zirconium toxicity. thesis, University of the Western Cape, 2016.

64. Kumar, V.; Guleria, P.; Kumar, V.; Yadav, S. K., Gold nanoparticle exposure induces growth and yield enhancement in Arabidopsis thaliana. Sci. Total Environ. 2013, 461, 462-468.

65. Arora, S.; Sharma, P.; Kumar, S.; Nayan, R.; Khanna, P.; Zaidi, M., Gold-nanoparticle induced enhancement in growth and seed yield of Brassica juncea. Plant Growth Regul. 2012, 66 (3), 303-310.

66. Falco, W.; Queiroz, A.; Fernandes, J.; Botero, E.; Falcão, E.; Guimarães, F.; M'Peko, J.-C.; Oliveira, S.; Colbeck, I.; Caires, A., Interaction between chlorophyll and silver nanoparticles: a close analysis of chlorophyll fluorescence quenching. J. Photochem. Photobiol., A 2015, 299, 203-209.

67. Govorov, A. O.; Carmeli, I., Hybrid structures composed of photosynthetic system and metal nanoparticles: plasmon enhancement effect. Nano Letters 2007, 7 (3), 620-625.

68. Avellan, A.; Yun, J.; Zhang, Y.; Spielman-Sun, E.; Unrine, J. M.; Thieme, J.; Li, J.; Lombi, E.; Bland, G.; Lowry, G. V., Nanoparticle size and coating chemistry control foliar uptake pathways, translocation and leaf-to-rhizosphere transport in wheat. ACS nano 2019.

69. Imai, S.; Tsuge, N.; Tomotake, M.; Nagatome, Y.; Sawada, H.; Nagata, T.; Kumagai, H., Plant biochemistry: an onion enzyme that makes the eyes water. Nature 2002, 419 (6908), 685.

70. Yoo, K. S.; Pike, L.; Crosby, K.; Jones, R.; Leskovar, D., Differences in onion pungency due to cultivars, growth environment, and bulb sizes. Sci. Hortic. 2006, 110 (2), 144-149.

71. Vavrina, C. S.; Smittle, D. A., Evaluating sweet onion cultivars for sugar concentrations and pungency. HortScience 1993, 28 (8), 804-806.

72. Silva, A. T.; Ligterink, W.; Hilhorst, H. W., Metabolite profiling and associated gene expression reveal two metabolic shifts during the seed-to-seedling transition in Arabidopsis thaliana. Plant Mol. Biol. 2017, 95 (4-5), 481-496.

73. Bian, F.; Su, J.; Liu, W.; Li, S., Dormancy release and germination of Taxus yunnanensis seeds during wet sand storage. Sci. Rep. 2018, 8 (1), 3205.

74. Shu, X.-L.; Frank, T.; Shu, Q.-Y.; Engel, K.-H., Metabolite profiling of germinating rice seeds. J. Agric. Food Chem. 2008, 56 (24), 11612-11620.

75. Seo, M.; Jikumaru, Y.; Kamiya, Y., Profiling of hormones and related metabolites in seed dormancy and germination studies. In Seed Dormancy, Springer: 2011; pp 99-111.

76. Han, C.; Yang, P., Studies on the molecular mechanisms of seed germination. Proteomics 2015, 15 (10), 1671-1679.

77. Hao, Y.; Yu, F.; Lv, R.; Ma, C.; Zhang, Z.; Rui, Y.; Liu, L.; Cao, W.; Xing, B., Carbon nanotubes filled with different ferromagnetic alloys affect the growth and development of rice seedlings by changing the C: N ratio and plant hormones concentrations. PloS one 2016, 11 (6), e0157264.

78. Kang, J.; Yim, S.; Choi, H.; Kim, A.; Lee, K. P.; Lopez-Molina, L.; Martinoia, E.; Lee, Y., Abscisic acid transporters cooperate to control seed germination. Nat. Commun. 2015, 6, 8113.

79. Lemmens, E.; Deleu, L. J.; De Brier, N.; De Man, W. L.; De Proft, M.; Prinsen, E.; Delcour, J. A., The Impact of Hydro-Priming and Osmo-Priming on Seedling Characteristics, Plant Hormone Concentrations, Activity of Selected Hydrolytic Enzymes, and Cell Wall and Phytate Hydrolysis in Sprouted Wheat (Triticum aestivum L.). ACS omega 2019.

80. Wasternack, C.; Kombrink, E., Jasmonates: structural requirements for lipid-derived signals active in plant stress responses and development. ACS Chem. Biol. 2009, 5 (1), 63-77.

81. Liu, S.; Wu, Y.; Fang, C.; Cui, Y.; Jiang, N.; Wang, H., Simultaneous Determination of 19 Plant Growth Regulator Residues in Plant-originated Foods by QuEChERS and Stable Isotope Dilution–Ultra Performance Liquid Chromatography–Mass Spectrometry. Anal. Sci. 2017, 33 (9), 1047-1052.

82. Acharya, P.; Jayaprakasha, G. K.; Crosby, K.; Jifon, J.; Patil, B. S., Nanoparticle-Mediated Seed Priming Improves Germination, Growth, Yield, and Quality of Watermelons (Citrullus lanatus) at multi-locations in Texas. Sci. Rep. 2020, 10 (1), 1-16.

83. Acharya, P.; Jayaprakasha, G. K.; Crosby, K.; Jifon, J.; Patil, B. S., Green-Synthesized Nanoparticles Enhanced Seedling Growth, Yield, and Quality of Onion (Allium cepa L.). ACS Sustainable Chem. Eng. 2019, 7 (17), 14580-14590.

84. Guha, T.; Gopal, G.; Kundu, R.; Mukherjee, A., Nanocomposites for Delivering Agrochemicals: A Comprehensive Review. J. Agric. Food Chem. 2020.

85. Raliya, R.; Saharan, V.; Dimkpa, C.; Biswas, P., Nanofertilizer for precision and sustainable agriculture: current state and future perspectives. J. Agric. Food Chem. 2017, 66 (26), 6487-6503.

86. Pradhan, S.; Mailapalli, D. R., Interaction of engineered nanoparticles with the agri-environment. J. Agric. Food Chem. 2017, 65 (38), 8279-8294.

87. Khodakovskaya, M. V.; De Silva, K.; Biris, A. S.; Dervishi, E.; Villagarcia, H., Carbon nanotubes induce growth enhancement of tobacco cells. ACS nano 2012, 6 (3), 2128-2135.

88. Pérez-de-Luque, A., Interaction of nanomaterials with plants: what do we need for real applications in agriculture? Front. Environ. Sci. 2017, 5, 12.

89. Khalilzadeh, M. A.; Borzoo, M., Green synthesis of silver nanoparticles using onion extract and their application for the preparation of a modified electrode for determination of ascorbic acid. J. Food Drug Anal. 2016, 24 (4), 796-803.

90. Jayaprakasha, G.; Negi, P.; Anandharamakrishnan, C.; Sakariah, K., Original Communications-Chemical Composition of Turmeric Oil-A By-product from Turmeric Oleoresin Industry and Its Inhibitory Activity against Different Fungi. Z Naturforsch C J Biosci. 2001, 56 (1-2), 40-44.

91. Murthy, K. C.; Monika, P.; Jayaprakasha, G.; Patil, B. S., Nanoencapsulation: An Advanced Nanotechnological Approach To Enhance the Biological Efficacy of Curcumin. In Advances in Plant Phenolics: From Chemistry to Human Health, ACS Publications: 2018; pp 383-405.

92. Uckoo, R. M.; Jayaprakasha, G. K.; Patil, B. S., Rapid separation method of polymethoxyflavones from citrus using flash chromatography. Sep. Purif. Technol. 2011, 81 (2), 151-158.

93. Raman, G.; Jayaprakasha, G.; Cho, M.; Brodbelt, J.; Patil, B. S., Rapid adsorptive separation of citrus polymethoxylated flavones in non-aqueous conditions. Sep. Purif. Technol. 2005, 45 (2), 147-152.

94. FAOSTAT http://www.fao.org/faostat/en/#data/QC.

95. Lv, S.; Gu, J.; Zhang, R.; Zhang, Y.; Tan, H.; McClements, D. J., Vitamin E Encapsulation in Plant-Based Nanoemulsions Fabricated Using Dual-Channel Microfluidization: Formation, Stability, and Bioaccessibility. J. Agric. Food Chem. 2018, 66 (40), 10532-10542.

96. Chang, Y.; McLandsborough, L.; McClements, D. J., Physical Properties and Antimicrobial Efficacy of Thyme Oil Nanoemulsions: Influence of Ripening Inhibitors. J. Agric. Food Chem. 2012, 60 (48), 12056-12063.

97. Zhao, L.; Huang, Y.; Hu, J.; Zhou, H.; Adeleye, A. S.; Keller, A. A., 1H NMR and GC-MS based metabolomics reveal defense and detoxification mechanism of cucumber plant under nano-Cu stress. Environ. Sci. Technol. 2016, 50 (4), 2000-2010.

98. Kasote, D. M.; Jayaprakasha, G. K.; Patil, B. S., Leaf Disc Assays for Rapid Measurement of Antioxidant Activity. Sci. Rep. 2019, 9 (1), 1884.

99. Gomez, M. K.; Singh, J.; Acharya, P.; Jayaprakasha, G.; Patil, B. S., Identification and Quantification of Phytochemicals, Antioxidant Activity, and Bile Acid-Binding Capacity of Garnet Stem Dandelion (Taraxacum officinale). J. Food Sci. 2018, 83 (6), 1569-1578.

100. Laware, S.; Raskar, S., Effect of titanium dioxide nanoparticles on hydrolytic and antioxidant enzymes during seed germination in onion. Int. J. Curr. Microbiol. App. Sci 2014, 3 (7), 749-760.

101. Haghighi, M.; da Silva, J. A. T., The effect of N-TiO 2 on tomato, onion, and radish seed germination. J. Crop Sci. Biotechnol. 2014, 17 (4), 221-227.

102. Kumar, V.; Sachdev, D.; Pasricha, R.; Maheshwari, P. H.; Taneja, N. K., Zinc-Supported Multiwalled Carbon Nanotube Nanocomposite: A Synergism to Micronutrient Release and a Smart Distributor To Promote the Growth of Onion Seeds in Arid Conditions. ACS Appl. Mater. Interfaces 2018, 10 (43), 36733-36745.

103. Raskar, S.; Laware, S., Effect of zinc oxide nanoparticles on cytology and seed germination in onion. Int. J. Curr. Microbiol. App. Sci. 2014, 3 (2), 467-73.

104. Siddiqui, M. H.; Al-Whaibi, M. H., Role of nano-SiO2 in germination of tomato (Lycopersicum esculentum seeds Mill.). Saudi J. Biol. Sci. 2014, 21 (1), 13-17.

105. Savithramma, N.; Ankanna, S.; Bhumi, G., Effect of nanoparticles on seed germination and seedling growth of Boswellia ovalifoliolata an endemic and endangered medicinal tree taxon. Nano Vision 2012, 2 (1), 2.

106. Lahiani, M. H.; Dervishi, E.; Chen, J.; Nima, Z.; Gaume, A.; Biris, A. S.; Khodakovskaya, M. V., Impact of carbon nanotube exposure to seeds of valuable crops. ACS Appl. Mater. Interfaces 2013, 5 (16), 7965-7973.

107. Srivastava, G.; Das, C. K.; Das, A.; Singh, S. K.; Roy, M.; Kim, H.; Sethy, N.; Kumar, A.; Sharma, R. K.; Singh, S. K., Seed treatment with iron pyrite (FeS 2) nanoparticles increases the production of spinach. RSC Adv. 2014, 4 (102), 58495-58504.

108. Jayaprakasha, G.; Patil, B. S., A metabolomics approach to identify and quantify the phytochemicals in watermelons by quantitative 1HNMR. Talanta 2016, 153, 268-277.

109. Soininen, T. H.; Jukarainen, N.; Auriola, S. O. K.; Julkunen-Tiitto, R.; Karjalainen, R.; Vepsäläinen, J. J., Quantitative metabolite profiling of edible onion species by NMR and HPLC–MS. Food Chem. 2014, 165, 499-505.

110. Miransari, M.; Smith, D., Plant hormones and seed germination. Environ. Exp. Bot. 2014, 99, 110-121.

111. Riefler, M.; Novak, O.; Strnad, M.; Schmülling, T., Arabidopsis cytokinin receptor mutants reveal functions in shoot growth, leaf senescence, seed size, germination, root development, and cytokinin metabolism. Plant Cell 2006, 18 (1), 40-54.

112. Mok, D. W., Cytokinins: chemistry, activity, and function. CRC press: 2019.

113. Rosental, L.; Nonogaki, H.; Fait, A., Activation and regulation of primary metabolism during seed germination. Seed Sci. Res. 2014, 24 (1), 1-15.

114. Zhang, Q.; Xiang, J.; Zhang, L.; Zhu, X.; Evers, J.; van der Werf, W.; Duan, L., Optimizing soaking and germination conditions to improve gamma-aminobutyric acid content in japonica and indica germinated brown rice. J. Funct. Foods 2014, 10, 283-291.

115. Yang, R.; Guo, Q.; Gu, Z., GABA shunt and polyamine degradation pathway on γ-aminobutyric acid accumulation in germinating fava bean (Vicia faba L.) under hypoxia. Food Chem. 2013, 136 (1), 152-159.

116. Fait, A.; Nesi, A. N.; Angelovici, R.; Lehmann, M.; Pham, P. A.; Song, L.; Haslam, R. P.; Napier, J. A.; Galili, G.; Fernie, A. R., Targeted enhancement of glutamate-to-γ-aminobutyrate conversion in Arabidopsis seeds affects carbon-nitrogen balance and storage reserves in a development-dependent manner. Plant Physiol. 2011, 157 (3), 1026-1042.

117. Graeber, K.; Linkies, A.; Müller, K.; Wunchova, A.; Rott, A.; Leubner-Metzger, G., Cross-species approaches to seed dormancy and germination: conservation and biodiversity of ABA-regulated mechanisms and the Brassicaceae DOG1 genes. Plant Mol. Biol. 2010, 73 (1-2), 67-87.

118. Dave, A.; Hernández, M. L.; He, Z.; Andriotis, V. M.; Vaistij, F. E.; Larson, T. R.; Graham, I. A., 12-Oxo-phytodienoic acid accumulation during seed development represses seed germination in Arabidopsis. Plant Cell 2011, 23 (2), 583-599.

119. Dave, A.; Graham, I. A., Oxylipin signaling: a distinct role for the jasmonic acid precursor cis-(+)-12-oxo-phytodienoic acid (cis-OPDA). Front. Plant Sci. 2012, 3, 42.

120. Dave, A.; Vaistij, F. E.; Gilday, A. D.; Penfield, S. D.; Graham, I. A., Regulation of Arabidopsis thaliana seed dormancy and germination by 12-oxo-phytodienoic acid. J. Exp. Bot. 2016, 67 (8), 2277-2284.

121. Steber, C. M., DE-repression of Seed Germination by GA Signaling. Annual Plant Reviews online 2018, 248-263.

122. Yamaguchi, S.; Kamiya, Y.; Nambara, E., Regulation of ABA and GA levels during seed development and germination in Arabidopsis. Annual Plant Reviews online 2018, 224-247.

123. Servin, A.; Elmer, W.; Mukherjee, A.; De la Torre-Roche, R.; Hamdi, H.; White, J. C.; Bindraban, P.; Dimkpa, C., A review of the use of engineered nanomaterials to suppress plant disease and enhance crop yield. Journal of Nanoparticle Research 2015, 17 (2), 92.

124. Shukla, P.; Chaurasia, P.; Younis, K.; Qadri, O. S.; Faridi, S. A.; Srivastava, G., Nanotechnology in sustainable agriculture: Studies from seed priming to post-harvest management. Nanotechnology for Environmental Engineering 2019, 4 (1), 11.

125. Shang, Y.; Hasan, M.; Ahammed, G. J.; Li, M.; Yin, H.; Zhou, J., Applications of nanotechnology in plant growth and crop protection: a review. Molecules 2019, 24 (14), 2558.

126. FAOSTAT. January 2019 ed.; 2019.

127. Marrelli, M.; Amodeo, V.; Statti, G.; Conforti, F., Biological Properties and Bioactive Components of Allium cepa L.: Focus on Potential Benefits in the Treatment of Obesity and Related Comorbidities. Molecules 2019, 24 (1), 119.

128. Galeone, C.; Pelucchi, C.; Levi, F.; Negri, E.; Franceschi, S.; Talamini, R.; Giacosa, A.; La Vecchia, C., Onion and garlic use and human cancer. The American journal of clinical nutrition 2006, 84 (5), 1027-1032.

129. Knekt, P.; Kumpulainen, J.; Järvinen, R.; Rissanen, H.; Heliövaara, M.; Reunanen, A.; Hakulinen, T.; Aromaa, A., Flavonoid intake and risk of chronic diseases. The American journal of clinical nutrition 2002, 76 (3), 560-568.

130. Murota, K.; Terao, J., Antioxidative flavonoid quercetin: implication of its intestinal absorption and metabolism. Archives of biochemistry and biophysics 2003, 417 (1), 12-17.

131. Lee, J.; Mitchell, A. E., Quercetin and isorhamnetin glycosides in onion (Allium cepa L.): varietal comparison, physical distribution, coproduct evaluation, and long-term storage stability. Journal of agricultural and food chemistry 2011, 59 (3), 857-863.

132. Lombard, K. A.; Geoffriau, E.; Peffley, E., Flavonoid quantification in onion by spectrophotometric and high performance liquid chromatography analysis. HortScience 2002, 37 (4), 682-685.

133. Patil, B. S.; Pike, L. M.; Yoo, K. S., Variation in the quercetin content in different colored onions (Allium cepa L.). Journal of the American Society for Horticultural Science 1995, 120 (6), 909-913.

134. Patil, B.; Pike, L.; Hamilton, B., Changes in quercetin concentration in onion (Allium cepa L.) owing to location, growth stage and soil type. New phytologist 1995, 130 (3), 349-355.

135. Mogren, L. M.; Olsson, M. E.; Gertsson, U. E., Quercetin content in field-cured onions (Allium cepa L.): effects of cultivar, lifting time, and nitrogen fertilizer level. Journal of agricultural and food chemistry 2006, 54 (17), 6185-6191.

136. Sharma, K.; Assefa, A. D.; Ko, E. Y.; Lee, E. T.; Park, S. W., Quantitative analysis of flavonoids, sugars, phenylalanine and tryptophan in onion scales during storage under ambient conditions. Journal of food science and technology 2015, 52 (4), 2157-2165.

137. Ko, E. Y.; Nile, S. H.; Sharma, K.; Li, G. H.; Park, S. W., Effect of different exposed lights on quercetin and quercetin glucoside content in onion (Allium cepa L.). Saudi journal of biological sciences 2015, 22 (4), 398-403.

138. Sharma, K.; Ko, E. Y.; Assefa, A. D.; Ha, S.; Nile, S. H.; Lee, E. T.; Park, S. W., Temperature-dependent studies on the total phenolics, flavonoids, antioxidant activities, and sugar content in six onion varieties. journal of food and drug analysis 2015, 23 (2), 243-252.

139. Lombard, K.; Peffley, E.; Geoffriau, E.; Thompson, L.; Herring, A., Quercetin in onion (Allium cepa L.) after heat-treatment simulating home preparation. Journal of Food Composition and Analysis 2005, 18 (6), 571-581.

140. Singh, J.; Metrani, R.; Jayaprakasha, G. K.; Crosby, K. M.; Ravishankar, S.; Patil, B. S., Multivariate Analysis of Amino Acids and Health Beneficial Properties of Cantaloupe Varieties Grown in Six Locations in the United States. Plants 2020, 9 (9), 1058.

141. Insani, E. M.; Cavagnaro, P.; Salomon, V. M.; Langman, L. E.; Sance, M.; Pazos, A. A.; Carrari, F.; Filippini, O.; Vignera, L.; Galmarini, C. R., Variation for health-enhancing compounds and traits in onion (Allium cepa L.) germplasm. 2016.

142. Hansen, S. L., Content of free amino acids in onion (Allium cepa L.) as influenced by the stage of development at harvest and long-term storage. Acta Agriculturae Scandinavica, Section B-Plant Soil Science 2001, 51 (2), 77-83.

143. Fredotović, Ž.; Soldo, B.; Šprung, M.; Marijanović, Z.; Jerković, I.; Puizina, J., Comparison of Organosulfur and Amino Acid Composition between Triploid Onion Allium cornutum Clementi ex Visiani, 1842, and Common Onion Allium cepa L., and Evidences for Antiproliferative Activity of Their Extracts. Plants 2020, 9 (1), 98.

144. Singh, J.; Jayaprakasha, G. K.; Patil, B. S., Rapid and efficient desulfonation method for the analysis of glucosinolates by high-resolution liquid chromatography coupled with quadrupole time-of-flight mass spectrometry. Journal of agricultural and food chemistry 2017, 65 (50), 11100-11108.

145. Corleto, K. A.; Singh, J.; Jayaprakasha, G.; Patil, B. S., A sensitive HPLC-FLD method combined with multivariate analysis for the determination of amino acids in l-citrulline rich vegetables. journal of food and drug analysis 2019, 27 (3), 717-728.

146. Pérez-Gregorio, R. M.; García-Falcón, M. S.; Simal-Gándara, J.; Rodrigues, A. S.; Almeida, D. P., Identification and quantification of flavonoids in traditional cultivars of red and white onions at harvest. Journal of Food Composition and Analysis 2010, 23 (6), 592-598.

147. Mogren, L. M.; Olsson, M. E.; Gertsson, U. E., Effects of cultivar, lifting time and nitrogen fertiliser level on quercetin content in onion (Allium cepa L.) at lifting. Journal of the Science of Food and Agriculture 2007, 87 (3), 470-476.

148. Rico, C. M.; Morales, M. I.; Barrios, A. C.; McCreary, R.; Hong, J.; Lee, W.-Y.; Nunez, J.; Peralta-Videa, J. R.; Gardea-Torresdey, J. L., Effect of cerium oxide nanoparticles on the quality of rice (Oryza sativa L.) grains. Journal of agricultural and food chemistry 2013, 61 (47), 11278-11285.

149. Lombard, K. A.; Geoffriau, E.; Peffley, E. B., Total quercetin content in onion: Survey of cultivars grown at various locations. HortTechnology 2004, 14 (4), 628-630.

150. Melandri, G.; AbdElgawad, H.; Riewe, D.; Hageman, J. A.; Asard, H.; Beemster, G. T.; Kadam, N.; Jagadish, K.; Altmann, T.; Ruyter-Spira, C., Biomarkers for grain yield stability in rice under drought stress. Journal of experimental botany 2020, 71 (2), 669-683.

151. Dini, I.; Tenore, G. C.; Dini, A., Chemical composition, nutritional value and antioxidant properties of Allium caepa L. Var. tropeana (red onion) seeds. Food chemistry 2008, 107 (2), 613-621.

152. Kato, H.; Rhue, M. R.; Nishimura, T., Role of free amino acids and peptides in food taste. ACS Publications: 1989.

153. Maynard, D., An introduction to the watermelon. ASHS Press, Alexandria: 2001; p 9-20.

154. Wang, T.; Cobb, B.; Sittertz-Bhatkar, H.; Leskovar, D. In An ultrastructural study of seed reserves in triploid watermelons, XXVI International Horticultural Congress: Issues and Advances in Transplant Production and Stand Establishment Research 631, 2002; pp 71-77.

155. Wang, T.; Sistrunk, L.; Leskovar, D.; Cobb, B., Characteristics of storage reserves of triploid watermelon seeds: association of starch and mean germination time. Seed Sci. Technol. 2011, 39 (2), 318-326.

156. Grange, S.; Leskovar, D. I.; Pike, L. M.; Cobb, B. G., Seedcoat structure and oxygen-enhanced environments affect germination of triploid watermelon. J. Am. Soc. Hortic. Sci. 2003, 128 (2), 253-259.

157. Yim, K.-O.; Bradford, K. J., Callose deposition is responsible for apoplastic semipermeability of the endosperm envelope of muskmelon seeds. Plant Physiol. 1998, 118 (1), 83-90.

158. Grange, S.; Leskovar, D.; Pike, L.; Cobb, B., Excess moisture and seedcoat nicking influence germination of triploid watermelon. HortScience 2000, 35 (7), 1355-1356.

159. Ashraf, M.; Rauf, H., Inducing salt tolerance in maize (Zea mays L.) through seed priming with chloride salts: Growth and ion transport at early growth stages. Acta Physiol. Plant. 2001, 23 (4), 407-414.

160. González-Melendi, P.; Fernández-Pacheco, R.; Coronado, M. J.; Corredor, E.; Testillano, P.; Risueño, M. C.; Marquina, C.; Ibarra, M. R.; Rubiales, D.; Pérez-de-Luque, A., Nanoparticles as smart treatment-delivery systems in plants: assessment of different techniques of microscopy for their visualization in plant tissues. Ann. Bot. 2007, 101 (1), 187-195.

161. Vurro, M.; Miguel-Rojas, C.; Pérez-de-Luque, A., Safe nanotechnologies for increasing effectiveness of environmentally friendly natural agrochemicals. Pest Manage. Sci. 2019.

162. Pariona, N.; Martínez, A. I.; Hernandez-Flores, H.; Clark-Tapia, R., Effect of magnetite nanoparticles on the germination and early growth of Quercus macdougallii. Sci. Total Environ 2017, 575, 869-875.

163. Jaskani, M. J.; Kwon, S. W.; Kim, D.; Abbas, H., Seed treatments and orientation affects germination and seedling emergence in tetraploid watermelon. Pak. J. Bot. 2006, 38 (1), 89.

164. Chaudhary, P.; Jayaprakasha, G.; Porat, R.; Patil, B. S., Degreening and postharvest storage influences 'Star Ruby'grapefruit (Citrus paradisi Macf.) bioactive compounds. Food Chem. 2012, 135 (3), 1667-1675.

165. Rosa, M.; Prado, C.; Podazza, G.; Interdonato, R.; González, J. A.; Hilal, M.; Prado, F. E., Soluble sugars: Metabolism, sensing and abiotic stress: A complex network in the life of plants. Plant Signaling Behav. 2009, 4 (5), 388-393.

166. Almutairi, Z. M.; Alharbi, A., Effect of silver nanoparticles on seed germination of crop plants. J. Adv. Agric 2015, 4 (1), 283-288.

167. Vannini, C.; Domingo, G.; Onelli, E.; De Mattia, F.; Bruni, I.; Marsoni, M.; Bracale, M., Phytotoxic and genotoxic effects of silver nanoparticles exposure on germinating wheat seedlings. J. Plant Physiol. 2014, 171 (13), 1142-1148.

168. Sharma, P.; Bhatt, D.; Zaidi, M.; Saradhi, P. P.; Khanna, P.; Arora, S., Silver nanoparticle-mediated enhancement in growth and antioxidant status of Brassica juncea. Appl. Biochem. Biotechnol. 2012, 167 (8), 2225-2233.

169. Parveen, A.; Rao, S., Effect of nanosilver on seed germination and seedling growth in Pennisetum glaucum. J. Cluster Sci. 2015, 26 (3), 693-701.

170. Yasur, J.; Rani, P. U., Environmental effects of nanosilver: impact on castor seed germination, seedling growth, and plant physiology. Environ. Sci. Pollut. Res. 2013, 20 (12), 8636-8648.

171. Sarabi, M.; Safipour Afshar, A.; Mahmoodzadeh, H., Physiological Analysis of Silver Nanoparticles and AgNO3 Effect to Brassica napus L. J. Chem. Health Risks 2015, 5 (4).

172. Cvjetko, P.; Milošić, A.; Domijan, A.-M.; Vrček, I. V.; Tolić, S.; Štefanić, P. P.; Letofsky-Papst, I.; Tkalec, M.; Balen, B., Toxicity of silver ions and differently coated silver nanoparticles in Allium cepa roots. Ecotoxicology and environmental safety 2017, 137, 18-28.

173. Pokhrel, L. R.; Dubey, B., Evaluation of developmental responses of two crop plants exposed to silver and zinc oxide nanoparticles. Science of the Total Environment 2013, 452, 321-332.

174. Wang, J.; Koo, Y.; Alexander, A.; Yang, Y.; Westerhof, S.; Zhang, Q.; Schnoor, J. L.; Colvin, V. L.; Braam, J.; Alvarez, P. J., Phytostimulation of poplars and Arabidopsis exposed to

silver nanoparticles and Ag+ at sublethal concentrations. Environmental science & technology 2013, 47 (10), 5442-5449.

175. Li, Y.; Qin, T.; Ingle, T.; Yan, J.; He, W.; Yin, J.-J.; Chen, T., Differential genotoxicity mechanisms of silver nanoparticles and silver ions. Archives of toxicology 2017, 91 (1), 509-519.

176. Salama, H. M., Effects of silver nanoparticles in some crop plants, common bean (Phaseolus vulgaris L.) and corn (Zea mays L.). Int Res J Biotechnol 2012, 3 (10), 190-197.

177. Zari, H.; Babak, P.; Asad, R., The effect of priming with nano-sliver on agronomic traits of safflower cultivars. J. Essent. Oil-Bear. Plants 2015, 18 (5), 1148-1156.

178. Sundaria, N.; Singh, M.; Upreti, P.; Chauhan, R. P.; Jaiswal, J.; Kumar, A., Seed priming with Iron oxide nanoparticles triggers Iron acquisition and biofortification in wheat (Triticum aestivum L.) grains. J. Plant Growth Regul. 2019, 38 (1), 122-131.

179. Wang, Z.; Xie, X.; Zhao, J.; Liu, X.; Feng, W.; White, J. C.; Xing, B., Xylem-and phloem-based transport of CuO nanoparticles in maize (Zea mays L.). Environ. Sci. Technol. 2012, 46 (8), 4434-4441.

180. Raliya, R.; Nair, R.; Chavalmane, S.; Wang, W.-N.; Biswas, P., Mechanistic evaluation of translocation and physiological impact of titanium dioxide and zinc oxide nanoparticles on the tomato (Solanum lycopersicum L.) plant. Metallomics 2015, 7 (12), 1584-1594.

181. Raliya, R.; Franke, C.; Chavalmane, S.; Nair, R.; Reed, N.; Biswas, P., Quantitative understanding of nanoparticle uptake in watermelon plants. Front. Plant Sci. 2016, 7, 1288.

182. Naz, A.; Butt, M. S.; Sultan, M. T.; Qayyum, M. M. N.; Niaz, R. S., Watermelon lycopene and allied health claims. EXCLI journal 2014, 13, 650.

183. Chen, L.; Stacewicz-Sapuntzakis, M.; Duncan, C.; Sharifi, R.; Ghosh, L.; Breemen, R. v.; Ashton, D.; Bowen, P. E., Oxidative DNA damage in prostate cancer patients consuming tomato sauce-based entrees as a whole-food intervention. J. Natl. Cancer Inst. 2001, 93 (24), 1872-1879.

184. Rao, A. V.; Agarwal, S., Role of antioxidant lycopene in cancer and heart disease. J. Am. Coll. Nutr. 2000, 19 (5), 563-569.

185. De, E. S.; Boffetta, P.; Brennan, P.; Deneo-Pellegrini, H.; Carzoglio, J.; Ronco, A.; Mendilaharsu, M., Dietary carotenoids and risk of gastric cancer: a case-control study in Uruguay. Eur. J. Cancer Prev. 2000, 9 (5), 329-334.

186. Edwards, A. J.; Vinyard, B. T.; Wiley, E. R.; Brown, E. D.; Collins, J. K.; Perkins-Veazie, P.; Baker, R. A.; Clevidence, B. A., Consumption of watermelon juice increases plasma concentrations of lycopene and β-carotene in humans. J. Nutr. 2003, 133 (4), 1043-1050.

187. Stahl, W.; Heinrich, U.; Wiseman, S.; Eichler, O.; Sies, H.; Tronnier, H., Dietary tomato paste protects against ultraviolet light–induced erythema in humans. J. Nutr. 2001, 131 (5), 1449-1451.

188. Wattanapenpaiboon, N.; Lukito, W.; Wahlqvist, M. L.; Strauss, B. J., Dietary carotenoid intake as a predictor of bone mineral density. Asia Pac. J. Clin. Nutr. 2003, 12 (4), 467-473.

189. Gupta, N. P.; Kumar, R., Lycopene therapy in idiopathic male infertility–a preliminary report. Int. Urol. Nephrol. 2002, 34 (3), 369-372.

190. Tarazona-Díaz, M. P.; Alacid, F.; Carrasco, M.; Martínez, I.; Aguayo, E., Watermelon juice: potential functional drink for sore muscle relief in athletes. J. Agric. Food Chem. 2013, 61 (31), 7522-7528.

191. Figueroa, A.; Sanchez-Gonzalez, M. A.; Perkins-Veazie, P. M.; Arjmandi, B. H., Effects of watermelon supplementation on aortic blood pressure and wave reflection in individuals with prehypertension: a pilot study. Am. J. Hypertens. 2011, 24 (1), 40-44.

192. Shiota, A.; Hotta, Y.; Kataoka, T.; Morita, M.; Maeda, Y.; Kimura, K., Oral l-citrulline supplementation improves erectile function in rats with acute arteriogenic erectile dysfunction. J. Sex. Med. 2013, 10 (10), 2423-2429.

193. Kader, A. A., Influence of preharvest and postharvest environment on nutritional composition of fruits and vegetables. In Horticulture and human health, contributions of fruits and vegetables Bliss, B. Q. F. A., Ed. Prentice-Hall, NJ: Englewood Cliffs.: 1988; pp 18-32.

194. Kader, A. A., Flavor quality of fruits and vegetables. Journal of the Science of Food and Agriculture 2008, 88 (11), 1863-1868.

195. Cisneros-Zevallos, L., The use of controlled postharvest abiotic stresses as a tool for enhancing the nutraceutical content and adding-value of fresh fruits and vegetables. J. Food Sci. 2003, 68 (5), 1560-1565.

196. Rushing, J.; Fonseca, J.; Keinath, A., Harvesting and postharvest handling. In: Maynard, D. (Ed.), Watermelons: Characteristics, Production, and Marketing. Am. Soc. Hort. Sci. Press, Alexandria, VA 22314: 2001.

197. Kyriacou, M. C.; Soteriou, G. A.; Rouphael, Y.; Siomos, A. S.; Gerasopoulos, D., Configuration of watermelon fruit quality in response to rootstock-mediated harvest maturity and postharvest storage. J. Sci. Food Agric. 2016, 96 (7), 2400-2409.

198. Perkins-Veazie, P.; Collins, J. K., Carotenoid changes of intact watermelons after storage. J. Agric. Food Chem. 2006, 54 (16), 5868-5874.

199. Nair, R.; Varghese, S. H.; Nair, B. G.; Maekawa, T.; Yoshida, Y.; Kumar, D. S., Nanoparticulate material delivery to plants. Plant Sci. 2010, 179 (3), 154-163.

200. Partila, A. M., Bioproduction of Silver Nanoparticles and Its Potential Applications in Agriculture. In Nanotechnology for Agriculture, Springer: 2019; pp 19-36.

201. Chebrolu, K. K.; Jayaprakasha, G.; Yoo, K. S.; Jifon, J. L.; Patil, B. S., An improved sample preparation method for quantification of ascorbic acid and dehydroascorbic acid by HPLC. LWT-Food Sci. Technol. 2012, 47 (2), 443-449.

202. Jayaprakasha, G.; Murthy, K. C.; Patil, B. S., Rapid HPLC-UV method for quantification of L-citrulline in watermelon and its potential role on smooth muscle relaxation markers. Food chem. 2011, 127 (1), 240-248.

203. Chisholm, D.; Picha, D., Effect of storage temperature on sugar and organic acid contents of watermelon. HortScience 1986, 21 (4), 1031-1033.

204. Kyriacou, M. C.; Soteriou, G., Quality and postharvest performance of watermelon fruit in response to grafting on interspecific cucurbit rootstocks. J. Food Qual. 2015, 38 (1), 21-29.

205. Perkins-Veazie, P.; Collins, J. K.; Davis, A. R.; Roberts, W., Carotenoid content of 50 watermelon cultivars. J. Agric. Food Chem. 2006, 54 (7), 2593-2597.

206. Leskovar, D.; Bang, H.; Crosby, K.; Maness, N.; Franco, A.; Perkins-Veazie, P., Lycopene, carbohydrates, ascorbic acid and yield components of diploid and triploid watermelon cultivars are affected by de® cit irrigation. J. Hortic. Sci. Biotechnol. 2004, 79 (1), 75-81.

207. Oms-Oliu, G.; Odriozola-Serrano, I.; Soliva-Fortuny, R.; Martín-Belloso, O., Effects of high-intensity pulsed electric field processing conditions on lycopene, vitamin C and antioxidant capacity of watermelon juice. Food Chem. 2009, 115 (4), 1312-1319.

208. Showalter, R.; Harmon, S.; Brantley, B.; Newson, D.; Pittman, J., Changes in Congo watermelons after harvest. Proc. Assoc. Southern Agric. Workers 1955, 52, 136-137.

209. Javanmardi, J.; Kubota, C., Variation of lycopene, antioxidant activity, total soluble solids and weight loss of tomato during postharvest storage. Postharvest Biol. Technol. 2006, 41 (2), 151-155.

210. Meléndez-Martínez, A. J.; Mapelli-Brahm, P.; Stinco, C. M., The colourless carotenoids phytoene and phytofluene: From dietary sources to their usefulness for the functional foods and nutricosmetics industries. J. Food Compos. Anal. 2018, 67, 91-103.

211. Srivastava, S.; Srivastava, A. K., Lycopene; chemistry, biosynthesis, metabolism and degradation under various abiotic parameters. J. Food Sci. Technol. 2015, 52 (1), 41-53.

212. Bianchi, G.; Rizzolo, A.; Grassi, M.; Provenzi, L.; Scalzo, R. L., External maturity indicators, carotenoid and sugar compositions and volatile patterns in ‘Cuoredolce®’and ‘Rugby’mini-watermelon (Citrullus lanatus (Thunb) Matsumura & Nakai) varieties in relation of ripening degree at harvest. Postharvest Biol. Technol. 2018, 136, 1-11.

213. Perkins-Veazie, P.; Collins, J. K.; Pair, S. D.; Roberts, W., Lycopene content differs among red-fleshed watermelon cultivars. J. Agric. Food Chem. 2001, 81 (10), 983-987.

214. Arias, R.; Lee, T.-C.; Logendra, L.; Janes, H., Correlation of lycopene measured by HPLC with the L*, a*, b* color readings of a hydroponic tomato and the relationship of maturity with color and lycopene content. J. Agric. Food Chem. 2000, 48 (5), 1697-1702.

215. Rimando, A. M.; Perkins-Veazie, P. M., Determination of citrulline in watermelon rind. J. Chromatogr. 2005, 1078 (1-2), 196-200.

216. Gil, M. I.; Aguayo, E.; Kader, A. A., Quality changes and nutrient retention in fresh-cut versus whole fruits during storage. J. Agric. Food Chem. 2006, 54 (12), 4284-4296.

217. Lee, S. K.; Kader, A. A., Preharvest and postharvest factors influencing vitamin C content of horticultural crops. Postharvest Biol. Technol. 2000, 20 (3), 207-220.

218. Pérez, A. G.; Luaces, P.; Oliva, J.; Ríos, J. J.; Sanz, C., Changes in vitamin C and flavour components of mandarin juice due to curing of fruits. Food Chem. 2005, 91 (1), 19-24.

219. Dewhirst, R. A.; Clarkson, G. J.; Rothwell, S. D.; Fry, S. C., Novel insights into ascorbate retention and degradation during the washing and post-harvest storage of spinach and other salad leaves. Food chem. 2017, 233, 237-246.

220. Szultka, M.; Buszewska-Forajta, M.; Kaliszan, R.; Buszewski, B., Determination of ascorbic acid and its degradation products by high-performance liquid chromatography-triple quadrupole mass spectrometry. Electrophoresis 2014, 35 (4), 585-592.

221. Liu, Y.; He, C.; Song, H., Comparison of fresh watermelon juice aroma characteristics of five varieties based on gas chromatography-olfactometry-mass spectrometry. Food Research International 2018, 107, 119-129.

222. Maoto, M. M.; Beswa, D.; Jideani, A. I., Watermelon as a potential fruit snack. International Journal of Food Properties 2019, 22 (1), 355-370.

223. Liu, Y.; Song, H.; Yang, X.; He, C., Influence of multiple environmental factors on the quality and flavor of watermelon juice. RSC advances 2019, 9 (27), 15289-15297.

224. Toivonen, P., Postharvest storage procedures and oxidative stress. HortScience 2004, 39 (5), 938.

225. Mahajan, P. V.; Caleb, O. J.; Singh, Z.; Watkins, C. B.; Geyer, M., Postharvest treatments of fresh produce. Philosophical Transactions of the Royal Society A: Mathematical, Physical and Engineering Sciences 2014, 372 (2017), 20130309.

226. Pech, J.-C.; Latché, A.; Van der Rest, B., Genes involved in the biosynthesis of aroma volatiles and biotechnological applications. In Fruit and Vegetable Flavour, Elsevier: 2008; pp 254-271.

227. Thomazini, M.; Franco, M., Methodology for analysis of the volatile constituints of flavor. Boletim da Sociedade Brasileira de Ciencia e Tecnologia de Alimentos (Brazil) 2000.

228. Xisto, A. L. R. P.; Boas, E. V. d. B. V.; Nunes, E. E.; Federal, B. M. V. B.; Guerreiro, M. C., Volatile profile and physical, chemical, and biochemical changes in fresh cut watermelon during storage. Food Science and Technology 2012, 32 (1), 173-178.

229. Bianchi, G.; Provenzi, L.; Rizzolo, A., Evolution of volatile compounds in 'Cuoredolce®'and 'Rugby'mini-watermelons (Citrullus lanatus (Thunb.) Matsumura and Nakai) in relation to ripening at harvest. Journal of the Science of Food and Agriculture 2020, 100 (3), 945-952.

230. Genthner, E. R. Identification of key odorants in fresh-cut watermelon aroma and structure-odor relationships of cis, cis-3, 6-nonadienal and ester analogs with cis, cis-3, 6-nonadiene, cis-3-nonene and cis-6-nonene backbone structures. University of Illinois at Urbana-Champaign, 2010.

231. Song, J.; Forney, C. F., Flavour volatile production and regulation in fruit. Canadian Journal of Plant Science 2008, 88 (3), 537-550.

232. Rizzolo, A.; Polesello, A.; Polesello, S., Use of headspace capillary GC to study the development of volatile compounds in fresh fruit. Journal of High Resolution Chromatography 1992, 15 (7), 472-477.

233. Yajima, I.; Sakakibara, H.; Ide, J.; Yanai, T.; Hayashi, K., Volatile flavor components of watermelon (Citrullus vulgaris). Agricultural and Biological Chemistry 1985, 49 (11), 3145-3150.

234. Dima, G.; Tripodi, G.; Condurso, C.; Verzera, A., Volatile constituents of mini-watermelon fruits. Journal of Essential Oil Research 2014, 26 (5), 323-327.

235. Fredes, A.; Sales, C.; Barreda, M.; Valcárcel, M.; Roselló, S.; Beltrán, J., Quantification of prominent volatile compounds responsible for muskmelon and watermelon aroma by purge and trap extraction followed by gas chromatography–mass spectrometry determination. Food chemistry 2016, 190, 689-700.

236. Pino, J. A.; Marbot, R.; Aguero, J., Volatile components of watermelon (Citrullus Ianatus [Thunb.] Matsum. et Nakai) fruit. Journal of Essential Oil Research 2003, 15 (6), 379-380.

237. Giuliano, G.; Al-Babili, S.; Von Lintig, J., Carotenoid oxygenases: cleave it or leave it. Trends in plant science 2003, 8 (4), 145-149.

238. Lewinsohn, E.; Sitrit, Y.; Bar, E.; Azulay, Y.; Meir, A.; Zamir, D.; Tadmor, Y., Carotenoid pigmentation affects the volatile composition of tomato and watermelon fruits, as revealed by comparative genetic analyses. Journal of Agricultural and Food Chemistry 2005, 53 (8), 3142-3148.

239. Liu, C.; Zhang, H.; Dai, Z.; Liu, X.; Liu, Y.; Deng, X.; Chen, F.; Xu, J., Volatile chemical and carotenoid profiles in watermelons [Citrullus vulgaris (Thunb.) Schrad (Cucurbitaceae)] with different flesh colors. Food Science and Biotechnology 2012, 21 (2), 531-541.

240. Kyriacou, M. C.; Leskovar, D. I.; Colla, G.; Rouphael, Y., Watermelon and melon fruit quality: The genotypic and agro-environmental factors implicated. Scientia Horticulturae 2018, 234, 393-408.

241. Vallone, S.; Sivertsen, H.; Anthon, G. E.; Barrett, D. M.; Mitcham, E. J.; Ebeler, S. E.; Zakharov, F., An integrated approach for flavour quality evaluation in muskmelon (Cucumis melo L. reticulatus group) during ripening. Food chemistry 2013, 139 (1-4), 171-183.

242. Gilbert, J. L.; Guthart, M. J.; Gezan, S. A.; de Carvalho, M. P.; Schwieterman, M. L.; Colquhoun, T. A.; Bartoshuk, L. M.; Sims, C. A.; Clark, D. G.; Olmstead, J. W., Identifying breeding priorities for blueberry flavor using biochemical, sensory, and genotype by environment analyses. PLoS One 2015, 10 (9), e0138494.

243. Samykanno, K.; Pang, E.; Marriott, P. J., Genotypic and environmental effects on flavor attributes of 'Albion'and 'Juliette'strawberry fruits. Scientia Horticulturae 2013, 164, 633-642.

244. Marsol-Vall, A.; Kortesniemi, M.; Karhu, S. T.; Kallio, H.; Yang, B., Profiles of volatile compounds in blackcurrant (Ribes nigrum) cultivars with a special focus on the influence of growth latitude and weather conditions. Journal of agricultural and food chemistry 2018, 66 (28), 7485-7495.

245. Vogele, A. C., Effect of environmental factors upon the color of the tomato and the watermelon. Plant physiology 1937, 12 (4), 929.

246. Wang, Y.-b.; Yue, M.; ZHAO, X.-y.; ZHANG, C. In Qualities and Aroma of Watermelon Juice during Storage at 4¯ C, 2nd International Conference on Biomedical and Biological Engineering 2017 (BBE 2017), Atlantis Press: 2017.

247. Saftner, R.; Luo, Y.; McEvoy, J.; Abbott, J. A.; Vinyard, B., Quality characteristics of fresh-cut watermelon slices from non-treated and 1-methylcyclopropene-and/or ethylene-treated whole fruit. Postharvest Biology and Technology 2007, 44 (1), 71-79.

248. Beaulieu, J. C.; Lea, J. M., Characterization and semiquantitative analysis of volatiles in seedless watermelon varieties using solid-phase microextraction. Journal of Agricultural and Food Chemistry 2006, 54 (20), 7789-7793.

APPENDIX A

SUPPLEMENTARY FILE FOR THE CHAPTER 2

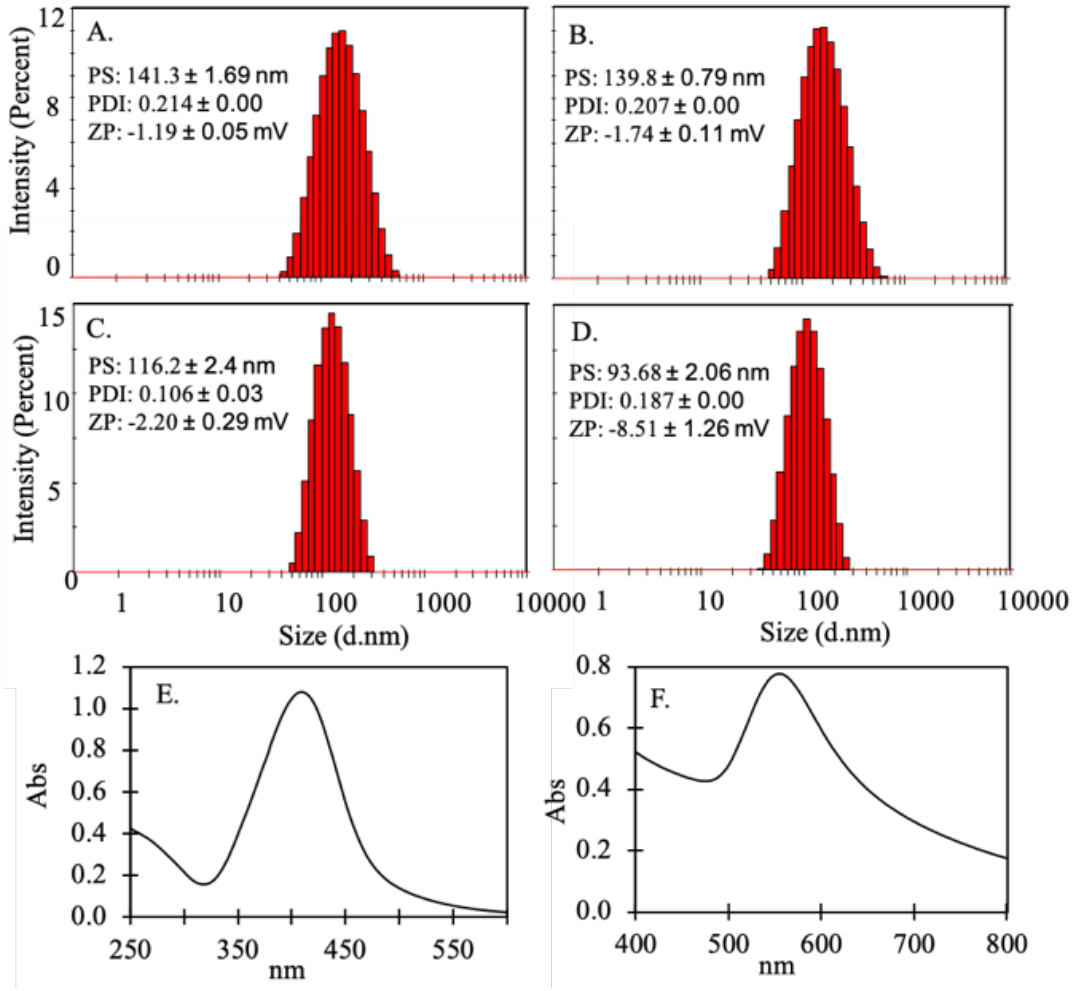

Figure A1 Histograms containing mean particle size (PS), zeta potential (ZP), and polydispersity index (PDI) for (A) turmeric nanoemulsion (TNE) (B) citrus nanoemulsion (CNE) (C) silver nanoparticles (AgNPs) (D) gold nanoparticles (AuNPs), respectively.

.

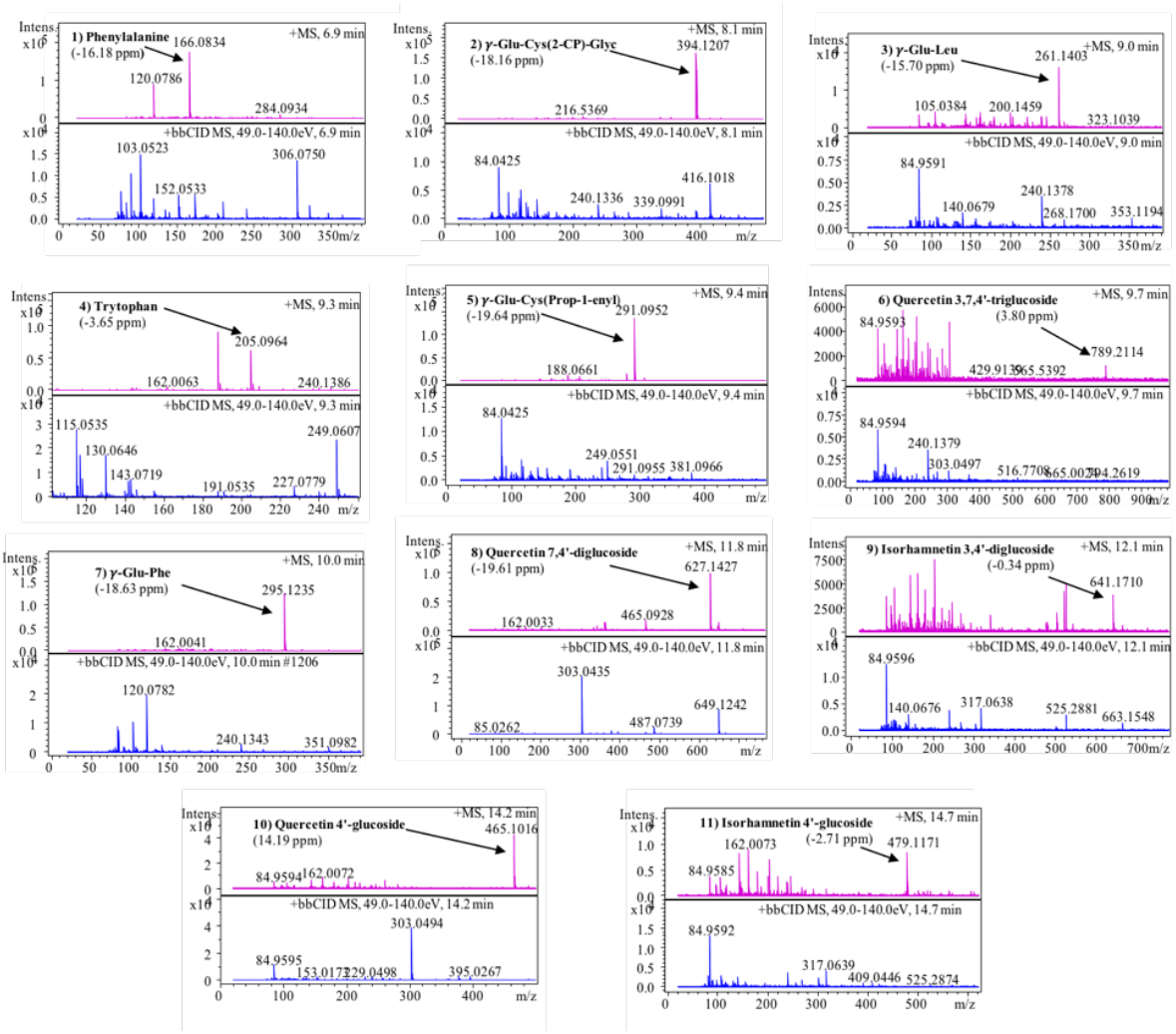

Figure A2 Tandem mass spectra in positive ionization mode. 1: phenylalanine; 2: γ-Glu-Cys(2-CP)-Glyc; 3: γ-Glu-Leu; 4: tryptophan; 5: γ-Glu-Cys (Prop-1-enyl); 6: quercetin 3,7,4′-triglucoside; 7: γ-Glu-Phe; 8: quercetin 7,4′-diglucoside; 9: isorhamnetin 3,4′-diglucoside; 10, quercetin 4-glucoside and 11: isorhamnetin 4′-glucoside.

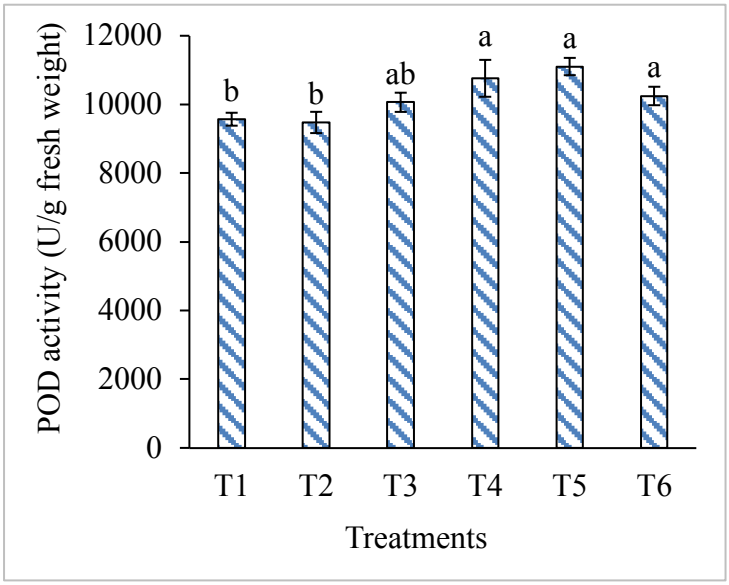

Figure A3 Effect of nanopriming in peroxidase activity of onion seeds. T1: unprimed, T2: hydroprimed, T3: turmeric oil nanoemulsion; T4: citrus oil nanoemulsion, T5: silver nanoparticle and T6: gold nanoparticle. Error bars represent standard error of the mean. Bars labeled with the same letters indicate no significant difference between the means at ($p \leq 0.05$).

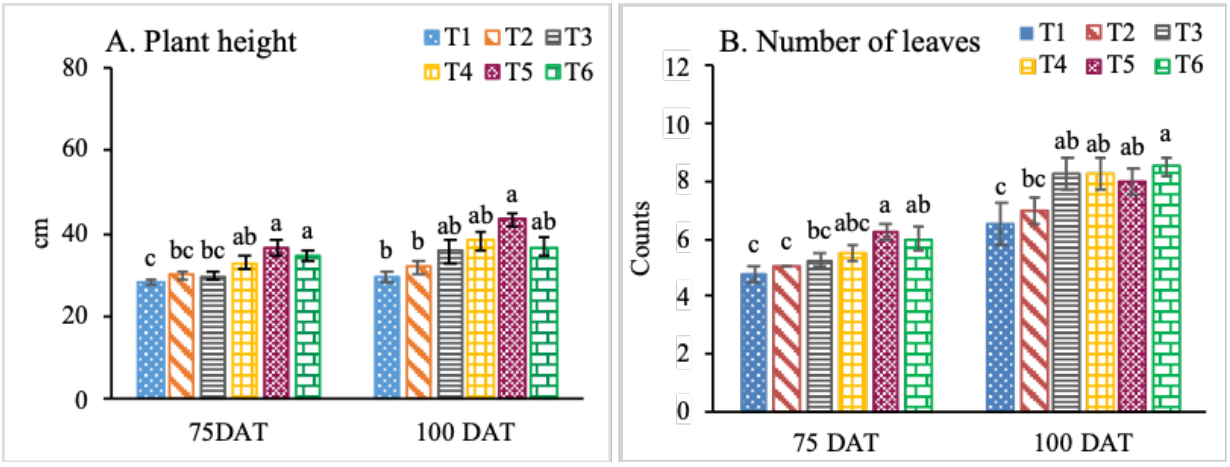

Figure A4 Effect of nanopriming in (A) plant height, (B) number of leaves of onions grown at College Station, 2015–2016. T1: unprimed, T2: hydroprimed, T3: turmeric oil nanoemulsion; T4: citrus oil nanoemulsion, T5: silver nanoparticle and T6: gold nanoparticle. Error bars represent standard error of the mean. Bars labeled with the same letters indicate no significant difference between the means at ($p \leq 0.05$). DAT: Days after transplanting

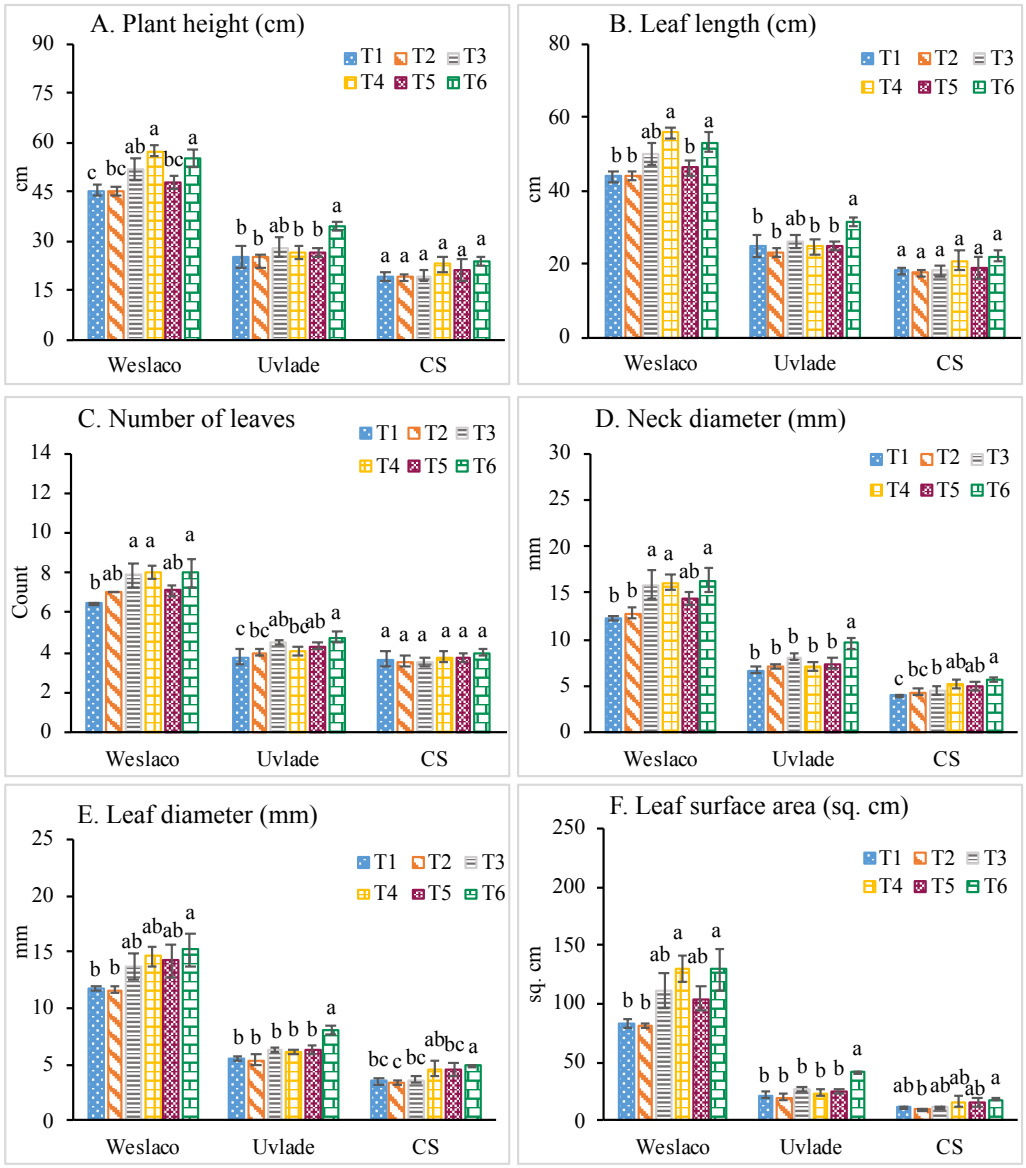

Figure A5 Effect of nanopriming on onion growth parameters. (A) Plant height (B) leaf length, (C) number of leaves per plant (D) neck diameter (E) leaf diameter, and (F) leaf surface area at 75 DAT (days after transplanting) of onions grown at Weslaco, Uvalde and College Station, 2016–2017. T1: unprimed, T2: hydroprimed, T3: turmeric oil nanoemulsion; T4: citrus oil nanoemulsion, T5: silver nanoparticle and T6: gold nanoparticle. Error bars represent standard error of the mean. Bars labeled with the same letters indicate no significant difference between the means at ($p \leq 0.05$).

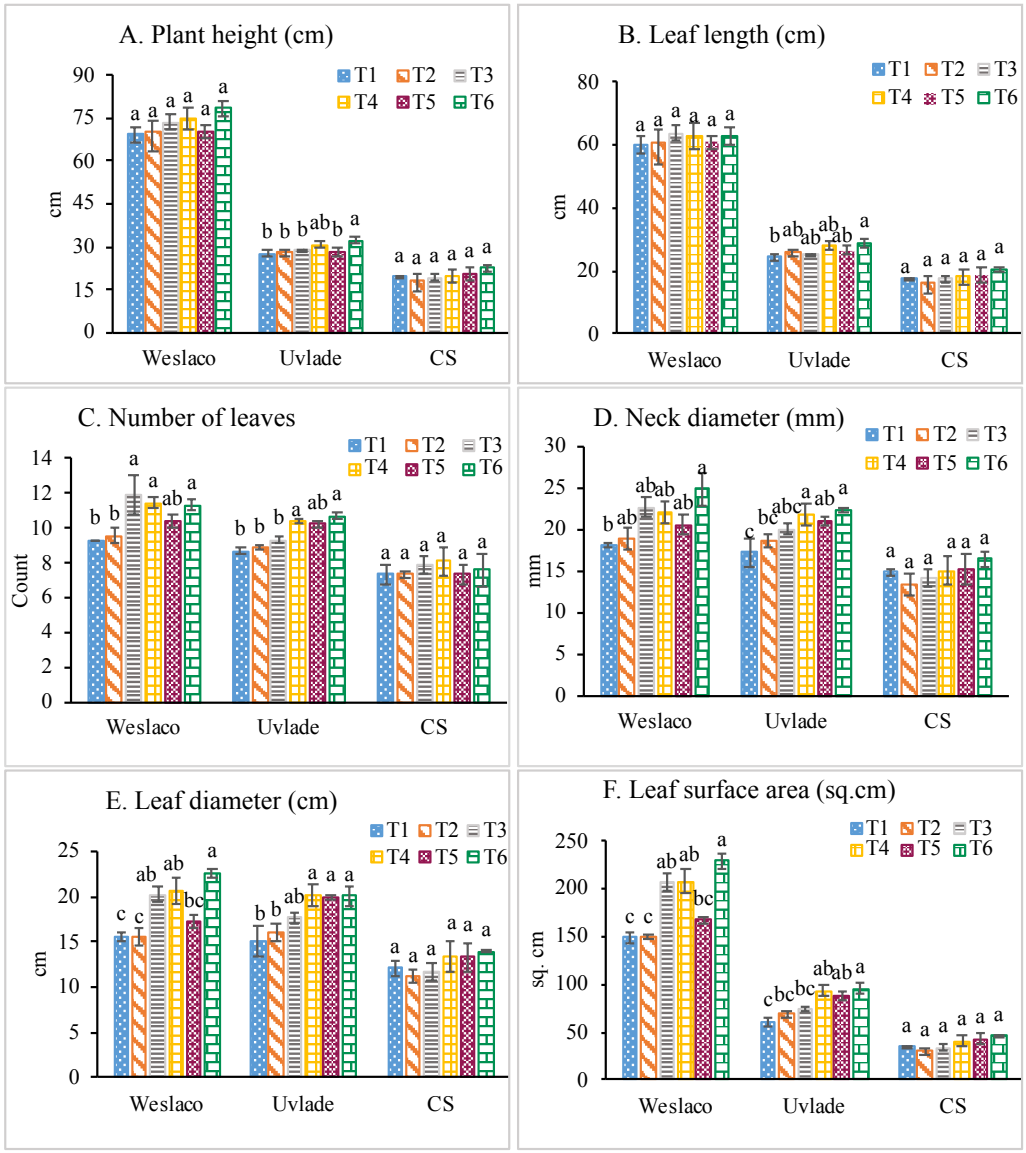

Figure A6 Effect of nanopriming on onion growth parameters. (A) Plant height (B) leaf length, (C) number of leaves per plant (D) neck diameter (E) leaf diameter and (F) leaf surface area at 100 DAT (days after transplanting) of onion grown at Weslaco, Uvalde and College Station, 2016–2017. T1: unprimed, T2: hydroprimed, T3: turmeric oil nanoemulsion; T4: citrus oil nanoemulsion, T5: silver nanoparticle and T6: gold nanoparticle. Error bars represent standard error of the mean. Bars labeled with the same letters indicate no significant difference between the means at ($p \leq 0.05$).

Table A1. Rainfall and maximum and minimum temperatures of growth conditions for both years

Months	2015–16			2016–17								
	College Station			Weslaco			Uvalde			College Station		
	Max (°C)	Min (°C)	Rain (in)	Max (°C)	Min (°C)	Rain (in)	Max (°C)	Min (°C)	Rain (in)	Max (°C)	Min (°C)	Rain (in)
Nov	28.3	1.1	0.5	35.0	5.6	0.2	31.1	1.7	0.2	30.6	1.1	0.3
Dec	26.7	1.1	0.7	30.6	1.7	0.1	28.3	-4.4	0.2	27.8	-5.6	0.3
Jan	26.7	-5.6	0.1	33.3	-1.7	0.1	28.9	-7.2	0.1	27.8	-8.3	0.3
Feb	26.7	-0.6	0.1	35.0	7.8	0.1	32.2	2.8	0.1	30.6	1.7	0.3
Mar	31.7	1.7	0.4	33.3	10.0	0.1	31.1	6.1	0.2	30.6	3.9	0.2

Table A2. Soil report for growth conditions for both years

Analysis	Units	2015–16	2016–17		
		College Station	Weslaco	Uvalde	College Station
pH	-	8	8.3	8.1	7.6
Conductivity	µmho/cm	301	212	383	2270
Nitrate-N	ppm	16	7	24	116
Phosphorus	ppm	83	51	60	163
Potassium	ppm	686	327	666	446
Calcium	ppm	4989	4619	11128	7911
Magnesium	ppm	110	310	274	321
Sulfur	ppm	13	20	26	18
Sodium	ppm	20	15	58	12

Table A3. Effect of nanopriming on the color measurements L*, a* and b* values and Brix values for different size onions grown at three different locations in 2016–17.

Location		Color values			°Brix			
		L*	a*	b*	Colossal	Large	Medium	Small
Weslaco	T1	27.18±2.32	-7.43±0.91	7.68±1.48	5.76±0.03	6.50±0.23	6.46±0.12	7.06±0.09
	T2	30.96±0.37	-8.21±0.14	9.12±0.17	6.00±0.10	6.10±0.21	6.30±0.15	6.66±0.03
	T3	30.59±0.21	-8.56±0.02	8.82±0.03	6.66±0.15	6.30±0.32	6.40±0.15	7.20±0.12
	T4	30.34±0.51	-8.40±0.04	9.02±0.01	6.10±0.15	6.03±0.07	6.03±0.17	6.90±0.06
	T5	31.97±0.22	-9.06±0.13	9.81±0.17	6.16±0.33	6.00±0.26	6.13±0.15	6.46±0.07
	T6	31.36±0.15	-9.19±0.12	10.35±0.13	6.30±0.06	6.06±0.15	6.00±0.20	6.33±0.03
Uvalde	T1	30.40±0.10	-8.41±0.04	9.19±0.09	6.53±0.23	6.86±0.27	6.43±0.09	7.13±0.03
	T2	29.83±0.12	-8.65±0.03	9.12±0.55	6.26±0.18	6.60±0.20	7.03±0.37	7.06±0.03
	T3	30.97±0.35	-8.89±0.04	10.05±0.05	6.46±0.32	6.96±0.09	6.40±0.06	6.80±0.06
	T4	30.20±0.17	-8.85±0.09	9.52±0.11	6.66±0.30	6.46±0.19	6.33±0.03	7.03±0.03
	T5	32.43±0.13	-9.07±0.01	10.40±0.01	6.33±0.43	6.40±0.12	6.26±0.20	6.86±0.03
	T6	30.44±0.53	-8.49±0.09	9.43±0.09	6.36±0.20	6.23±0.03	6.73±0.15	7.23±0.03
College Station	T1	29.77±0.15	-7.70±0.01	11.53±0.06	-	5.33±0.03	7.43±0.09	7.86±0.03
	T2	30.26±0.24	-7.91±0.09	11.84±0.16	5.13±0.03	5.30±0.10	6.36±0.12	6.66±0.07
	T3	31.21±0.07	-8.27±0.12	12.89±0.13	6.80±0.15	6.10±0.35	5.73±0.03	6.10±0.06
	T4	29.81±0.03	-7.86±0.06	11.77±0.05	5.73±0.07	5.50±0.10	6.33±0.03	9.40±0.31
	T5	29.25±0.14	-7.02±0.02	10.22±0.05	7.03±0.03	8.26±0.29	9.26±0.33	9.36±0.03
	T6	29.71±0.39	-7.50±0.40	11.62±0.33	7.03±0.03	7.06±0.87	8.43±0.73	8.60±0.00

T1: unprimed, T2: hydroprimed, T3: turmeric oil nanoemulsion; T4: citrus oil nanoemulsion; T5: silver nanoparticle; and T6: gold nanoparticle. Values represent mean ± standard error of mean (n = 3)

APPENDIX B

SUPPLEMENTARY FILE FOR THE CHAPTER 3

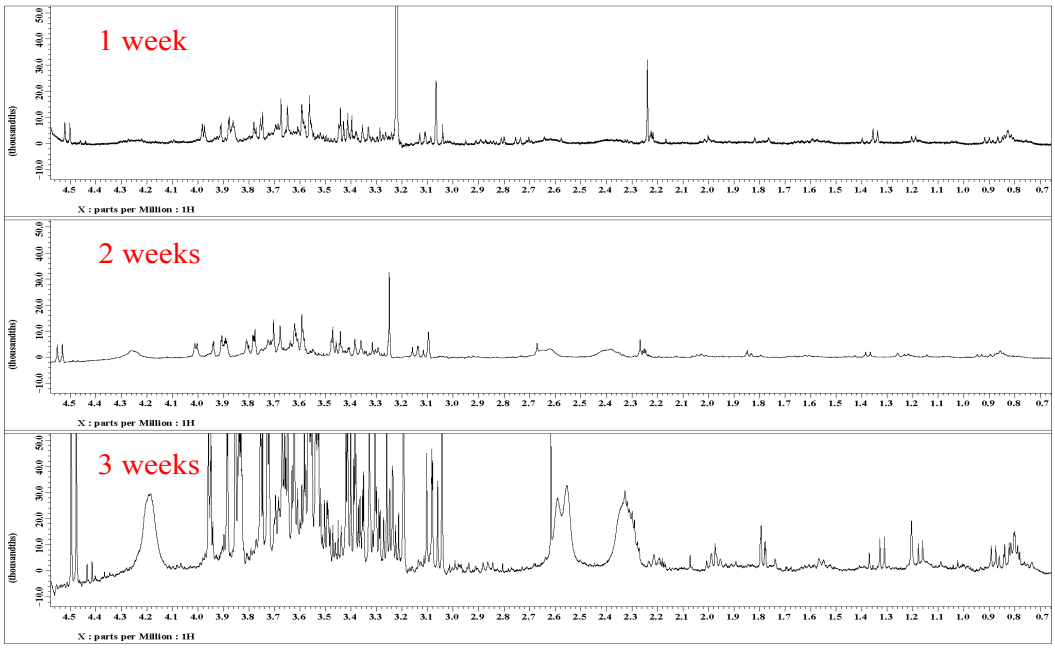

Figure B1 Identified metabolites of 1-week, 2-week and 3-week old unprimed onion seedlings by ^{1}H NMR spectra recorded at 400 MHz JEOL spectrometer.

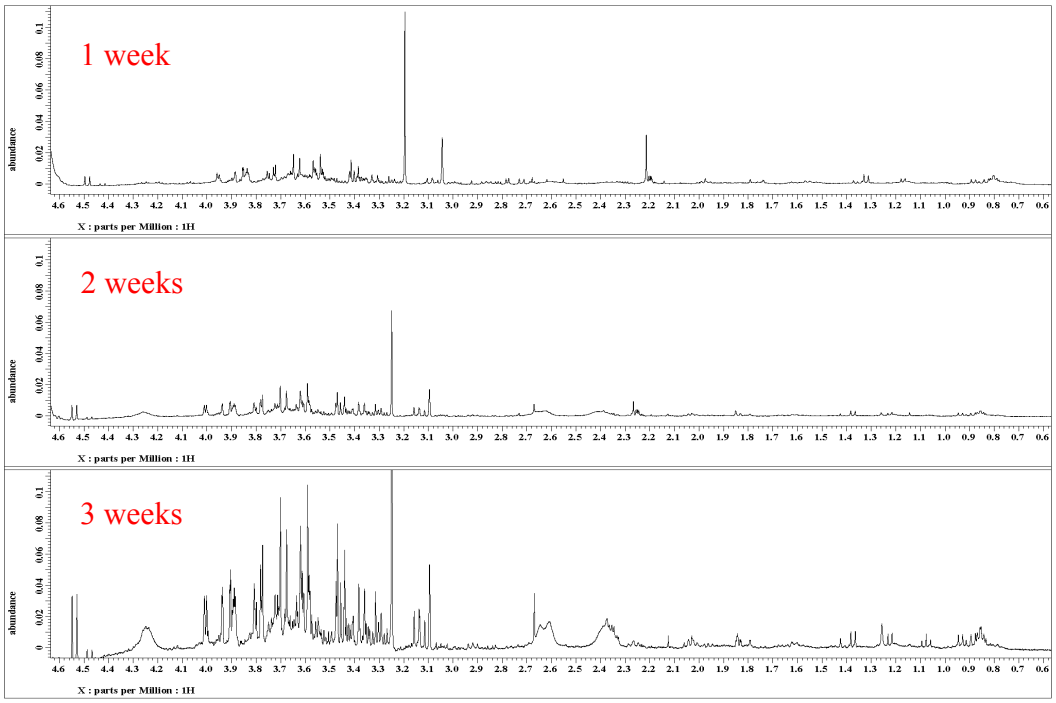

Figure B2 Overlay ^{1}H NMR spectra of 1-week, 2-week and 3-week old hydroprimed onion seedlings.

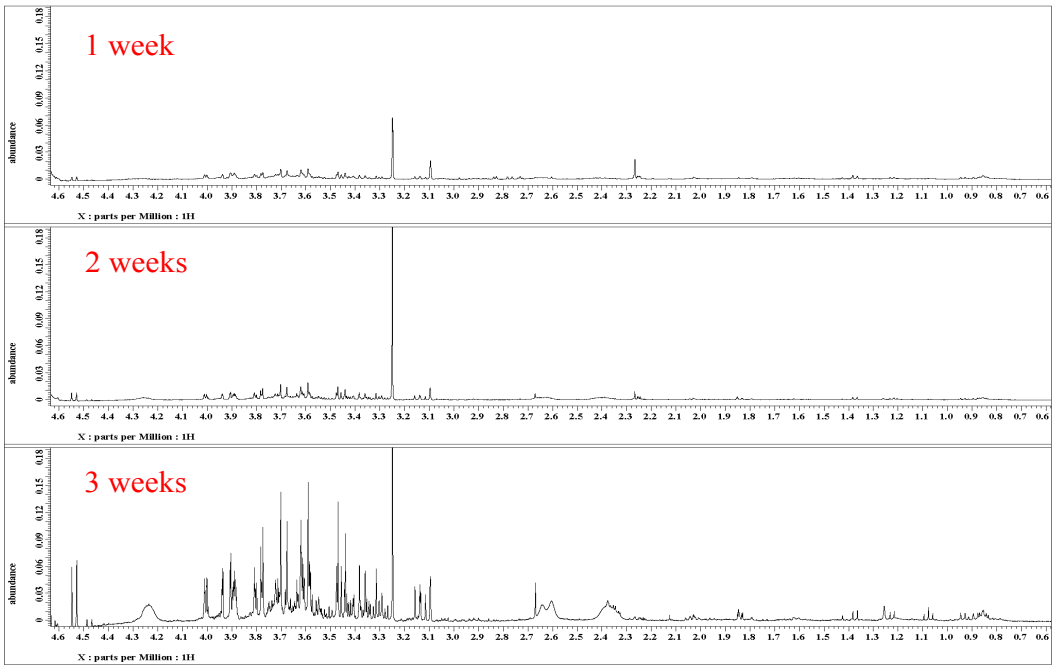

Figure B3 Overlay ^{1}H NMR spectra of 1-week, 2-week and 3-week old turmeric nanoemulsion treated onion seedlings.

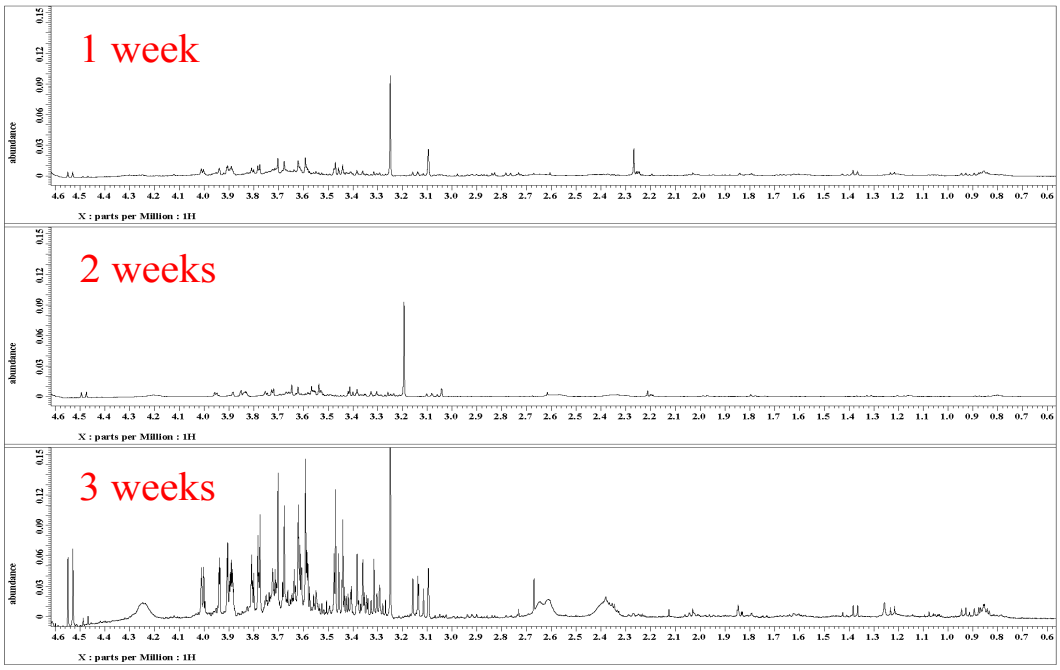

Figure B4 Overlay ^{1}H NMR spectra of 1-week, 2-week and 3-week old citrus nanoemulsion treated onion seedlings.

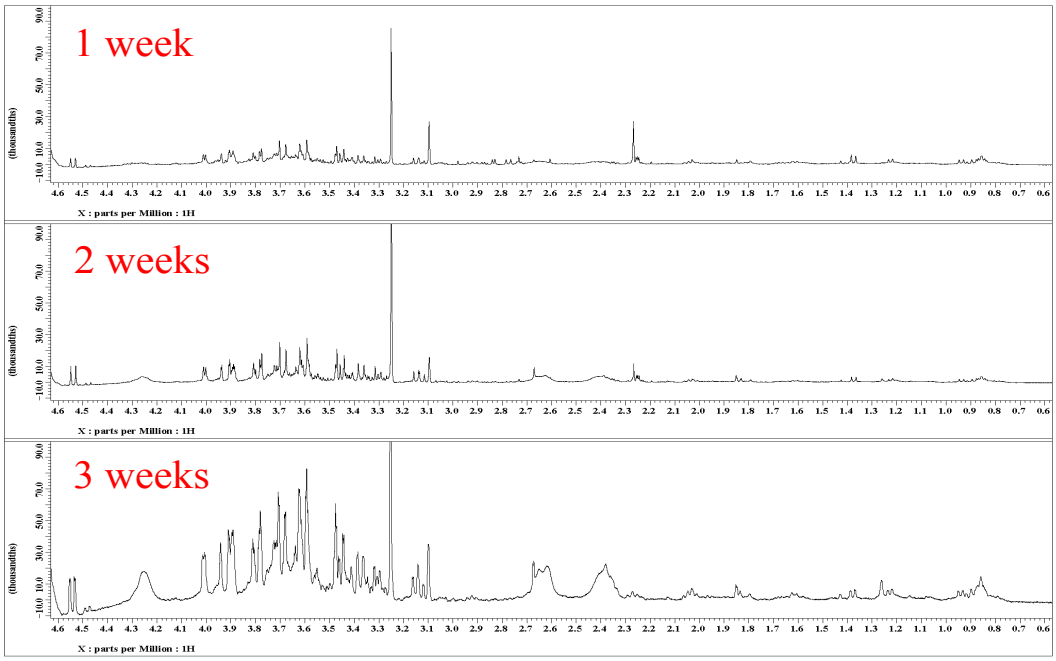

Figure B5 Overlay ^{1}H NMR spectra of 1-week, 2-week and 3-week old silver nanoparticle treated onion seedlings.

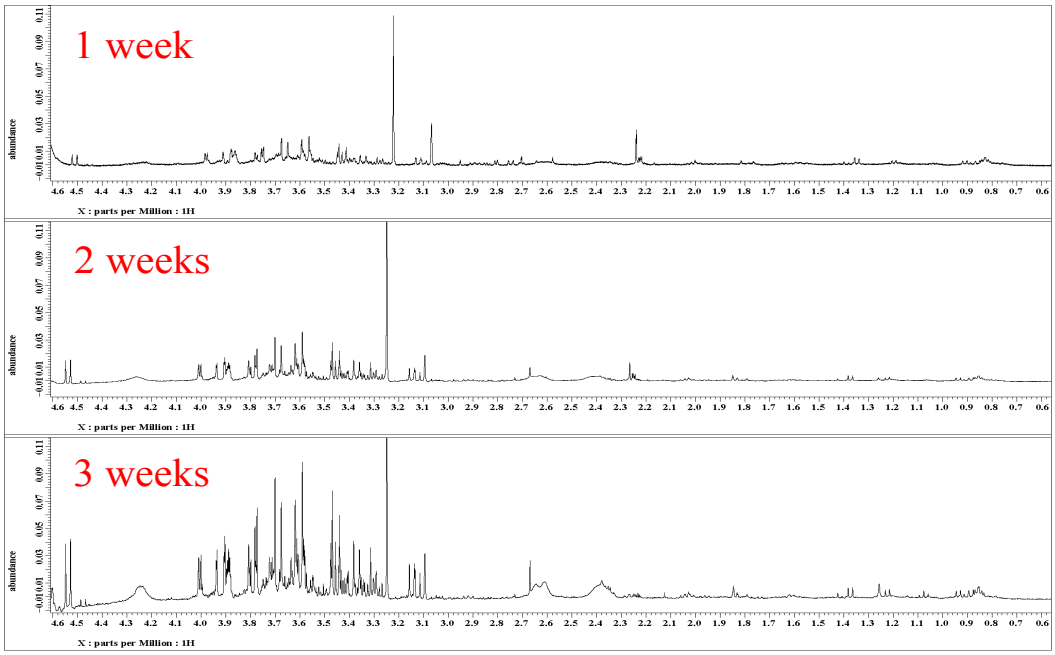

Figure B6 Overlay ^{1}H NMR spectra of 1-week, 2-week and 3-week old gold nanoparticle treated onion seedlings.

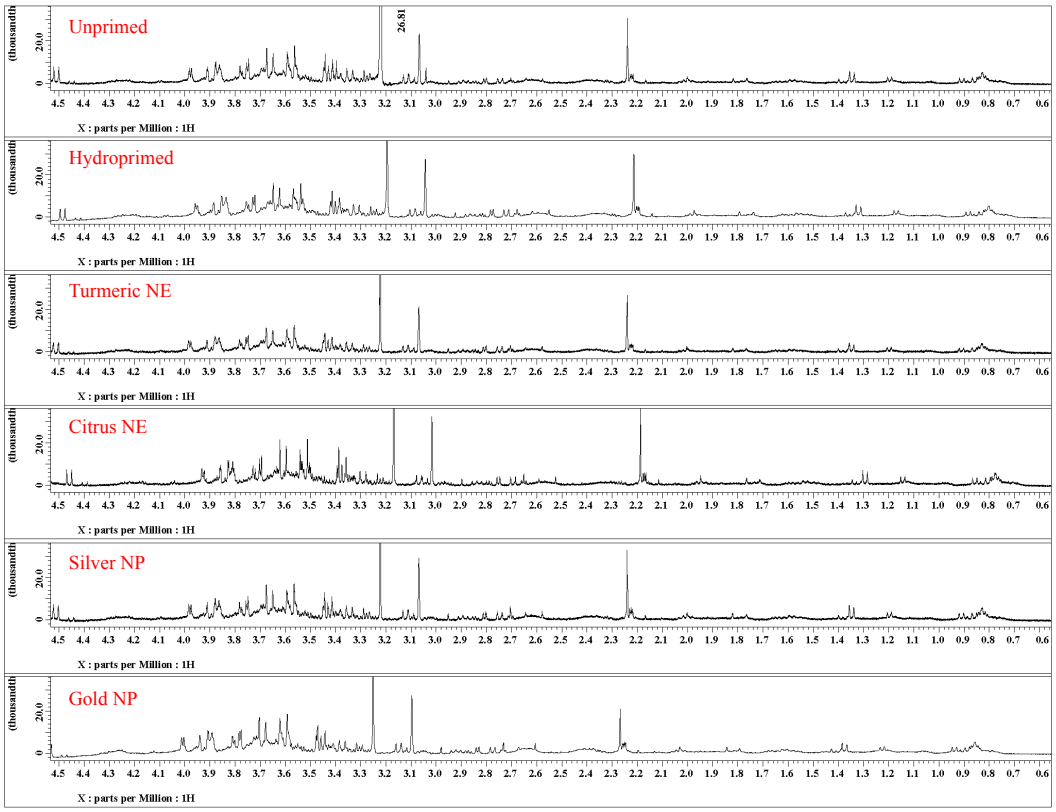

Figure B7 Overlay ^{1}H NMR spectra of one-week old onion seedlings extract obtained from different green nanoparticle treatments.

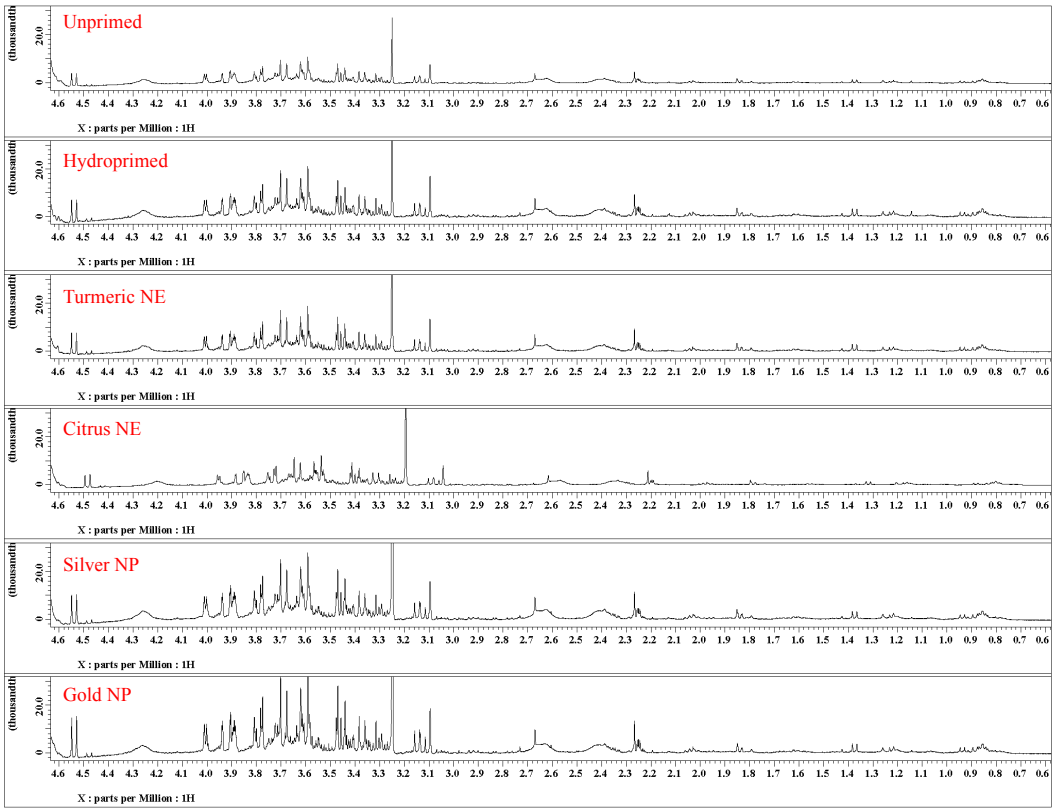

Figure B8 Overlay ^{1}H NMR spectra of two-weeks old onion seedlings extract obtained from different green nanoparticle treatments.

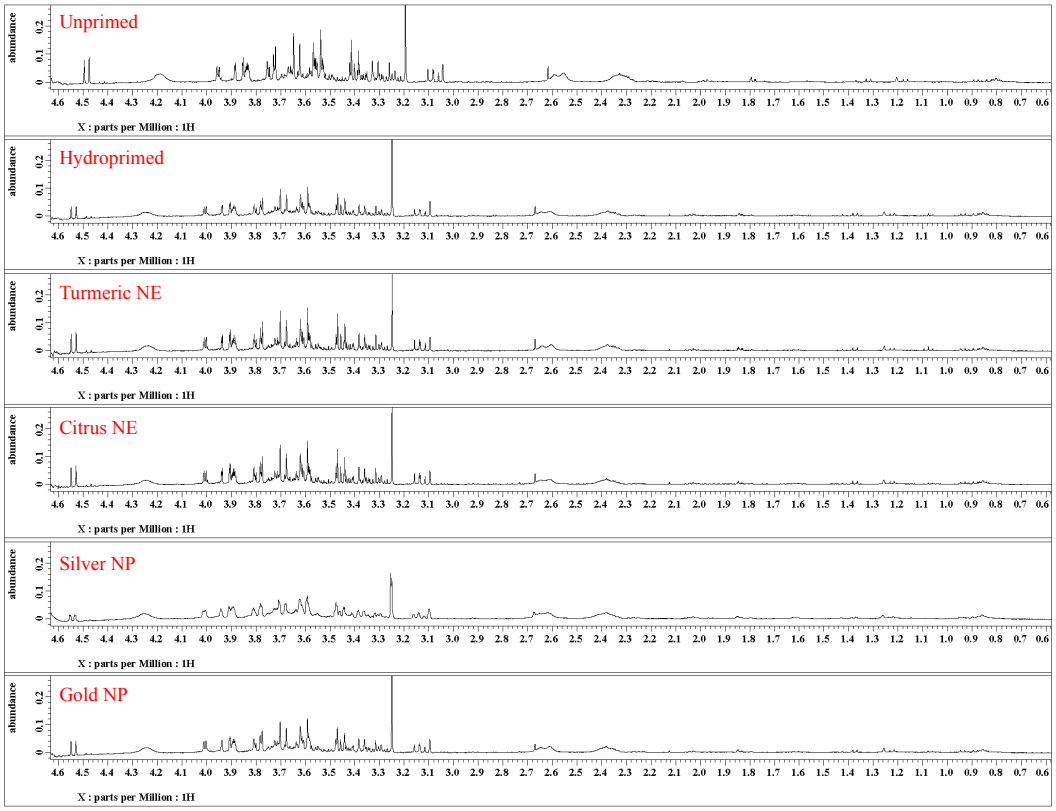

Figure B9 Overlay ^{1}H NMR spectra of three-weeks old onion seedlings extract obtained from different green nanoparticle treatments.

APPENDIX C

SUPPLEMENTARY FILE FOR THE CHAPTER 4

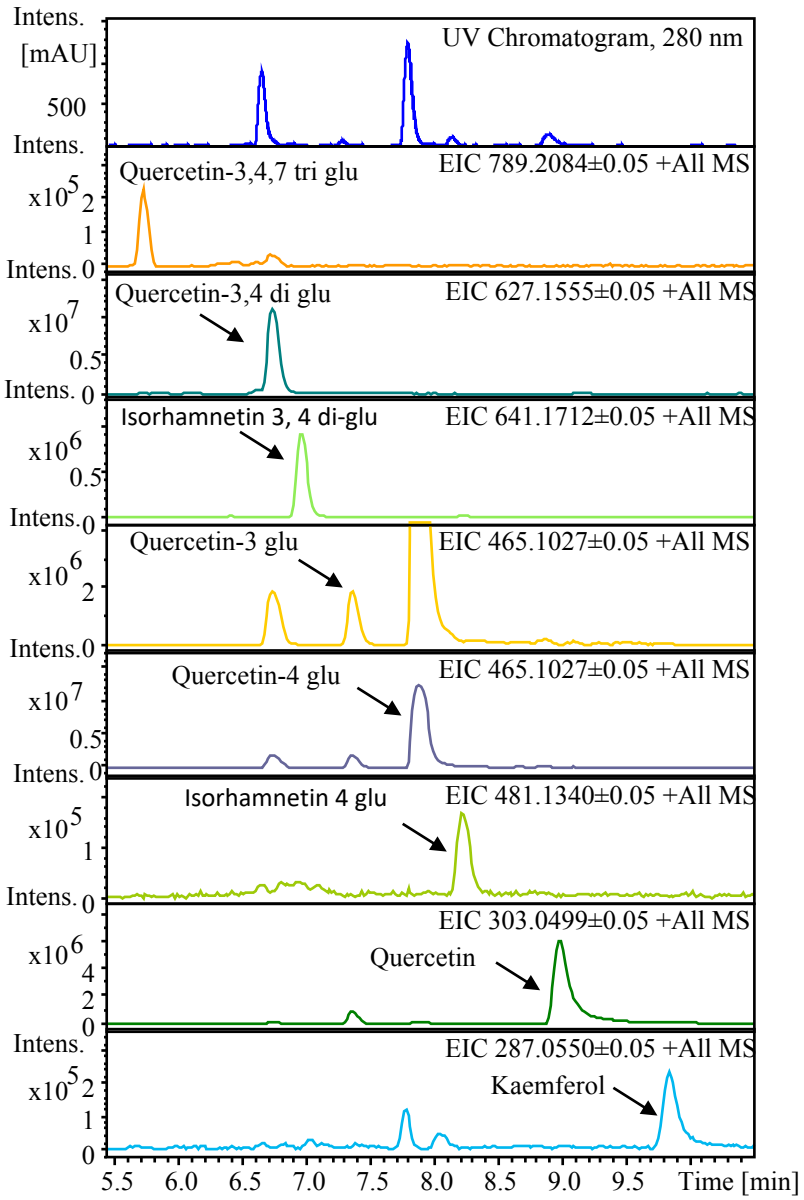

Figure C1 UHPLC-UV chromatogram and extracted ion chromatograms of onion flavonoids obtained from HR-ESI-QTOFMS analysis in positive ionization mode.

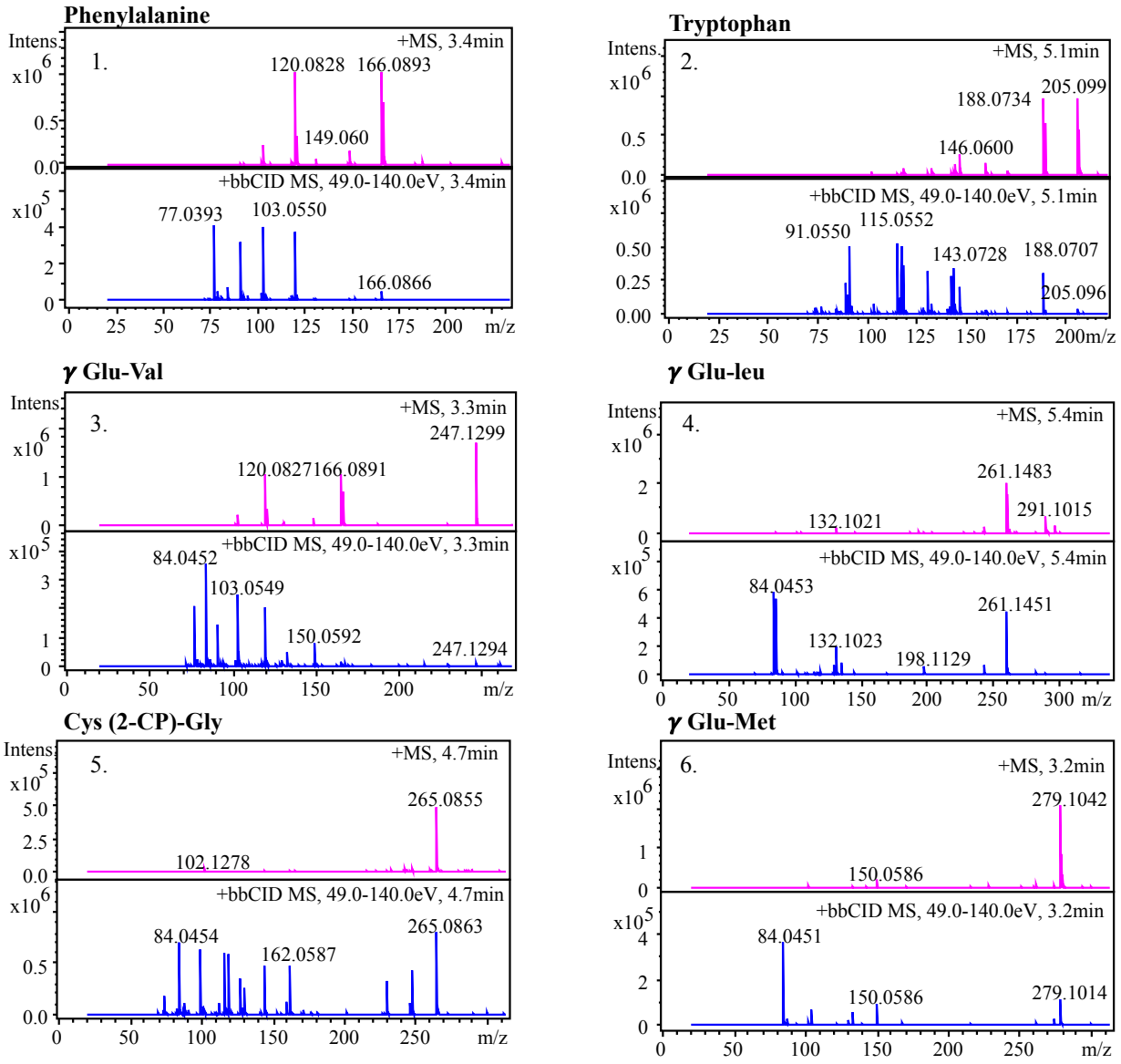

Figure C2 Identified metabolites in onion using HR-ESI-QTOFMS analysis in positive ionization mode.

Figure C2 continued

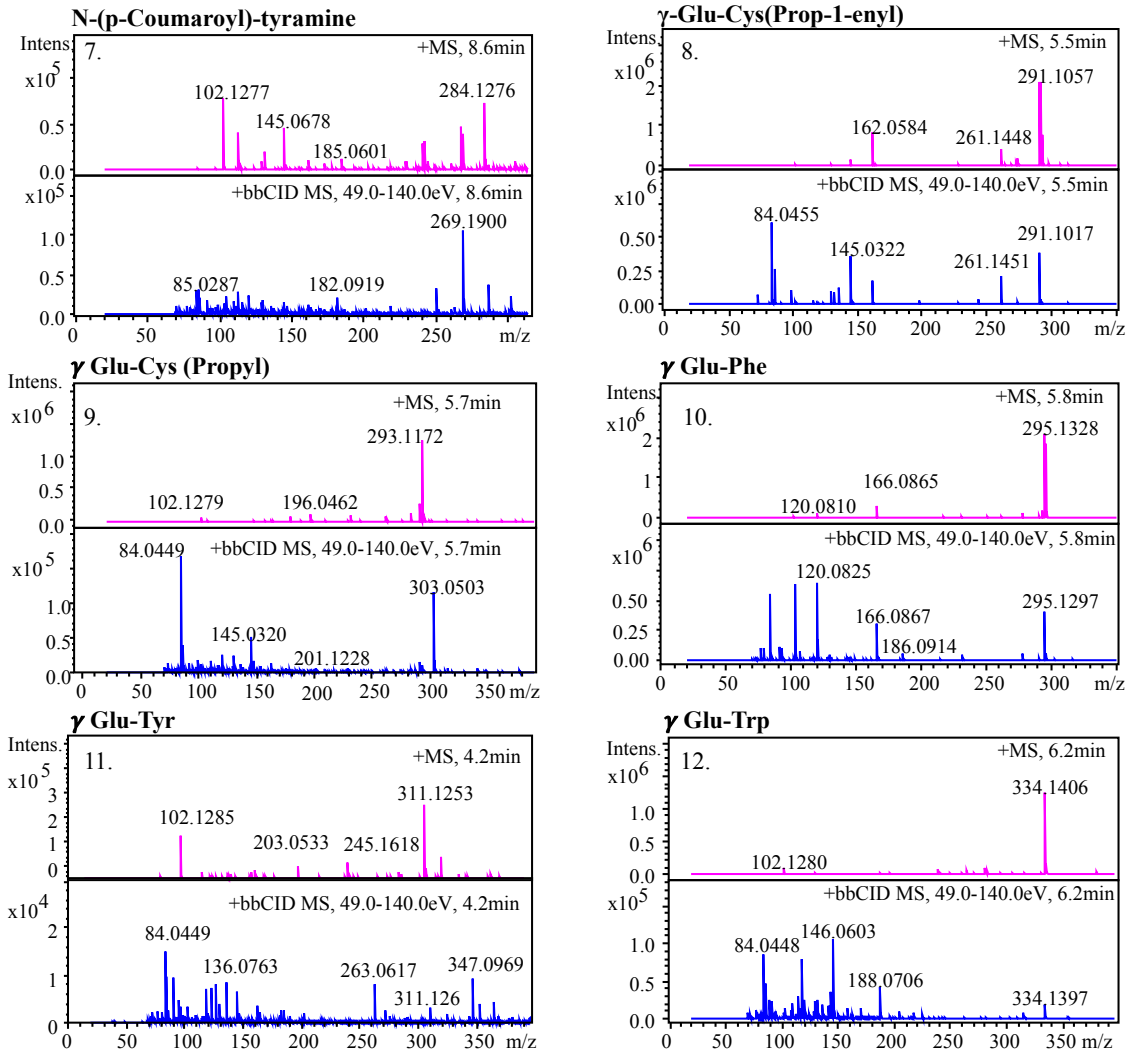

Figure C2 continued

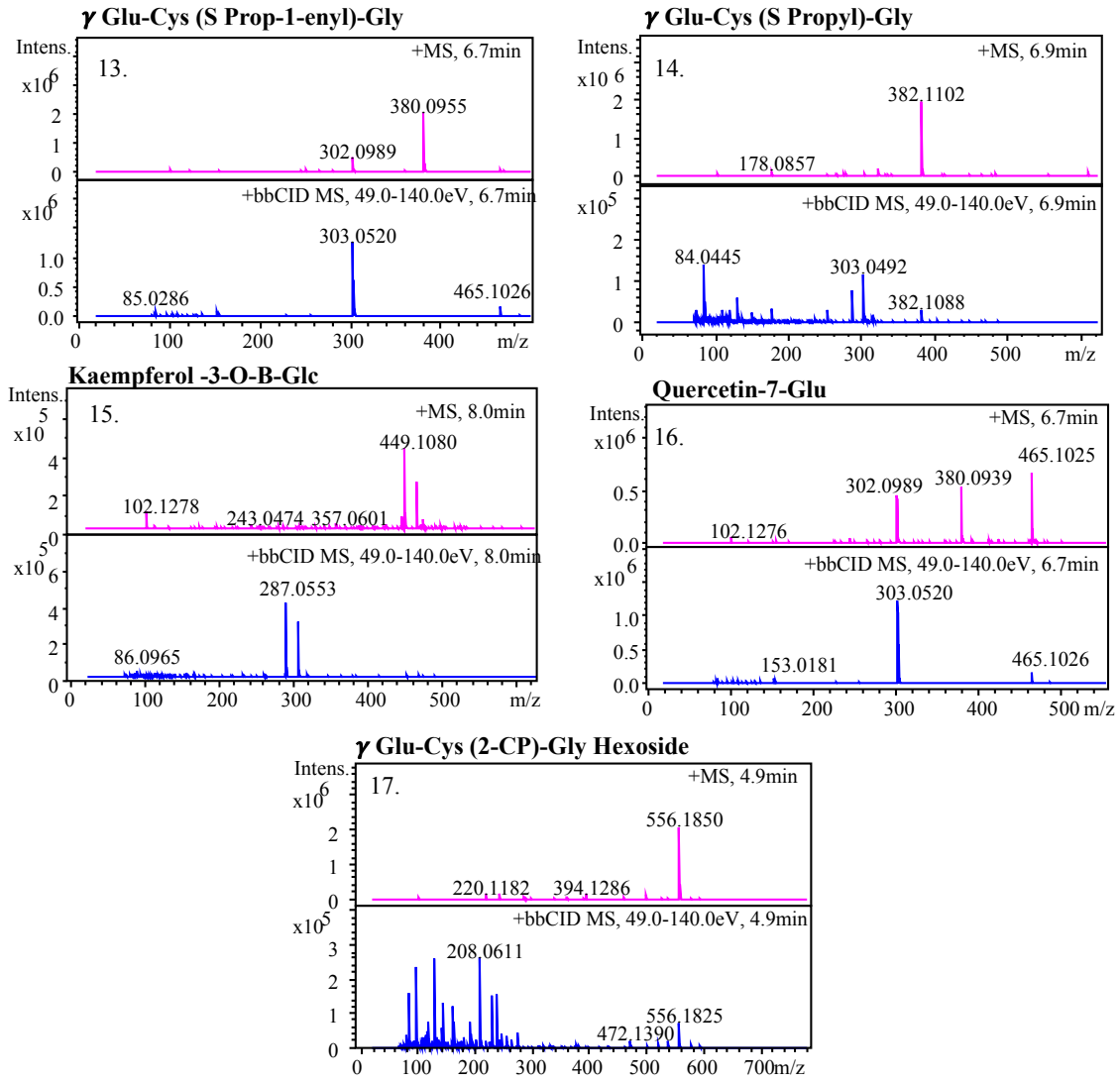

APPENDIX D

SUPPLEMENTARY FILE FOR THE CHAPTER 5

Figure D1 Map of Texas, USA with all the growing environment conditions. First year, watermelon plants were grown at four locations of Texas; Edinburg (26°18′15″N 98°9′50″W), Snook (30°29′25″N 96°28′11″W), Pecos (31°24′56″N 103°30′0″W), and Grapeland (31°29′30″N 95°28′49″W) in the grower's field during the summer season of 2016/17. Moreover, in order to validate the result of the first year, another field trial was conducted in Texas A&M AgriLife Research and Extension Center at Weslaco (26º15'N, 97º98'W) in 2017/18. TAMU: Texas A&M University, College Station where all the harvested samples were collected and analyzed.

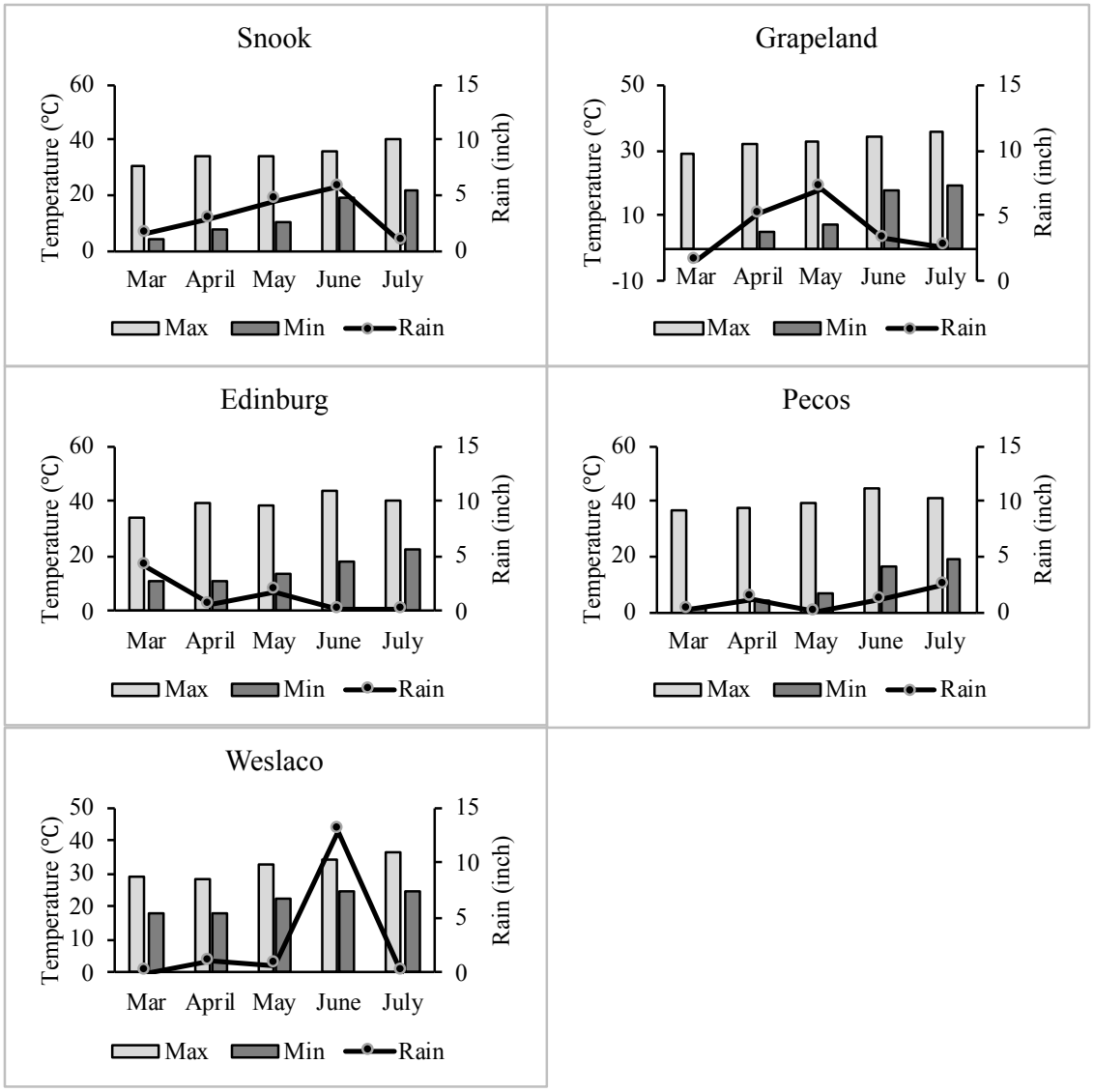

Figure D2 Rainfall (inches), maximum and minimum temperature (°C) of all the growing environments. During harvesting time (June) in Weslaco, there was heavy storm and rainfall that led to flooding in the watermelon fields so we were able to harvest only once.
Source: http://www.texmesonet.org/HistoricalData

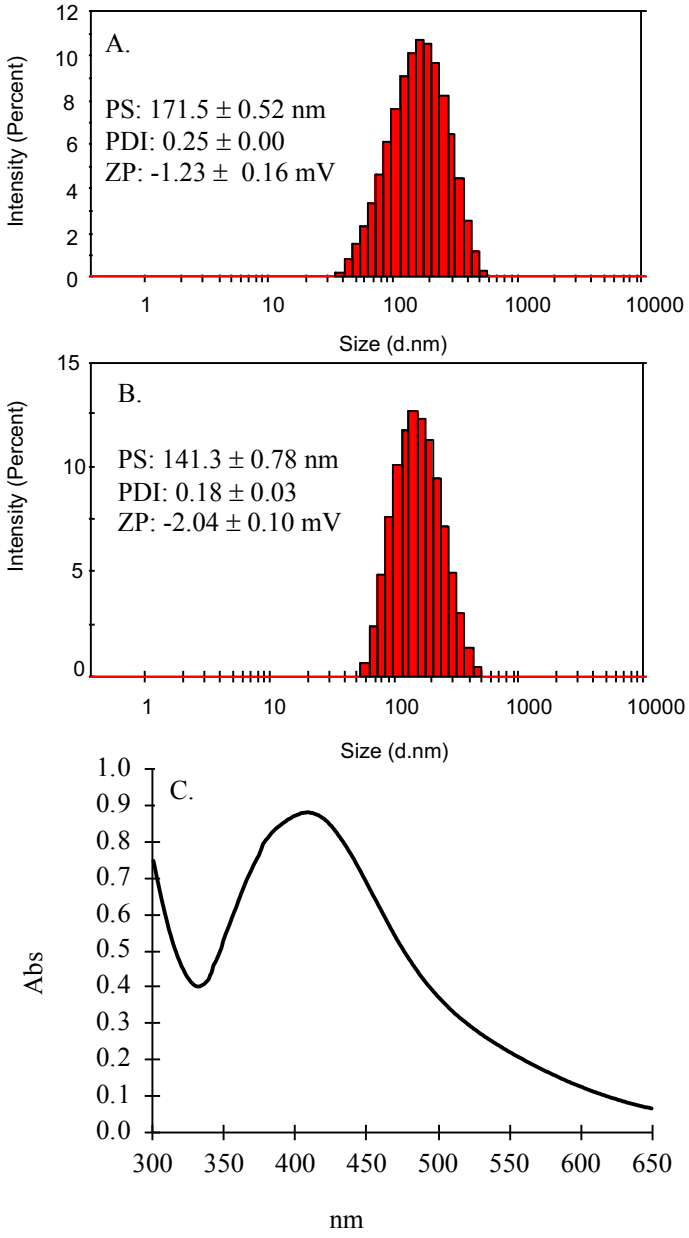

Figure D3 Histograms containing mean particle size (PS), polydispersity index (PDI) and the zeta potential (ZP) from photon correlation spectroscopy for (A) turmeric nanoemulsion (B) silver nanoparticles, (C) UV-Vis spectra of silver nanoparticles. A single, strong, and broad surface plasmon resonance (SPR) peak was observed for silver nanoparticles at 410 nm. Data represent mean ± SEM (n = 3).

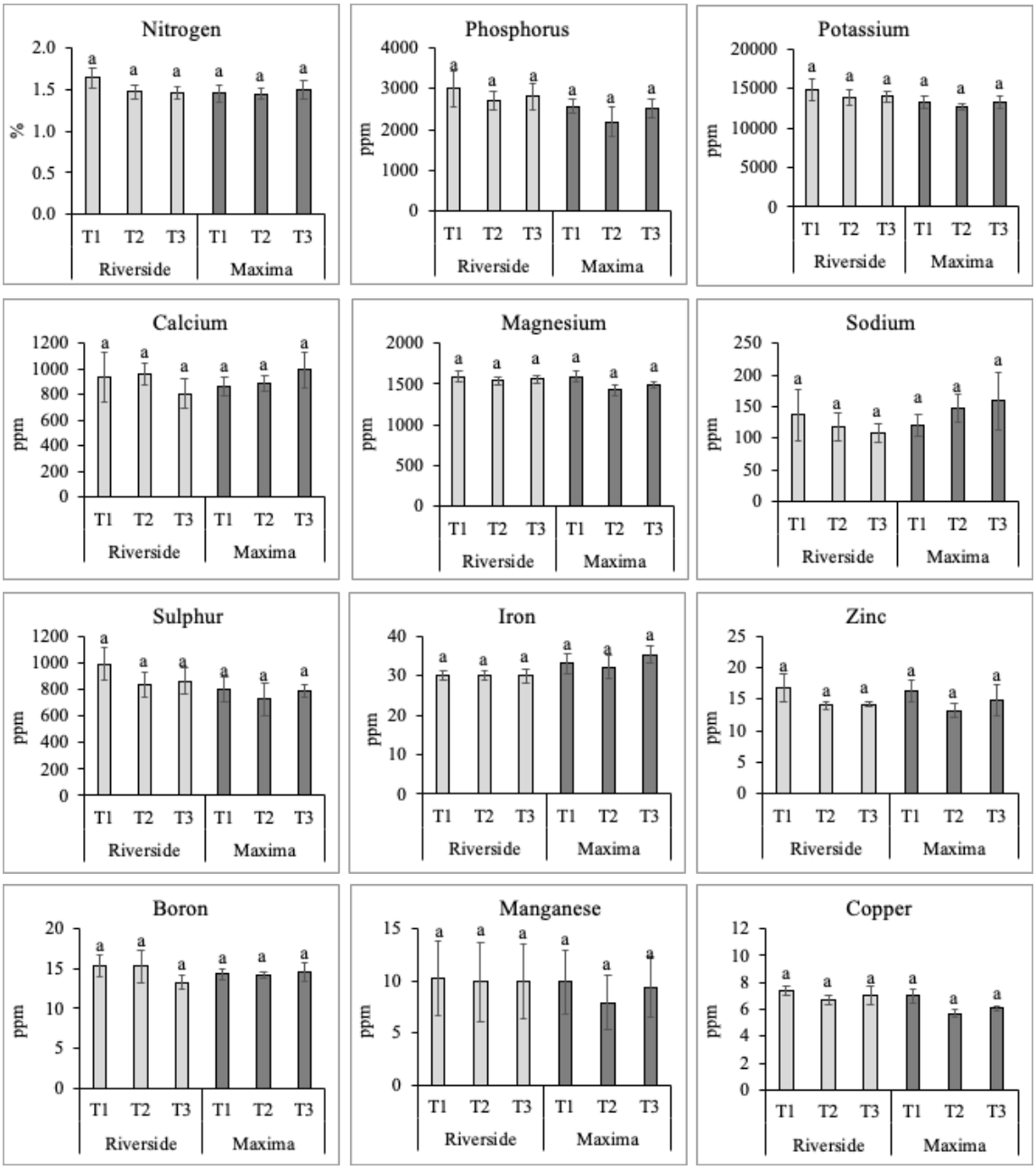

Figure D4 Elemental analysis of nanoparticle treated and untreated watermelon fruits. T1: unprimed, T2: turmeric oil nanoemulsion and T3: silver nanoparticle. Same letters above a bar indicate there was no significant difference at ($p \leq 0.05$) between the treatments. Data represent mean ± SEM (n = 15).

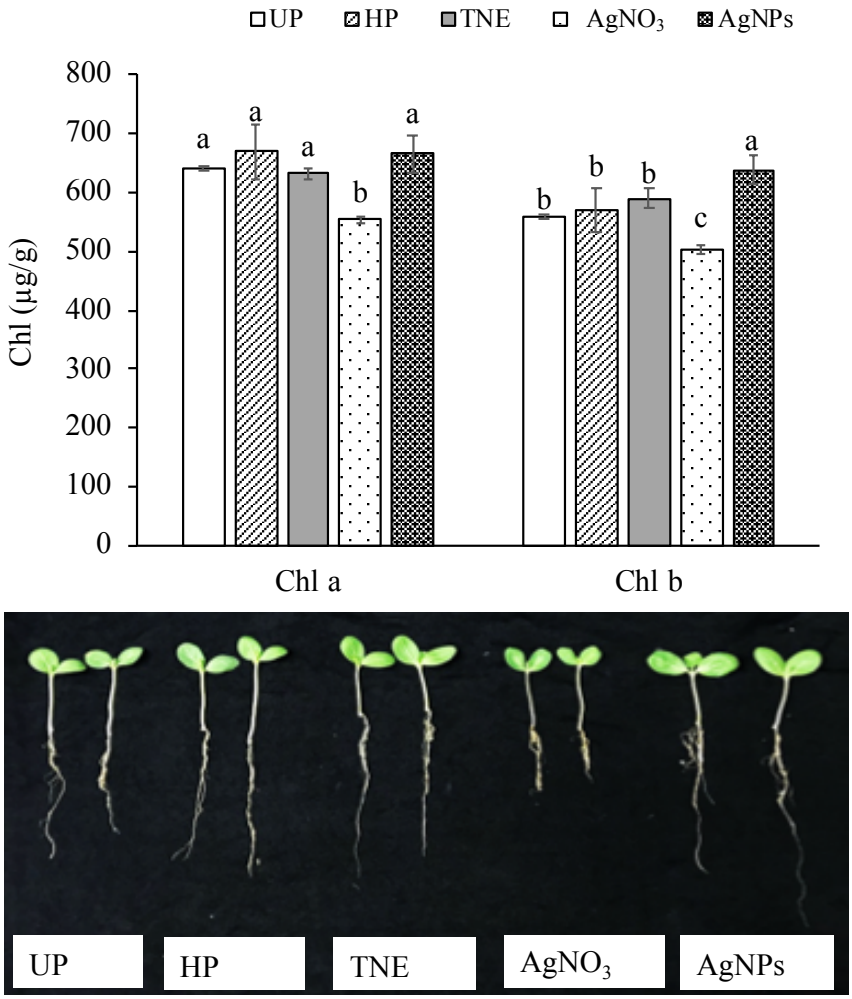

Figure D5 Influence of seed priming treatments on the levels of chlorophyll *a* and *b* of 14-day-old Riverside watermelon seedlings. Values are average ± standard error of three replicates. The post hoc test significant differences ($p \leq 0.05$) among different treatments are shown by different letters. UP, unprimed; HP, hydroprimed; TNE, turmeric oil nanoemulsion; $AgNO_3$; silver nitrate; and AgNPs, silver nanoparticles.

Table D1. Calculation of the average crystallite size of AgNPs synthesized with onion peel extracts, using Debye Scherer's equation.

S. No	2θ (degrees)	FWHM (β) (radians)	d-spacing (°A)	Miller indices	Crystallite size (nm)
1	38.19	0.118	2.354	111	47.5
2	44.38	0.156	2.04	200	39.7
3	64.49	0.186	1.443	220	33.3
4	77.45	0.277	1.231	311	25.3
				Average size (D) = 36.5	

Table D2. Soil analysis of growing environment conditions for both years.

		2017				2018
Analysis	Units	Grapeland	Edinburg	Pecos	Snook	Weslaco
pH	-	5.9	8.5	8	7.9	7.9
Conductivity	umho/cm	75	129	2240	892	367
Nitrate-N	ppm	8	4	207	124	23
Phosphorus	ppm	39	39	61	121	54
Potassium	ppm	30	203	1112	419	387
Calcium	ppm	314	4484	9974	4783	3594
Magnesium	ppm	34	150	676	156	307
Sulfur	ppm	3	879	23	3	51
Sodium	ppm	8	264	34	1	99

Soil samples were analyzed by the Soil, Water and Forage Testing Laboratory, Department of Soil and Crop Sciences, Texas A&M University, College Station, TX.

Table D3. Internalization of silver nanoparticles (μg/g FW) and turmeric nanoemulsion in treated Riverside (diploid) and Maxima (triploid) watermelon seeds. * value was below detection limit of INAA analysis (40 ng/g for Ag).

Cultivar	Nanopriming solution	Compound	Control seed	Treated seed (μg/g FW)
Riverside	Turmeric oil nanoemulsion	Ar-Turmerone	N.D.	2250.18 ± 67.65
	Silver nanoparticles	Silver	N.D.*	20.86 ± 7.21
Maxima	Turmeric oil nanoemulsion	Ar-Turmerone	N.D.	2422.46 ± 111.95
	Silver nanoparticles	Silver	N.D.*	15.63 ± 3.84

Control and silver nanoparticle (AgNPs) primed watermelon seeds were tested by instrumental neutron activation analysis to determine the silver concentration. Turmeric oil nanoemulsion treated watermelon seeds were tested by GC-MS analysis to determine the active compound. Ar-Turmerone is the major compound found in turmeric oil nanoemulsion. Values are means of three replicates ± SEM.

APPENDIX E

SUPPLEMENTARY FILE FOR THE CHAPTER 6

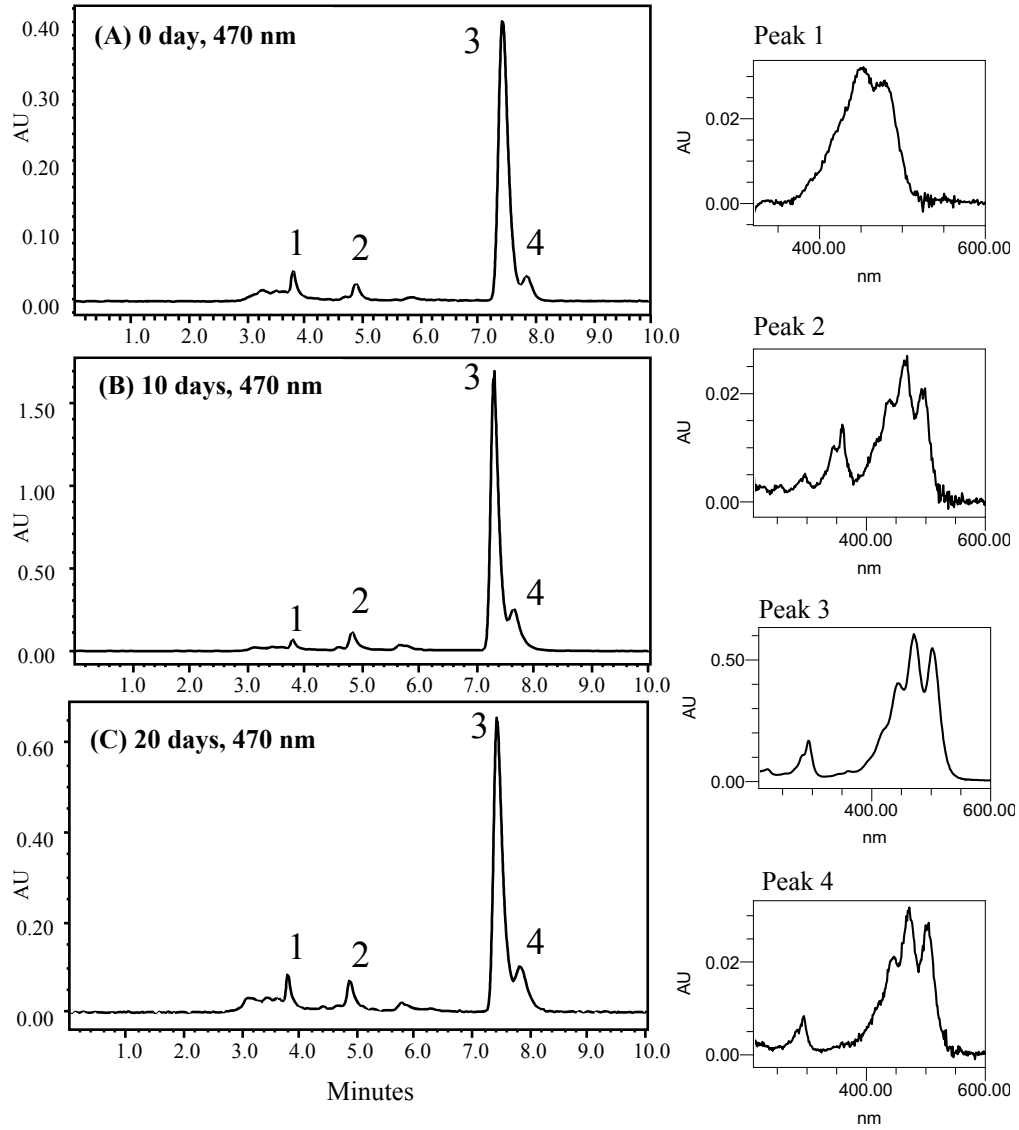

Figure E1 HPLC overlaid chromatograms for carotenoids of watermelons at (A) 0 d (B) 10 d and (C) 20 d after harvesting at 450 nm wavelength. Peaks represent (1) *β*-carotene (2) 13 cis-lycopene (3) trans-lycopene and (4) 5 cis lycopene. The level of trans and cis lycopenes were higher at 10 d storage as compared to 0 and 20 d of storage.

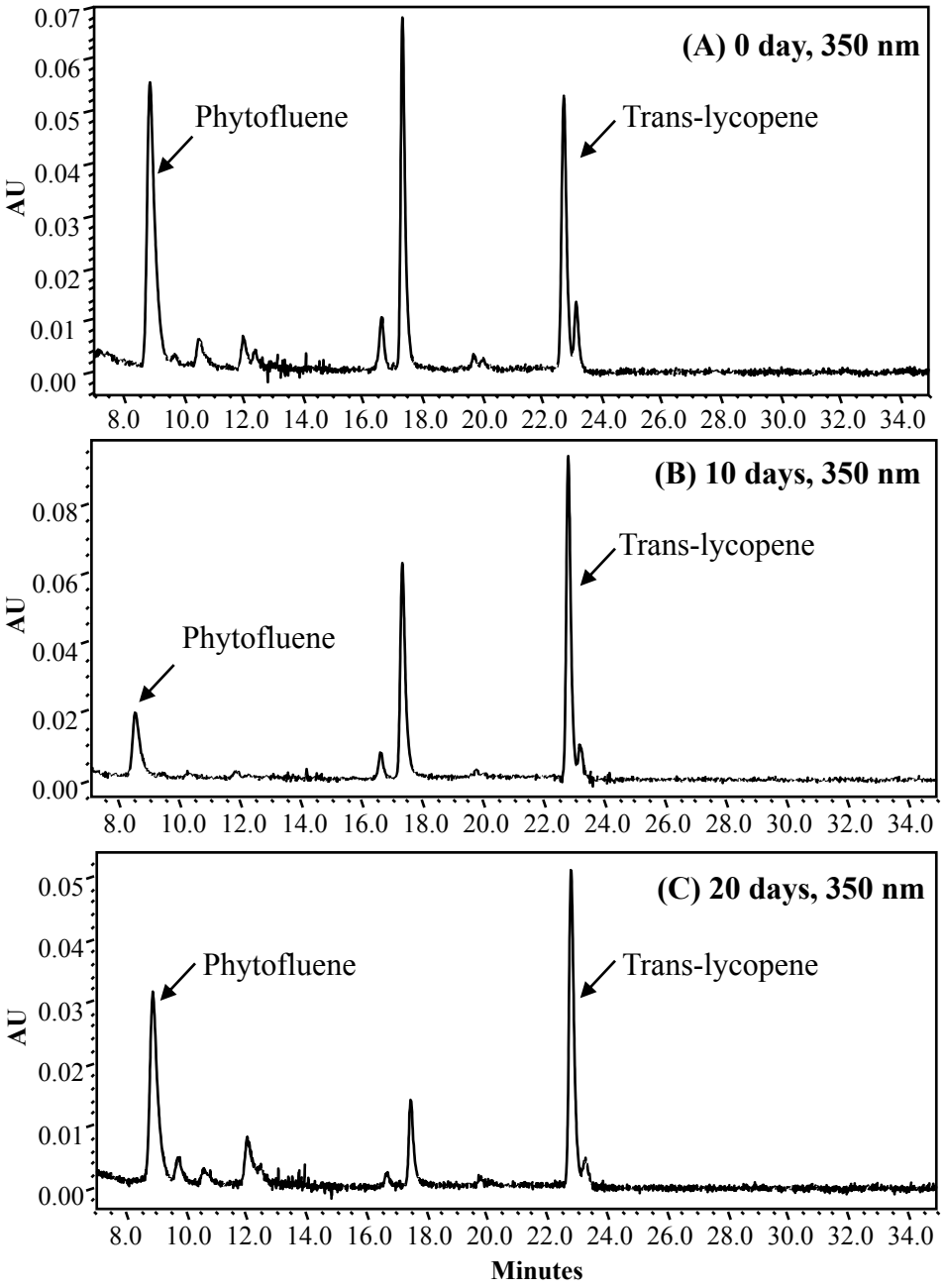

Figure E2 HPLC overlaid chromatograms for carotenoids of watermelons at (A) 0 d (B) 10 d and (C) 20 d after harvesting at 350 nm wavelength. Phytofluene content was reduced at 10 d of storage as compared to the 0 d watermelons. Inversely, trans-lycopene was found to be higher at 10 d of storage.

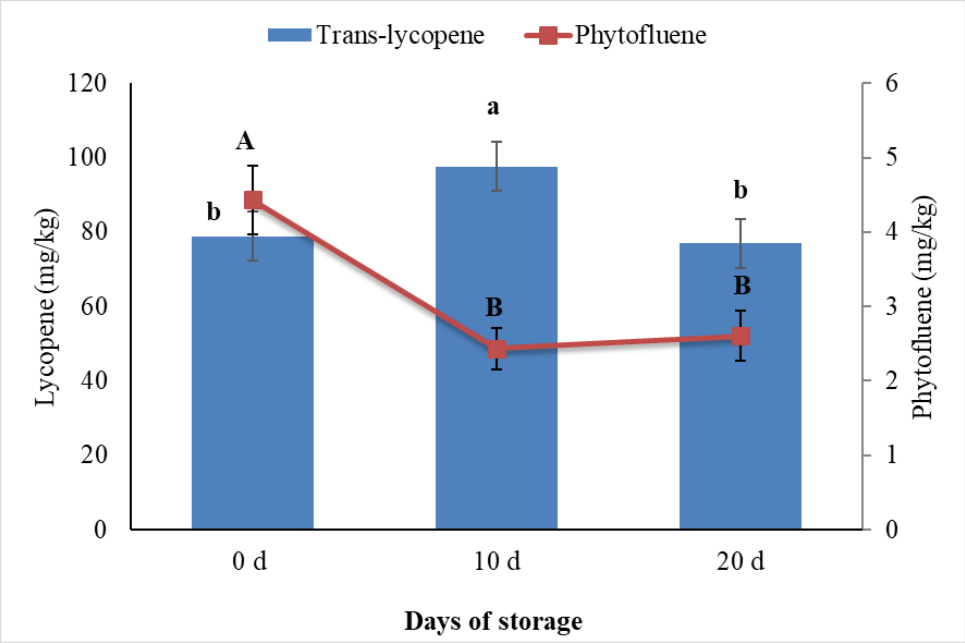

Figure E3 Phytofluene and trans-lycopene level in the watermelon samples at 0, 10, and 20 days of storage. Statistical analysis was performed using one-way ANOVA and means were compared using Student's t-test. Different letters indicate significant differences at $P < 0.05$.

Table E1. Color values for watermelon fruit, Maxima and Riverside with three treatments harvested from five different locations and stored for 0, 10, and 20 days. Statistical analysis was performed using two-way ANOVA and means were compared using Student's t-test. Different letters indicate significant differences at $*p < 0.05$, $**p < 0.01$.

Edinburg	Treatments	Maxima					Riverside				
		L*	**a***	**b***	**C***	h°	**L***	**a***	**b***	**C***	h°
Storage (S)	0	47.12a	40.39b	20.27b	26.71a	45.21c	46.98a	39.29b	19.37b	26.08b	43.82b
	10	44.82b	44.67a	21.17a	25.35b	49.44a	46.46a	44.47a	23.05a	27.41a	50.11a
	20	41.69c	43.73a	20.14b	24.75b	48.16b	46.18a	44.25a	22.45a	26.90a	49.63a
Treatments (T)	Control	42.60c	42.42a	20.09b	25.40ab	46.96a	47.52a	38.81b	19.80b	26.76a	43.60b
	TNE	44.39b	43.19a	20.33b	25.24b	47.75a	45.30b	44.69a	22.33a	26.56a	49.97a
	AgNPs	46.64a	43.17a	21.16a	26.17a	48.10a	46.80a	44.51a	22.73a	27.07a	49.99a
	(S x T)	NS	NS	NS	NS	NS	*	**	**	**	**
Grapeland											
Storage (S)	0	48.80a	41.07a	22.57b	28.77b	46.84b	47.84a	42.64a	22.51a	27.85a	48.24a
	10	46.42b	41.50a	23.46b	29.47b	47.73ab	47.78a	42.84a	22.74a	27.93a	48.51a
	20	49.64a	41.50a	25.19a	31.31a	48.70a	46.92a	42.41a	23.29a	28.80a	48.42a
Treatments (T)	Control	47.49b	41.42a	22.92b	28.97b	47.46a	47.11a	42.13a	22.32a	27.86a	47.67a
	TNE	47.82ab	41.74a	23.42b	29.26b	47.86a	47.45a	42.63a	23.00a	28.39a	48.48a
	AgNPs	49.55a	40.91a	24.88a	31.31a	47.94a	47.98a	42.13a	23.33a	28.34a	49.02a
	(S x T)	NS	NS	*	*	NS	NS	NS	NS	NS	NS
Pecos											
Storage (S)	0	43.85a	44.52a	20.35b	24.55b	48.96a	49.02a	42.80b	21.24c	26.41b	47.79b
	10	42.21b	44.08a	20.42b	24.84b	48.59a	48.65a	44.71a	22.57b	27.52ab	50.10a
	20	42.44b	44.59a	21.29a	25.52a	49.43a	47.54a	42.83b	23.59a	28.82a	48.93ab
Treatments (T)	Control	42.06b	44.33a	20.19b	24.47b	48.72b	49.11a	43.23a	22.54a	28.27a	48.77a
	TNE	42.80ab	43.97a	20.59b	25.08b	48.57b	48.69a	43.28a	22.36a	27.32a	48.75a
	AgNPs	43.64a	44.89a	21.28a	25.35a	49.69a	47.41a	43.83a	22.51a	27.16a	49.30a
	(S x T)	NS	*	NS	NS	NS	NS	NS	NS	NS	NS
Snook											
Storage (S)	0	47.03a	43.48a	20.97a	25.77a	48.29a	53.99a	38.35b	21.10a	28.94a	43.79b
	10	44.42a	43.34a	20.69a	25.51a	48.04a	46.76b	42.14a	21.08a	26.08b	47.13a
	20	44.92a	43.64a	20.91a	25.60a	48.41a	46.28b	42.52a	21.24a	26.52a	47.56a
Treatments (T)	Control	46.22a	42.60b	20.49a	25.71a	47.29b	49.71a	40.36a	20.73a	26.84a	45.40a
	TNE	44.33a	44.10a	20.97a	25.42a	48.84a	48.88a	41.26a	20.97a	26.95a	46.31a
	AgNPs	45.81a	43.76a	21.11a	25.74a	48.60a	48.43a	41.38	21.73a	27.75a	46.77a
	(S x T)	NS	NS	NS	NS	NS	NS	*	NS	NS	*
Weslaco											
Storage (S)	0	43.49a	45.60a	21.36b	50.38a	25.06b	50.08a	43.86b	21.14a	48.70b	25.75ab
	10	41.89b	45.15a	20.51b	49.62a	24.46b	45.00b	45.58a	21.48a	50.40a	25.23b
	20	44.07a	44.32a	23.07a	50.05a	27.52a	44.72b	44.40b	21.97a	49.19b	26.37a
Treatments (T)	Control	42.93a	45.37a	21.42a	50.25a	25.31a	47.24a	44.24a	21.81a	48.98a	26.31a
	TNE	42.71a	45.06a	21.72a	50.07a	25.71a	46.03a	44.85a	21.33a	49.68a	25.43b
	AgNPs	43.81a	44.65a	21.80a	49.72a	26.02a	46.52a	44.75a	21.45a	49.63a	25.60b
	(S x T)	NS	NS	NS	NS	NS	NS	NS	*	NS	NS

APPENDIX F

SUPPLEMENTARY FILE FOR THE CHAPTER 7

Table F1. Volatile compounds quantified (μg/kg) in watermelons harvested from Snook. Values are means ± SE.

RT	Compounds	Snook					
		Riverside			Maxima		
		0 day	10 day	20 day	0 day	10 day	20 day
2.30	Ethanol	-	-	415.1±35.4	-	-	395.53±15.3
3.64	Hexanal	-	-	-	-	-	-
5.04	D-limonene	-	-	-	-	-	-
5.48	β-limonene	-	-	-	-	-	-
5.50	Pyridine	-	-	-	-	-	-
5.71	2-Pentylfuran	1066.77±103.88	364.5±62.44	1011.78±38.54	-	446.21±87.06	258.68±4.98
5.80	(E)-2-Hexenal	-	-	-	-	-	-
6.54	Cyclodecane	-	-	-	-	-	-
6.58	Acetoin	-	-	-	174.83±14.56	-	-
6.80	trans-2-(2-Pentenyl)furan	305.4±10.1	88.58±2.55	142.26±11.7	-	68.32±14.6	196.38±1.66
6.99	Octanal	-	-	-	-	-	-
7.57	6-Methyl-5-hepten-2-one	409.35±36.49	646.5±91.64	234.43±33.26	433.43±32.47	805.46±41.65	19.08±4.91
7.84	(E)-2-Heptenal	-	-	-	-	-	-
8.53	1 Hexanol	-	-	-	-	-	-
8.60	Nonanal	1537.5±135.17	535.48±30.28	1716.27±134.03	-	127.31±20.26	16.83±1.45
9.07	Perilline	-	-	-	28.6±0	45.68±5.26	-
9.58	Acetic acid	-	-	-	2031.16±42.46	-	-
9.79	1-Octen-3-ol	-	-	-	-	-	-
9.85	(E)-2-Octenal	-	-	-	-	-	-
10.00	(E)-4-Nonenal	22.35±4.06	140.85±1	-	-	-	-
10.26	(Z)-6-Nonenal	3129.3±337.87	192.9±13.41	1667.43±126.25	-	-	44.04±4.03
10.42	(E)-6-Nonenal	10.58±0.1	20.38±0	-	-	-	-
10.70	6-Methyl-5-hepten-2-ol	-	-	-	51.28±6.63	-	-
10.76	(Z)-2-Nonenal	71.29±6.13	65.63±1.3	98.36±3.42	-	43.94±9.2	30.9±1.25
11.03	Benzaldehyde	-	-	-	-	56.79±6.6	-
11.20	Methyl nonanoate	-	-	-	-	-	-
11.23	Decanal	-	-	-	-	-	-
11.35	(E)-2-Nonenal	1523.95±248.15	1954.52±49.52	2372.63±55.91	143.52±8.55	1400.52±286.92	1502.45±45.24
11.90	Pinocarvone	-					
11.92	1-Octanol	18.3±3.14	59.45±6.15	51.43±5.07	-	93.84±7.54	161.29±5.42

Table F1. continued

RT	Compounds	Snook					
		Riverside			Maxima		
		0 day	10 day	20 day	0 day	10 day	20 day
12.33	(E,Z)-2,6-Nonadienal	1474.81±25.59	1676.77±69.48	1656.69±45.85	-	856.3±57.81	518.34±70.79
12.33	Ethyl-3-nonenoate	-	-	-	145.98±5.97	-	-
12.34	6-Methyl-3,5-heptadien-2-one	-	-	-	-	-	-
12.72	(Z)-3-Nonenyl acetate	-	-	-	361.07±23.98	-	-
12.89	β-cyclocitral	-	28.6±1.94	21.27±0.44	-	44.25±1.33	38.88±3.92
12.98	(Z)-5-Octen-1-ol	15.99±0.21	19.34±2.59	18.27±0.53	-	-	9.7±0.57
13.34	(E)-2-Decenal	-	-	-	-	-	-
13.35	cis-Pinocarveol	-	-	-	-	-	-
13.48	Methyl 6-nonynoate	12.66±0.33	7.13±0.88	6.17±0.35	84.05±8.12	-	-
13.77	4,5-Difluoroctane	-	-	174.91±5.87	565.29±19.76	-	199.56±0.1
13.88	1-Nonanol	500.38±7.73	1780.43±144	1074.94±92.01	1604.81±52.44	-	1731.72±62.73
14.10	pentadecanal	57.91±6.26	140.38±1.45	94.6±6.39	-	99.68±32.27	67.46±5.56
14.32	(Z)-3-Nonen-1-ol	1064.32±92.5	4516.26±68.33	1464.7±225.29	5473.49±248.29	3948.79±56.92	5589.98±614.03
14.44	(E,E)-2,4-Nonadienal	86.01±8.08	217.28±0.32	85.9±4.57	-	-	191.43±12.74
14.68	(Z)-6-Nonen-1-ol	-	-	-	-	2367.36±1334.87	-
14.83	(E)-2-Nonen-1-ol	-	-	-	342.51±7.09	-	-
14.92	(E)-6-Nonen-1-ol	750.81±75.54	2054.53±73.92	1013.99±93.25	803.13±126.46	1973.58±280.93	582.97±63.33
15.03	(E)-Citral	140.03±9.74	280.98±27.37	156.76±4.45	-	229.77±15.42	144.62±7.21
15.52	(Z,Z)-3,6-Nonadien-1-ol	1418.37±85.6	5052.47±196.95	1940.36±173.11	3881.69±166.35	4007.57±287.77	3491.04±113.81
15.82	(E,Z)-2,6-Nonadien-1-ol	107.43±13.23	291.68±39.08	162.35±19.67	-	614.93±31.93	292.94±51.38
15.85	L-Perrillaldehyde	-	-	-	-	607.23±129.53	-
15.91	Methoxy-phenyl-oxime	375.34±8.15	258.54±17.83	113.04±1.41	-	-	144.32±2.89
16.35	(E,E)-2,4-Decadienal	-	-	-	-	-	-
16.36	(E)-Geraniol	-	-	-	-	-	-
16.74	cis-Geranylacetone	-	-	-	-	-	-
16.95	Myrtenol	-	-	-	-	-	-
17.07	α-Ionone	-	-	-	-	-	-
18.18	Benzene ethanol	-	-	-	136.48±49.53	48.58±20.25	-
18.30	Tetradecanal	-	-	-	-	-	-
18.54	β-Ionone	21.76±2.16	80.01±8.93	87.7±4.49	93.15±12.77	134.9±5.77	120.08±7.61
18.66	cis-Jasmone	-	-	-	-	-	-
18.77	Benzothiazole	16.17±0.54	23.97±1.57	13.41±0.6	-	-	15.66±2.04
18.97	6,10 Dimethyl-5,9 undecadien-2-ol	-	-	-	128.58±8.39	-	-
19.43	β-Ionone-5,6-epoxide	-	-	7.35±0.2	-	-	25.66±3.47
19.89	2 Hexenoic acid	-	-	-	-	-	-
19.97	γ-Nonalactone	-	-	-	-	-	-

Table F1. continued

RT	Compounds	Snook					
		Riverside			Maxima		
20.07	Pentadecanal	26.97±2.95	29.52±2.75	34.73±5.78	36.91±6.21	263.66±21.4	5.52±0.15
21.23	Cuminol	14.42±0.5	12.99±0.35	12.31±0.18	-	-	13.35±0.46
21.35	Octanoic acid	-	-	-	-	-	-
21.59	(E,E)-Pseudoionone	7.56±0.5	19.45±1.11	11.69±1.05	-	35.38±3.27	10.85±1.52
21.98	Nonanoic acid	15.36±1.24	34.07±4.94	30.37±4.32	-	22.27±1.38	22.37±1.12
22.35	Methyl hexadecanoate	-	-	-	-	-	-
22.62	Ethyl pentadecanoate	-	-	-	176.81±4.17	-	-
22.63	Ethyl hexadecanoate	19.36±1.76	53.21±3.07	-	-	102.07±4.32	58.34±0.35
22.71	3-Nonenoic acid	-	-	18.13±1.94	1108.05±19.85	-	59.27±3.64
23.18	Dihydroactinidiolide	-	-	-	-	-	-
23.35	Farnesyl acetone	15.16±3.93	78.05±6.8	55.09±5.48	-	87.44±6.97	58.64±7.63
23.80	Methyl 9-octadecenoate	-	-	-	-	24.51±3.88	-
24.00	2 Decenoic acid	-	-	-	-	-	-
24.03	Methyl octadecanoate	-	-	-	-	-	-
24.14	Ethyl 9-octadecenoate	-	44.95±8.26	23.05±3.17	133.02±21.09	58.2±5.65	146.13±11.06
24.19	Methyl octadecadienoate	-	-	-	-	-	-

Table F2. Volatile compounds quantified (μg/kg) in watermelons harvested from Pecos. Values are means ± SE.

RT	Compounds	Pecos					
		Riverside			Maxima		
		0 day	10 day	20 day	0 day	10 day	20 day
2.30	Ethanol	338.54±15.81	110.33±9.35	308.87±28.61	-	208.11±11.94	350.84±16.94
3.64	Hexanal						
5.04	D-limonene	-	-	-	-	-	-
5.48	β-limonene	-	-	-	-	-	-
5.50	Pyridine	-	-	-	-	-	-
5.71	2-Pentylfuran	259.87±28.26	264.87±39.29	297.65±17.84	-	73.97±0	-
5.80	(E)-2-Hexenal	-	-	-	-	-	-
6.54	Cyclodecane	-	-	-	-	-	-
6.58	Acetoin	-	-	-	-	-	-
6.80	trans-2-(2-Pentenyl)furan	126.43±16.27	135.42±13.46	54.1±6.55	-	-	-
6.99	Octanal	-	-	-	-	-	-
7.57	6-Methyl-5-hepten-2-one	310.56±23.19	340.19±11.83	317.08±47.66	1084.71±98.19	443.82±93.01	483.27±38.41
7.84	(E)-2-Heptenal	-	-	-	-	-	-
8.53	1 Hexanol	-	-	-	-	-	-
8.60	Nonanal	2046.26±106.01	1761.8±230.3	1649.21±369.14	918.9±22	579.52±12.9	867.47±65.09
9.07	Perilline	-	-	-	-	27.18±1	-
9.58	Acetic acid	-	-	-	-	151.42±0	-
9.79	1-Octen-3-ol	-	-	-	-	-	-
9.85	(E)-2-Octenal	-	-	-	-	-	-
10.00	(E)-4-Nonenal	-	-	-	-	-	-
10.26	(Z)-6-Nonenal	1469.87±219.58	1530.7±286.01	1047.21±271.65	367.25±22.68	150.01±19.52	398.67±58.1
10.42	(E)-6-Nonenal	-	-	-	-	-	-
10.70	6-Methyl-5-hepten-2-ol	-	-	-	-	397.45±0	-
10.76	(Z)-2-Nonenal	10.01±0.56	96.54±3.96	108.54±2.87	124.6±14.08	66.03±9.8	92.91±6.73
11.03	Benzaldehyde	-	-	-	-	-	36.86±0.77
11.20	Methyl nonanoate	-	-	-	-	-	-
11.23	Decanal	-	-	-	-	-	-
11.35	(E)-2-Nonenal	2100.56±161.82	2783.83±191.01	3049.62±89.52	2763.07±178.32	3011.94±1.9	2515.1±48.23
11.90	Pinocarvone	-	-	-	-	-	-
11.92	1-Octanol	26.57±1.26	28.71±2.74	66.22±6.08	53.67±4.91	81.71±6.66	102.34±3.88
12.33	(E,Z)-2,6-Nonadienal	1072.57±139.72	1503.53±57.22	1409.07±38.95	1452.22±86.26	1371.82±18.78	1258.27±25.26
12.33	Ethyl-3-nonenoate	-	-	-	-	-	-
12.34	6-Methyl-3,5-heptadien-2-one	-	-	-	-	-	-
12.72	(Z)-3-Nonenyl acetate	-	-	-	-	-	-
12.89	β-cyclocitral	-	18.39±3.21	47.69±3.58	48.38±8.22	45.53±1.54	77.12±7.42

Table F2. continued

RT	Compounds	Pecos					
		Riverside			Maxima		
		0 day	10 day	20 day	0 day	10 day	20 day
12.98	(Z)-5-Octen-1-ol	11.78±0.98	18.65±0.37	19.88±0.76	12.11±2.13	18.88±0.85	35.17±3.85
13.34	(E)-2-Decenal	-	-	-	-	-	-
13.35	cis-Pinocarveol	-	-	-	14.12±2.29	-	-
13.48	Methyl 6-nonynoate	-	9.45±2.38	5.85±1.57	-	13.73±0	-
13.77	4,5-Difluoroctane	136.04±12.11	176.96±8.32	194.48±8.39	176.36±5.26	265.9±20.38	308.29±25.86
13.88	1-Nonanol	723.08±7.52	599.05±53.99	1669.01±8.85	1211.31±45.13	1634.96±68.24	1552.8±156.28
14.10	pentadecanal	75.18±8.38	112.33±4.41	90.46±11.07	253.74±25.34	172.5±9.73	162.17±6.26
14.32	(Z)-3-Nonen-1-ol	1170.97±34.37	1645.13±138.97	3185.33±243.88	2860.18±147.63	4265.6±104.8	4584.84±345.49
14.44	(E,E)-2,4-Nonadienal	-	-	-	-	-	-
14.68	(Z)-6-Nonen-1-ol	-	-	-	-	-	-
14.83	(E)-2-Nonen-1-ol	-	-	-	155.86±12.45	493.71±12.07	298.21±10.73
14.92	(E)-6-Nonen-1-ol	427.8±30.59	406.14±32.5	989.75±103.76	599.15±39.45	739.82±49.75	758.27±80.75
15.03	(E)-Citral	152.39±12.95	206.7±4.54	169.04±19.32	382.13±32.56	242.81±36.53	286.32±12.88
15.52	(Z,Z)-3,6-Nonadien-1-ol	792.82±66.08	1262.78±138.58	1973.11±107.02	1839.6±47.75	2613.86±71.21	2890.19±133.46
15.82	(E,Z)-2,6-Nonadien-1-ol	19.39±3.26	163.97±34.92	191.21±23.61	126.6±9.09	241.12±42.55	263.62±31.35
15.85	L-Perrillaldehyde	-	-	-	-	-	-
15.91	Methoxy-phenyl-oxime	106.88±8.11	108.29±8.04	119.05±3.88	140.74±10.34	151.16±15.29	188.49±5.08
16.35	(E,E)-2,4-Decadienal	-	-	-	11.64±3.09	-	-
16.36	(E)-Geraniol	-	-	-	-	65.3±1	-
16.74	cis-Geranylacetone	-	-	-	-	-	-
16.95	Myrtenol	-	-	-	-	-	-
17.07	α-Ionone	-	-	-	-	-	-
17.20	trans-Geranylacetone	290.2±21.84	601.05±50.15	899.01±87.95	1027.98±29.89	1241.35±43.59	1398.88±60.67
17.59	Benzyl alcohol	-	-	-	27.55±1.36	90.63±4.17	108.12±21.86
17.76	Isolimonene	-	-	-	-	-	-
17.84	Hexanoic acid	-	-	-	-	-	-
18.18	Benzene ethanol	-	-	6.11±0.5	8.08±0.1	9.32±0.1	108.6±49.02
18.30	Tetradecanal	-	-	-	60.55±8.26	-	-
18.54	β-Ionone	27.07±1.08	59.65±6.69	123.92±9.85	187.24±23.21	147.16±5.48	190.29±14.88
18.66	cis-Jasmone	-	-	-	11.74±1.26	16.37±1.12	9.1±1.71
18.77	Benzothiazole	11.18±0.21	3.46±0.44	16.25±0.63	17.54±1.05	2.98±0.43	19.02±0.62
18.97	6,10 Dimethyl-5,9 undecadien-2-ol	-	-	-	-	134.78±59.27	5.82±0.3
19.43	β-Ionone-5,6-epoxide	-	9.79±1.22	14.42±1.73	23.97±3.81	17.62±0.18	21.34±1.42
19.89	2 Hexenoic acid	-	-	-	-	-	-
19.97	γ-Nonalactone	-	-	23.68±2.82	-	-	25.39±3.09
20.07	Pentadecanal	-	47.81±3.94	-	297.15±104.77	45.36±2.63	455.77±232.88

Table F2. continued

RT	Compounds	Pecos					
		Riverside			Maxima		
		0 day	10 day	20 day	0 day	10 day	20 day
20.74	5 Pentyl-2(5H)-furanone	-	-	-	-	-	-
21.23	Cuminol	10.73±0.66	12.61±0.48	14.02±0.41	12.45±0.86	17.33±0.37	12.05±0.27
21.35	Octanoic acid	-	-	-	-	-	-
21.59	(E,E)-Pseudoionone	8.83±0.57	15.54±0.99	17.86±1	79.14±9.87	40.14±2.21	36.54±3.12
21.98	Nonanoic acid	28.32±0.89	21.9±0.18	53.11±7.27	-	18.88±1.68	20.63±3.29
22.35	Methyl hexadecanoate	-	-	-	-	-	39.54±3.64
22.62	Ethyl pentadecanoate	-	-	-	25.74±1	-	-
22.63	Ethyl hexadecanoate	6.49±0.93	41.65±3.51	83.18±6.39	-	178.66±6.74	70.37±8.83
22.71	3-Nonenoic acid	-	12.28±0.88	19.62±1.59	-	-	-
23.18	Dihydroactinidiolide	-	-	-	-	-	-
23.35	Farnesyl acetone	9.64±0.34	32.12±4.88	62.25±6.92	78.99±6.23	91.94±2.45	106.07±3.25
23.80	Methyl 9-octadecenoate	-	-	72.18±7.3	37.99±3.58	43.63±5.79	44.26±7.2
24.00	2 Decenoic acid	-	-	-	-	-	-
24.03	Methyl octadecanoate	-	-	-	-	-	-
24.14	Ethyl 9-octadecenoate	-	26.99±1.98	188.88±17.13	32.24±2.83	197.21±13.7	112.42±17.58
24.19	Methyl octadecadienoate	11.22±0.23	-	-	-	-	-

Table F3. Volatile compounds quantified (μg/kg) in watermelons harvested from Grapeland. Values are means ± SE.

RT	Compounds	Grapeland					
		Riverside			Maxima		
		0 day	10 day	20 day	0 day	10 day	20 day
2.30	Ethanol	163.93±2.92	167.31±5	289.16±11.15	-	125.06±7.63	437.22±24.52
3.64	Hexanal						
5.04	D-limonene	-	-	-	-	-	120.44±14.58
5.48	β-limonene	-	-	-	-	-	-
5.50	Pyridine	-	-	-	-	-	-
5.71	2-Pentylfuran	248.72±16.61	110.92±19.4	634.14±70.01	96.95±3.9	25.75±1.97	-
5.80	(E)-2-Hexenal	-	-	-	-	-	-
6.54	Cyclodecane	-	-	-	-	-	-
6.58	Acetoin	-	-	-	-	-	-
6.80	trans-2-(2-Pentenyl)furan	-	-	-	-	-	-
6.99	Octanal	-	-	-	-	-	-
7.57	6-Methyl-5-hepten-2-one	669.62±35.82	930.68±84.1	353.29±20.91	1010.19±72.82	510.39±69.36	79.53±1.13
7.84	(E)-2-Heptenal	-	-	-	-	-	-
8.53	1 Hexanol	-	-	-	-	-	-
8.60	Nonanal	319.74±48.13	975.88±66.89	394.23±21.89	933.02±64.67	167.77±24.5	175.1±27.48
9.07	Perilline	12.54±0.1	76.74±5.98	-	84.03±7.79	25.73±5.32	-
9.58	Acetic acid	-	-	-	-	-	-
9.79	1-Octen-3-ol	-	-	40.34±3.59	56±5.45	22.39±3.83	12.67±0.23
9.85	(E)-2-Octenal	19.39±3.16	107.68±13.06	38.28±3.49	104.96±6.57	22.82±2.88	-
10.00	(E)-4-Nonenal	98.46±18.39	115.35±14.65	88.22±22.95	119.22±23.02	37.77±4.8	16.74±0.9
10.26	(Z)-6-Nonenal	39.31±8.01	110.39±15.43	37.15±8.13	89.86±14.45	18.96±4.09	13.87±2.89
10.42	(E)-6-Nonenal	-	-	-	-	-	-
10.70	6-Methyl-5-hepten-2-ol	4.69±0	35.33±1.98	-	16.51±3.16	14.32±1.69	-
10.76	(Z)-2-Nonenal	134.04±21.73	113.63±14.98	115.2±19.51	107.43±16.66	51.64±4.9	46.53±4.89
11.03	Benzaldehyde	192.9±91.71	88.85±9.48	832.91±124.54	85.32±7.96	23.79±3.07	99.65±39.57
11.20	Methyl nonanoate	-	-	-	-	-	-
11.23	Decanal	-	-	-	-	-	-
11.35	(E)-2-Nonenal	3030.85±359.66	2221.06±238.01	3506.66±252.82	2599.02±296.14	1360.8±110.83	1689.13±117.47
11.90	Pinocarvone	-	-	-	-	-	-
11.92	1-Octanol	39.49±0.69	118.77±14.78	51.98±1.57	126.72±8.81	71.82±0.66	134.79±15.81
12.33	(E,Z)-2,6-Nonadienal	1089.29±117.35	611.57±84.43	689.74±41.38	750.78±107.07	458.95±50.43	692.26±47.51
12.33	Ethyl-3-nonenoate	-	-	-	-	-	-
12.34	6-Methyl-3,5-heptadien-2-one	-	-	-	-	-	-
12.72	(Z)-3-Nonenyl acetate	-	-	-	-	-	-
12.89	β-cyclocitral	40.72±3.7	186.87±15.41	71.31±8.43	185.5±14.53	65.37±8.55	67.23±10.77

Table F3. continued

RT	Compounds	Grapeland					
		Riverside			Maxima		
		0 day	10 day	20 day	0 day	10 day	20 day
12.98	(Z)-5-Octen-1-ol	10.37±1.12	13.81±1.25	15.29±1.91	12.05±0.65	9.68±1.59	15.28±0.72
13.34	(E)-2-Decenal	-	163.66±17.57	-	155.59±17.51	13.39±1.96	8.05±1.8
13.35	cis-Pinocarveol	-	-	-	-	-	-
13.48	Methyl 6-nonynoate	-	-	-	-	-	-
13.77	4,5-Difluoroctane	241.31±9.76	311.14±37.05	214.75±18.35	245.5±11.81	117.81±3.76	372.62±28.57
13.88	1-Nonanol	1358.48±111.66	1383.76±104.65	1251.09±41.06	1484.5±118.93	910.92±71.06	1340.44±109.16
14.10	pentadecanal	123.83±7.38	157.54±13.12	67.77±3.67	171.34±13.22	83.61±15.41	48±8.76
14.32	(Z)-3-Nonen-1-ol	4517.87±234.56	4276.77±509.42	3772.27±133.25	4725.7±196.97	2316.5±44.68	4666.1±302.38
14.44	(E,E)-2,4-Nonadienal	-	-	-	-	-	-
14.68	(Z)-6-Nonen-1-ol	-	-	-	52.13±3.19	-	22.97±0.4
14.83	(E)-2-Nonen-1-ol	414.82±86.75	152.64±8.59	349.44±3.63	178.33±17.13	177.85±43.4	472.37±46.51
14.92	(E)-6-Nonen-1-ol	396.16±28.3	280.49±25.12	980.53±27.96	335.79±20.24	202.16±14.04	356.17±33.25
15.03	(E)-Citral	210.38±12.87	290.09±31.58	89.96±8.76	313.93±37.38	139.6±24.93	97.12±15.1
15.52	(Z,Z)-3,6-Nonadien-1-ol	1672.95±69.48	1551.32±129.02	1127.08±128.31	1657.79±48.44	1006.93±13.27	1827.28±90.33
15.82	(E,Z)-2,6-Nonadien-1-ol	101.86±8.28	78.3±2.01	192.3±6.57	89.9±9.53	67.72±14.71	198.12±8.06
15.85	L-Perrillaldehyde	-	-	-	-	-	-
15.91	Methoxy-phenyl-oxime	291.6±88.46	151.71±5.03	341.77±65.48	149.99±5.41	88.81±2.43	255.74±15.8
16.35	(E,E)-2,4-Decadienal	-	13.75±0.28	10.06±2.38	14.96±0.67	7.56±1.27	-
16.36	(E)-Geraniol	-	-	-	-	-	-
16.74	cis-Geranylacetone	-	60.05±4.3	35.76±1.67	58.19±4.39	32.69±2.13	-
16.95	Myrtenol	-	-	-	-	-	-
17.07	α-Ionone	-	9.86±0.65	-	10.54±0.69	-	-
17.20	trans-Geranylacetone	534.45±19.53	1595.33±142.31	578.6±17.78	1632.04±158.04	900.86±107.57	823.83±48.35
17.59	Benzyl alcohol	33.11±0.81	80.87±6.83	136.99±7.19	80.75±7.36	121.92±32.32	389.5±98.48
17.76	Isolimonene	-	15.43±1.51	6.14±0.31	14.63±1.23	-	-
17.84	Hexanoic acid	-	-	-	-	-	-
18.18	Benzene ethanol	7.2±1.03	-	-	-	-	-
18.30	Tetradecanal	-	-	-	-	-	-
18.54	β-Ionone	129.6±6.58	686.1±85.95	158.22±10.8	736.7±55.77	153.91±16.13	231.84±42.08
18.66	cis-Jasmone	-	-	-	-	-	-
18.77	Benzothiazole	18.8±1.29	5.04±0.13	6.65±2.05	5.01±0.2	13.43±1.18	7.4±0.96
18.97	6,10 Dimethyl-5,9 undecadien-2-ol	-	60.38±10.59	14.19±1.51	62.76±8.27	30.59±3.82	40.38±4.34
19.43	β-Ionone-5,6-epoxide	16.38±0.97	95.68±13.4	25.9±3.65	101.23±11.08	18.3±2.2	34.38±8.59
19.89	2 Hexenoic acid	-	-	-	-	-	-
19.97	γ-Nonalactone	80.94±4.19	110.03±14.52	73.92±9.33	117.98±8.63	36±4.32	37.02±3.77
20.07	Pentadecanal	20.15±6.11	-	-	-	-	-

Table F3. continued

RT	Compounds	Grapeland					
		Riverside			Maxima		
		0 day	10 day	20 day	0 day	10 day	20 day
20.74	5 Pentyl-2(5H)-furanone	-	25.57±1.93	37.17±6.61	27.03±2.23	11.82±2.86	12.98±0.32
21.23	Cuminol	9.17±0.73	12.07±0.19	9.14±0.28	11.75±0.23	11.88±0.39	15.19±0.14
21.35	Octanoic acid	-	-	-	-	-	-
21.59	(E,E)-Pseudoionone	17.86±2.6	77.32±6.59	17.96±2.5	84.29±5.76	23.29±4.28	17.71±2.7
21.98	Nonanoic acid	6.92±0.85	4.74±0.52	-	4.4±0.4	3.37±0.84	10.28±2.08
22.35	Methyl hexadecanoate	-	-	-	-	-	-
22.62	Ethyl pentadecanoate	-	-	-	-	-	-
22.63	Ethyl hexadecanoate	20.32±0.55	27.34±2.2	11.53±1.59	30.49±3.86	39.94±3.89	16.13±3.18
22.71	3-Nonenoic acid	-	-	-	-	-	-
23.18	Dihydroactinidiolide	13.47±0.03	34.08±4.76	13.22±0.57	36.64±3.88	11.08±0.83	25.49±4.02
23.35	Farnesyl acetone	30.76±2.55	161.62±20.66	-	186.98±19.55	76.54±9.43	106.07±10.52
23.80	Methyl 9-octadecenoate	35.88±1.8	112.16±4.58	-	123.87±7.5	119.97±8.12	146.28±8.7
24.00	2 Decenoic acid	-	-	-	-	-	-
24.03	Methyl octadecanoate	-	-	-	-	-	-
24.14	Ethyl 9-octadecenoate	13.88±0.97	19.59±0.55	-	-	24.49±2.44	489.41±88.9
24.19	Methyl octadecadienoate	-	-	-	-	-	-

Table F4. Volatile compounds quantified (μg/kg) in watermelons harvested from Edinburg. Values are means ± SE.

RT	Compounds	Edinburg					
		Riverside			Maxima		
		0 day	10 day	20 day	0 day	10 day	20 day
2.30	Ethanol	99.97±16.93	102.69±1.26	161.97±1.96	141.16±11.18	170.81±16.86	194.26±5.57
3.64	Hexanal						
5.04	D-limonene	-	-	-	-	-	-
5.48	β-limonene	-	-	-	-	-	-
5.50	Pyridine	-	-	-	-	-	-
5.71	2-Pentylfuran	429.25±40.16	1668.16±9.15	1046.69±6.42	246.49±19.29	676.8±116.69	845.31±52.85
5.80	(E)-2-Hexenal	-	-	-	-	-	-
6.54	Cyclodecane	-	-	-	-	-	-
6.58	Acetoin	-	-	-	-	-	-
6.80	trans-2-(2-Pentenyl)furan	-	39.74±1.99	35.86±6.98	35.96±4.23	60.25±16.15	67.14±22.16
6.99	Octanal	-	-	-	-	-	-
7.57	6-Methyl-5-hepten-2-one	697.25±82.54	1041.63±54.82	602.78±20.75	503.32±50.31	1319.94±40.3	1603.47±76.6
7.84	(E)-2-Heptenal	-	-	-	-	-	-
8.53	1 Hexanol	-	-	-	-	-	-
8.60	Nonanal	2836.43±277.58	850.12±40.9	1299.82±49.07	901.9±82.84	731.85±71.45	1187.86±56.85
9.07	Perilline	-	-	-	-	39.72±3.64	152.85±10.79
9.58	Acetic acid	-	-	-	-	-	-
9.79	1-Octen-3-ol	-	-	-	-	-	66.45±0
9.85	(E)-2-Octenal	-	13.29±1.2	82.99±0.35	20.34±2.77	20.53±1.79	117.43±11.52
10.00	(E)-4-Nonenal	-	57.43±5.46	147±10.88	40.89±4.1	40.69±4.76	175.16±10.88
10.26	(Z)-6-Nonenal	644.01±98.82	157.73±58.89	253±5.66	353.65±52.1	52.25±13.62	302.34±44.35
10.42	(E)-6-Nonenal	-	-	-	-	-	-
10.70	6-Methyl-5-hepten-2-ol	-	-	10.5±1.24	-	-	-
10.76	(Z)-2-Nonenal	94.03±12.87	113.13±11.18	97.68±8.05	111.46±9.86	80.56±13.22	124.26±3.34
11.03	Benzaldehyde	-	33.19±2.61	18.25±3.64	-	47.68±8.62	-
11.20	Methyl nonanoate	-	-	-	-	-	-
11.23	Decanal	-	-	-	-	-	-
11.35	(E)-2-Nonenal	2240.55±50.77	2531.03±213.99	2401.87±9.65	2682.91±164.85	1993.32±132.44	2993.9±111.41
11.90	Pinocarvone	-	-	-	-	-	-
11.92	1-Octanol	34.15±2	14.85±1.54	16.99±2.04	31.88±3.22	62.39±18.52	36.19±4.59
12.33	(E,Z)-2,6-Nonadienal	444.26±16.59	620.92±81.46	595.74±28.12	1135.71±86.6	619.21±60.31	1117.58±13.74
12.33	Ethyl-3-nonenoate	-	-	-	-	-	-
12.34	6-Methyl-3,5-heptadien-2-one	-	-	-	-	-	-

Table F4. continued

RT	Compounds	Edinburg					
		Riverside			Maxima		
		0 day	10 day	20 day	0 day	10 day	20 day
12.72	(Z)-3-Nonenyl acetate	-	-	-	19.49±0.57	-	-
12.89	β-cyclocitral	28.31±1.54	26.04±3.91	46.92±5.82	30.84±0.42	74.24±6.18	99.72±7.04
12.98	(Z)-5-Octen-1-ol	4.86±0.61	3.32±0.26	6.38±0.57	-	12.24±2.37	-
13.34	(E)-2-Decenal	-	5.43±0.1	9.46±1.42	14.14±1.67	27.75±0.98	-
13.35	cis-Pinocarveol	-	-	-	-	-	-
13.48	Methyl 6-nonynoate	-	-	-	-	-	-
13.77	4,5-Difluoroctane	294.38±133.46	113.72±9.31	62.98±1.56	149.7±20.15	119.59±15.63	101.13±2.64
13.88	1-Nonanol	925.95±59.81	131.7±10.61	420.56±73.01	893.19±97.74	873.95±283.25	378.76±59.73
14.10	pentadecanal	126.38±29.68	175.12±29.23	138.56±4.48	162.75±17.72	206.74±45.67	355.93±19.64
14.32	(Z)-3-Nonen-1-ol	1222.95±39.24	762.41±53.44	900.05±138.51	1403.77±41.66	1539.88±262.78	1240.89±39.3
14.44	(E,E)-2,4-Nonadienal	-	130.83±17.69	118.37±8.45	-	158.51±5.83	177.57±13.27
14.68	(Z)-6-Nonen-1-ol	-	-	-	-	30.83±5.85	20.08±0.4
14.83	(E)-2-Nonen-1-ol	53.89±17.57	83.74±7.23	260.12±62.82	253.91±1.36	402.02±121.2	379.87±40.99
14.92	(E)-6-Nonen-1-ol	147.11±9.05	70.03±11.96	-	336.85±55.07	362.98±135.06	-
15.03	(E)-Citral	333.85±52.16	216.33±30.26	251.08±8.09	283.02±31.44	352.74±48.81	515.94±15.71
15.52	(Z,Z)-3,6-Nonadien-1-ol	294.91±21.06	226.64±62.21	240.91±63.14	625.09±32.27	404.64±31.89	484.15±32.19
15.82	(E,Z)-2,6-Nonadien-1-ol	-	35.82±8.28	46.45±14.98	181.09±67.38	228.62±78.5	156.35±37.13
15.85	L-Perrillaldehyde	-	126.26±16.67	-	-	215.87±56.54	156.35±37.13
15.91	Methoxy-phenyl-oxime	171.71±48.12	-	60.23±0.22	126.26±16.31	-	-
16.35	(E,E)-2,4-Decadienal	-	-	-	-	-	-
16.36	(E)-Geraniol	-	-	-	-	26.43±10.04	59.88±23.93
16.74	cis-Geranylacetone	-	-	-	-	-	-
16.95	Myrtenol	-	-	-	-	-	-
17.07	α-Ionone	-	-	-	-	-	-
17.20	trans-Geranylacetone	451.44±8.3	333.34±28.68	598.29±58.05	1286.19±6.25	1652.38±44.53	2051.14±261.07
17.59	Benzyl alcohol	-	106.81±20.93	116.5±21.05	-	110.33±32.35	81.26±11.75
17.76	Isolimonene	-	-	-	-	-	-
17.84	Hexanoic acid	-	-	-	-	-	-
18.18	Benzene ethanol	-	5.11±0.63	5.12±0.58	-	36.51±12.19	13.11±2.83
18.30	Tetradecanal	-	-	-	-	-	-
18.54	β-Ionone	96.47±0.55	-	136.61±14.58	159.06±2.05	258.11±19.18	258.68±14.43
18.66	cis-Jasmone	-	-	-	-	-	-
18.77	Benzothiazole	12.45±1.82	8.49±0.4	3.19±0.16	-	13.52±0.56	14.5±0.51
18.97	6,10 Dimethyl-5,9 undecadien-2-ol	-	-	3.35±0.35	-	17.37±4.99	10.25±2.09

Table F4. continued

RT	Compounds	Edinburg					
		Riverside			Maxima		
		0 day	10 day	20 day	0 day	10 day	20 day
19.43	β-Ionone-5,6-epoxide	16.68±0.23	12.26±1.38	20.87±1.53	23.1±1.02	42.8±4.77	36.6±2.57
19.89	2 Hexenoic acid	-	-	-	-	-	-
19.97	γ-Nonalactone	-	16.81±1.48	10.55±2.87	11.73±3.59	23.55±6.86	-
20.07	Pentadecanal	-	-	4.02±0.35	-	5.74±0.38	9.76±1.78
20.74	5 Pentyl-2(5H)-furanone	-	-	-	-	-	-
21.23	Cuminol	7.74±0.77	12.03±0.9	11.97±0.89	14.76±2.73	21.46±2.12	11.4±1.1
21.35	Octanoic acid	-	-	-	-	-	-
21.59	(E,E)-Pseudoionone	31.77±2.25	16.61±1.39	33.71±2.71	69.9±5.54	104.32±2.59	101.14±3.96
21.98	Nonanoic acid	31.51±3.49	4.59±0.3	-	29.96±1.77	29.75±7.91	18.27±2.04
22.35	Methyl hexadecanoate	-	-	34.61±2.68	-	-	-
22.62	Ethyl pentadecanoate	-	-	-	-	-	-
22.63	Ethyl hexadecanoate	42.18±9.63	12.21±1.1	19.06±0.86	93.14±11.62	14.85±2.05	67±9.39
22.71	3-Nonenoic acid	-	-	-	9.16±0.52	-	-
23.18	Dihydroactinidiolide	-	-	-	-	-	-
23.35	Farnesyl acetone	21.89±0.51	13.11±2.57	47.36±6.78	141.02±8.75	138.36±3.49	189.48±26.85
23.80	Methyl 9-octadecenoate	64.6±13.69	32.27±5.4	61.77±6.41	62.54±6.66	116.41±6.66	133.82±17.08
24.00	2 Decenoic acid	-	-	-	-	-	-
24.03	Methyl octadecanoate	-	-	-	-	-	-
24.14	Ethyl 9-octadecenoate	58.25±14.11	26.32±2.66	69.7±8.74	66.52±10.64	38.08±5.88	74.77±16.06
24.19	Methyl octadecadienoate	-	-	-	-	-	-

Table F5. Volatile compounds quantified (μg/kg) in watermelons harvested from Weslaco. Values are means ± SE.

RT	Compounds	Weslaco					
		Riverside			Maxima		
		0 day	10 day	20 day	0 day	10 day	20 day
2.30	Ethanol	-	-	-	-	-	-
3.64	Hexanal	162.05±26.4	12.95±0.97	44.41±3.49	38.75±4.39	23.58±0.9	19.22±2.15
5.04	D-limonene	-	18.17±3.65	17.65±0.86	26.86±3.38	17.39±0.41	12.29±1.64
5.48	β-limonene	20.03±3.93	-	-	-	-	-
5.50	Pyridine	-	42.26±6.79	227.58±5.81	156.23±32.75	81.93±11.06	63.33±9.95
5.71	2-Pentylfuran	365.51±51.75	188.35±9.5	224.8±5.69	128.19±16.74	105.57±6.91	75.61±12.98
5.80	(E)-2-Hexenal	76.66±12.67	-	-	137.73±4.89	-	-
6.54	Cyclodecane	812.71±106.68	280.95±29.51	333.72±4.3	62.77±15.69	41.19±3.48	77.5±14.28
6.58	Acetoin	-	-	-	-	-	-
6.80	trans-2-(2-Pentenyl)furan	-	-	-	-	-	-
6.99	Octanal	9.03±1.41	-	-	5.73±0.08	6.36±0.52	3±0.1
7.57	6-Methyl-5-hepten-2-one	1444.64±138.14	1952.79±145.43	211.79±28.13	304.21±42.24	278.81±16.36	527.35±98.84
7.84	(E)-2-Heptenal	23.12±2.6	-	-	-	-	-
8.53	1 Hexanol	-	95.22±2.89	-	23.32±4.17	24.29±2.21	3.27±0.1
8.60	Nonanal	1333.99±216.91	206.99±69.89	959.68±182.34	158.06±24.71	62.19±7.63	276.88±38.66
9.07	Perilline	-	92.74±14.22	-	28.01±2.72	15.19±0.81	25.31±3.94
9.58	Acetic acid	-	322.04±59.8	-	-	-	-
9.79	1-Octen-3-ol	-	-	-	-	-	81.95±29.11
9.85	(E)-2-Octenal	84.39±11.02	-	38.8±7.3	23.21±3.2	16.1±0.74	23.65±2.7
10.00	(E)-4-Nonenal	71.33±7.05	-	90.79±9.27	30.26±2.79	25.81±4.9	42.17±1.58
10.26	(Z)-6-Nonenal	534.19±203.49	-	239.48±65.33	48.52±11.49	30.72±9.4	46.31±16.1
10.42	(E)-6-Nonenal	129.93±10.37	-	447.4±73.77	42.02±3.63	56.75±4.21	69.32±0.1
10.70	6-Methyl-5-hepten-2-ol	21.96±0.63	142.83±29.93	4.03±0.54	4.97±0.39	14.14±2.05	5.82±0.79
10.76	(Z)-2-Nonenal	48.36±1.95	24.18±1.56	109.31±7.93	-	464.23±74.48	53.43±7.16
11.03	Benzaldehyde	19.1±1.59	11±1.11	12.09±1.12	-	-	10.78±0.95
11.20	Methyl nonanoate	20.21±2.79	-	45.04±3.81	-	15.48±1.3	9.43±1.06
11.23	Decanal	21.16±0.7	-	-	16.61±0.51	-	-
11.35	(E)-2-Nonenal	2617.28±191.85	402.89±136.02	3329.57±342.94	1437.75±134.58	967.13±211.96	1855.11±150.39
11.90	Pinocarvone	-	-	-	60.64±1.98	82.04±5.86	36.95±5.31
11.92	1-Octanol	48.94±4.5	65.63±5.76	29.07±2.92	-	-	-
12.33	(E,Z)-2,6-Nonadienal	1010.82±60.51	149.85±40.53	1270.76±66.82	488.73±63.09	751.4±81.64	785.13±132.04
12.33	Ethyl-3-nonenoate	-	-	-	-	-	-
12.34	6-Methyl-3,5-heptadien-2-one	-	60.54±2.62	-	-	-	-

Table F5. continued

RT	Compounds	Weslaco					
		Riverside			Maxima		
		0 day	10 day	20 day	0 day	10 day	20 day
12.72	(Z)-3-Nonenyl acetate	-	-	-	-	-	-
12.89	β-cyclocitral	28.45±1.62	62.81±5.72	21.5±1.56	23.04±3.14	31.79±0.87	27.08±2.63
12.98	(Z)-5-Octen-1-ol	-	-	-	-	-	-
13.34	(E)-2-Decenal	-	-	-	47.56±8.86	36.26±1.56	56.82±8.93
13.35	cis-Pinocarveol	-	-	-	-	-	-
13.48	Methyl 6-nonynoate	-	-	-	-	-	-
13.77	4,5-Difluoroctane	-	204.8±9.35	147.72±6.28	253.68±5.04	145.62±3.78	79.49±5.27
13.88	1-Nonanol	565.61±107.08	1427.03±141.95	371.81±52.73	1092.51±79.33	1721.48±183.36	356.64±31.59
14.10	pentadecanal	63.95±5.55	111.73±26.8	61.32±4.96	94.13±14.49	98.47±10.19	90.51±9.46
14.32	(Z)-3-Nonen-1-ol	951.87±169.45	1279.68±50.3	944.3±64.73	3080.92±130.03	3156.07±157.58	1636.82±163.09
14.44	(E,E)-2,4-Nonadienal	-	-	-	597.5±78.38	-	-
14.68	(Z)-6-Nonen-1-ol	-	-	-	-	-	-
14.83	(E)-2-Nonen-1-ol	54.32±12.17	1412.74±294.51	150.04±14.06	405.06±105.48	68.94±15.22	168.78±37.93
14.92	(E)-6-Nonen-1-ol	186.04±13.3	1315.15±175.07	148.38±7.18	439.96±68.99	585.58±70.84	148.97±33.19
15.03	(E)-Citral	119.92±7.68	134.11±46.43	137.6±8.77	153.55±16.01	211.93±12.19	166±16.79
15.52	(Z,Z)-3,6-Nonadien-1-ol	383.18±64.86	1056.49±97.73	585.7±2.05	1848.05±74.02	2209.7±100.8	890.4±80.47
15.82	(E,Z)-2,6-Nonadien-1-ol	40.13±2.08	679.94±56.52	96.5±2.37	320.38±59.9	84.66±4.68	92.11±17.57
15.85	L-Perrillaldehyde	41.5±4.33	20.78±1.94	30.93±1	44.53±1.88	33.28±0.8	31.83±2
15.91	Methoxy-phenyl-oxime	-	-	-	-	-	-
16.35	(E,E)-2,4-Decadienal	2.77±0.22	-	-	-	-	-
16.36	(E)-Geraniol	200.05±25.99	-	-	-	-	-
16.74	cis-Geranylacetone	-	-	-	-	-	-
16.95	Myrtenol	-	-	-	3.97±0	7.53±2.03	-
17.07	α-Ionone	-	-	-	-	-	-
17.20	trans-Geranylacetone	-	818.65±95.4	294.96±40.06	630.68±84.7	592.83±10.8	519.46±30.68
17.59	Benzyl alcohol	-	58.8±12.53	172.21±5.78	-	-	71.83±2.01
17.76	Isolimonene	-	-	-	-	-	-
17.84	Hexanoic acid	29.35±7.12	54.62±2.27	6.27±0.89	15.29±2.08	10.94±1.05	6.24±0.02
18.18	Benzene ethanol	8.87±0.12	13.85±2.05	-	-	-	-
18.30	Tetradecanal	-	-	-	-	-	-
18.54	β-Ionone	35.35±8.74	75.98±5.58	58.78±3.78	62.58±4.85	71.84±3.41	84.56±15.5
18.66	cis-Jasmone	-	-	-	-	-	-
18.77	Benzothiazole	20.39±2.58	29.75±8.45	53.89±1.48	39.39±10.44	14.32±0.13	16.66±2.45
18.97	6,10 Dimethyl-5,9 undecadien-2-ol	-	-	-	-	-	-

Table F5. continued

RT	Compounds	Weslaco					
		Riverside			Maxima		
		0 day	10 day	20 day	0 day	10 day	20 day
19.43	β-Ionone-5,6-epoxide	7.55±1.17	15.5±0.37	12.91±1.63	9.01±1	15.08±1.67	17.8±4.03
19.89	2 Hexenoic acid	-	7.27±0.44	2.08±0.24	-	-	-
19.97	γ-Nonalactone	35.96±3.38	-	45.66±6.24	-	-	27.72±3.17
20.07	Pentadecanal	-	-	-	-	-	-
20.74	5 Pentyl-2(5H)-furanone	14.95±3.22	13.04±0.66	13.58±0.8	-	-	-
21.23	Cuminol	10.17±0.43	9.32±0.31	10.33±0.59	10.39±0.29	16.58±4.4	8.64±0.12
21.35	Octanoic acid	10.11±0.39	20.2±2.77	7.37±0.87	-	-	-
21.59	(E,E)-Pseudoionone	-	-	-	-	-	-
21.98	Nonanoic acid	51.94±2.23	152±22.56	46.04±4.28	19.2±2.54	61.62±4.5	48.03±6.54
22.35	Methyl hexadecanoate	64.22±5.18	268.93±4.1	887.61±35.14	703.89±55.39	1127.95±88.84	344.83±104.99
22.62	Ethyl pentadecanoate	-	-	-	-	-	-
22.63	Ethyl hexadecanoate	-	-	-	-	-	-
22.71	3-Nonenoic acid	-	-	-	-	-	-
23.18	Dihydroactinidiolide	-	-	-	-	-	-
23.35	Farnesyl acetone	-	-	-	-	-	-
23.80	Methyl 9-octadecenoate	-	-	-	94.83±6.4	-	-
24.00	2 Decenoic acid	-	52.43±8.39	48.72±10.98	-	-	-
24.03	Methyl octadecanoate	-	-	22.79±2.86	-	-	15.05±5.3
24.14	Ethyl 9-octadecenoate	-	-	-	-	-	-
24.19	Methyl octadecadienoate	-	-	-	-	-	-